

Gratian Dragoslav Miclaus
Horia Ples

Atlas of CT Angiography

Normal and Pathologic
Findings

 Springer

Atlas of CT Angiography

Gratian Dragoslav Miclaus • Horia Ples

Atlas of CT Angiography

Normal and Pathologic Findings



Springer

Gratian Dragoslav Miclaus
Department of Computed Tomography
SCM Neuromed
Timisoara
Romania

Horia Ples
Department of Neurosurgery
University of Medicine and Pharmacy
“Victor Babes”
Timisoara
Romania

ISBN 978-3-319-05283-0 ISBN 978-3-319-05284-7 (eBook)
DOI 10.1007/978-3-319-05284-7
Springer Cham Heidelberg New York Dordrecht London

Library of Congress Control Number: 2014942079

© Springer International Publishing Switzerland 2014

This work is subject to copyright. All rights are reserved by the Publisher, whether the whole or part of the material is concerned, specifically the rights of translation, reprinting, reuse of illustrations, recitation, broadcasting, reproduction on microfilms or in any other physical way, and transmission or information storage and retrieval, electronic adaptation, computer software, or by similar or dissimilar methodology now known or hereafter developed. Exempted from this legal reservation are brief excerpts in connection with reviews or scholarly analysis or material supplied specifically for the purpose of being entered and executed on a computer system, for exclusive use by the purchaser of the work. Duplication of this publication or parts thereof is permitted only under the provisions of the Copyright Law of the Publisher's location, in its current version, and permission for use must always be obtained from Springer. Permissions for use may be obtained through RightsLink at the Copyright Clearance Center. Violations are liable to prosecution under the respective Copyright Law.

The use of general descriptive names, registered names, trademarks, service marks, etc. in this publication does not imply, even in the absence of a specific statement, that such names are exempt from the relevant protective laws and regulations and therefore free for general use.

While the advice and information in this book are believed to be true and accurate at the date of publication, neither the authors nor the editors nor the publisher can accept any legal responsibility for any errors or omissions that may be made. The publisher makes no warranty, express or implied, with respect to the material contained herein.

Printed on acid-free paper

Springer is part of Springer Science+Business Media (www.springer.com)

Preface

Permanent research in the field of medical radio-imaging concerning the non-invasive exploration of the circulatory system has led to the appearance and increasing use of the CT multislice for diagnostic purposes.

The acquisition by Neuromed Timisoara of the first computed tomography 64 multislice has placed Romania among the countries using state-of-the art non-invasive technologies for diagnostic purposes. It is used not only for routine investigations but also in the diagnosis of cardiovascular pathology.

Worldwide the existence and use of this technique avoids almost entirely the use invasive methods for diagnostic purposes, which takes place only in exceptional circumstances. The invasive part of the diagnosis, which is extremely unpleasant to the patient, is thus eliminated from the diagnostic process, and patients now have the possibility of the diagnosis of vascular pathology without hospitalization.

The technique is also beneficial to the doctors, as it enables them to identify and visualize the exact location of the damaged area, the anatomic details, the severity of lesions leading to a more appropriate planning of the operating techniques by the use of 3D reconstruction.

The present atlas aims to present some of the more challenging cases explored in our clinic during a period of 7 years. During this period, we explored more than 3,500 CT coronary angiographies and more than 18,000 CT angiographies of other anatomic segments.

While the imagistic radiographs presented in this paper do not fully cover the vascular pathology, we consider it useful to present them in the hope that a great number of doctors will become familiar with the exploration possibilities given by this non-invasive method.

The present paper is subject to constant improvement, as our acquired experience and inventory of cases studied, provides us with new and interesting insight to be presented in order to discover more the possibilities of non-invasive exploration of the circulatory system.

Technical Principles

Computed tomography is a diagnostic technique which utilizes X-rays, in which a small fascicle of X-rays axially traverses the patient's body from different angles. Parallel collimation is used to model the fascicle of rays into a small slot, which defines the width of the scanning plan. Detectors measure

the intensity of the reduction of emerging radiation from the patient's body. A mathematical algorithm is used (inverse radon transformation) to calculate the reduction in each part of the CT section. These local reduction coefficients are then transformed into "CT numbers" and are finally converted into shades of grey which are then, in turn, shown as images.

Multislice tomographs allow the acquisition during a single rotation of the tube of a variable number of images (2-6-4), respectively, of a larger volume. The width of the slice is variable, with the spatial resolution growing in reverse proportion with the width. Therefore, for obtaining isotropy, the use of sub-millimetric widths is necessary. Isotropic acquisition allows us to reconstruct images in all three dimensions without modifying the spatial resolution. Thus, diagnostic accuracy in the case of isotropic acquisition is the same, indifferent of the spatial dimension in which the images are later reconstructed.

In the case of Somatom Sensation 64, the spatial resolution of an image is lower than 0.4 mm, and the acquired volume unit (voxel) has the same size for all 3 dimensions (under 0.4 mm for the x , y and z axes).

Obtaining such a resolution is possible due to the technical parameters offered by this machine and, particularly, the high rotation speed of the tube (330 ms) and the technical ability of the STRATON tube to generate two fascicles of X-rays which intertwine, generating the spatial resolution of 0.3 mm.

The length which may be scanned is also important; this machine permits the acquiring of images for a length of up to 1,540 mm, which makes its use possible in peripheral angiographic studies.

All of these technical details, the high scanning speed and high temporal and spatial resolution, allow the use of the computed tomograph in coronary angiographic studies, where the investigation of small arteries belonging to a continually moving organ is necessary.

The study does not aim to become a technical treaty or one of the CT exam protocols, but we consider it necessary to present a couple of technical possibilities for examination as well as a couple of advantages offered by the use of this type of computed tomograph, in relation to the investigated area.

Cerebral CT Angiography

In our clinic, we use a scanning protocol which includes a native scan and a scan which follows the injection of intravenous contrast substance. We apply this protocol in order to obtain the subtraction of the bone, which allows the evaluation of the circulation in the cerebral arteries, without the presence of the bone structures of the neurocranium.

Following the bone subtraction, 3D MIP and 3D VRT reconstructions are used to visualize aneurysms as well as artery-vein malformations (MAV). Coming to the aid of neurosurgeons, we also use 3D VRT reconstructions without bone subtraction, which allows the planning of craniotomies in such a way that the remaining bone defect is at a minimum.

The method is also used to check post-operative evolution in the case of applying metal clips or for selective arterial embolising procedures of the MAV.

CT Angiography of the Cervical Region

This is used to visualize arterial circulation at the level of the cervical region as well as arterial pathology at this level. Thus, we are able to identify stenoses of the common carotid arteries, internal and external; of other arteries at the base of the neck; and of vertebral arteries, as well as perform post-operative or post-interventional checks at the level of the before-mentioned arteries. Thus, one can check the patency of carotid stenting, showing the presence or absence of restenosis in the stent.

Pre-operative details regarding the parietal calcification at the level of the carotid arteries may be given.

As an examination protocol, we use 64×0.6 mm acquisition, with 1 mm reconstruction, and the optimization of the presence of contrast in the carotid arteries is performed through bolus tests.

Post-processing consists of 3D MIP, 3D VRT and 3D MPR reconstructions.

Thoracoabdominal CT Angiography

This is used for visualizing the pathology of the ascending aorta, of the aortic arch and the descending aorta, of the thoracic and abdominal portions and of the branches emerging from these, as well as for studying pulmonary arteries for pulmonary thromboembolism or for malformative pathology.

As a scanning protocol, we use 64×0.6 mm scanning, with a variable rotation of the tube, according to the pathology, with 1 mm reconstructions; in order to find SDC presence in the arterial circulation, we use bolus tests.

Peripheral CT Angiography

This is used for discerning arterial pathology at the level of the lower and upper limbs. It shows the presence of arterial stenoses in obliterating arteriopathy, allows the evaluation of the venous or synthetic graphs used in bypass interventions, as well as the evaluation of the patency of the stents placed at different levels.

It may identify arthero-venous fistulas as well as malformative lesions at the level of the limbs' circulatory bed.

CT Coronary Angiography

CT coronary angiography currently represents one of the most important non-invasive diagnostic possibilities offered by computed tomography.

In our clinic, over the course of 1 year, over 500 patients were investigated with the purpose of detecting coronary affections, as well as patients with stents and aorto-coronary bypasses with the purpose of determining their patency.

In our CT coronary angiography examining protocol, we use native scanning in order to detect and quantify coronary calcifications (Agatston calcium score), followed, if the calcifications are not severe, by the proper angiographic phase. Optimization of the presence of the contrast substance at the coronary level is done through bolus tests, with the quantity of contrast substance administered depending on the scanned surface. In order to reduce the dose administered to the patient, we use CareDOSE 4D and modulated ECG acquisition with pulsed ECG.

The images are acquired in the format 64×0.6 mm, with the reconstruction of axial images at 0.75 mm. Post-processing consists of 3D VRT, 3D MPR and 3D MIP reconstructions. The software of the post-processing unit allows the quantification of the degree of stenosis, expressing the result either as an area or percentage.

Timisoara, Romania

Gratian Dragoslav Miclaus

Contents

1	Cerebral Angiography	1
1.1	Normal Cerebral Angiography	2
1.2	Arteriovenous Malformation at the Level of Pars Precentralis Dextra	4
1.3	Arteria Basilaris Aneurysm at the Level of Pars Proximalis	6
1.4	Arteria Cerebri Media Sinistra Aneurysm	9
1.5	Arteria Cerebri Media Dextra Aneurysm	11
1.6	Aneurysm of Arteria Pericallosa	13
1.7	Aneurysm of Persistent Primitive Hypoglossal Artery	15
1.8	Aneurysm of Arteria Communicans Posterior	17
2	Carotid Angiography	19
2.1	Normal Carotid Angiography	20
2.2	Anomalous Origin of Arteria Carotis Communis	22
2.3	Calcified Atheromatous Plaques at the Level of Arteria Carotis	24
2.4	Carotid Angiography: Nonobstructive Calcified Atheromatous Plaques	26
2.5	Carotid Angiography: Calcified Atheromatous Lesions and Kinking of Arteria Carotis Interna Sinistra	29
2.6	Short Lesion, Moderate Stenosis of Arteria Carotis Internra Sinistra	32
2.7	Carotid Angiography Emphasising a Severe Stenotic Lesion (Subocclusive) at the Level of Arteria Carotis Internra Dextra	35
2.8	Carotid Angiography Emphasising a Subocclusive Lesion at the Level of the Emerging Arteria Carotis Internra Sinistra	38
2.9	Carotid Angiography Ostial Occlusive Lesion at the Level of Arteria Carotis Interna Sinistra	40
2.10	Carotid Angiography: Complete Occlusion of the Arteria Carotis Interna Dextra	43

2.11	Carotid Angiography: Severe Stenotic Lesion at the Level of the Pars Proximalis of Arteria Subclavia Sinistra	45
2.12	Carotid Angiography: Stent Occlusion at the Level of Arteria Subclavia Sinistra.....	47
3	Thoracic Angiography.....	49
3.1	Aneurysm of the Aorta Ascendens	50
3.2	Supravalvular Aortic Stenosis.....	53
3.3	Aneurysm of the Aorta Ascendens: Isthmic Stenosis	56
3.4	Aneurysm of the Arcus Aortae	58
3.5	Aneurysm of the Aorta Ascendens: Chronic Dissection of the Aorta	60
3.6	Post-traumatic Aneurysm of the Aorta Descendens	63
3.7	Gigantic Aneurysm at the Level of the Aorta Descendens	65
3.8	Chronic Dissection of the Aorta Descendens	68
3.9	Stenosis of A. Pulmonalis Dextra	71
3.10	Aneurysm and Dissection of the Aorta ascendens After Valvular Aortic Replacement.....	73
3.11	Pulmonary Thromboembolism	75
3.12	Right Partially Anomalous Venous Drainage	77
3.13	Partially Aberrant Venous Drainage	79
3.14	Interrupted Arcus Aortae.....	82
4	Coronary Angiography	85
4.1	Normal Arteriae Coronariae	86
4.2	Abnormal Emergence of the R. Circumflexus	89
4.3	Abnormal Emergence of the A. Coronaria Dextra Placed on the Posterior Aortic Wall	91
4.4	Emergence Through Separate Ostium of the Three A. Coronariae	93
4.5	Abnormal A. Coronaria dextra emergence from the Truncus A. Pulmonalis	95
4.6	Coronary and Aortopulmonary Fistulas	98
4.7	Coronary Calcification	101
4.8	Monovascular Coronary Disease: A. Coronaria Dextra Occlusion.....	103
4.9	Occlusive Lesion at the Middle Segment of the R. Interventricularis Anterior – Collateral Circulation A. Coronaria Dextra – R. Interventricularis Anterior	105
4.10	Bivascular Coronary Disease	107
4.11	Trivascular Coronary Disease	110
4.12	Aneurysm of the Left Ventricle and R. Interventricularis Anterior Occlusion	113
4.13	Monovascular Coronary Disease Patent Stent in the Middle Segment of R. Interventricularis Anterior ..	116

4.14	Restenosis at Stent Level.....	119
4.15	Occlusion of R. Interventricularis Anterior	122
4.16	Coronary Bypass Evaluation.....	124
4.17	Fallot Tetralogy.....	126
4.18	Fallot Tetralogy in an Adult Patient	128
5	Abdominal Angiography.....	131
5.1	Normal Abdominal Angiography	132
5.2	Aneurysm of Truncus Coeliacus and Stenotic Lesion of A. Hepatica Communis.....	135
5.3	Left Renal Arteriovenous Fistula	137
5.4	Aorta Abdominalis Aneurysm with Aortoduodenal Fistula	140
5.5	Operated Aorta Abdominalis Aneurysm: Post-operative Complications.....	143
5.6	Stenosis of A. Renalis Sinistra	145
5.7	Right A. Renalis Dextra Occlusion Collateral Circulation for Renal Parenchyma	148
5.8	Dissection of Aorta Abdominalis	151
5.9	Separate Emergence of A. Hepatica Communis and A. Splenica Additional Polar Left Superior A. Renalis Sinistra.....	153
5.10	Multiple Aneurysms of A. Splenica Associated with Aneurysm of A. Renalis Dexter	156
6	Peripheral Angiography	159
6.1	Normal Peripheral Angiography.....	160
6.2	Leriche Syndrome.....	165
6.3	Leriche Syndrome Axillofemoral Bypass	167
6.4	Leriche Syndrome Aortobifemoral and Femoropopliteal Graft	170
6.5	Aortobifemoral Graft and Aneurysms at the Level of Anastomosis	174
6.6	Right Arm Occlusion of the Aortobifemoral Graft	177
6.7	Right Femoro-fibular Graft: Occlusion of the Left Lower Limb Arteries.....	179
6.8	Iliac and Femoral Stents: In-Stent Restenosis.....	182
6.9	Iliac and Femoral Stents: Occluded Iliac Stents	185
6.10	Autoimmune Vasculitis.....	187
6.11	Tumour of the Leg.....	190
6.12	Giant Tumour of the Thigh.....	192
6.13	CT Angiography of the Right Upper Limb: Occlusion of the Arteria Radialis Dextra	194
6.14	Arteriovenous Malformation in Deltoid Region.....	196
6.15	CTA Run-Off: Incidental Finding	198

Contents

1.1	Normal Cerebral Angiography	2
1.2	Arteriovenous Malformation at the Level of Pars Precentralis Dextra	4
1.3	Arteria Basilaris Aneurysm at the Level of Pars Proximalis	6
1.4	Arteria Cerebri Media Sinistra Aneurysm	9
1.5	Arteria Cerebri Media Dextra Aneurysm	11
1.6	Aneurysm of Arteria Pericallosa	13
1.7	Aneurysm of Persistent Primitive Hypoglossal Artery	15
1.8	Aneurysm of Arteria Communicans Posterior	17

1.1 Normal Cerebral Angiography

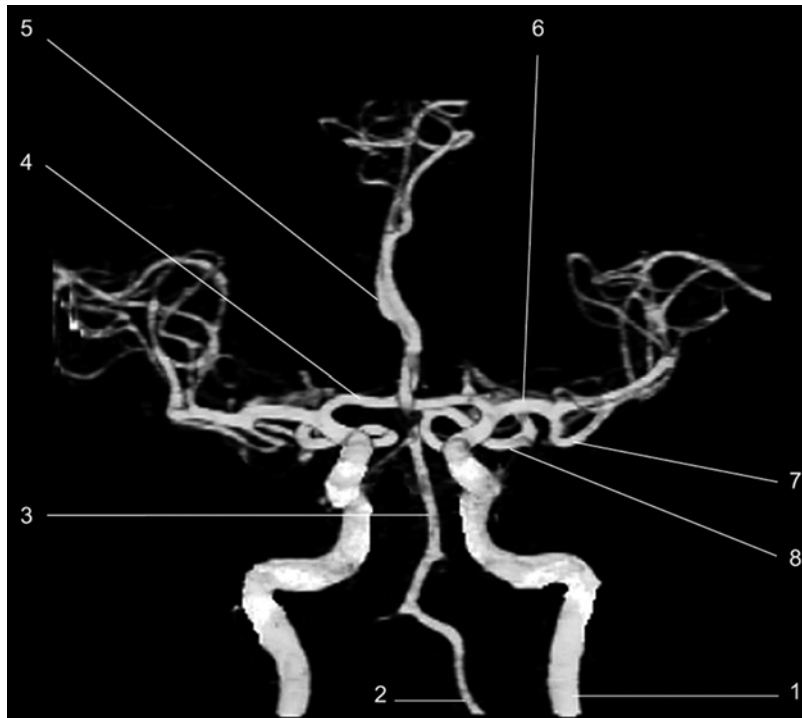


Fig. 1.1 Neuro DSA – VRT
1. A. carotis interna
2. A. vertebralis
3. A. basilaris
4. A. cerebri anterior
5. A. cerebri anterior – segmentum A2
6. A. cerebri media – segmentum M1
7. A. cerebri media – segmentum M2
8. A. cerebri posterior



Fig. 1.2 Neuro DSA – MIP



Fig. 1.3 Neuro DSA – VRT

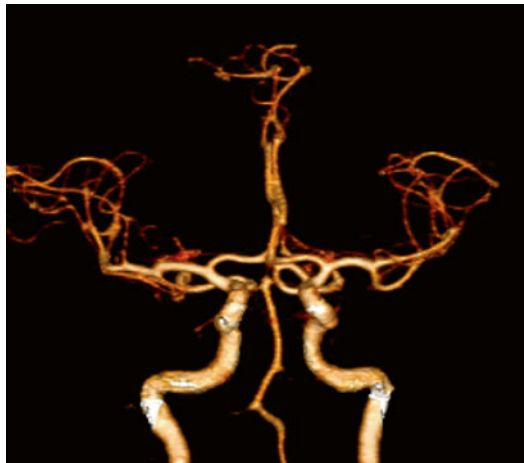


Fig. 1.4 Neuro DSA – VRT colour



Fig. 1.6 Cerebral angiography 3D VRT reconstruction



Fig. 1.5 Neuro DSA – VRT colour

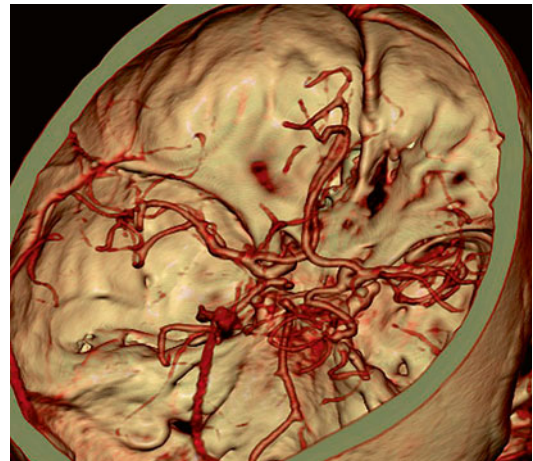


Fig. 1.7 Cerebral angiography 3D VRT reconstruction

1.2 Arteriovenous Malformation at the Level of Pars Precentralis Dextra

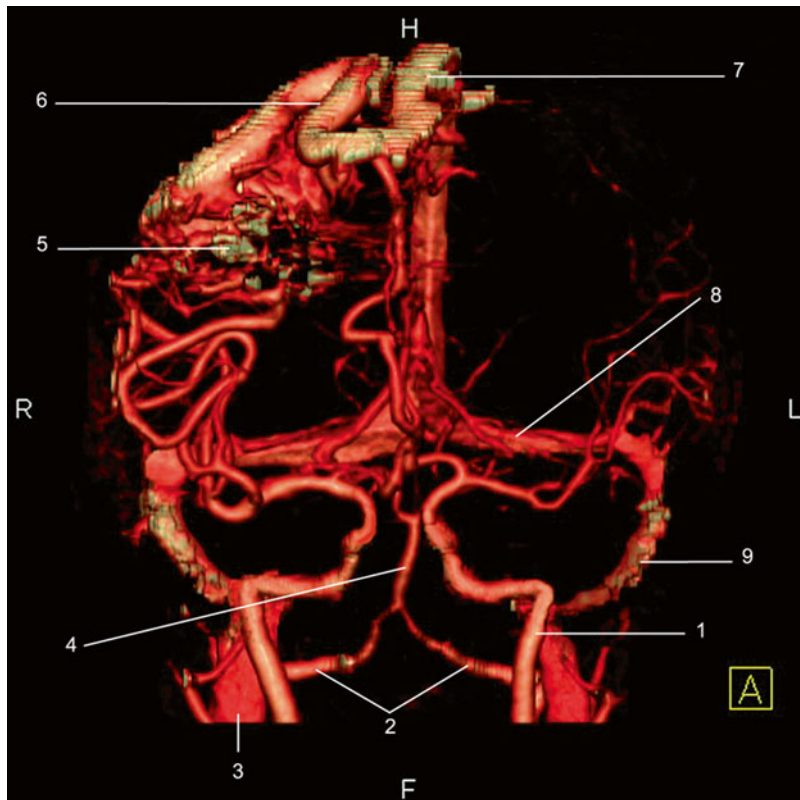


Fig. 1.8 Arteriovenous malformation at the level of pars precentralis dextra

1. A. carotis interna
2. A. vertebralis
3. V. jugularis interna
4. A. basilaris
5. Partially embolised arteriovenous malformation
6. Drainage vein
7. Sinus sagittalis superior
8. Sinus transversalis
9. Sinus sigmoideus

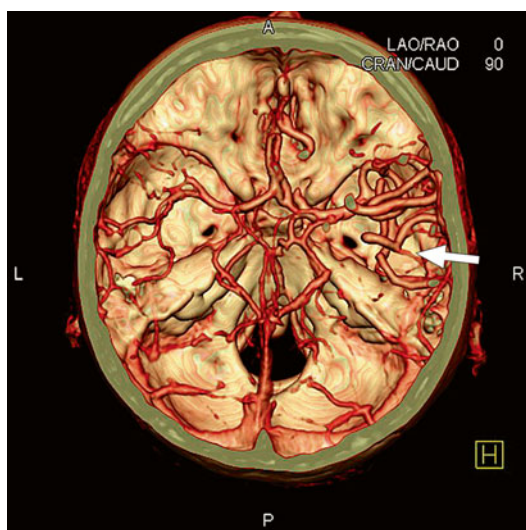


Fig. 1.9 Cerebral angiography in the case of an arteriovenous malformation (arrow) (a. cerebra media) with accentuation of the vascularisation at the level of a. cerebra media (3D axial reconstruction)

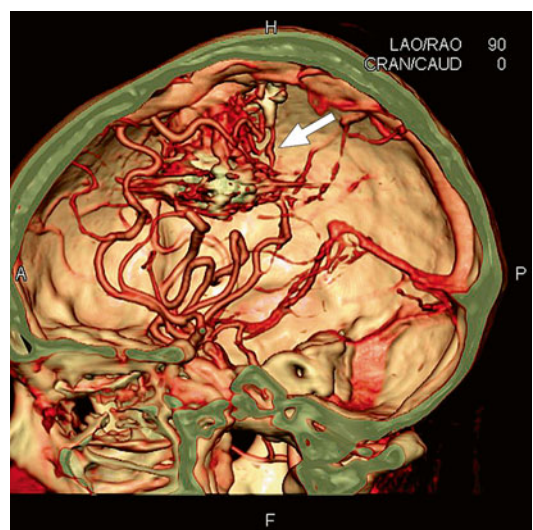


Fig. 1.10 Cerebral angiography of a partially embolised arteriovenous malformation (arrow)

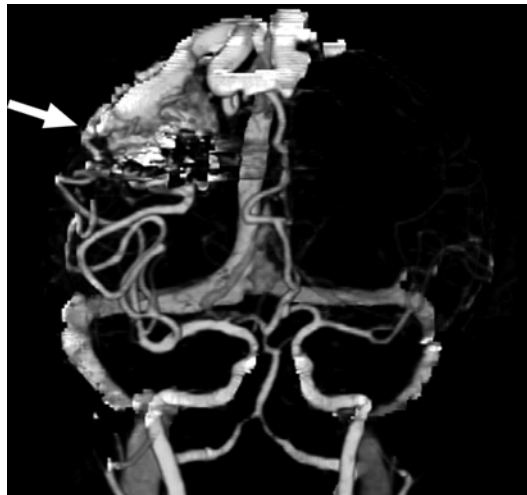


Fig. 1.11 Neuro DSA 3D MIP reconstruction, anterior plan. The *arrow* indicates the arteriovenous malformation

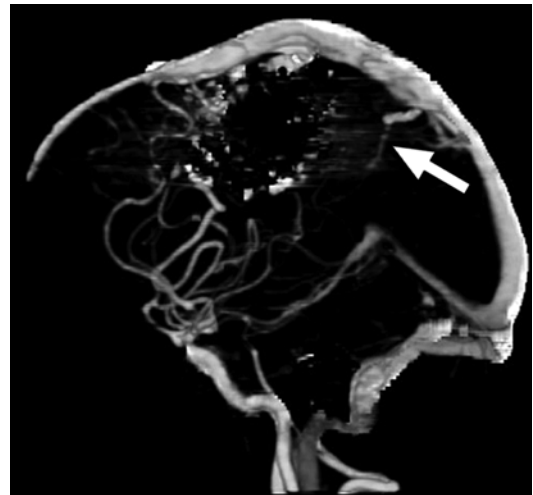


Fig. 1.13 Neuro DSA 3D MIP reconstruction, lateral right plan. The *arrow* indicates the arteriovenous malformation



Fig. 1.12 Neuro DSA 3D MIP reconstruction, posterior view

1.3 Arteria Basilaris Aneurysm at the Level of Pars Proximalis

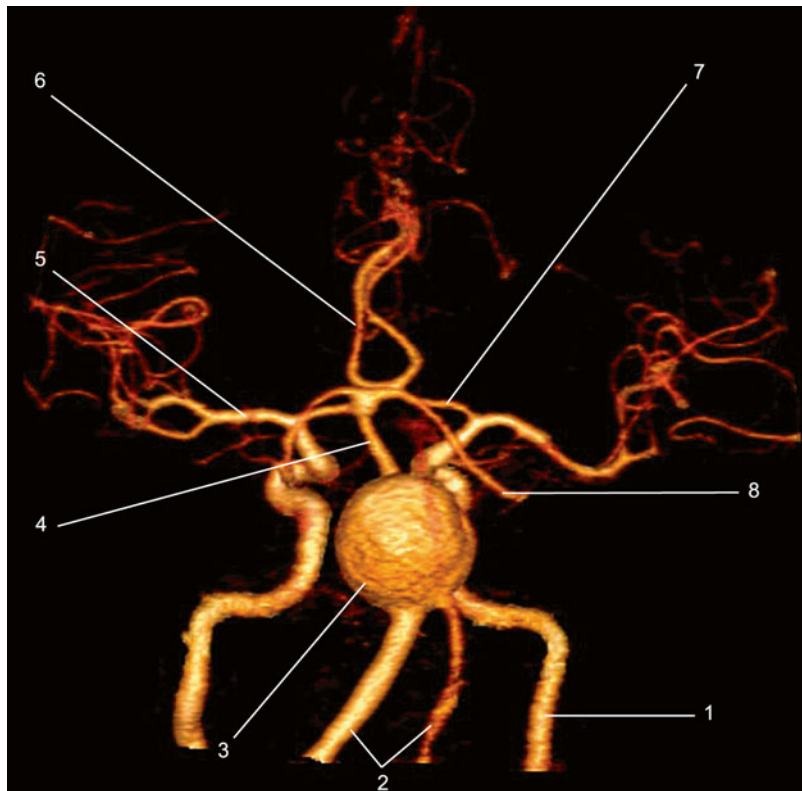


Fig. 1.14 Neuro DSA 3D VRT colour reconstruction
1. A. carotis interna
2. A. vertebralis
3. Giant aneurysm
4. A. basilaris
5. A. cerebri media – segmentum M1
6. A. cerebri anterior – segmentum A2
7. A. cerebri anterior – segmentum A1
8. A. cerebri posterior



Fig. 1.15 Neuro DSA 3D MIP reconstruction



Fig. 1.16 Neuro DSA 3D MIP reconstruction

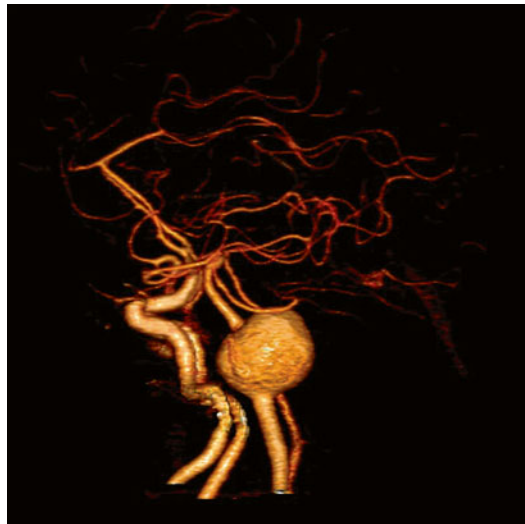


Fig. 1.17 Neuro DSA 3D VRT colour reconstruction

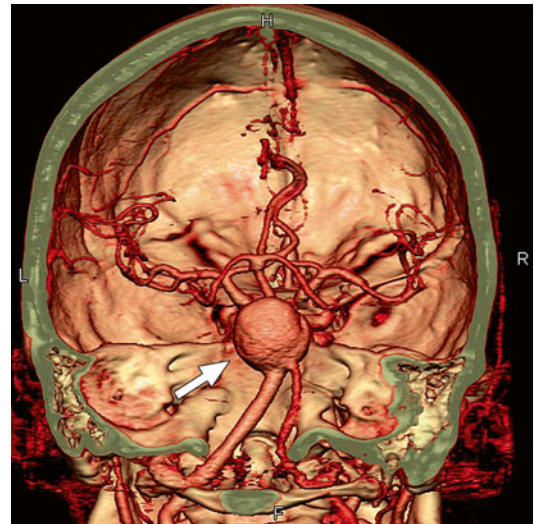


Fig. 1.19 Cerebral angiography 3D VRT reconstruction in posterior coronal plan. The *arrow* indicates the aneurysm

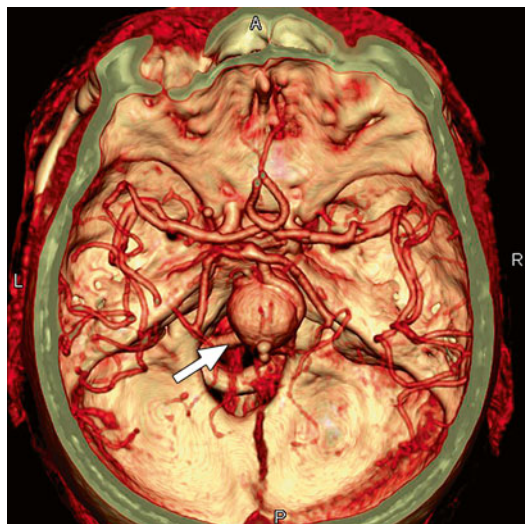


Fig. 1.18 Cerebral angiography axial 3D VRT reconstruction. The *arrow* indicates the aneurysm



Fig. 1.20 Cerebral angiography 3D VRT reconstruction, sagittal plan. The *arrow* indicates the aneurysm

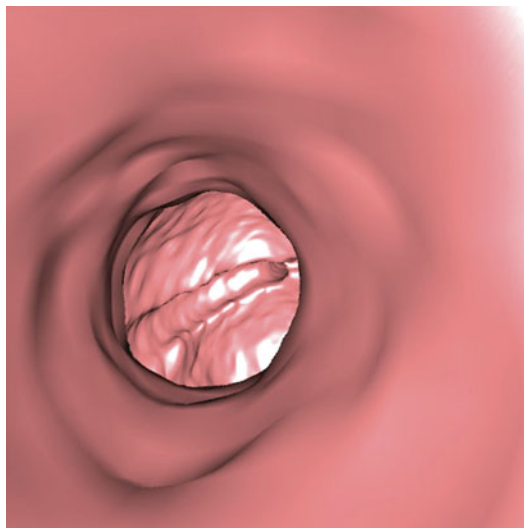


Fig. 1.21 Endoluminal navigation

1.4 Arteria Cerebri Media Sinistra Aneurysm



Fig. 1.22 Neuro DSA 3D VRT reconstruction

1. A. carotis interna
2. A. vertebralis
3. A. cerebri anterior – segmentum A1
4. A. cerebri anterior – segmentum A2
5. A. cerebri media – segmentum M1
6. A. cerebri media – segmentum M2
7. Aneurysm
8. A. basilaris



Fig. 1.23 Neuro DSA 3D VRT colour reconstruction.
The arrow indicates the aneurysm

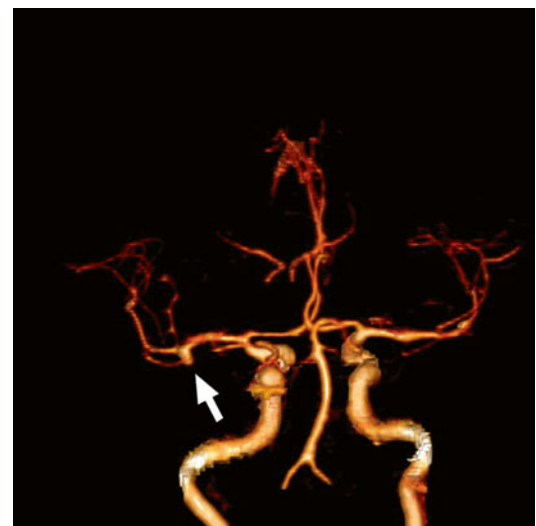


Fig. 1.24 Neuro DSA 3D VRT colour reconstruction.
The arrow indicates the aneurysm



Fig. 1.25 Neuro DSA 3D VRT reconstruction. The *arrow* indicates the aneurysm

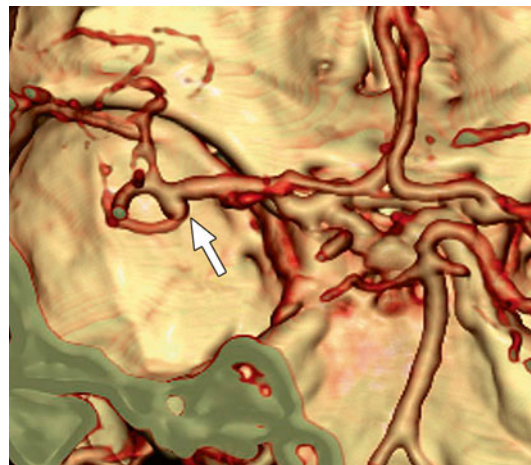


Fig. 1.28 Neuro DSA 3D VRT colour reconstruction, enlarged image. The *arrow* indicates the aneurysm

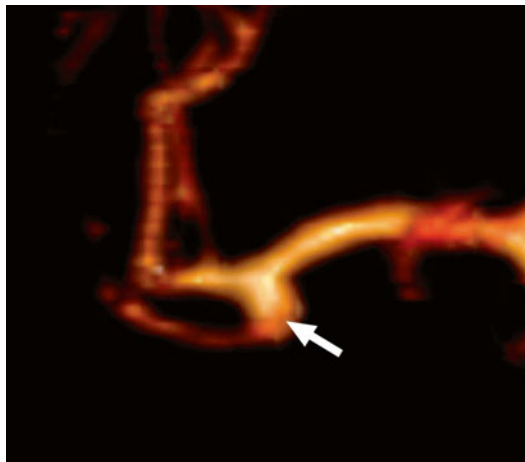


Fig. 1.26 Neuro DSA 3D VRT colour reconstruction, enlarged image. The *arrow* indicates the aneurysm

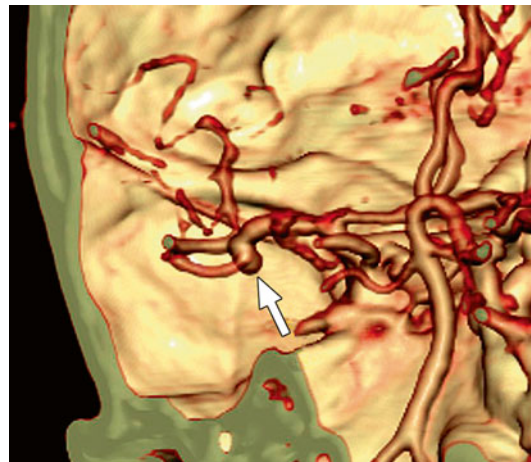


Fig. 1.29 Neuro DSA 3D VRT colour reconstruction, enlarged image. The *arrow* indicates the aneurysm

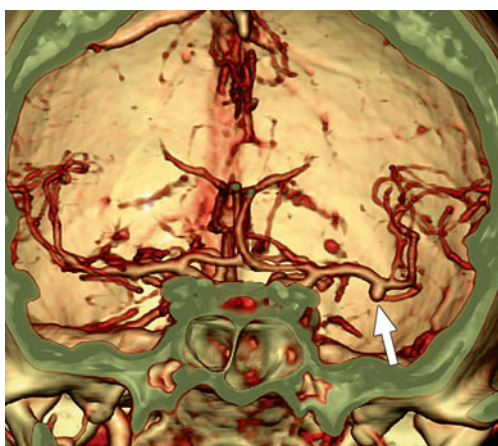


Fig. 1.27 Cerebral angiography 3D VRT colour reconstruction, enlarged image. The *arrow* indicates the aneurysm

1.5 Arteria Cerebri Media Dextra Aneurysm

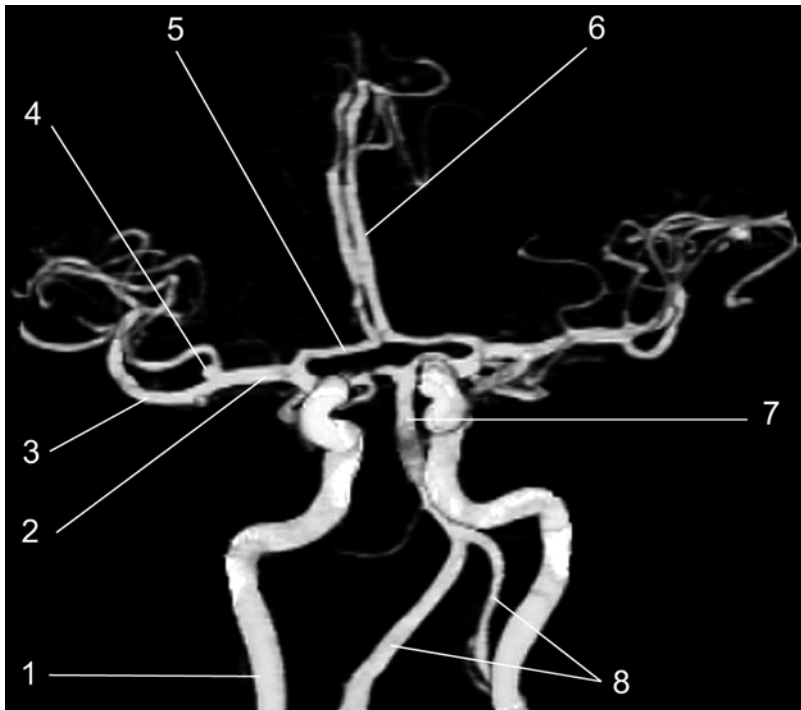


Fig. 1.30 Neuro DSA 3D

- VRT reconstruction
1. Arteria carotis interna
 2. Arteria cerebri media – segmentum M1
 3. Arteria cerebri media – segmentum M2
 4. Aneurysm
 5. Arteria cerebri anterior – segmentum A1
 6. Arteria cerebri anterior – segmentum A2
 7. Arteria basilaris
 8. Arteria vertebralis

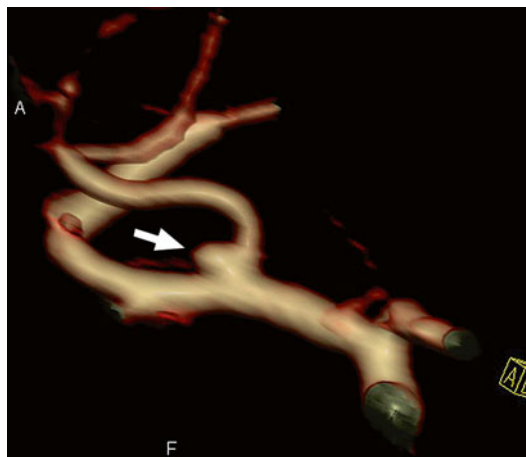


Fig. 1.31 Neuro DSA 3D VRT colour reconstruction, enlarged image. The arrow indicates the aneurysm



Fig. 1.32 Neuro DSA 3D VRT colour reconstruction. The arrow indicates the aneurysm



Fig. 1.33 Neuro DSA 3D VRT colour reconstruction. The arrow indicates the aneurysm



Fig. 1.35 Cerebral angiography, 3D VRT colour reconstruction, intraventricular catheter for external drainage. The arrow indicates the aneurysm

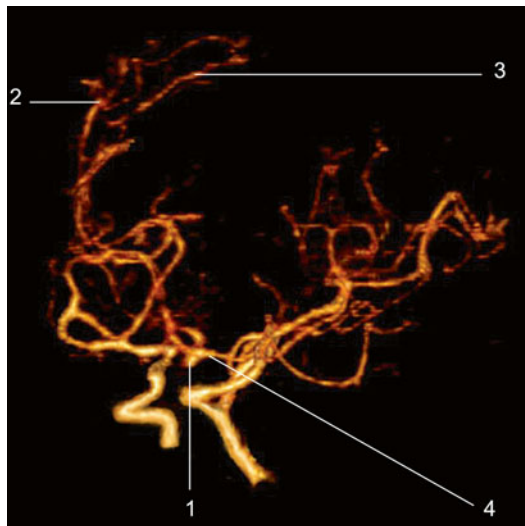


Fig. 1.34 Arteria communicans anterior aneurysm
1. Aneurysm
2. Arteria callosomarginalis
3. Arteria pericallosa
4. Arteria cerebri anterior – segmentum (A1)

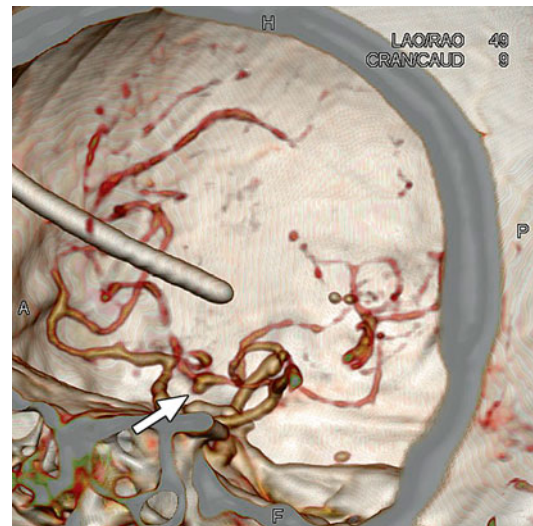


Fig. 1.36 Cerebral angiography, 3D VRT colour reconstruction, intraventricular catheter for external drainage. The arrow indicates the aneurysm

1.6 Aneurysm of Arteria Pericallosa

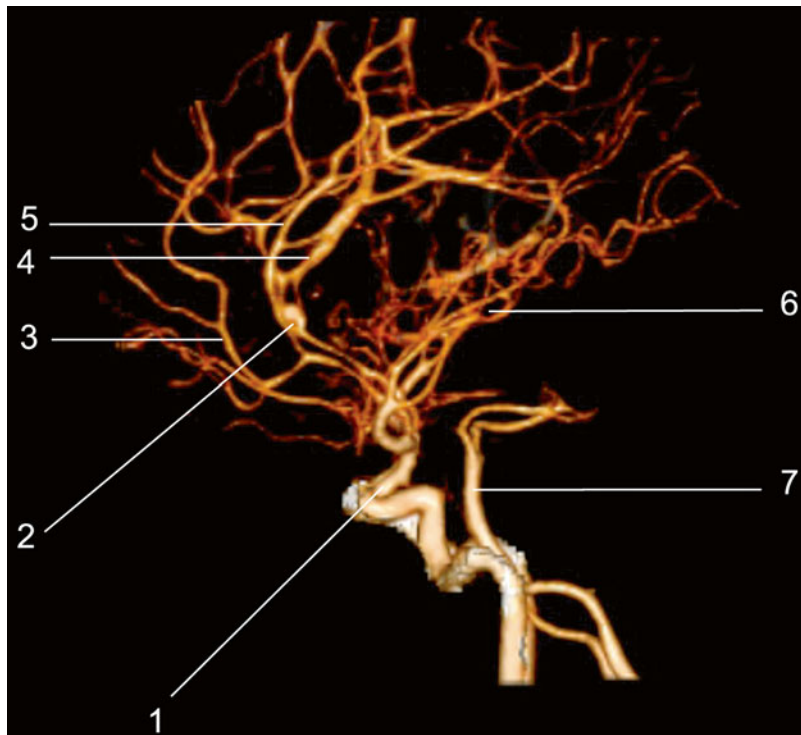


Fig. 1.37 Neuro DSA, 3D VRT colour reconstruction
1. Arteria carotis interna
2. Aneurysm
3. Arteria frontobasalis medialis
4. Arteria pericallosa
5. Arteria callosomarginalis
6. Arteria cerebri media
7. Arteria basilaris

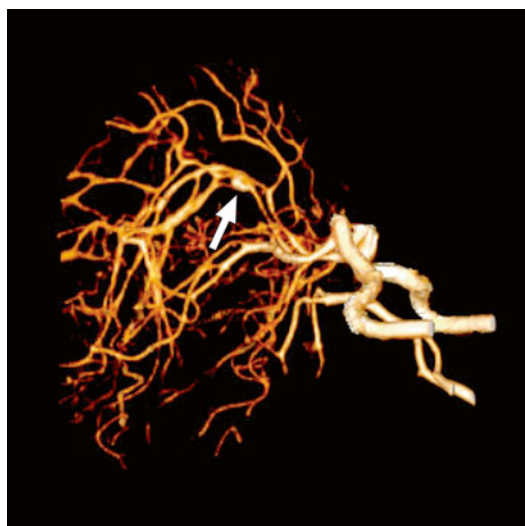


Fig. 1.38 Neuro DSA, 3D VRT colour reconstruction. The arrow indicates the aneurysm

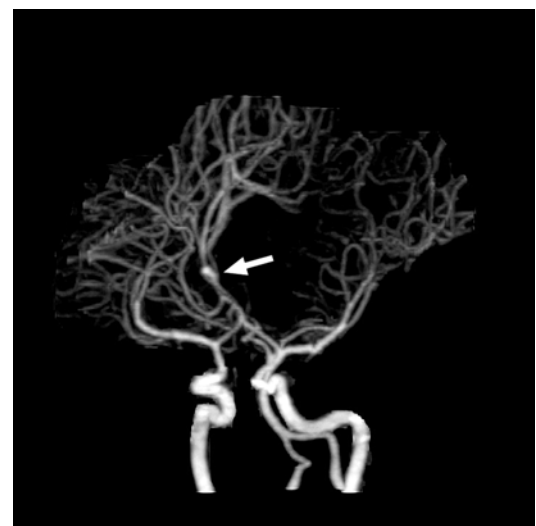


Fig. 1.39 Neuro DSA, 3D MIP reconstruction. The arrow indicates the aneurysm

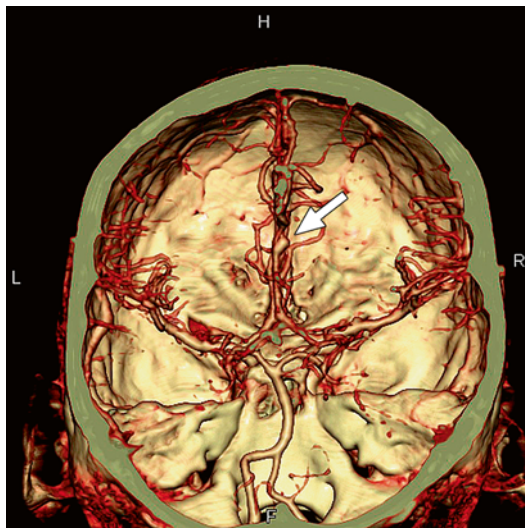


Fig. 1.40 Cerebral angiography 3D VRT colour reconstruction, aneurysm (arrow) of arteria pericallosa

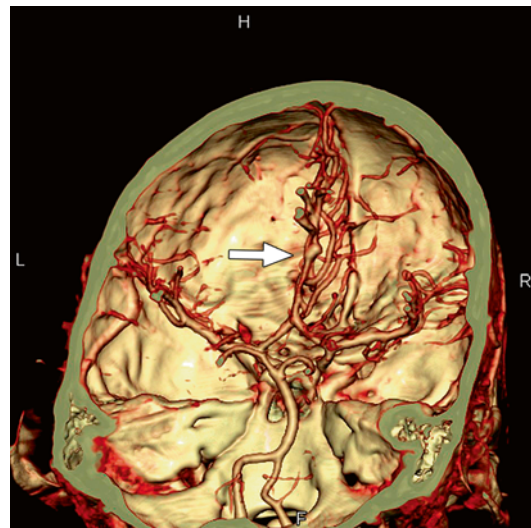


Fig. 1.42 Cerebral angiography 3D VRT colour reconstruction, aneurysm (arrow) of arteria pericallosa

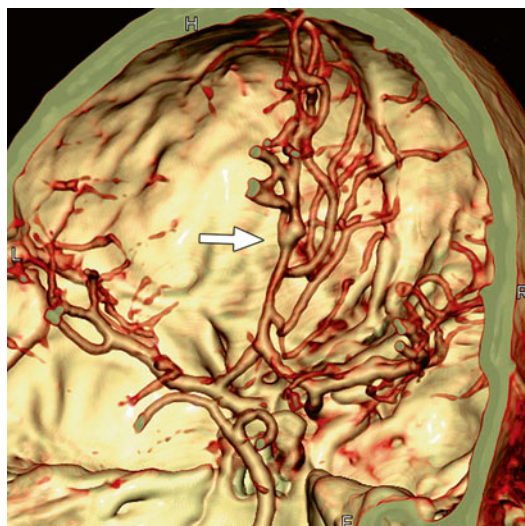


Fig. 1.41 Cerebral angiography 3D VRT colour reconstruction, aneurysm (arrow) of arteria pericallosa

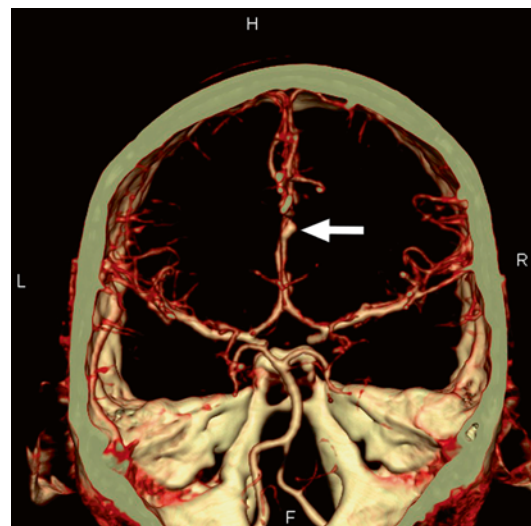


Fig. 1.43 Cerebral angiography 3D VRT colour reconstruction, aneurysm (arrow) of arteria pericallosa

1.7 Aneurysm of Persistent Primitive Hypoglossal Artery

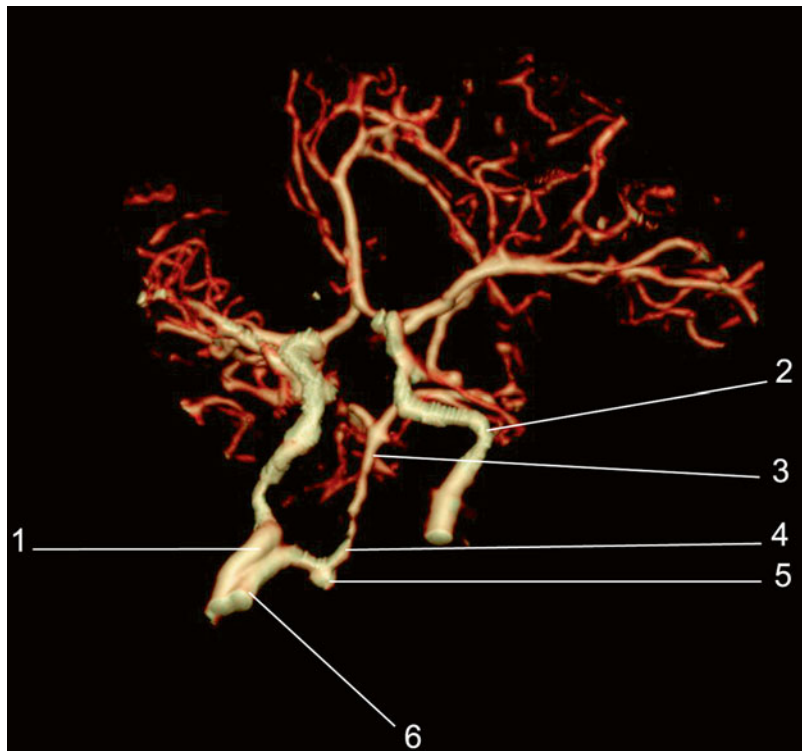


Fig. 1.44 Arteria hypoglossi primitiva persistent aneurysm
 1. Arteria carotis interna dextra
 2. Arteria carotis interna sinistra
 3. Arteria basilaris
 4. Persistent arteria hypoglossi primitiva
 5. Aneurysm
 6. Doubled internal carotid artery which is tributary to the posterior circulation



Fig. 1.45 Neuro DSA 3D MIP reconstruction with the visualisation of the aneurysm. The *full arrow* indicates aneurysm

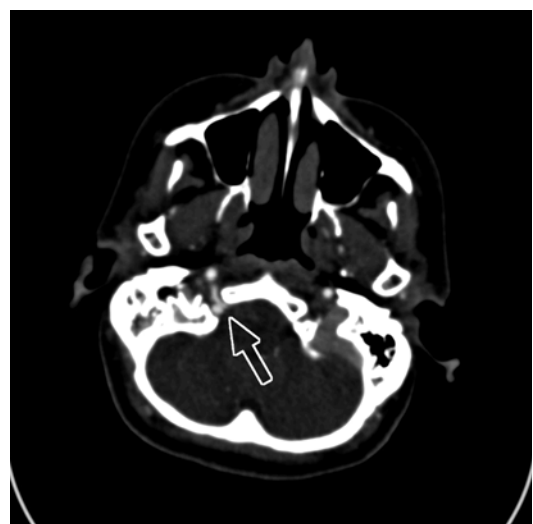


Fig. 1.46 Axial image with the visualisation of the persistent a. hypoglossi primitiva in the canalis nervi hypoglossi and presence of the aneurysm. The *arrow with contour* indicates a. hypoglossi + aneurysm

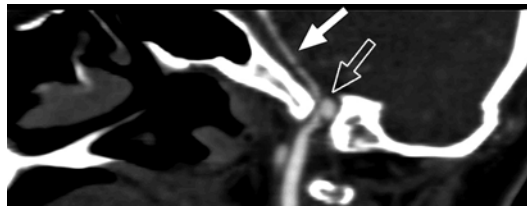


Fig. 1.47 The trajectory of a. hypoglossi in the canalis nervi hypoglossi with the visualisation of the aneurysm
Full arrow=arteria basilaris
Arrow with contour=aneurysm

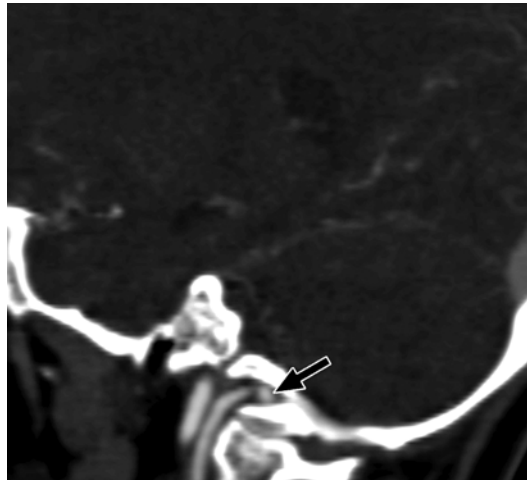


Fig. 1.48 The trajectory of a. hypoglossi in the canalis nervi hypoglossi with visualisation of the aneurysm
Arrow with contour=aneurysm



Fig. 1.49 The trajectory of a. hypoglossi in the canalis nervi hypoglossi with the visualisation of the aneurysm
Arrow with contour=aneurysm

1.8 Aneurysm of Arteria Communicans Posterior

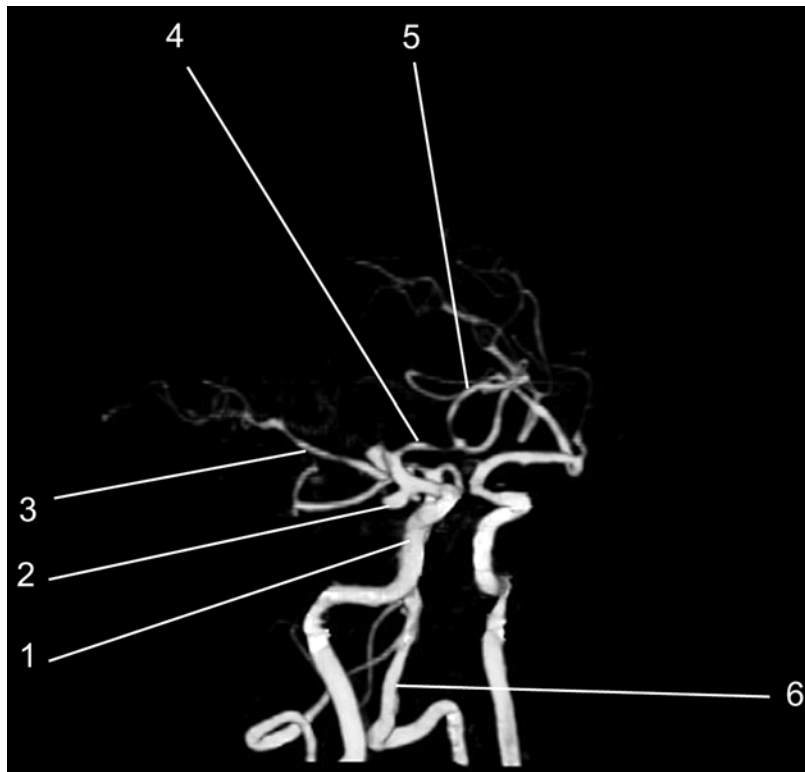


Fig. 1.50 Neuro DSA, 3D VRT reconstruction
1. A. carotis interna
2. Aneurysm
3. A. cerebri media
4. A. cerebri anterior – segmentum A1
5. A. cerebri anterior – segmentum A2
6. A. vertebralis



Fig. 1.51 Neuro DSA, 3D VRT reconstruction. The arrow indicates the aneurysm



Fig. 1.52 Neuro DSA, 3D VRT reconstruction. The arrow indicates the aneurysm

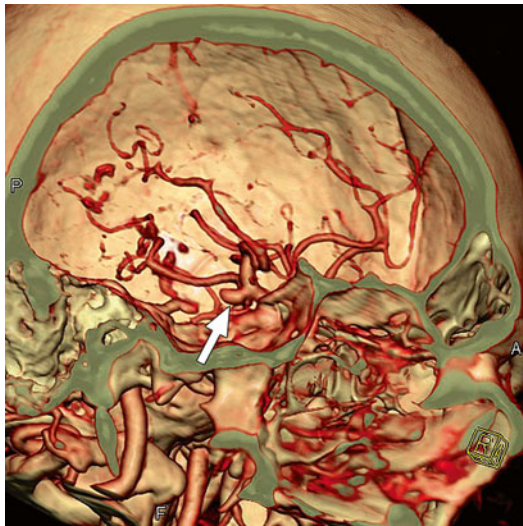


Fig. 1.53 Cerebral angiography 3D VRT colour reconstruction. The *arrow* indicates the aneurysm

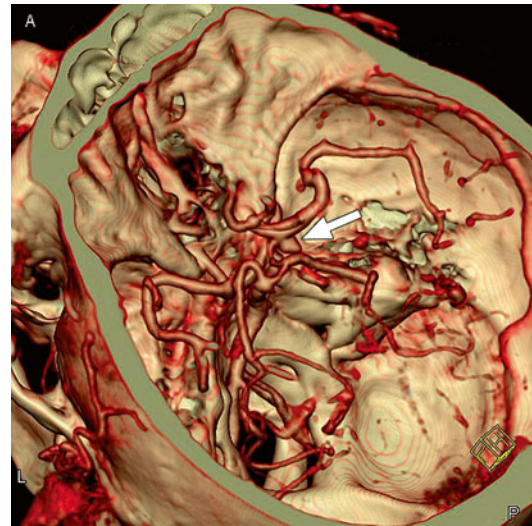


Fig. 1.55 Cerebral angiography 3D VRT colour reconstruction. The *arrow* indicates the aneurysm

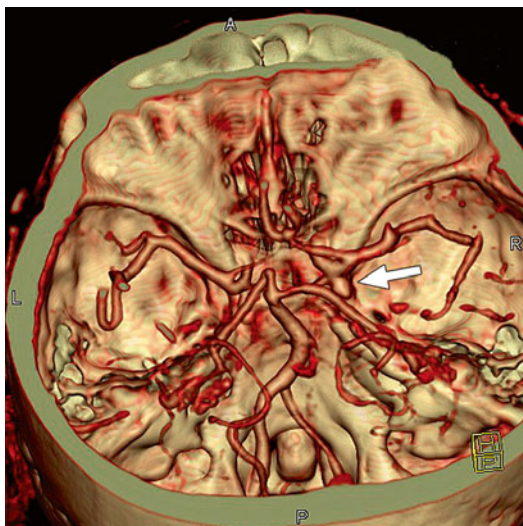


Fig. 1.54 Cerebral angiography 3D VRT colour reconstruction. The *arrow* indicates the aneurysm

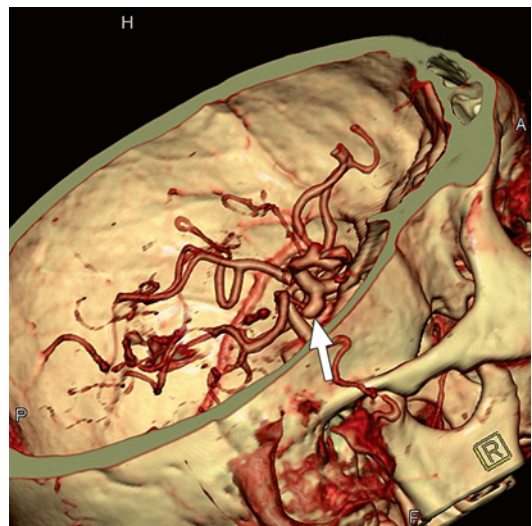


Fig. 1.56 Cerebral angiography 3D VRT colour reconstruction. The *arrow* indicates the aneurysm

Contents

2.1	Normal Carotid Angiography	20
2.2	Anomalous Origin of Arteria Carotis Communis	22
2.3	Calcified Atheromatous Plaques at the Level of Arteria Carotis	24
2.4	Carotid Angiography: Nonobstructive Calcified Atheromatous Plaques	26
2.5	Carotid Angiography: Calcified Atheromatous Lesions and Kinking of Arteria Carotis Interna Sinistra	29
2.6	Short Lesion, Moderate Stenosis of Arteria Carotis Interna Sinistra	32
2.7	Carotid Angiography Emphasising a Severe Stenotic Lesion (Subocclusive) at the Level of Arteria Carotis Interna Dextra	35
2.8	Carotid Angiography Emphasising a Subocclusive Lesion at the Level of the Emerging Arteria Carotis Interna Sinistra	38
2.9	Carotid Angiography Ostial Occlusive Lesion at the Level of Arteria Carotis Interna Sinistra	40
2.10	Carotid Angiography: Complete Occlusion of the Arteria Carotis Interna Dextra	43
2.11	Carotid Angiography: Severe Stenotic Lesion at the Level of the Pars Proximalis of Arteria Subclavia Sinistra	45
2.12	Carotid Angiography: Stent Occlusion at the Level of Arteria Subclavia Sinistra	47

2.1 Normal Carotid Angiography

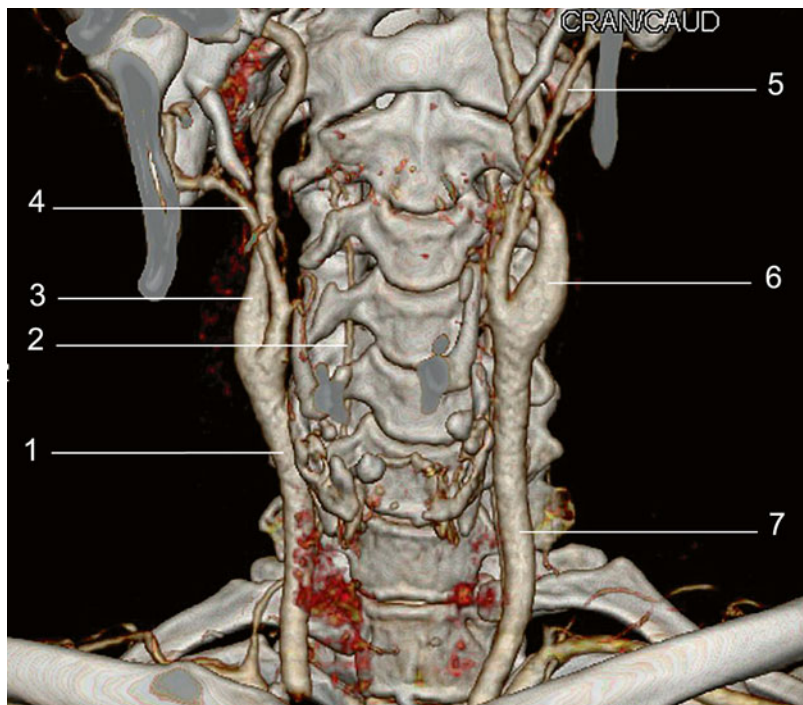


Fig. 2.1 Normal carotid angiography

1. A. carotis communis dextra
2. A. vertebralis dextra
3. A. carotis interna dextra
4. A. carotis externa dextra
5. A. carotis communis sinistra
6. A. carotis interna sinistra
7. A. carotis externa sinistra



Fig. 2.2 Normal carotid angiography 3D VRT colour reconstruction anterior coronal plane



Fig. 2.3 Normal carotid angiography 3D VRT colour reconstruction oblique anterior plane

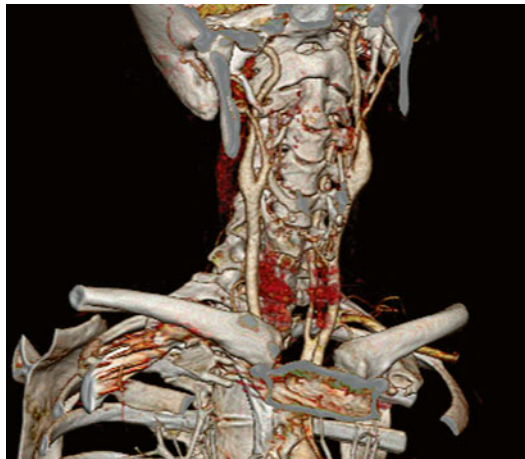


Fig. 2.4 Normal carotid angiography 3D VRT colour reconstruction left anterior oblique plane



Fig. 2.6 Normal carotid angiography 3D MIP reconstruction with visualisation of a. carotis communis dextra and a. carotis interna dextra



Fig. 2.5 Normal carotid angiography 3D MIP reconstruction with visualisation of a. carotis communis sinistra and a. carotis interna sinistra

2.2 Anomalous Origin of Arteria Carotis Communis

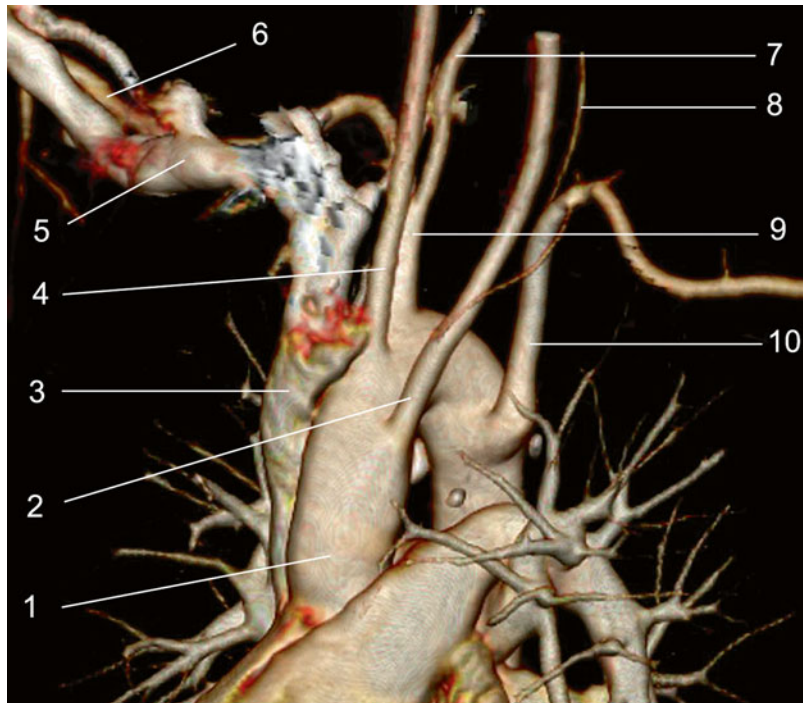


Fig. 2.7 Anomalous origin of common carotid arteries

- 1. Aorta ascendens
- 2. A. carotis communis sinistra
- 3. Vena cava superior
- 4. A. carotis communis dextra
- 5. V. subclavia dextra
- 6. A. subclavia dextra
- 7. A. vertebralis dextra
- 8. A. vertebralis sinistra
- 9. Truncus brachiocephalicus
- 10. A. subclavia sinistra

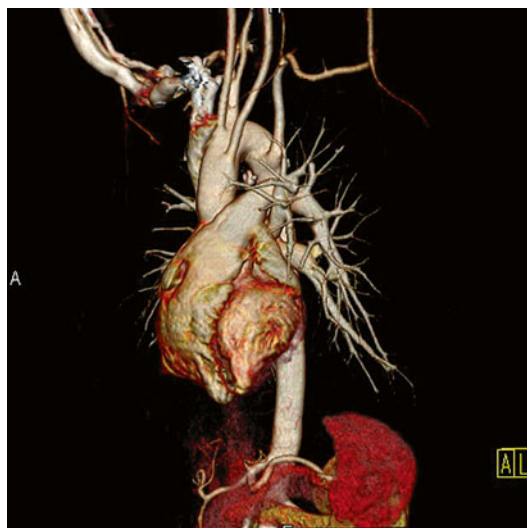


Fig. 2.8 Colour reconstruction 3D VRT

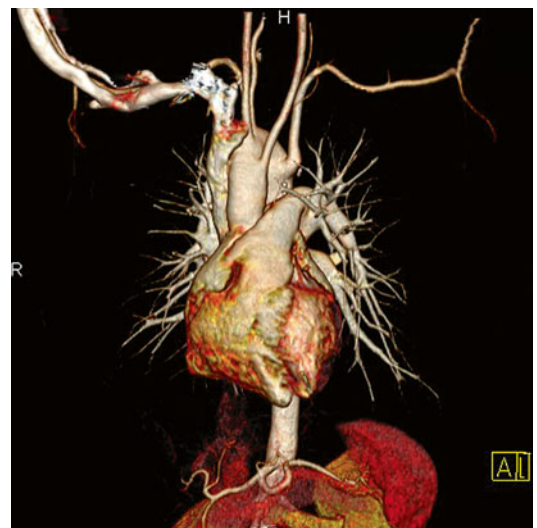


Fig. 2.9 Colour reconstruction 3D VRT



Fig. 2.10 Colour reconstruction 3D VRT, enlarged image, anterior plane



Fig. 2.12 3D VRT reconstruction, posterior plane

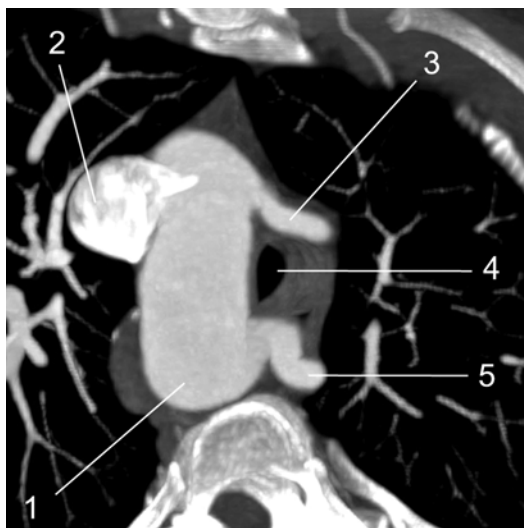


Fig. 2.11 Axial image, 3D MIP

1. Arcus aortae
2. Vena cava superior
3. A. carotis communis sinistra
4. Trachea
5. A. subclavia sinistra with retrotracheal and retro-oesophageal trajectory

2.3 Calcified Atheromatous Plaques at the Level of Arteria Carotis

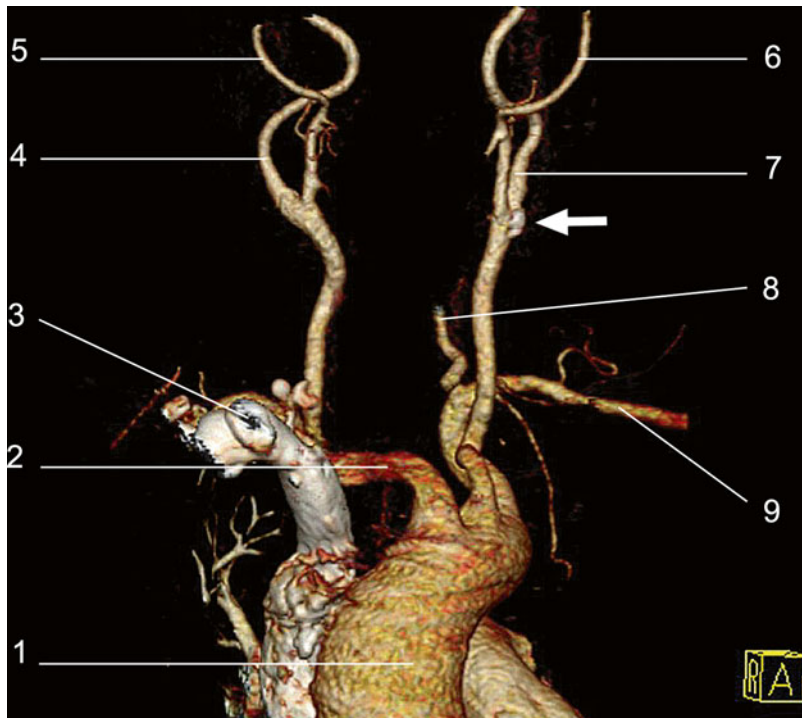


Fig. 2.13 Normal carotid angiography. The arrow indicate calcified plaques

1. Aorta ascendens
2. Truncus brachiocephalicus
3. V. cava superior
4. A. carotis communis dextra
5. A. carotis externa dextra
6. A. carotis externa sinistra
7. A. carotis interna sinistra
8. A. vertebralis sinistra
9. A. subclavia sinistra
10. A. carotis communis sinistra



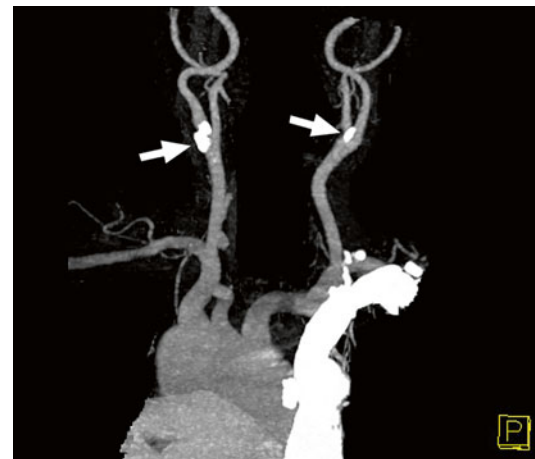
Fig. 2.14 3D VRT colour reconstruction, posterior plane. The arrow indicate calcified plaques



Fig. 2.15 3D VRT colour reconstruction, posterior plane. The arrows indicate calcified atheromatous plaques

**Fig. 2.16** 3D VRT reconstruction

The *arrows* indicate calcified atheromatous plaques placed at the level of the emerging a. carotis interna

**Fig. 2.18** 3D VRT reconstruction

The *arrows* indicate calcified atheromatous plaques placed at the level of the emerging a. carotis interna

**Fig. 2.17** 3D VRT reconstruction

The *arrows* indicate calcified atheromatous plaques placed at the level of the emerging a. carotis interna

2.4 Carotid Angiography: Nonobstructive Calcified Atheromatous Plaques

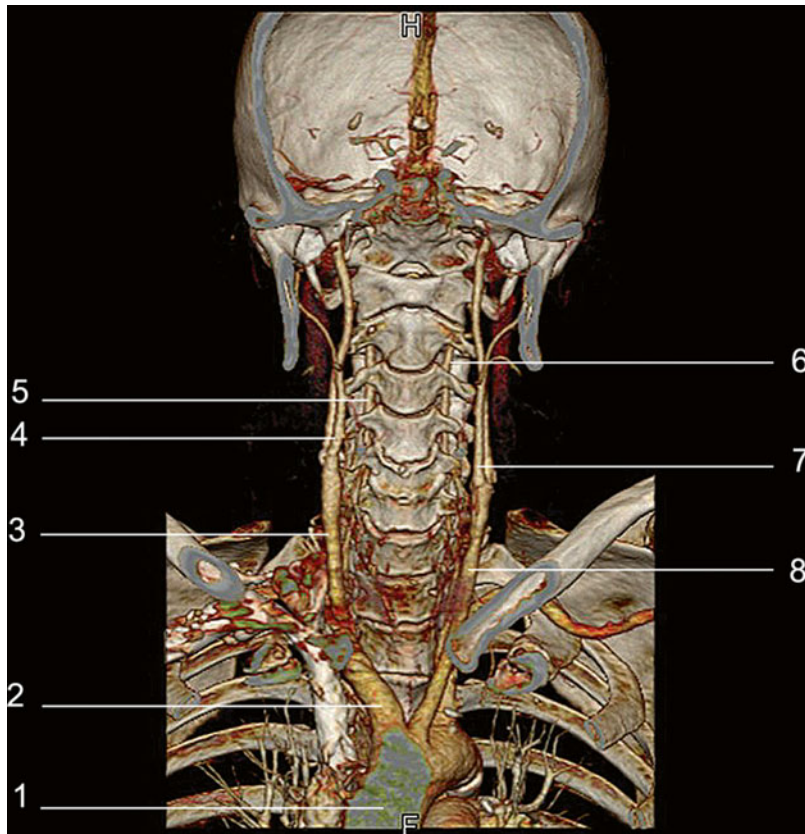


Fig. 2.19 Reconstruction 3D VRT colour, frontal plane

1. Aorta ascendens
2. Truncus brachiocephalicus
3. A. carotis communis dextra
4. A. carotis interna dextra
5. A. vertebralis dextra
6. A. carotis interna sinistra
7. A. vertebralis sinistra
8. A. carotis communis sinistra

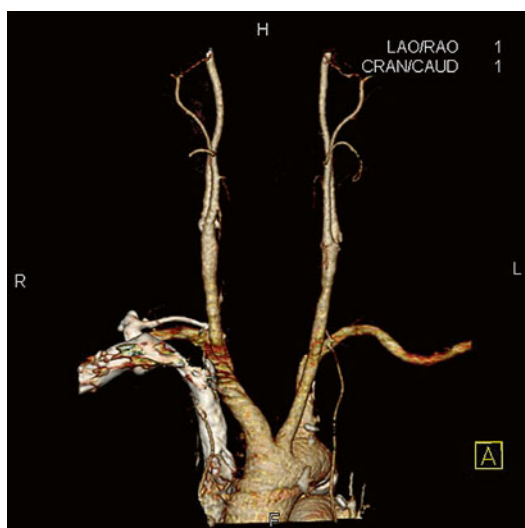


Fig. 2.20 3D VRT colour reconstruction, after removal of the bone structure

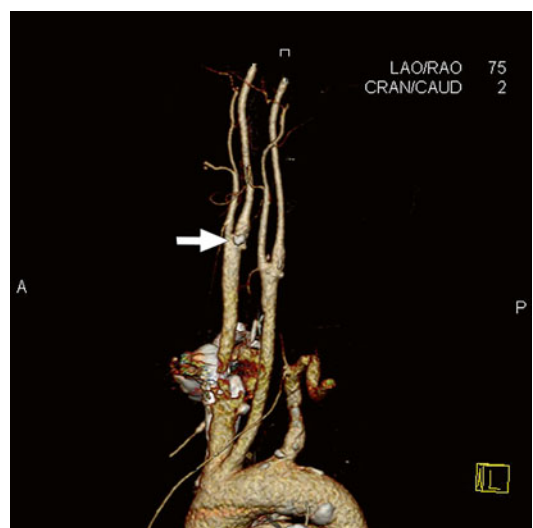


Fig. 2.21 3D VRT colour reconstruction, oblique and sagittal planes

The arrows indicate calcified atheromatous plaques

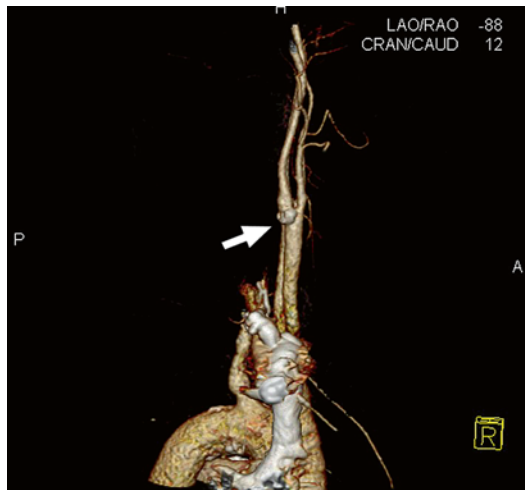


Fig. 2.22 3D VRT colour reconstruction, oblique and sagittal planes
The arrows indicate calcified atheromatous plaques



Fig. 2.24 3D MPR reconstruction
Full arrow=a. carotis communis sinistra
Arrow with contour=a. carotis interna sinistra
Tip of the arrow=atheromatous calcified plaque



Fig. 2.23 3D MIP reconstruction
Full arrow=a. carotis communis sinistra
Arrow with contour=a. carotis interna sinistra
Tip of the arrow=atheromatous calcified plaque



Fig. 2.25 3D MIP reconstruction
Full arrow=a. carotis communis dextra
Arrow with contour=a. carotis interna dextra
Tip of the arrow=atheromatous calcified plaque



Fig. 2.26 3D MPR reconstruction

Full arrow=a. carotis communis dextra

Arrow with contour=a. carotis interna dextra

Tip of the arrow=atheromatous calcified plaque

2.5 Carotid Angiography: Calcified Atheromatous Lesions and Kinking of Arteria Carotis Interna Sinistra

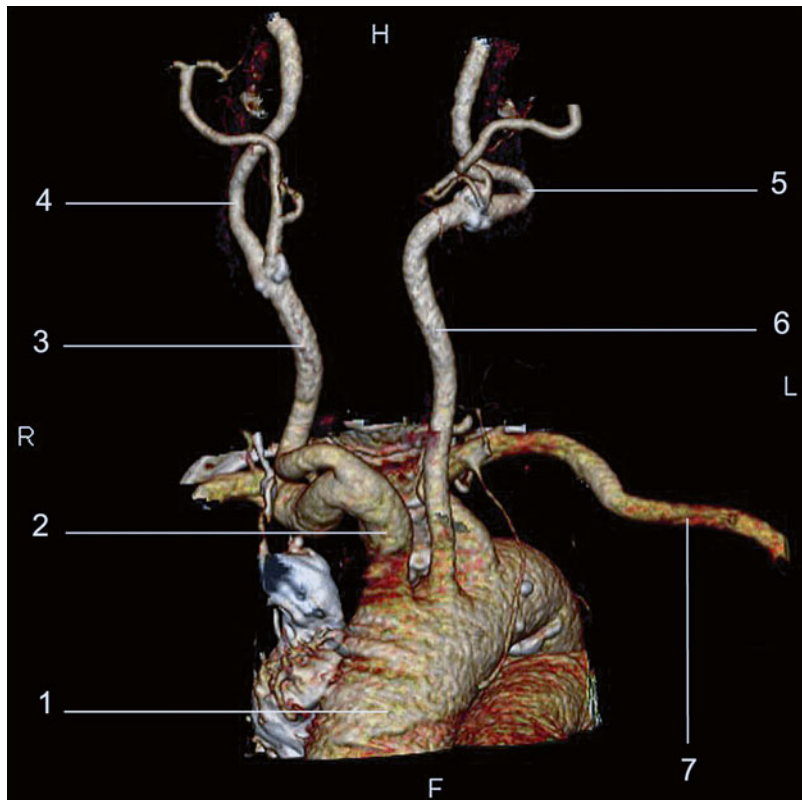


Fig. 2.27 3D VRT colour reconstruction, after removal of the bone structure

1. Aorta ascendens
2. Truncus brachiocephalicus
3. A. carotis communis dextra
4. A. carotis interna dextra
5. A. carotis interna sinistra
6. A. carotis communis sinistra
7. A. subclavia sinistra

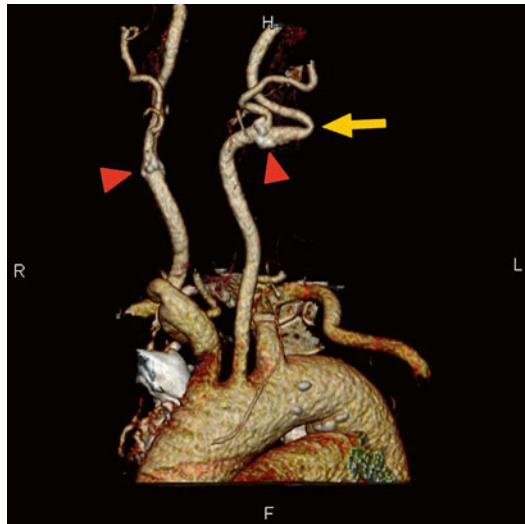


Fig. 2.28 3D VRT colour reconstruction, anterior plane
Yellow arrow=kinking of a. carotis interna sinistra
Tip of the arrow=calcified atheromatous plaques

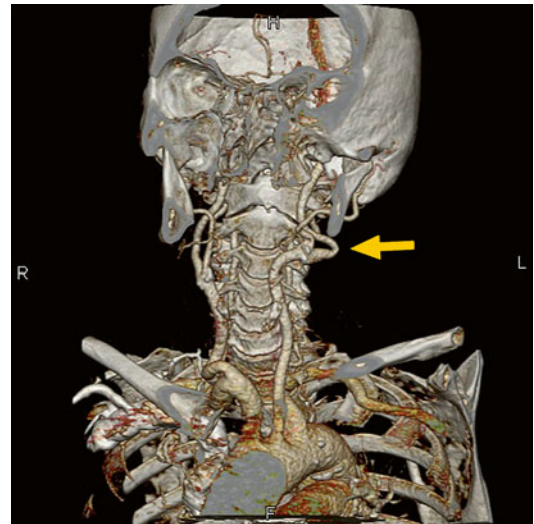


Fig. 2.30 3D VRT colour reconstruction, with bone structure, frontal plane
Yellow arrow=kinking of a. carotis interna sinistra
Tip of the arrow=calcified atheromatous plaques

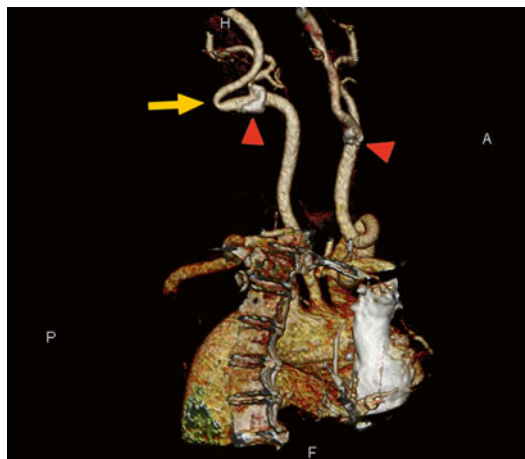
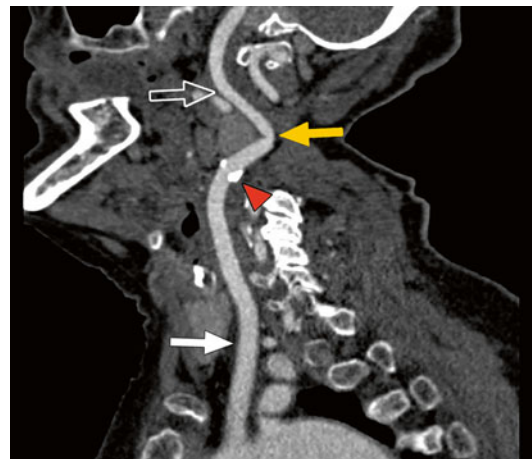


Fig. 2.29 3D VRT colour reconstruction, posterior plane
Yellow arrow=kinking of a. carotis interna sinistra
Tip of the arrow=calcified atheromatous plaques



Fig. 2.31 Reconstruction 3D MIP
Full arrow=a. carotis communis sinistra
Arrow with contour=a. carotis interna sinistra
Tip of the arrow=calcified atherosomatous plaques
Yellow arrow=kinking of a. carotis interna sinistra

**Fig. 2.32** Reconstruction 3D MIP*Full arrow=a. carotis communis sinistra**Arrow with contour=a. carotis interna sinistra**Tip of the arrow=calcified atheromatous plaques**Yellow arrow=kinking of a. carotis interna sinistra***Fig. 2.34** Reconstruction 3D MPR*Full arrow=a. carotis communis sinistra**Arrow with contour=a. carotis interna sinistra**Tip of the arrow=calcified atheromatous plaques**Yellow arrow=kinking of a. carotis interna sinistra***Fig. 2.33** Reconstruction 3D MPR*Full arrow=a. carotis communis dextra**Arrow with contour=a. carotis interna dextra**Tip of the arrow=calcified atheromatous plaques*

2.6 Short Lesion, Moderate Stenosis of Arteria Carotis Interna Sinistra

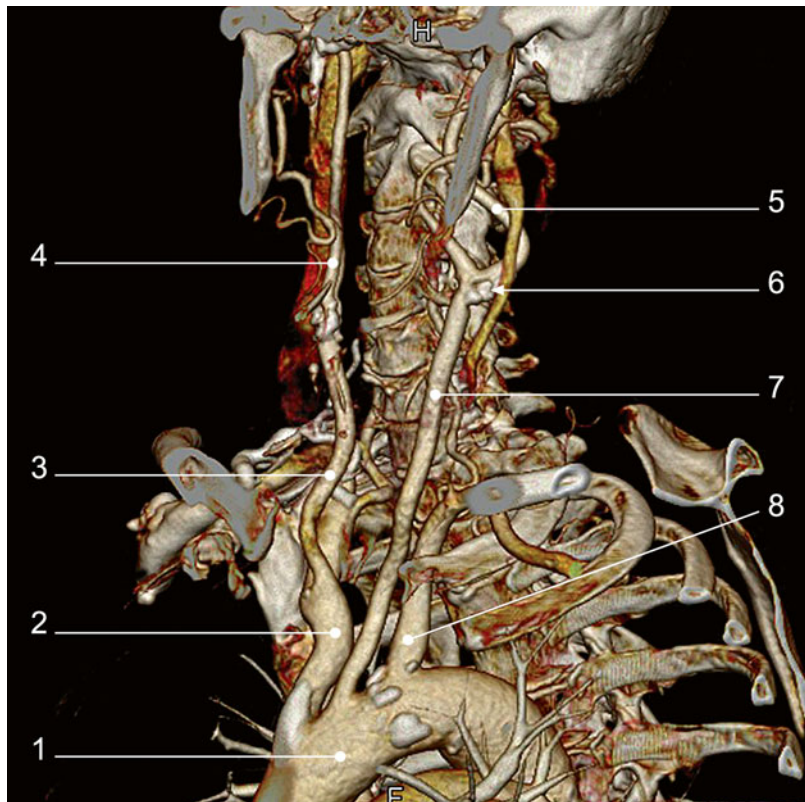


Fig. 2.35 Colour reconstruction 3D VRT oblique plane

1. Arcus aortae
2. Truncus brachiocephalicus
3. A. carotis communis dextra
4. A. carotis interna dextra
5. A. carotis interna sinistra
6. Moderate stenosis of a. carotis interna sinistra by mixed atheromatous plaques
7. A. carotis communis sinistra
8. A. subclavia sinistra

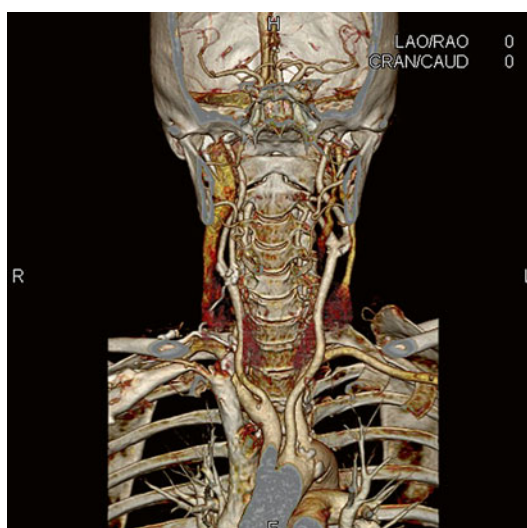


Fig. 2.36 Colour reconstruction 3D VRT, frontal plane

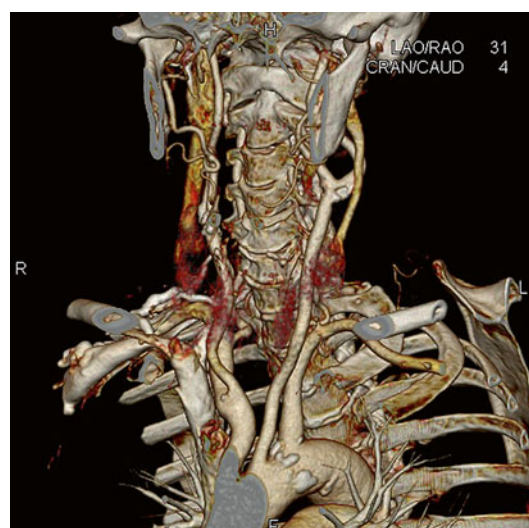


Fig. 2.37 3D VRT colour reconstruction, left oblique plane

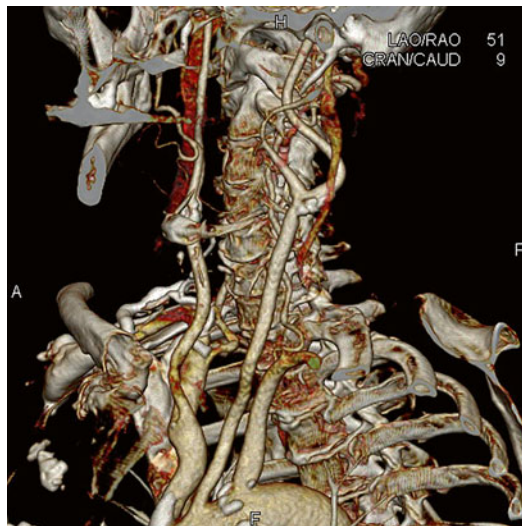


Fig. 2.38 3D VRT colour reconstruction, left oblique plane

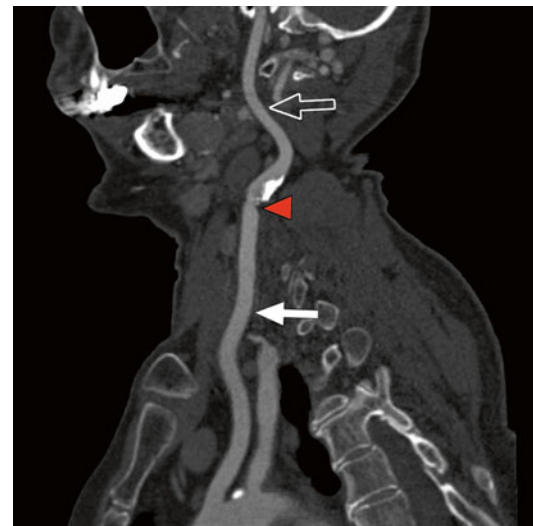


Fig. 2.40 3D MIP reconstruction
Full arrow=a. carotis communis sinistra
Arrow with contour=a. carotis interna sinistra
Tip of the arrow=left calcified lesion moderate stenosis

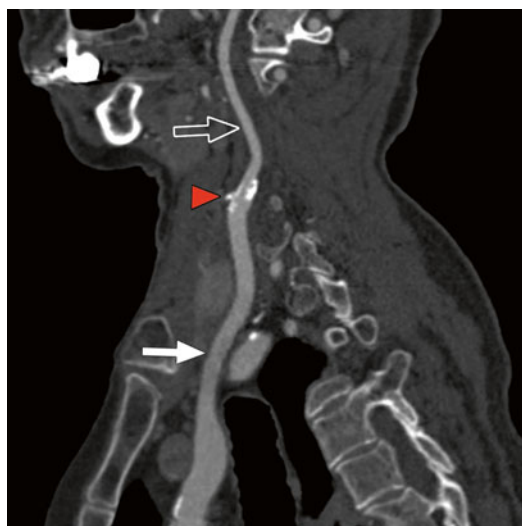


Fig. 2.39 3D MIP reconstruction
Full arrow=a. carotis communis sinistra
Arrow with contour=a. carotis interna sinistra
Tip of the arrow=left calcified lesion moderate stenosis

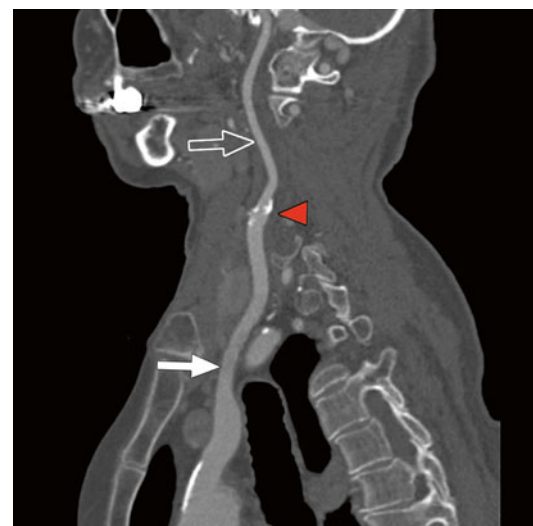


Fig. 2.41 3D MPR reconstruction
Full arrow=a. carotis communis dextra
Arrow with contour=a. carotis interna dextra
Tip of the arrow=left moderate stenosis



Fig. 2.42 3D MPR reconstruction

Full arrow=a. carotis communis dextra

Arrow with contour=a. carotis interna dextra

Tip of the arrow=left moderate stenosis

2.7 Carotid Angiography Emphasising a Severe Stenotic Lesion (Subocclusive) at the Level of Arteria Carotis Interna Dextra

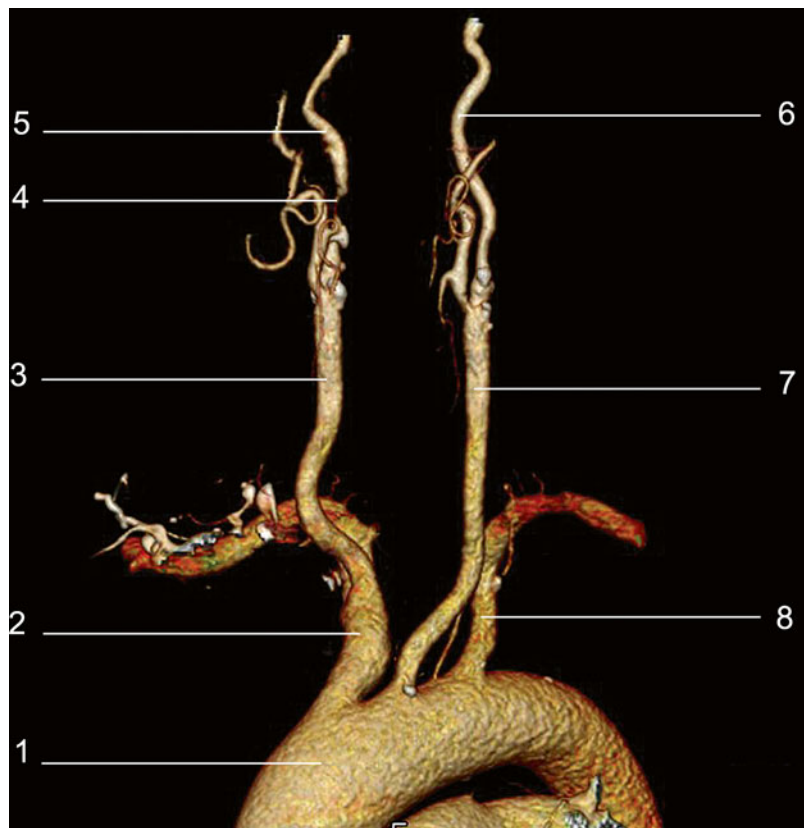


Fig. 2.43 3D VRT colour reconstruction after removal of the bone structure

1. Aorta
2. Truncus brachiocephalicus
3. A. carotis communis dextra
4. Subocclusive lesion
5. A. carotis interna dextra
6. A. carotis interna sinistra
7. A. carotis communis sinistra
8. A. subclavia sinistra

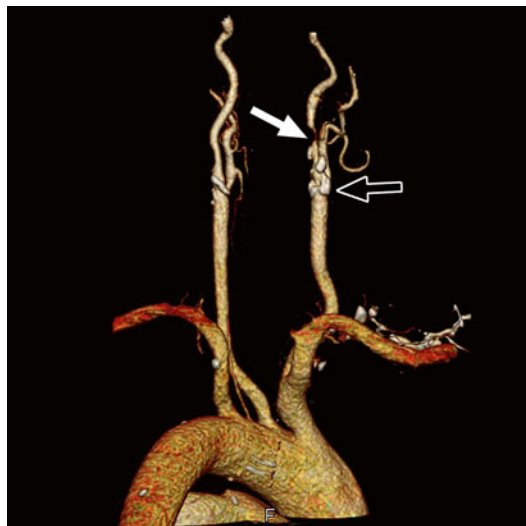


Fig. 2.44 3D VRT colour reconstruction after removal of the bone structure, posterior plane
Full arrow=subocclusive lesion
Arrow with contour=calcified plaques

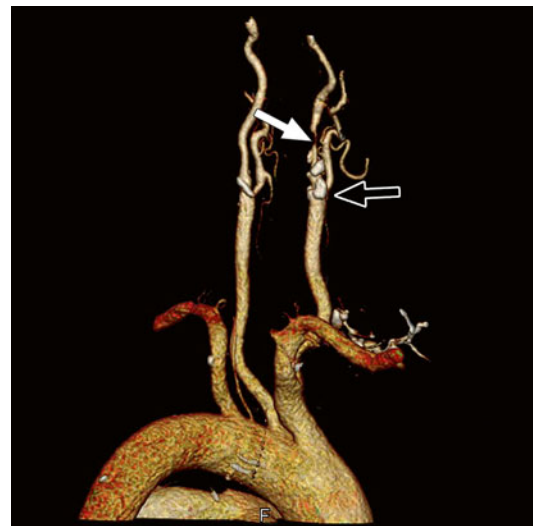
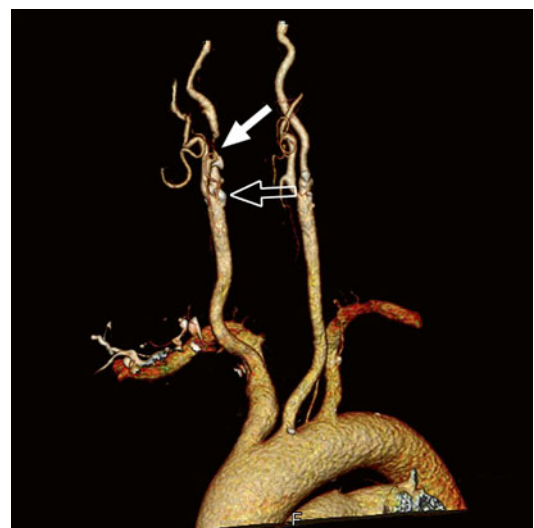


Fig. 2.45 3D VRT colour reconstruction after removal of the bone structure, posterior oblique plane
Full arrow=subocclusive lesion
Arrow with contour=calcified plaques

Fig. 2.46 3D VRT colour reconstruction after removal of the bone structure anterior oblique plane
Full arrow=subocclusive lesion
Arrow with contour=calcified plaques

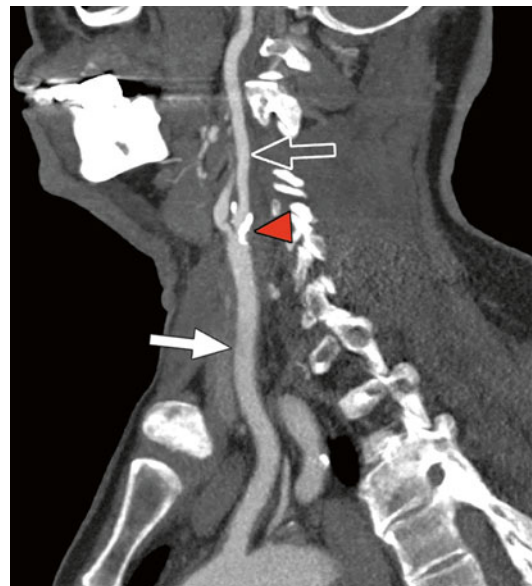


**Fig. 2.47** 3D MIP reconstruction

Full arrow=a. carotis interna dextra

Arrow with contour=a. carotis communis dextra

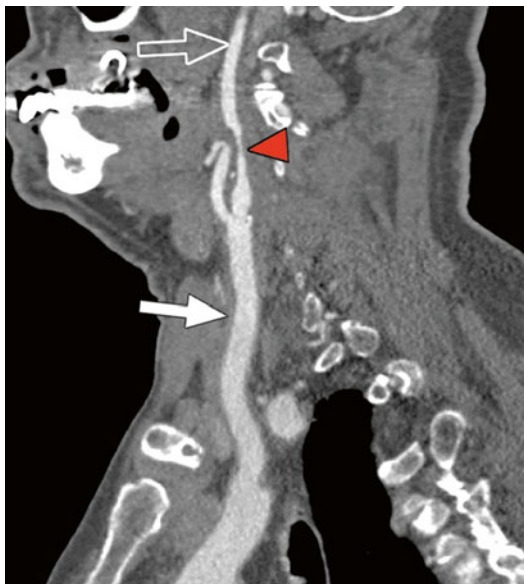
Tip of the arrow=subocclusive lesion a. carotis interna dextra

**Fig. 2.49** 3D MIP reconstruction

Full arrow=a. carotis communis sinistra

Arrow with contour=a. carotis interna sinistra

Tip of the arrow=calcified plaques

**Fig. 2.48** 3D MPR reconstruction

Full arrow=a. carotis interna dextra

Arrow with contour=a. carotis communis dextra

Tip of the arrow=subocclusive lesion a. carotis interna dextra

**Fig. 2.50** 3D MPR reconstruction

Full arrow=a. carotis communis sinistra

Arrow with contour=a. carotis interna sinistra

Tip of the arrow=calcified plaques

2.8 Carotid Angiography Emphasising a Subocclusive Lesion at the Level of the Emerging Arteria Carotis Interna Sinistra

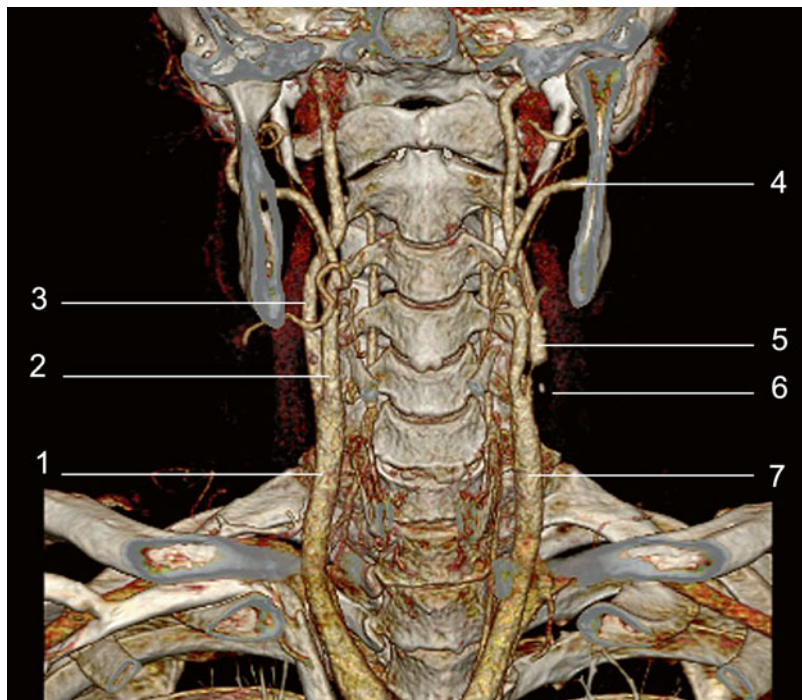


Fig. 2.51 3D VRT colour reconstruction frontal plane

1. A. carotis communis dextra
2. A. carotis externa dextra
3. A. carotis interna dextra
4. A. carotis externa sinistra
5. A. carotis interna sinistra
6. Subocclusive lesion
7. A. carotis communis sinistra

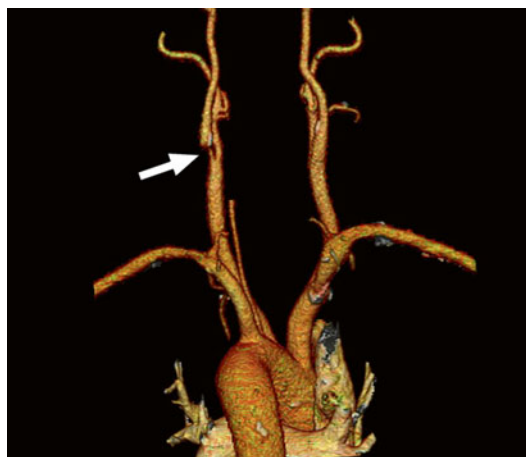


Fig. 2.52 3D VRT colour reconstruction after removal of the bone structure, posterior plane
Full arrow = subocclusive lesion a. carotis interna sinistra



Fig. 2.53 3D VRT colour reconstruction after removal of the bone structure, posterior oblique plane
Full arrow = subocclusive lesion a. carotis interna sinistra

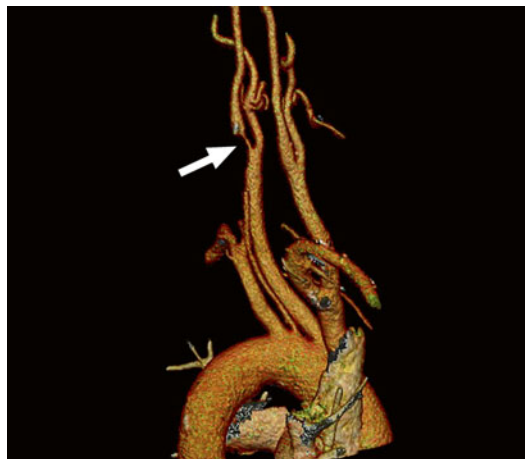


Fig. 2.54 3D VRT colour reconstruction after removal of the bone structure, sagittal plane
Full arrow=subocclusive lesion a. carotis interna sinistra



Fig. 2.55 3D VRT colour reconstruction after removal of the bone structure, anterior plane
Full arrow=subocclusive lesion at the level of a. carotis interna sinistra



Fig. 2.56 3D VRT colour reconstruction after removal of the bone structure, anterior oblique plane
Full arrow=subocclusive lesion at the level of a. carotis interna sinistra

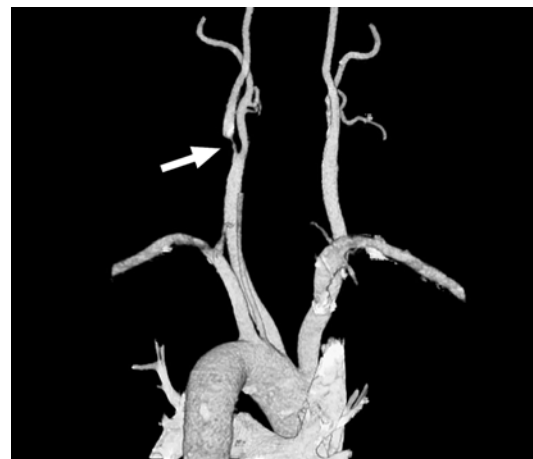


Fig. 2.57 3D VRT colour reconstruction after removal of the bone structure, posterior plane
Full arrow=subocclusive lesion at the level of a. carotis interna sinistra

2.9 Carotid Angiography Ostial Occlusive Lesion at the Level of Arteria Carotis Interna Sinistra

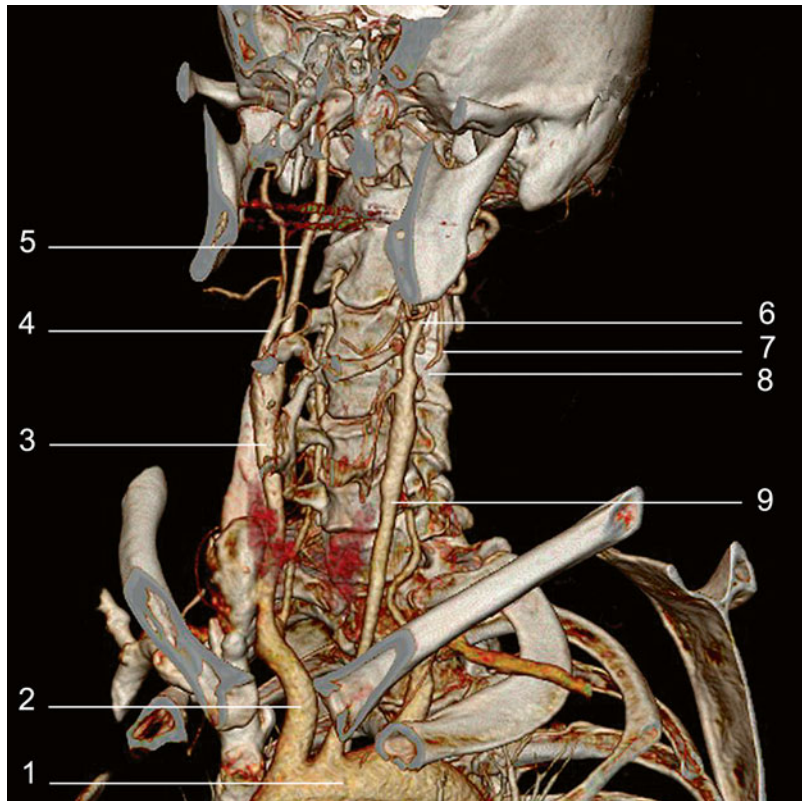


Fig. 2.58 3D VRT colour reconstruction, oblique plane

1. Aorta
2. Truncus brachiocephalicus
3. A. carotis communis dextra
4. A. carotis externa dextra
5. A. carotis interna dextra
6. A. carotis externa sinistra
7. A. carotis interna sinistra
8. Occlusive lesion
9. A. carotis communis sinistra

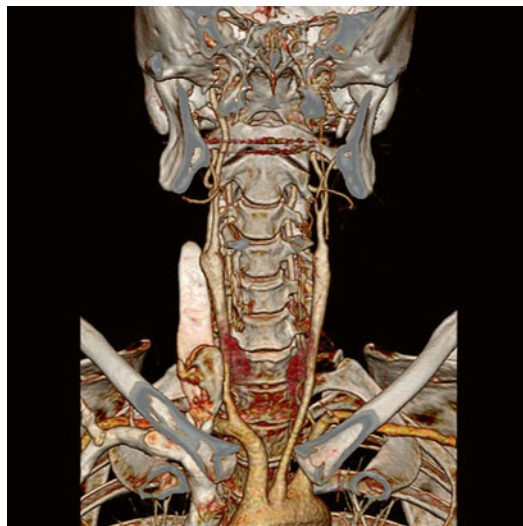


Fig. 2.59 3D VRT colour reconstruction frontal plane

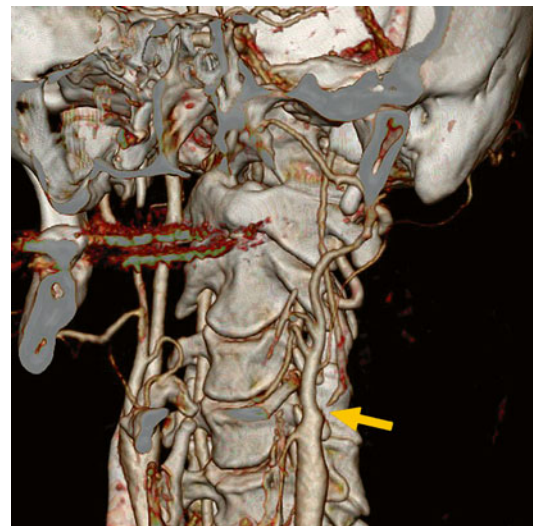


Fig. 2.61 3D VRT colour reconstruction, oblique plane
The yellow arrow indicates ostial occlusive lesion

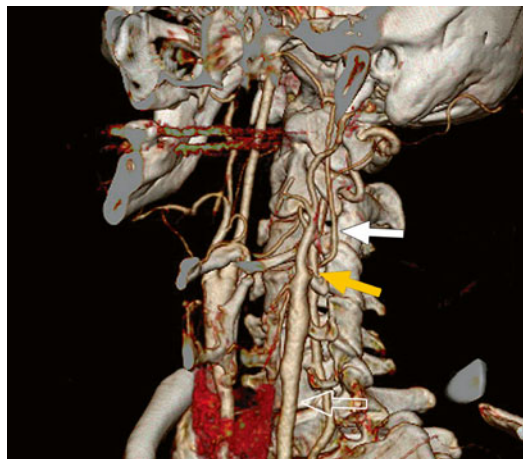


Fig. 2.60 3D VRT colour reconstruction enlarged image
Arrow with contour=a. carotis communis sinistra
Full arrow=a. carotis interna sinistra
Yellow arrow=ostial occlusive lesion



Fig. 2.62 3D MIP colour reconstruction
Arrow with contour=a. carotis communis dextra
Full arrow=a. carotis interna dextra

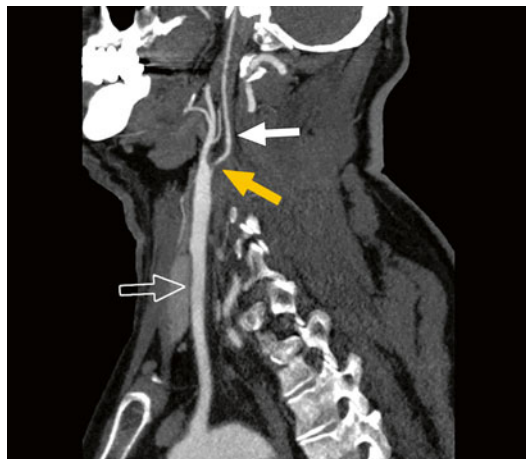


Fig. 2.63 3D MIP colour reconstruction

Arrow with contour=a. carotis communis sinistra

Full arrow=a. carotis interna sinistra

Yellow arrow=ostial occlusive lesion

2.10 Carotid Angiography: Complete Occlusion of the Arteria Carotis Interna Dextra

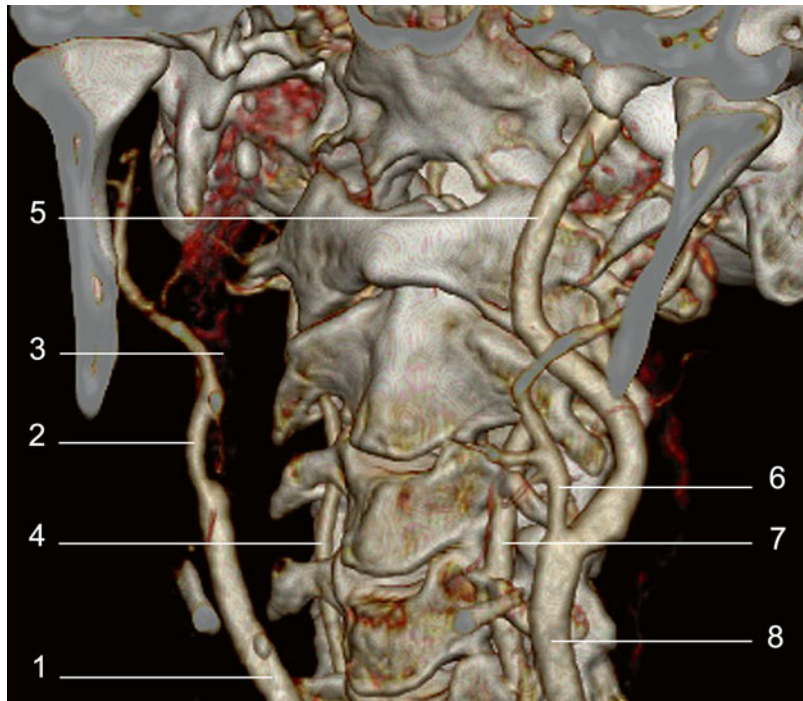


Fig. 2.64 3D VRT colour reconstruction, enlarged image, oblique plane

1. A. carotis communis dextra
2. A. carotis externa dextra
3. Occluded a. carotis interna dextra
4. A. vertebralis dextra
5. A. carotis interna sinistra
6. A. carotis externa sinistra
7. A. vertebralis sinistra
8. A. carotis communis sinistra

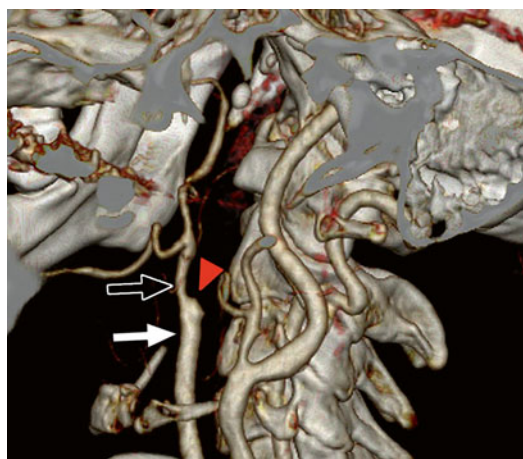


Fig. 2.65 3D VRT colour reconstruction, sagittal plane, enlarged image

Full arrow=a. carotis communis dextra

Arrow with contour=a. carotis externa dextra

At the tip of the arrow=a. carotis interna dextra, chronic occlusion

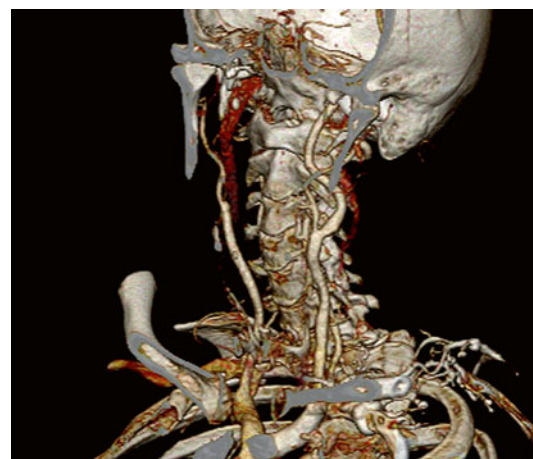


Fig. 2.66 3D VRT colour reconstruction, oblique plane

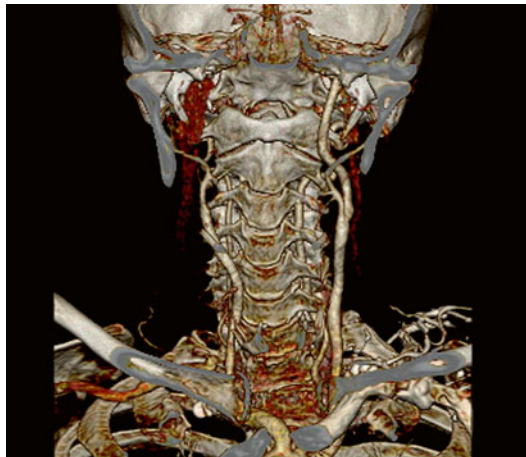


Fig. 2.67 3D VRT colour reconstruction, frontal plane



Fig. 2.69 3D MIP reconstruction
Full arrow=a. carotis communis dextra
Arrow with contour=a. carotis interna dextra
Tip of the arrow=ostium of a. carotis interna dextra with chronic occlusion

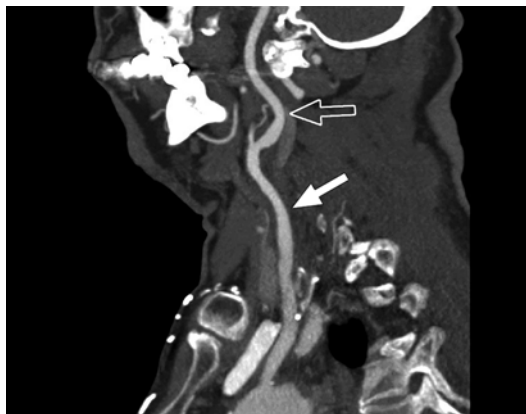


Fig. 2.68 3D MIP reconstruction
Full arrow=a. carotis communis sinistra
Arrow with contour=a. carotis interna sinistra

2.11 Carotid Angiography: Severe Stenotic Lesion at the Level of the Pars Proximalis of Arteria Subclavia Sinistra



Fig. 2.70 3D VRT colour reconstruction, after removal of the bone structure

1. Aorta
2. Truncus brachiocephalicus
3. Vena cava superior
4. A. carotis communis dextra
5. A. carotis externa dextra
6. A. carotis interna dextra
7. A. carotis interna sinistra
8. A. carotis externa sinistra
9. A. subclavia sinistra
10. Severe stenotic lesion

Fig. 2.71 3D VRT colour reconstruction, after removal of the bone structure, posterior plane
The full arrow indicates stenotic lesion





Fig. 2.72 3D VRT colour reconstruction, after removal of the bone structure, enlarged image, anterior plane
The full arrow indicates stenotic lesion



Fig. 2.74 3D MPR reconstruction, frontal plane
Full arrow = stenotic lesion

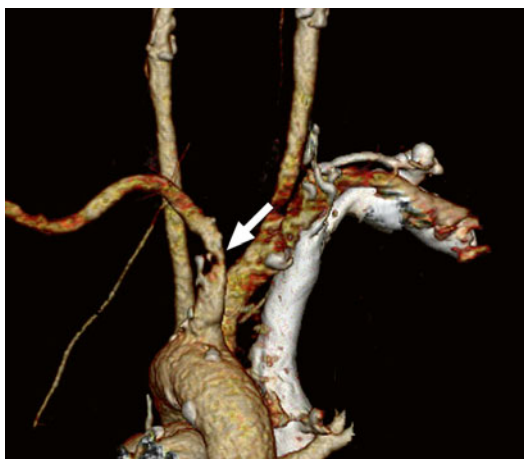


Fig. 2.73 3D VRT colour reconstruction, after removal of the bone structure, enlarged image, posterior plane
The full arrow indicates stenotic lesion

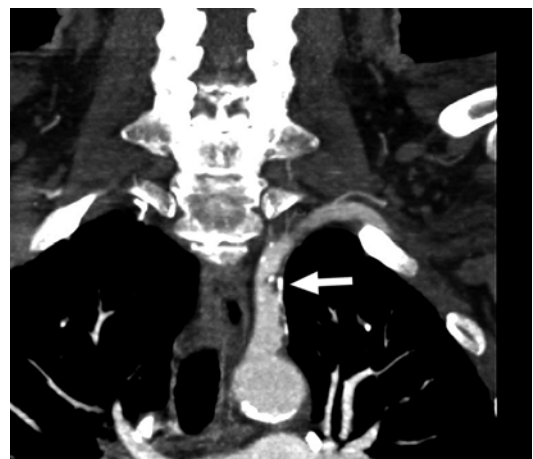


Fig. 2.75 3D MIP reconstruction, frontal plane
Full arrow = stenotic lesion

2.12 Carotid Angiography: Stent Occlusion at the Level of Arteria Subclavia Sinistra

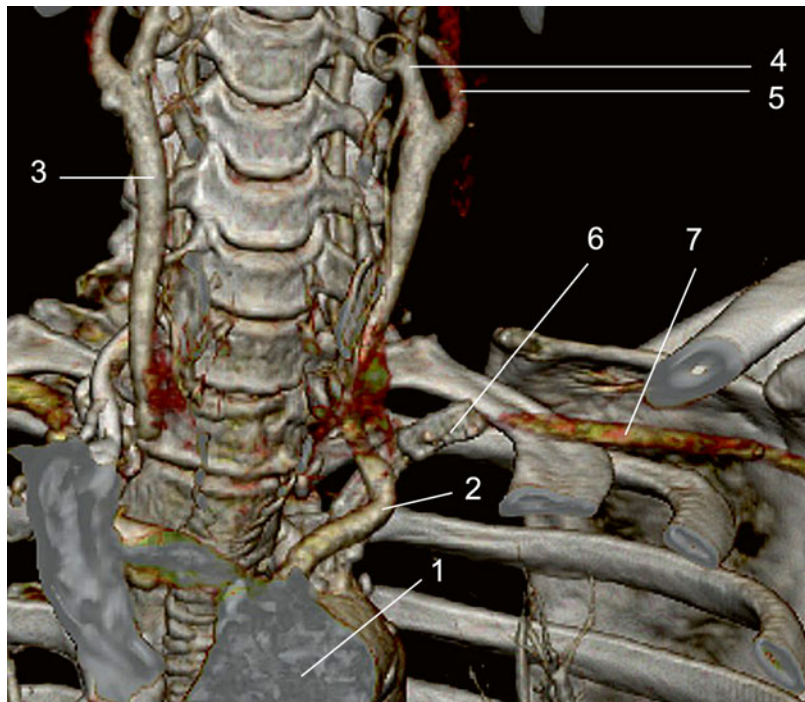


Fig. 2.76 3D VRT colour reconstruction, frontal plane, enlarged image

1. Aorta
2. A. carotis communis sinistra
3. A. carotis communis dextra
4. A. carotis interna sinistra
5. A. carotis externa sinistra
6. Stent
7. A. subclavia sinister

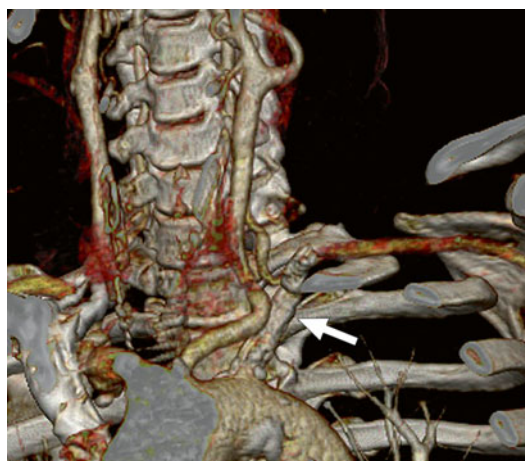


Fig. 2.77 3D VRT colour reconstruction, oblique plane, enlarged image. The *full arrow* indicates stent

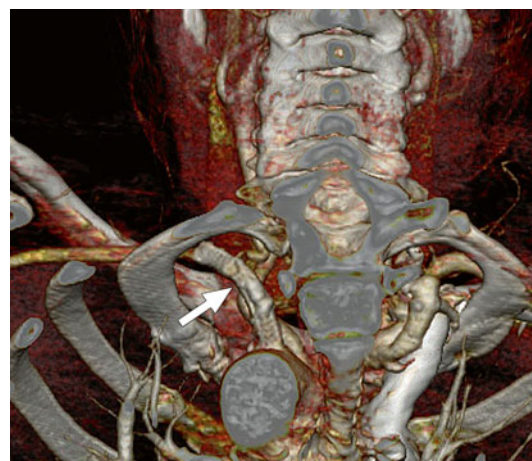


Fig. 2.78 3D VRT colour reconstruction, posterior plane, enlarged image. The *full arrow* indicates stent



Fig. 2.79 3D curved MPR reconstruction

Full arrow = stent occlusion

Arrow with contour = a. subclavia sinistra

Contents

3.1	Aneurysm of the Aorta Ascendens	50
3.2	Supravalvular Aortic Stenosis	53
3.3	Aneurysm of the Aorta Ascendens: Isthmic Stenosis	56
3.4	Aneurysm of the Arcus Aortae	58
3.5	Aneurysm of the Aorta Ascendens: Chronic Dissection of the Aorta.....	60
3.6	Post-traumatic Aneurysm of the Aorta Descendens.....	63
3.7	Gigantic Aneurysm at the Level of the Aorta Descendens.....	65
3.8	Chronic Dissection of the Aorta Descendens.....	68
3.9	Stenosis of A. Pulmonalis Dextra.....	71
3.10	Aneurysm and Dissection of the Aorta ascendens After Valvular Aortic Replacement.....	73
3.11	Pulmonary Thromboembolism.....	75
3.12	Right Partially Anomalous Venous Drainage.....	77
3.13	Partially Aberrant Venous Drainage.....	79
3.14	Interrupted Arcus Aortae	82

3.1 Aneurysm of the Aorta Ascendens

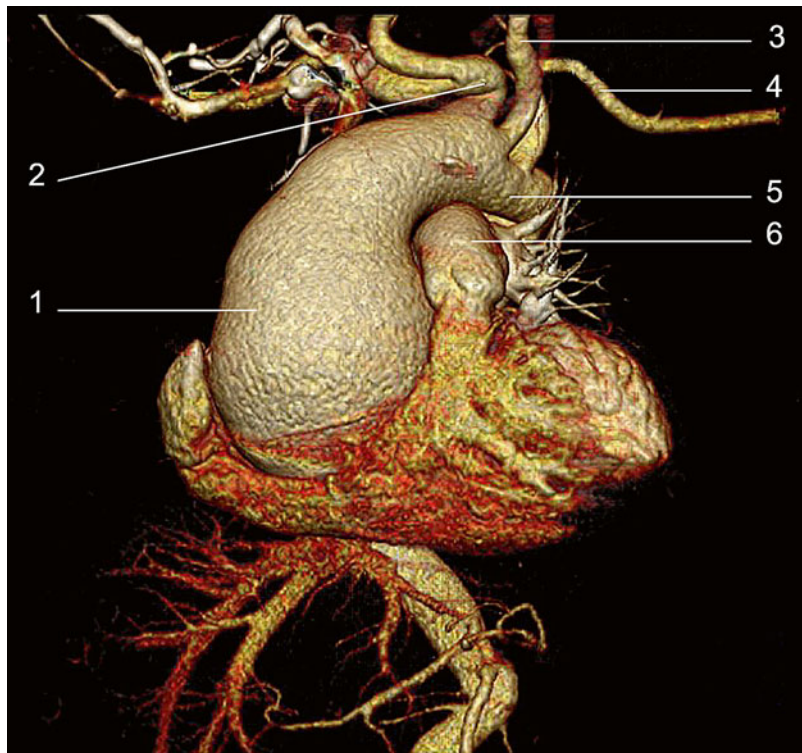


Fig. 3.1 3D VRT colour reconstruction, after removal of the thoracic cage

1. Aorta ascendens.
Aneurysmal dilatation
2. Truncus brachiocephalicus
3. A. carotis communis sinistra
4. A. subclavia sinistra
5. Arcus aortae
6. Truncus a. pulmonalis

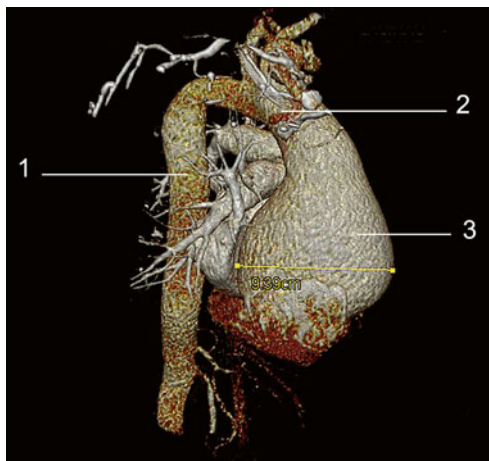


Fig. 3.2 3D VRT colour reconstruction, after removal of the thoracic cage

1. Aorta descendens thoracica
2. Arcus aortae
3. Aneurysm

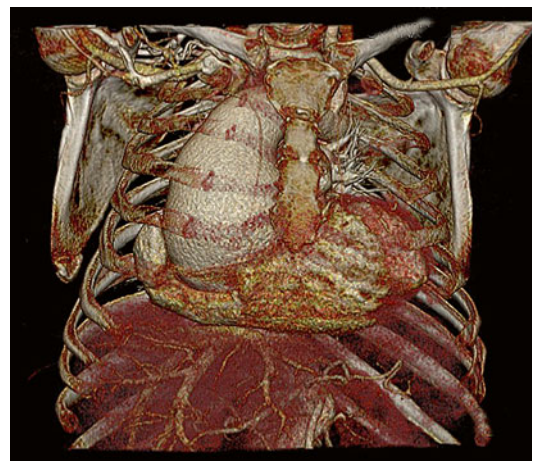


Fig. 3.3 3D VRT colour reconstruction, anterior plane

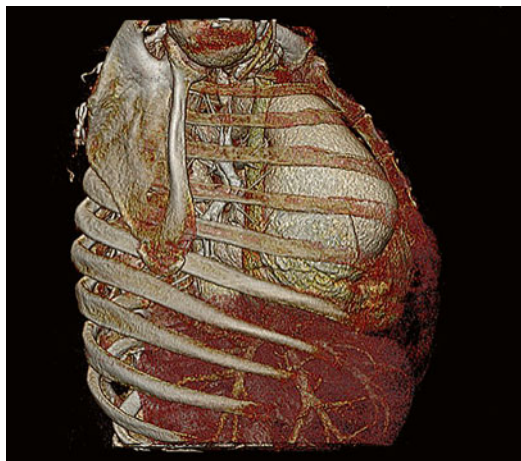


Fig. 3.4 3D VRT colour reconstruction, right sagittal plane

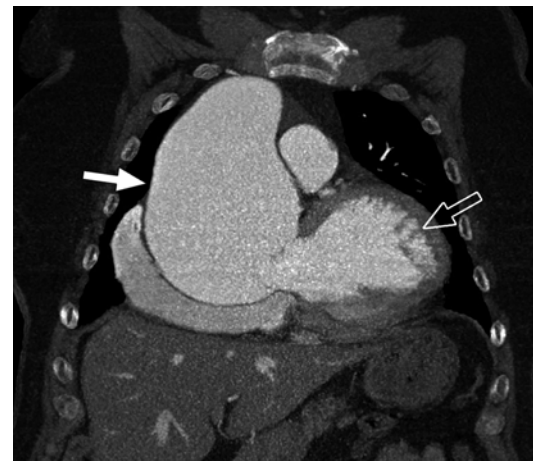


Fig. 3.6 3D MIP reconstruction, coronal plane

Full arrow = aneurysm

Arrow with contour = ventriculus sinister

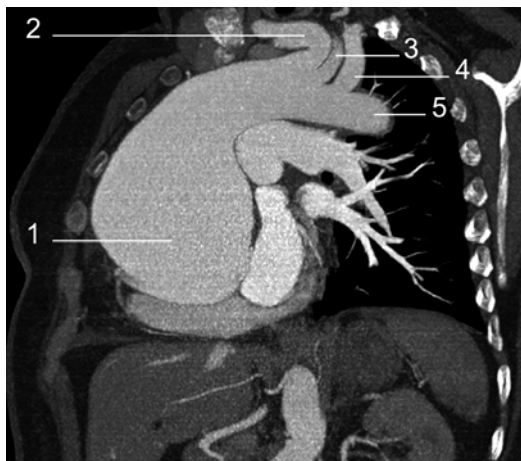


Fig. 3.5 3D MIP reconstruction, coronal plane

1. Aneurysm
2. Truncus brachiocephalicus
3. A. carotis communis sinistra
4. A. subclavia sinistra
5. A. aorta descendens

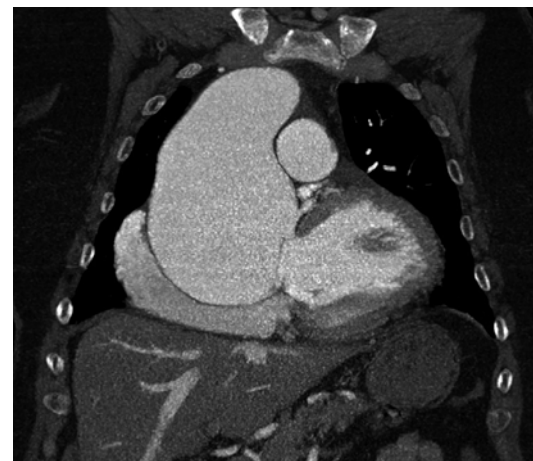


Fig. 3.7 3D MIP reconstruction, coronal plane

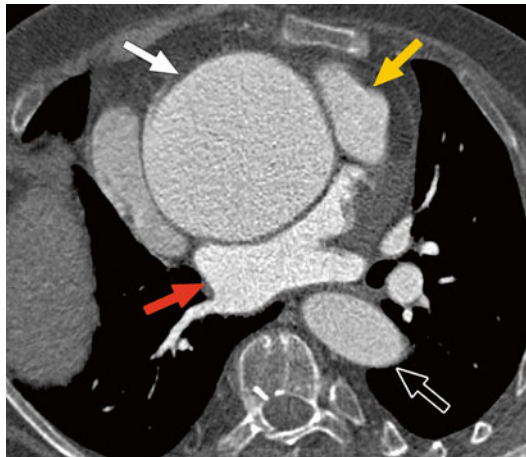


Fig. 3.8 3D MIP reconstruction, axial plane

Full arrow = aneurysm

Arrow with contour = aorta descendens

Yellow arrow = ventriculus sinister

Red arrow = atrium sinister

3.2 Supravalvular Aortic Stenosis

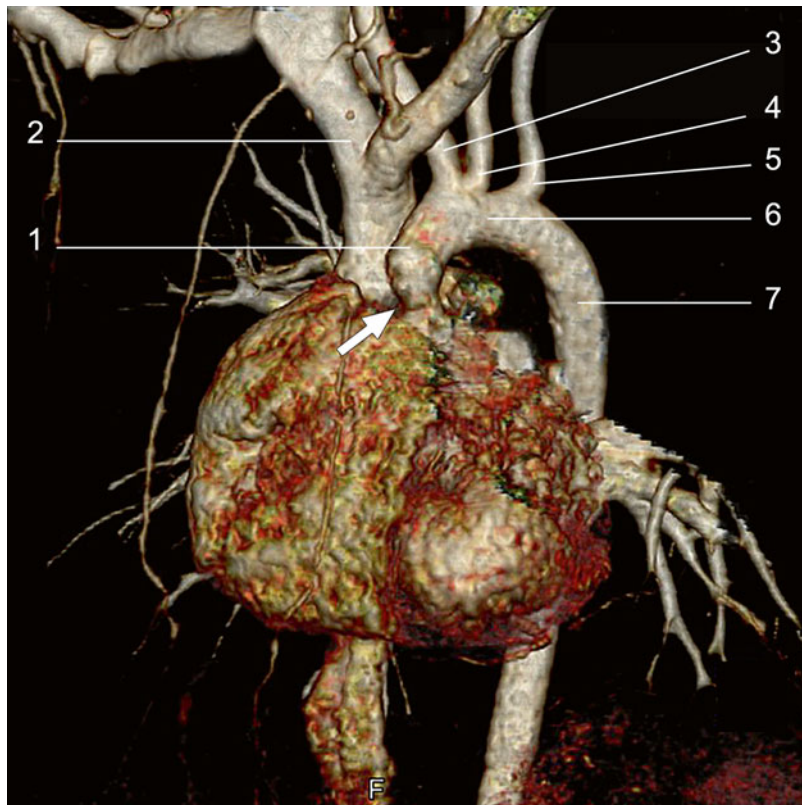


Fig. 3.9 3D VRT colour reconstruction, after removal of the bone structure
1. A. ascendens
2. V. brachiocephalica dextra
3. Truncus brachiocephalicus
4. A. carotis communis sinistra
5. A. subclavia sinistra
6. Arcus aortae
7. Aorta descendens
The full arrow indicates stenotic area



Fig. 3.10 3D VRT colour reconstruction, after removal of the bone structure, oblique anterior plane
Full arrow = supravalvular stenotic area



Fig. 3.11 3D VRT colour reconstruction, after removal of the bone structure, posterior oblique plane
Full arrow = supravalvular stenotic area

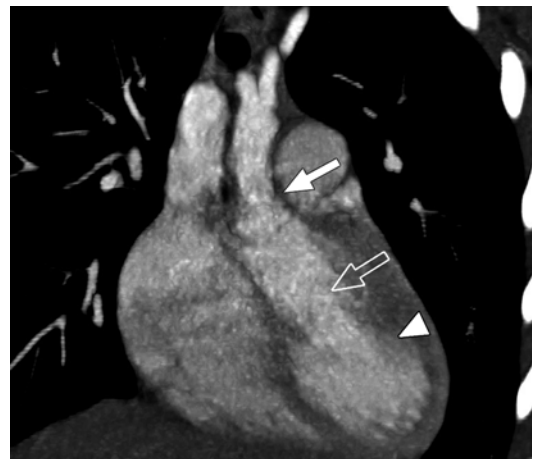


Fig. 3.13 3D MIP reconstruction, tract of ejection ventriculus sinister
Full arrow = supravalvular stenotic area
Arrow with contour = tract of ejection ventriculus sinister
Tip of the arrow = ventriculus sinister

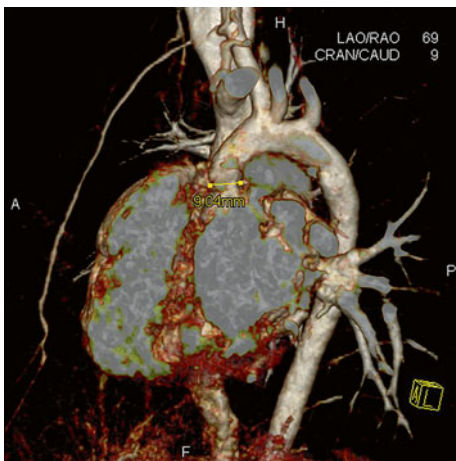


Fig. 3.12 3D VRT colour reconstruction, enlarged image

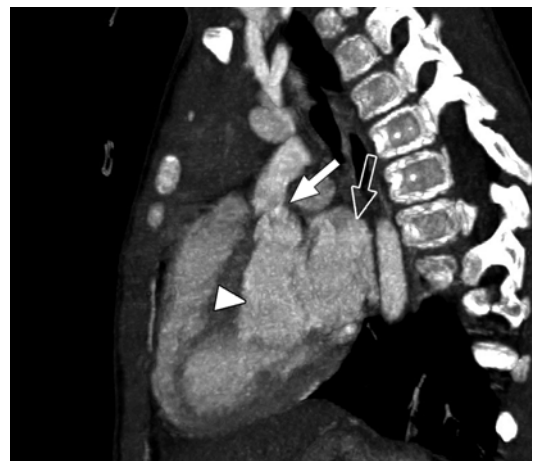


Fig. 3.14 3D MIP reconstruction
Full arrow = supravalvular stenotic area
Arrow with contour = atrium sinistrum
Tip of the arrow = tract of ejection ventriculus sinister



Fig. 3.15 3D MIP reconstruction, axial plane

Full arrow=aorta ascendens

Arrow with contour=aorta descendens

Tip of the arrow=truncus a. pulmonalis

3.3 Aneurysm of the Aorta Ascendens: Isthmic Stenosis

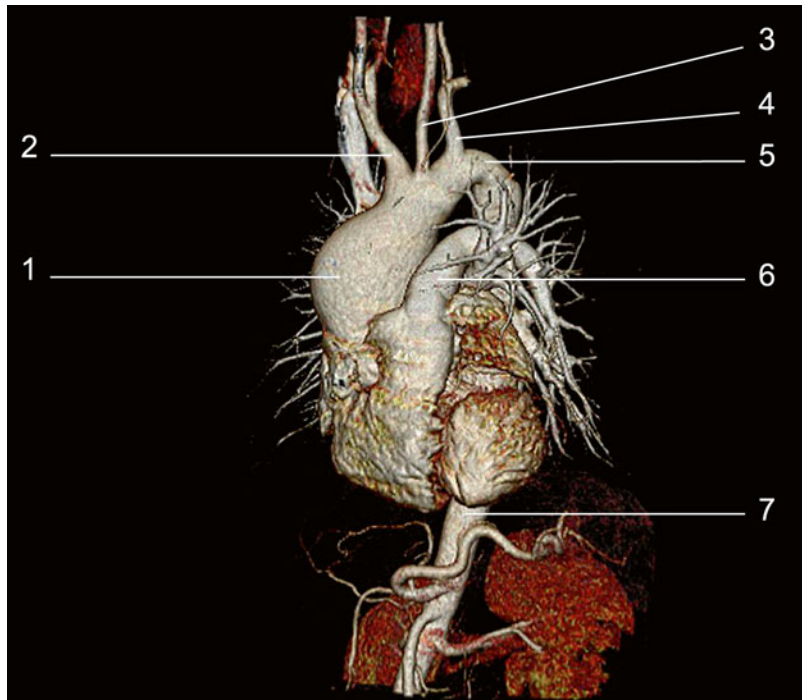


Fig. 3.16 3D VRT colour reconstruction, after removal of the bone structure, left anterior oblique plane
 1. Aorta ascendens
 2. Truncus brachiocephalicus
 3. A. carotis communis sinistra
 4. A. subclavia sinistra
 5. Area of isthmic stenosis
 6. Truncus a. pulmonalis
 7. Aorta descendens

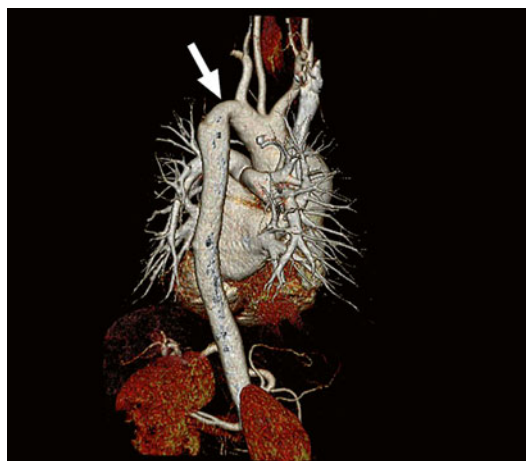


Fig. 3.17 3D VRT colour reconstruction, after removal of the bone structure, posterior oblique plane
Full arrow = area of isthmic stenosis

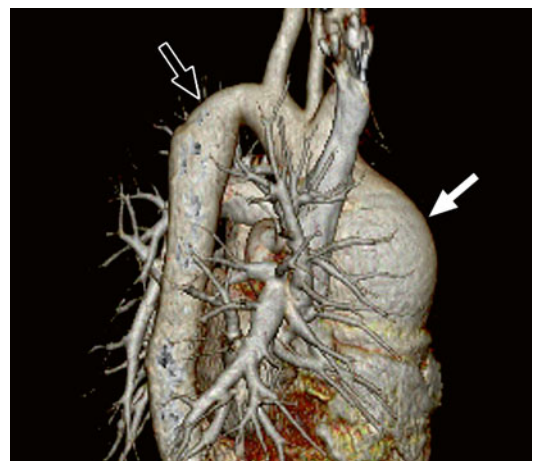


Fig. 3.18 3D VRT colour reconstruction, after removal of the bone structure, posterior oblique plane
*Full arrow = dilated aneurysm at the aorta ascendens
 Arrow with contour = area of isthmic stenosis*

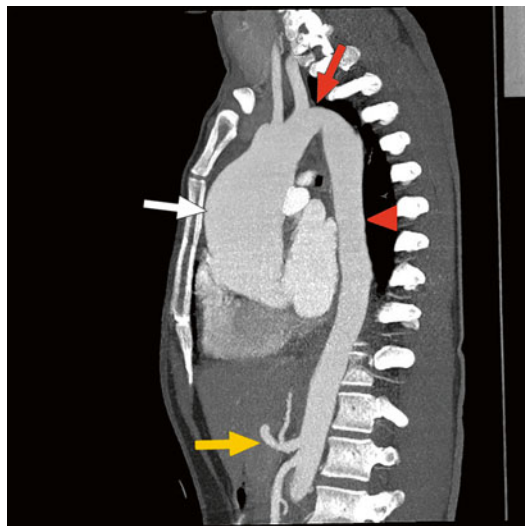


Fig. 3.19 3D MIP reconstruction, sagittal plane
Full arrow=aneurysm of the aorta ascendens
Full red arrow=isthmic stenotic area
At the tip of the *red arrow*=aorta thoracica
Yellow arrow=truncus coeliacus and arteria mesenterica superior

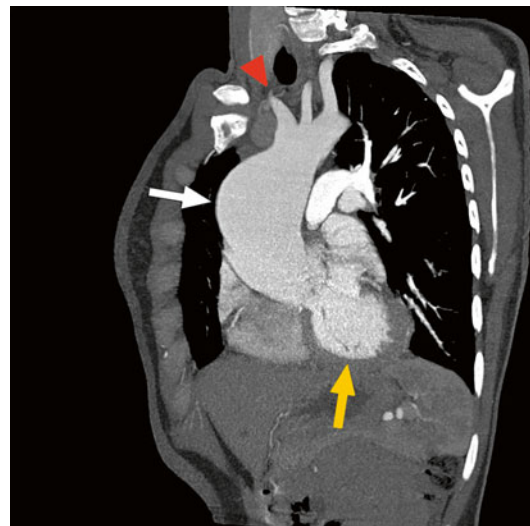


Fig. 3.21 3D MIP reconstruction, sagittal plane
Full arrow=aneurysm of the aorta ascendens
Yellow arrow=ventriculus sinister
At the tip of the *red arrow*=emerging vessels from the arcus aortae

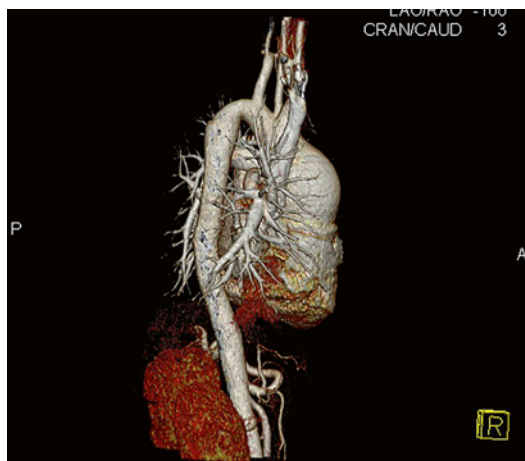


Fig. 3.20 3D VRT colour reconstruction, right sagittal plane

3.4 Aneurysm of the Arcus Aortae

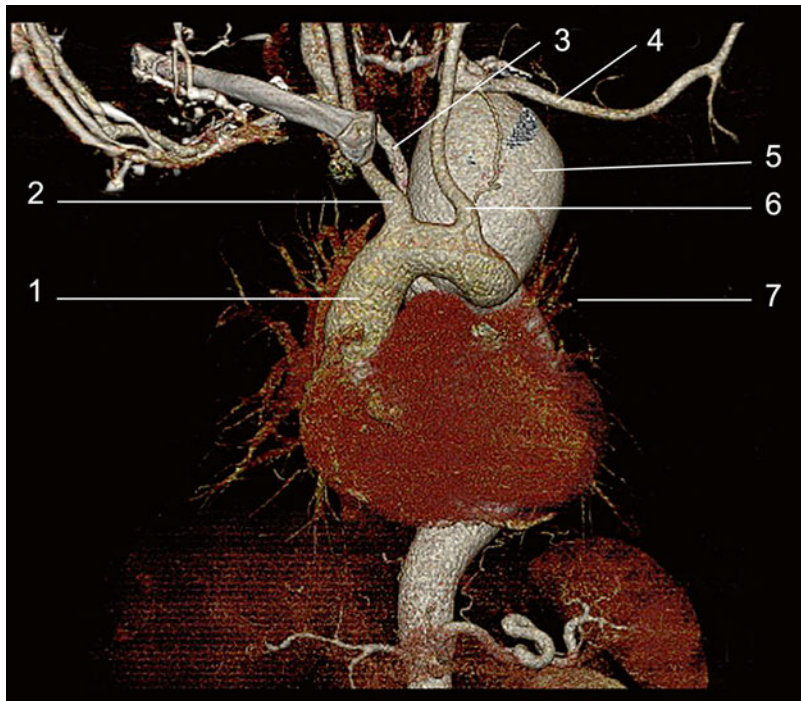


Fig. 3.22 3D VRT colour reconstruction, after removal of the bone structure, anterior view
 1. Aorta ascendens
 2. A. carotis communis dextra
 3. A. subclavia dextra
 4. A. subclavia sinistra
 5. Aneurysm of arcus aortae
 6. A. carotis communis sinistra
 7. Aorta descendens

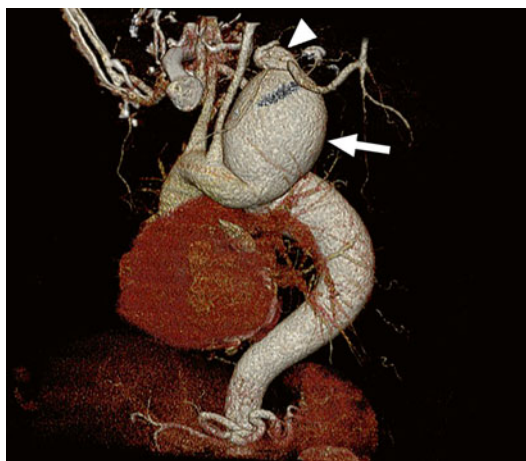


Fig. 3.23 3D VRT colour reconstruction, after removal of the bone structure, left anterior oblique view

Full arrow=aneurysm of the arcus aortae

At the tip of the arrow=abnormal emergence of the a. subclavia sinister from the level of the superior pole of the aneurysm

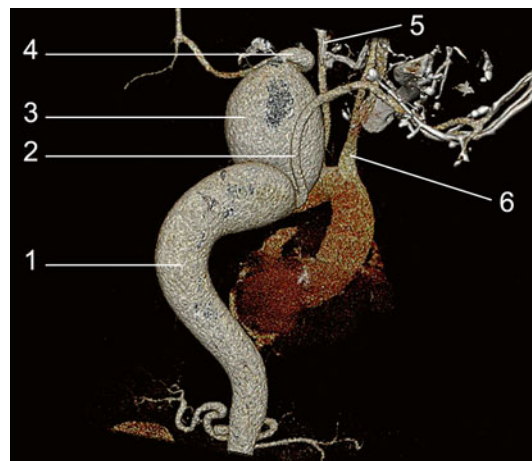


Fig. 3.24 3D VRT colour reconstruction, after removal of the bone structure, posterior view

1. Aorta thoracica
2. A. subclavia dextra
3. Aneurysm
4. A. subclavia sinistra
5. A. carotis communis sinistra
6. A. carotis communis dextra

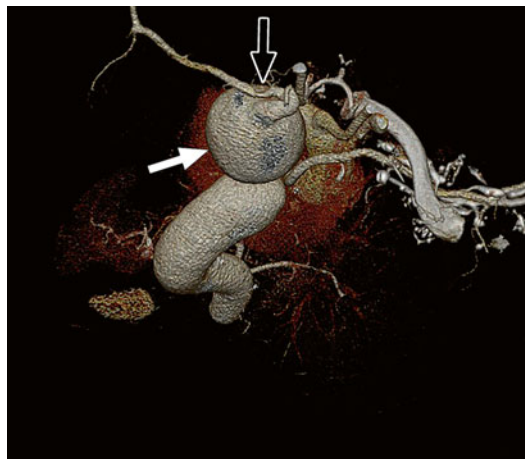


Fig. 3.25 3D VRT colour reconstruction, after removal of the bone structure, posterior cranial view

Full arrow=aneurysm

Arrow with contour=emergence of a. subclavia sinistra from the cranial extremity of the aneurysm



Fig. 3.27 3D VRT colour reconstruction, after removal of the bone structure, posterior view

The *full arrow* indicates aneurysm



Fig. 3.26 3D VRT colour reconstruction, after removal of the bone structure, anterior cranial view

Full arrow=aneurysm

Tip of the *yellow arrow*=a. carotis communis dextra

Tip of the *red arrow*=a. carotis communis sinistra

3.5 Aneurysm of the Aorta Ascendens: Chronic Dissection of the Aorta

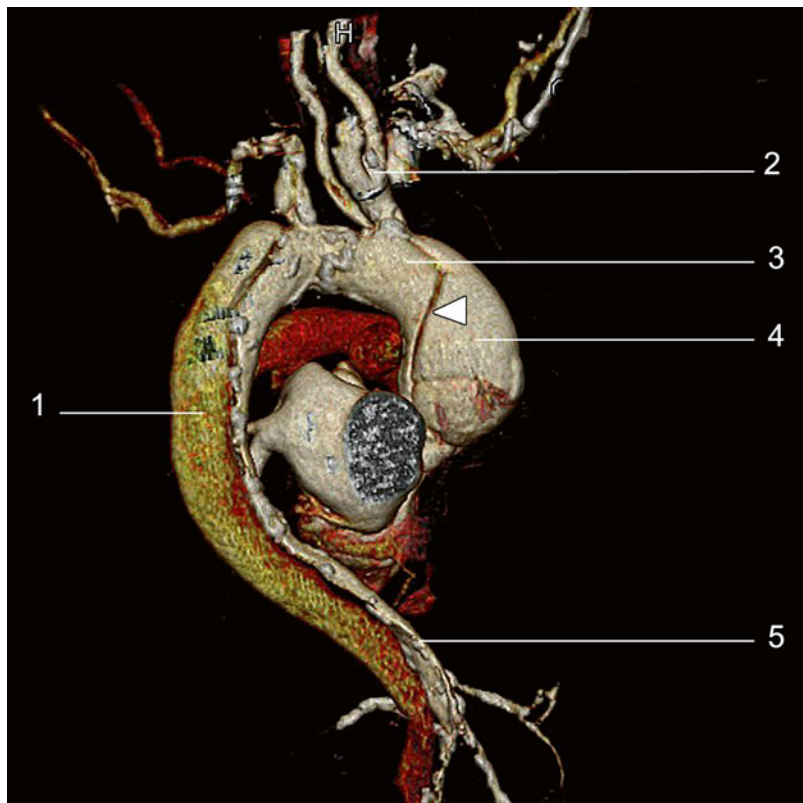


Fig. 3.28 3D VRT colour reconstruction, right oblique view

1. Aorta ascendens
 2. Truncus brachiocephalicus
 3. Aorta ascendens
 4. Dissected aortic aneurysm
 5. “True” lumen of aorta descendens
- Tip of the arrow=fold dissection



Fig. 3.29 3D VRT colour reconstruction, right oblique view
The *full arrow* indicates fold dissection

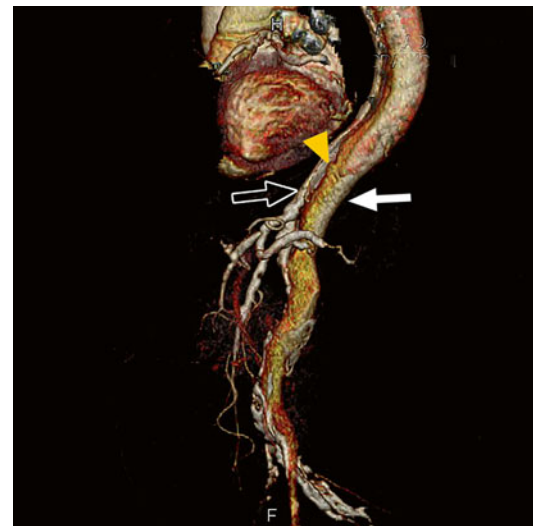


Fig. 3.31 3D VRT colour reconstruction, enlarged image of the aorta descendens
Full arrow = false lumen
Arrow with contour = true lumen
Tip of the *yellow arrow* = dissection fold

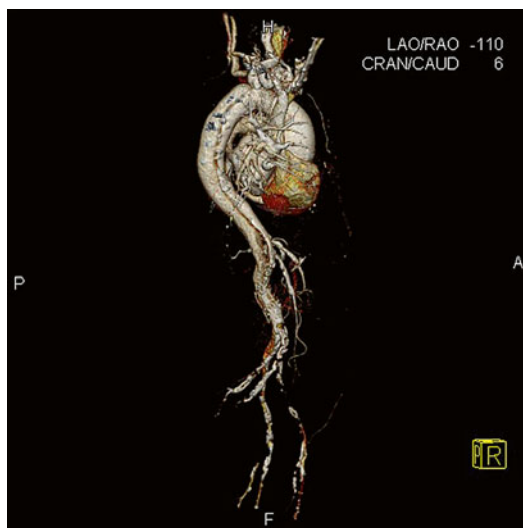


Fig. 3.30 3D VRT colour reconstruction, lateral view with visualisation of the abdominal aorta

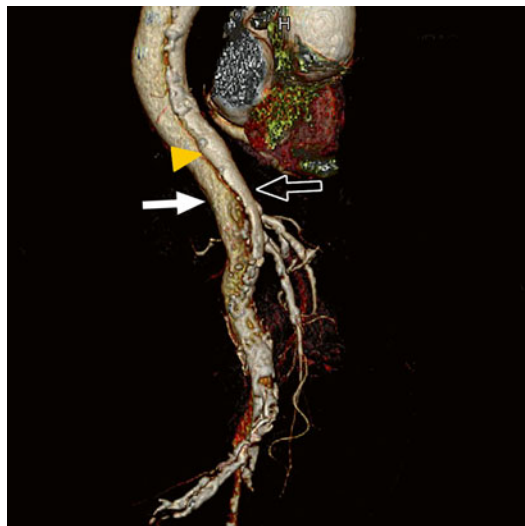


Fig. 3.32 3D VRT colour reconstruction, enlarged image of the aorta descendens

Full arrow = false lumen

Arrow with contour = true lumen

Tip of the yellow arrow = dissection fold

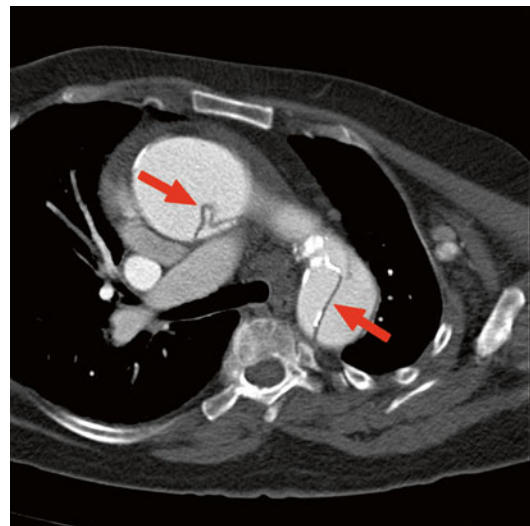


Fig. 3.33 3D MIP reconstruction, axial plane

Red arrow = dissection fold

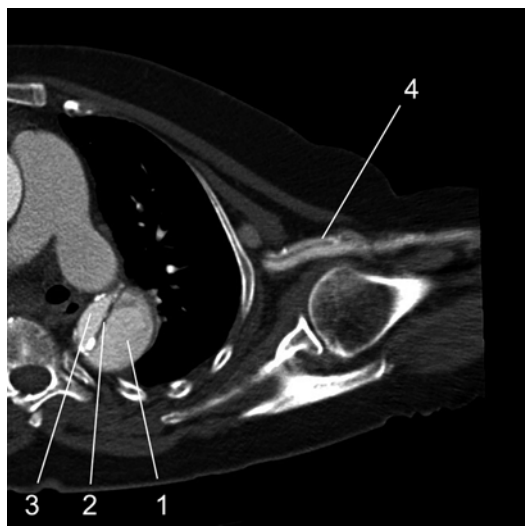


Fig. 3.34 3D MIP reconstruction, axial plane

1. False lumen

2. Dissection fold

3. True lumen of the aorta descendens

4. A. subclavia sinister with dissection

3.6 Post-traumatic Aneurysm of the Aorta Descendens

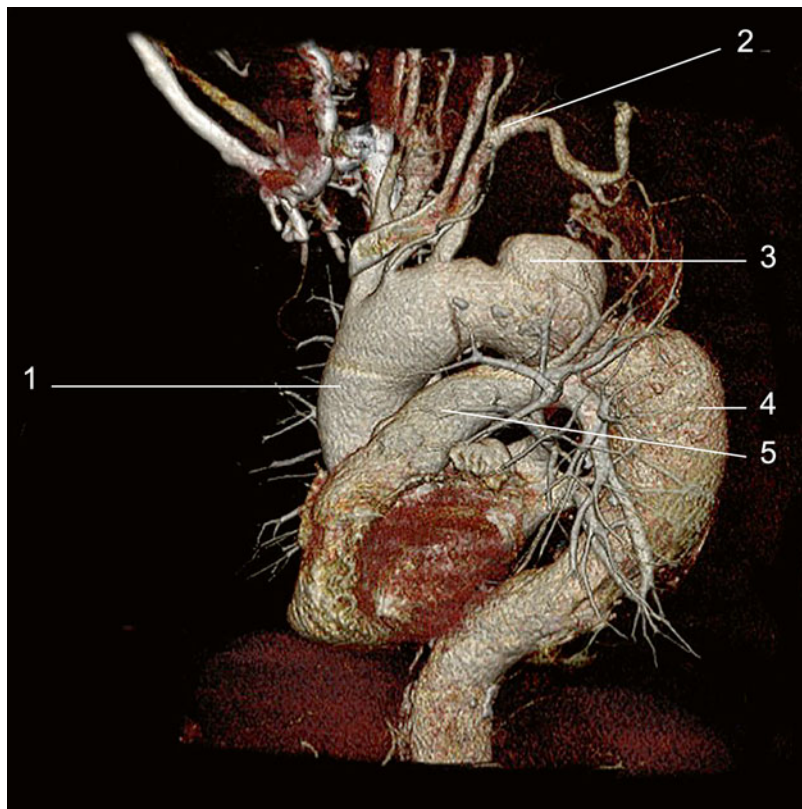


Fig. 3.35 3D VRT colour reconstruction, after removal of the bone structure, left anterior oblique view

1. Aorta ascendens
2. A. subclavia sinistra
3. Aneurysm of isthmic area
4. Aneurysmal dilatation of the aorta descendens
5. Truncus a. pulmonalis

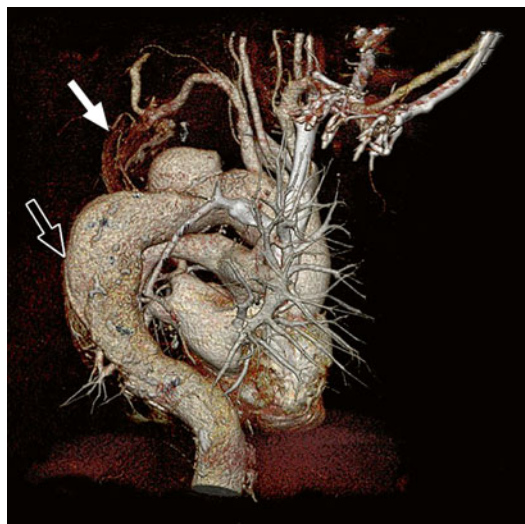


Fig. 3.36 3D VRT colour reconstruction, after removal of the bone structure, right posterior oblique view
Full arrow = dissection fold
Arrow with contour = aneurysmal dilatation of the aorta descendens

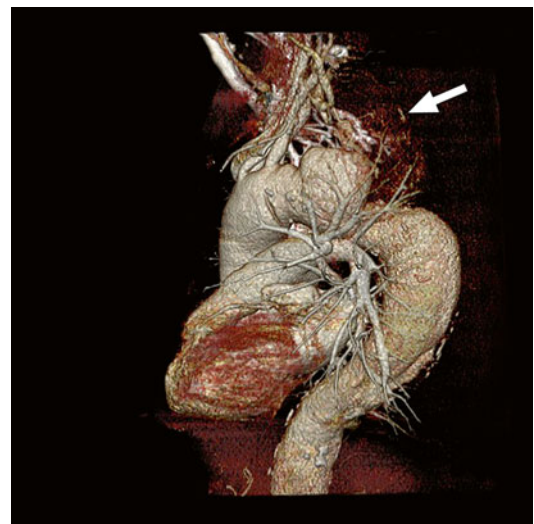


Fig. 3.37 3D VRT colour reconstruction; left lateral view
Full arrow = aneurysm



Fig. 3.38 3D MIP reconstruction, sagittal plane

1. Aorta ascendens
2. A. subclavia sinistra
3. Aneurysm with parietal thrombosis
4. Aneurysm of the aorta descendens with thrombosis and mural calcifications

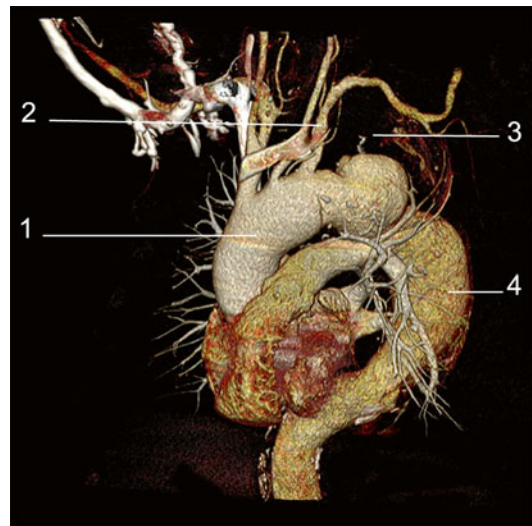


Fig. 3.40 3D VRT reconstruction

1. Aorta ascendens
2. A. subclavia sinistra
3. Aneurysm with parietal thrombosis
4. Aneurysm of the aorta descendens with thrombosis and mural calcifications

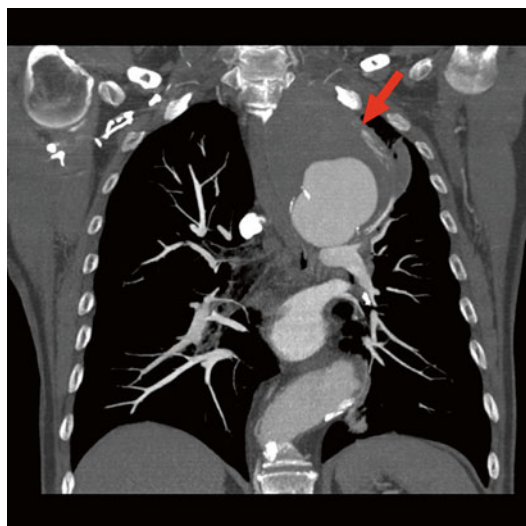


Fig. 3.39 3D MIP reconstruction, frontal plane

Red arrow = thrombosed aneurysm

3.7 Gigantic Aneurysm at the Level of the Aorta Descendens

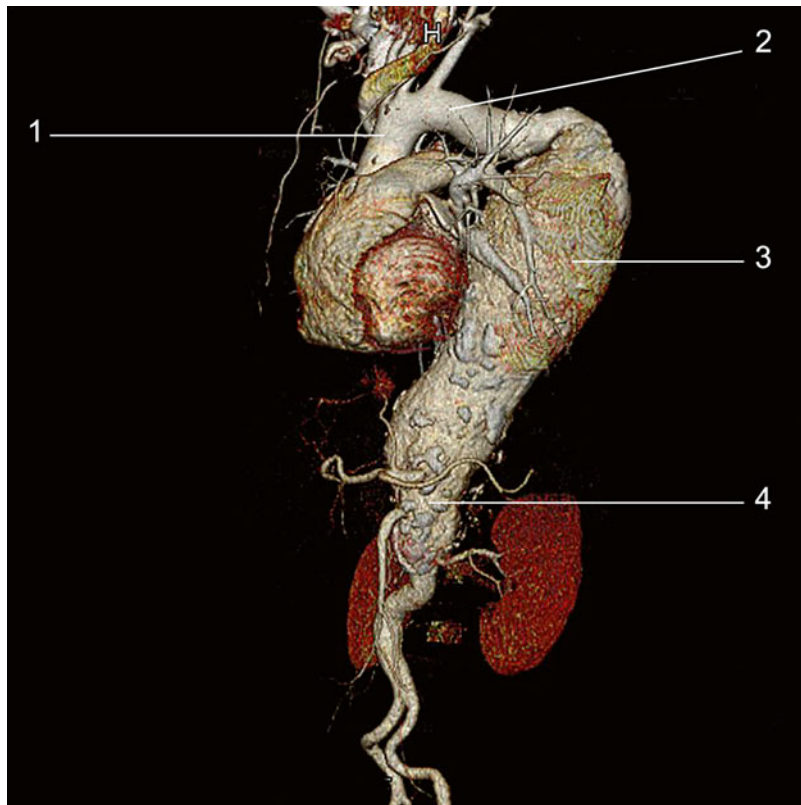


Fig. 3.41 3D VRT colour reconstruction, left anterior oblique view

1. Aorta ascendens
2. Arcus aortae
3. Aorta thoracica
4. Aorta abdominalis

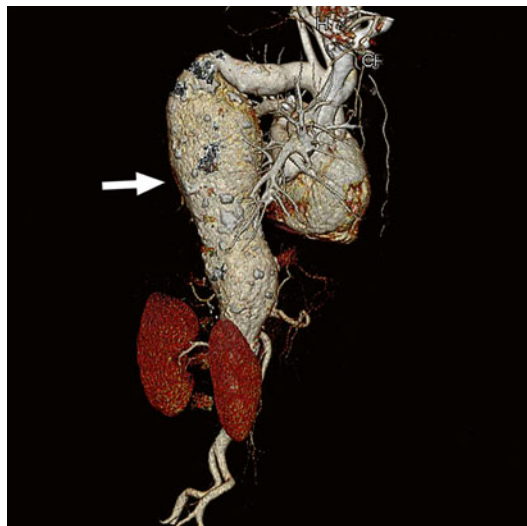


Fig. 3.42 3D VRT colour reconstruction, right posterior oblique view
The *full arrow* indicates gigantic aneurysm of aorta descendens

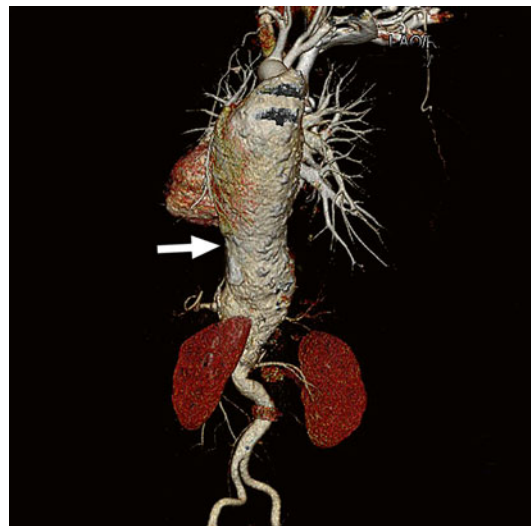


Fig. 3.43 3D VRT colour reconstruction, posterior view
The *full arrow* indicates aorta descendens with a gigantic aneurysm

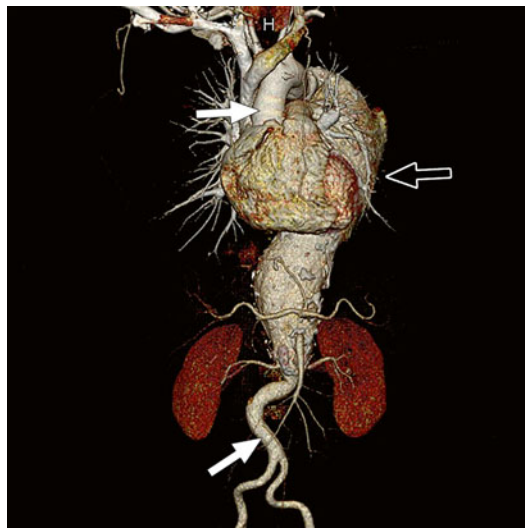


Fig. 3.44 3D VRT colour reconstruction, anterior view
Full arrows=normal calibre of aorta ascendens and aorta abdominalis
Arrow with contour=gigantic aneurysm

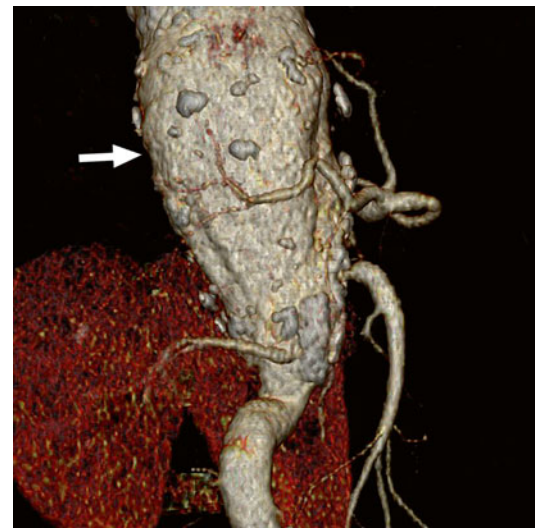


Fig. 3.45 3D VRT colour reconstruction, enlarged image
The *full arrow* indicates aneurysm of aorta abdominalis with calcified parietal plaques

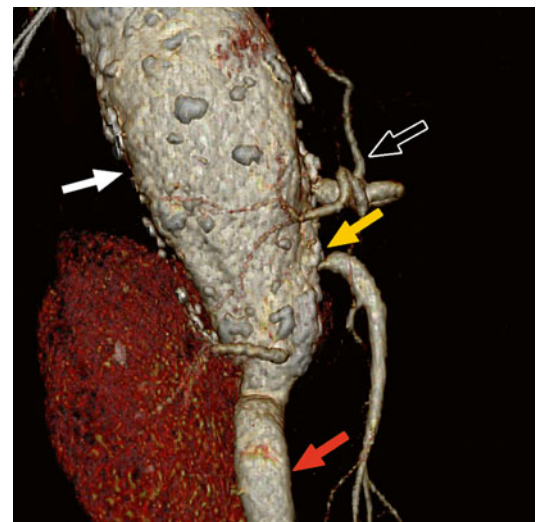


Fig. 3.46 3D VRT colour reconstruction, enlarged image
Full arrow=aneurysm
Arrow with contour=truncus coeliacus
Yellow arrow=a. mesenterica superior with a severe ostial stenotic lesion
Red arrow=normal calibre of aorta abdominalis

3.8 Chronic Dissection of the Aorta Descendens

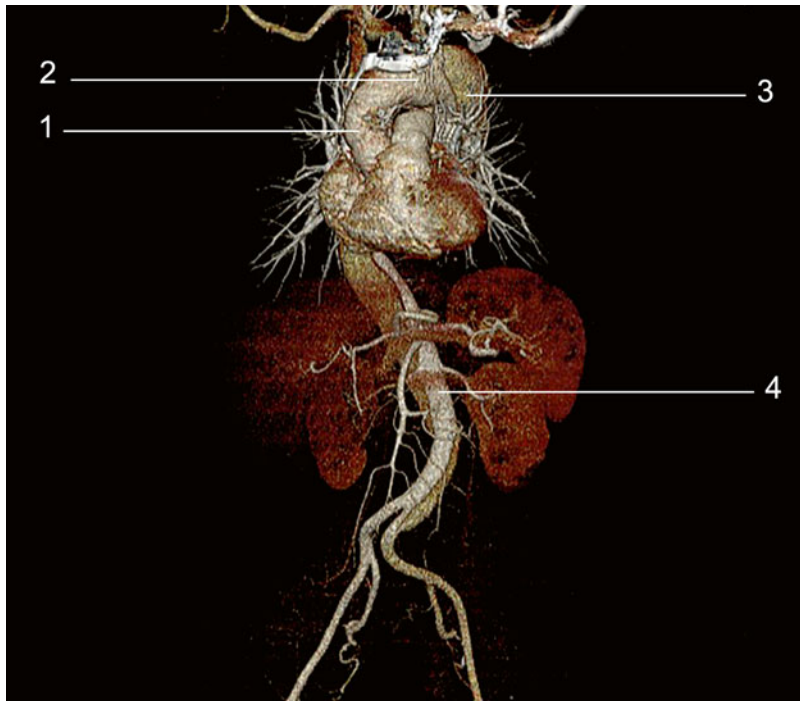


Fig. 3.47 3D VRT colour reconstruction, frontal plane

1. Aorta ascendens
2. Arcus aortae
3. Aorta thoracica dissected
4. Aorta abdominalis dissected



Fig. 3.48 3D VRT colour reconstruction, left anterior oblique plane

Full arrow = false lumen

Arrow with contour = true lumen



Fig. 3.49 3D VRT colour reconstruction, posterior plane

Full arrow = false lumen

Arrow with contour = true lumen

Tip of the arrow = dissection fold

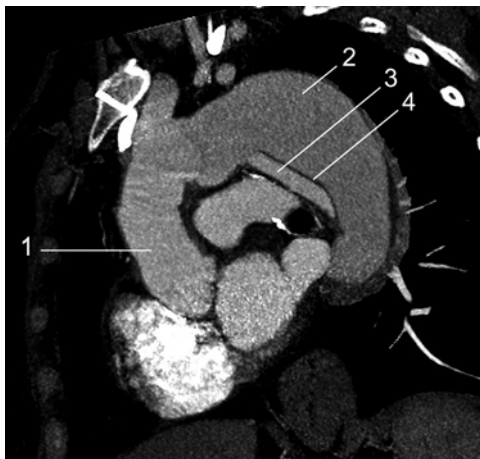


Fig. 3.50 3D MIP reconstruction

- 1. Aorta ascendens
- 2. False lumen
- 3. True lumen
- 4. Dissection fold



Fig. 3.52 3D MIP reconstruction, frontal plane at the level of aorta abdominalis, pars distalis

- Full arrow = false lumen
- Arrow with contour = true lumen
- At the tip of the red arrow = dissection fold

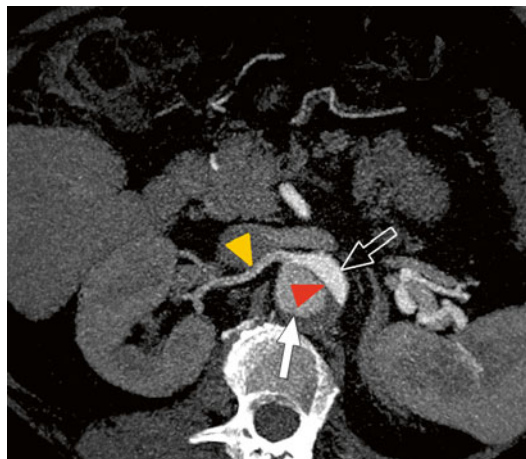


Fig. 3.51 3D MIP reconstruction, axial plane

- Full arrow = false lumen
- Arrow with contour = true lumen
- Tip of the red arrow = dissection fold
- Tip of the yellow arrow = a. renalis dextra with proximal dissection

3.9 Stenosis of A. Pulmonalis Dextra

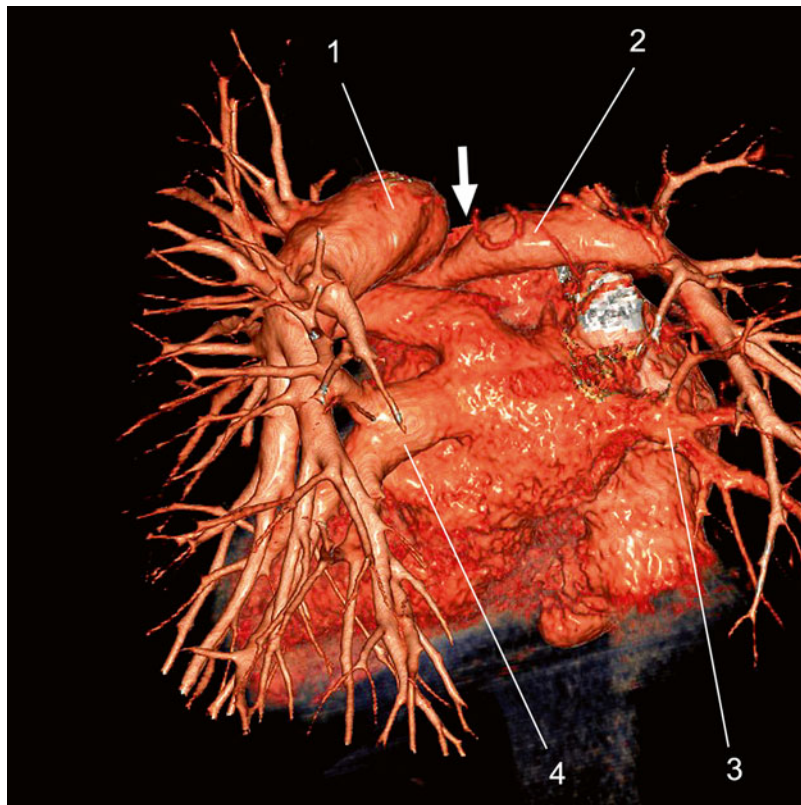


Fig. 3.53 3D VRT colour reconstruction, after removal of the thoracic cage

1. A. pulmonalis sinistra
 2. A. pulmonalis dextra
 3. V. pulmonalis dextra
 4. V. pulmonalis sinistra
- The full arrow indicates stenotic area at the emergence of the a. pulmonalis dextra



Fig. 3.54 3D VRT colour reconstruction, after removal of the thoracic cage, cranial view
The *full arrow* indicates stenotic area

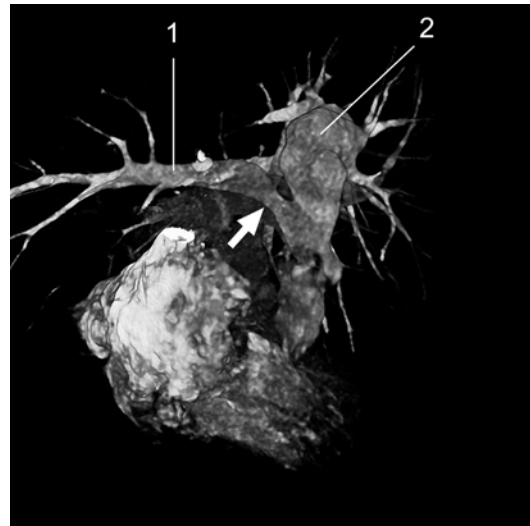


Fig. 3.56 3D VRT reconstruction, anterior view
1. A. pulmonalis dextra
2. A. pulmonalis sinistra
The *full arrow* indicates stenotic area

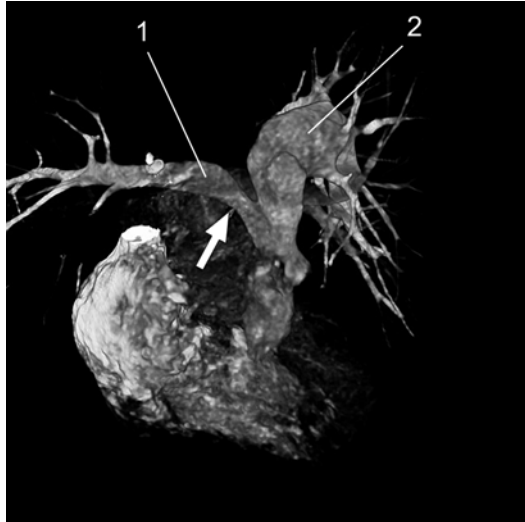


Fig. 3.55 3D VRT reconstruction, anterior view
1. A. pulmonalis dextra
2. A. pulmonalis sinistra
The *full arrow* indicates stenotic area

3.10 Aneurysm and Dissection of the Aorta ascendens After Valvular Aortic Replacement

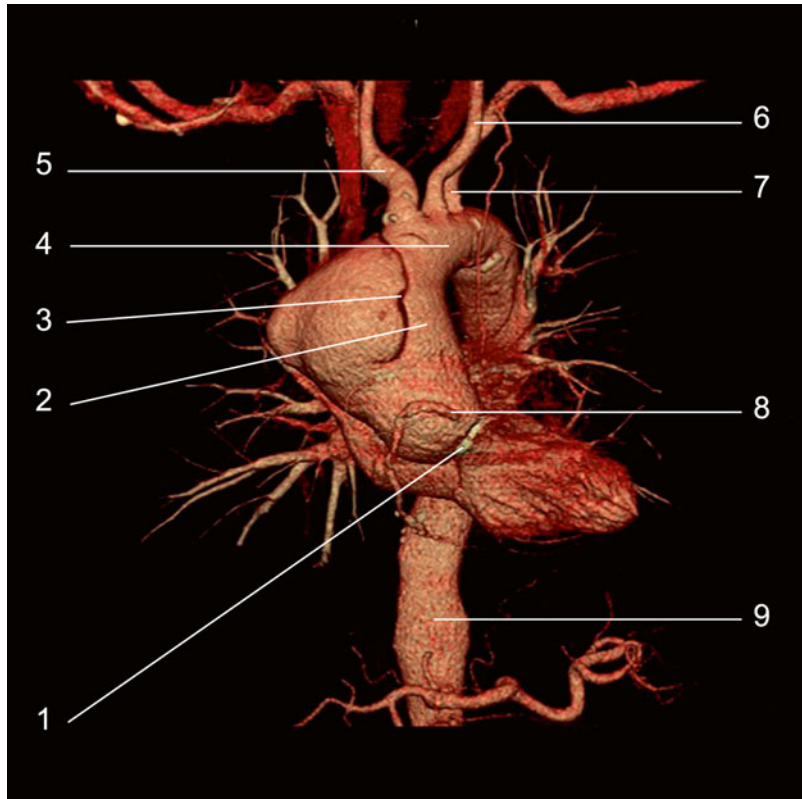


Fig. 3.57 3D VRT colour reconstruction, after removal of the thoracic cage, frontal plane

1. Valvular aortic prosthesis
2. Aorta ascendens dilated
3. Dissection fold
4. Arcus aortae
5. Truncus brachiocephalicus
6. A. carotis communis sinistra
7. A. subclavia sinistra
8. A. coronaria dextra
9. Aorta descendens

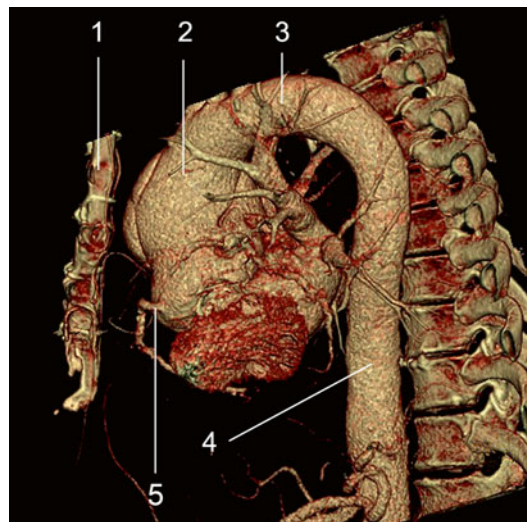


Fig. 3.58 3D VRT colour reconstruction, lateral plane

1. Sternum
2. Aorta ascendens with aneurysm
3. Arcus aortae
4. Aorta descendens
5. A. coronaria dextra

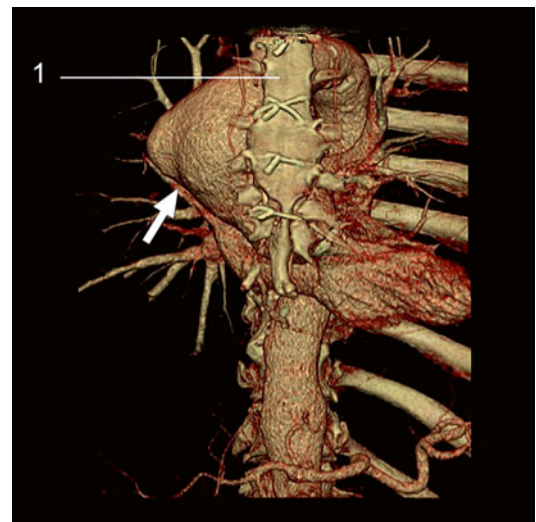


Fig. 3.59 3D VRT colour reconstruction, frontal plane

1. Sternum with metallic suture
- Full arrow = aneurysm

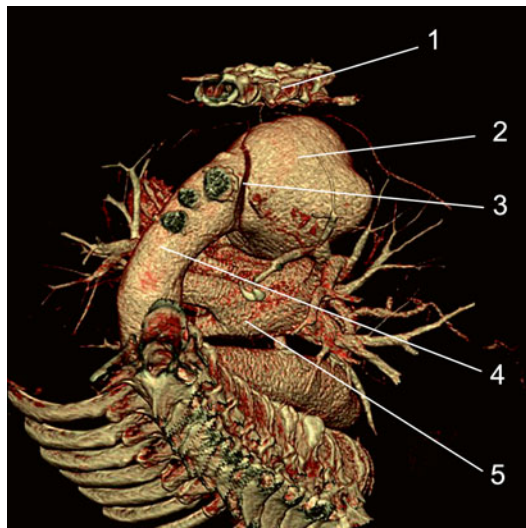


Fig. 3.60 3D VRT colour reconstruction, cranial plane

- 1. Sternum
- 2. Aneurysm
- 3. Dissection fold
- 4. Arcus aortae
- 5. Atrium sinistrum



Fig. 3.62 3D MIP reconstruction, transversal plane

- 1. True lumen of the aorta ascendens
- 2. Dissection fold
- 3. False lumen of the aorta ascendens
- 4. Aorta descendens

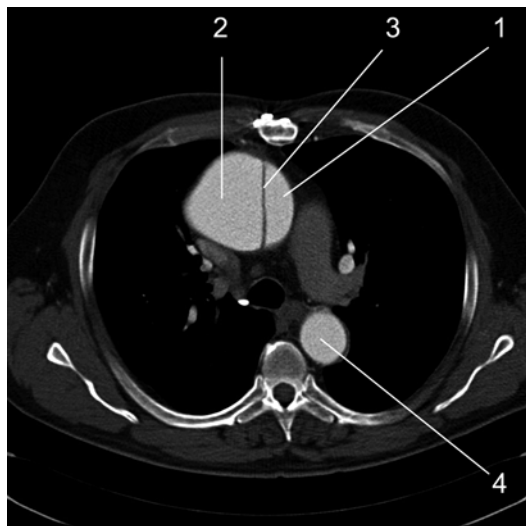


Fig. 3.61 3D VRT colour reconstruction, transversal plane

- 1. True lumen of the aorta ascendens
- 2. False lumen of the aorta ascendens
- 3. Dissection fold
- 4. Aorta descendens

3.11 Pulmonary Thromboembolism

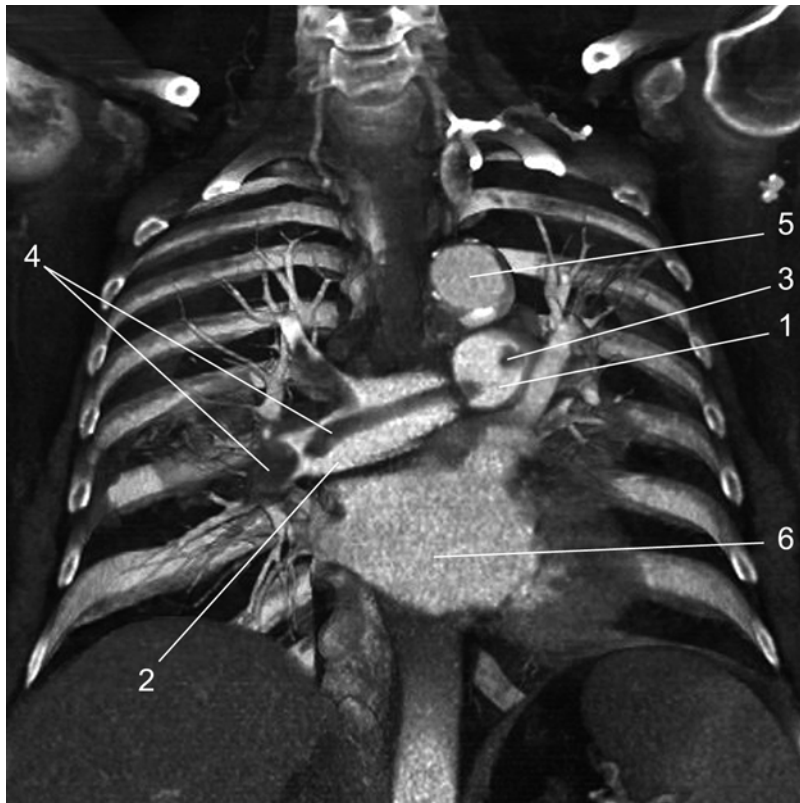


Fig. 3.63 3D MIP reconstruction, frontal plane

1. A. pulmonalis sinistra
2. A. pulmonalis dextra
3. Thrombus in a. pulmonalis sinistra
4. Thrombus in a. pulmonalis dextra
5. Aorta
6. Atrium sinistrum

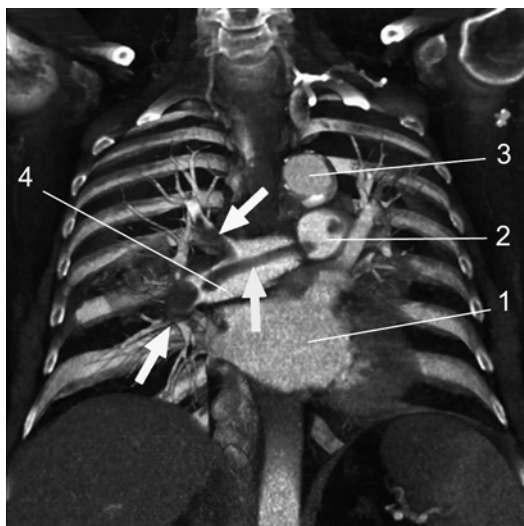


Fig. 3.64 3D MIP reconstruction, frontal plane

1. Atrium sinistrum
 2. A. pulmonalis sinistra
 3. Aorta
 4. A. pulmonalis dextra
- The full arrow indicates thrombus



Fig. 3.65 3D MIP reconstruction, frontal plane

The full arrow indicates thrombus



Fig. 3.66 3D MIP reconstruction, frontal plane
The full arrow indicates thrombus

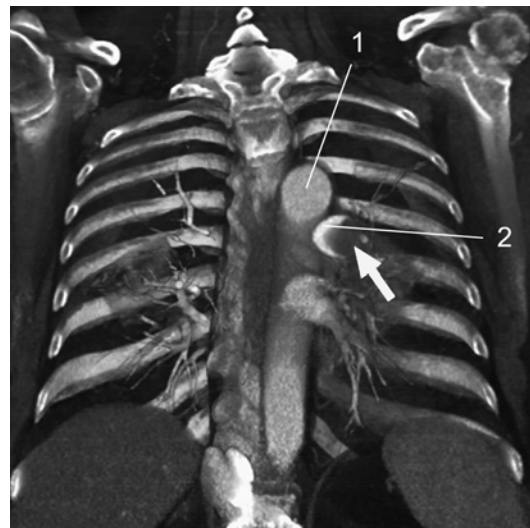


Fig. 3.68 3D MIP reconstruction, frontal plane
1. Aorta
2. A. pulmonalis sinistra
Full arrow indicates voluminous thrombus

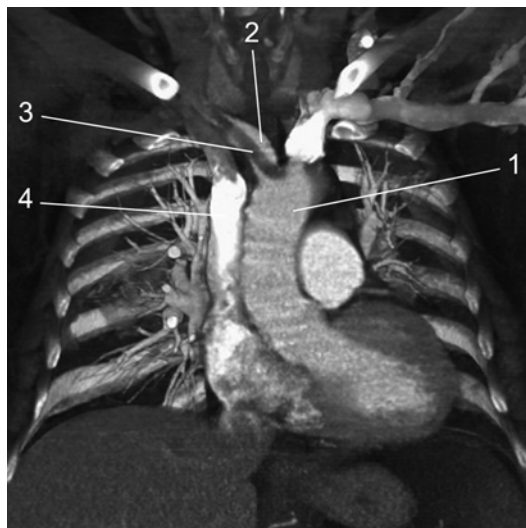


Fig. 3.67 3D MIP reconstruction, frontal plane
1. Aorta ascendens
2. Truncus brachiocephalicus
3. Thrombus at the level of the truncus brachiocephalicus
4. V. cava superior

3.12 Right Partially Anomalous Venous Drainage

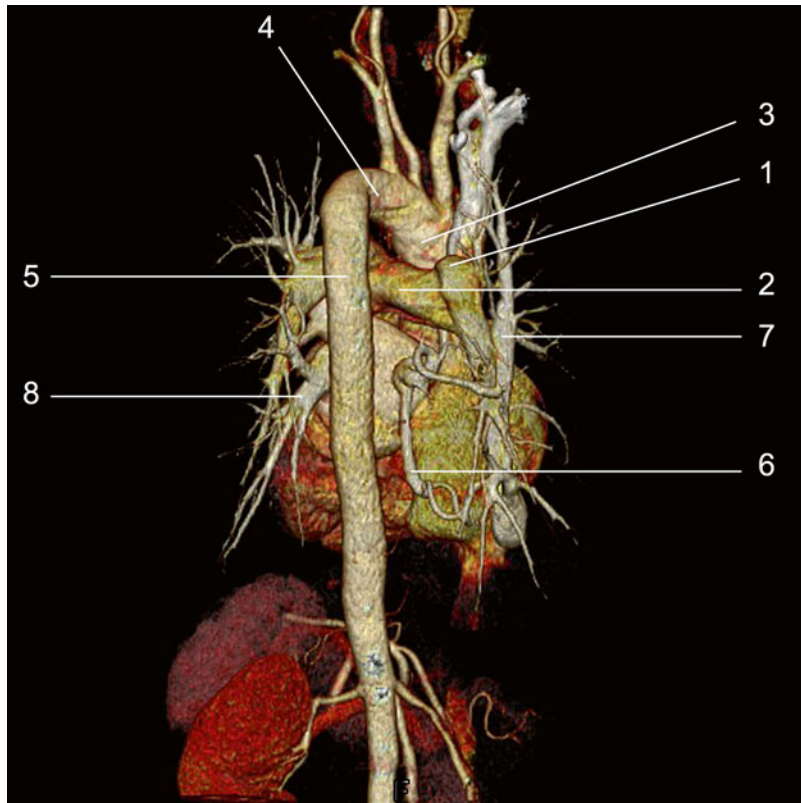


Fig. 3.69 3D VRT colour reconstruction, after removal of the thoracic cage, posterior plane

1. A. pulmonalis dextra
2. A. pulmonalis sinistra
3. Aorta ascendens
4. Arcus aortae
5. Aorta descendens
6. V. pulmonalis dextra superior
7. Aberrant collector with drainage in v. cava inferior
8. V. pulmonalis sinistra

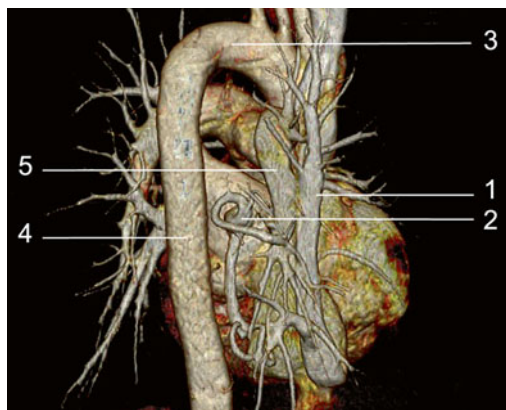


Fig. 3.70 3D VRT colour reconstruction, after removal of the thoracic cage, right posterior oblique plane

1. Aberrant venous collector
2. V. pulmonalis dextra
3. Arcus aortae
4. Aorta descendens
5. A. pulmonalis dextra

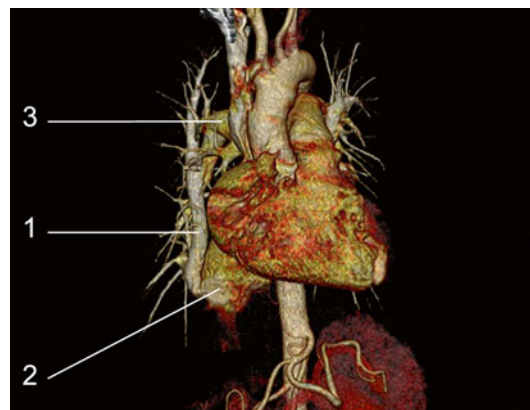


Fig. 3.71 3D VRT colour reconstruction, frontal plane

1. Pulmonary aberrant venous collector
2. V. cava superior
3. A. pulmonalis dextra

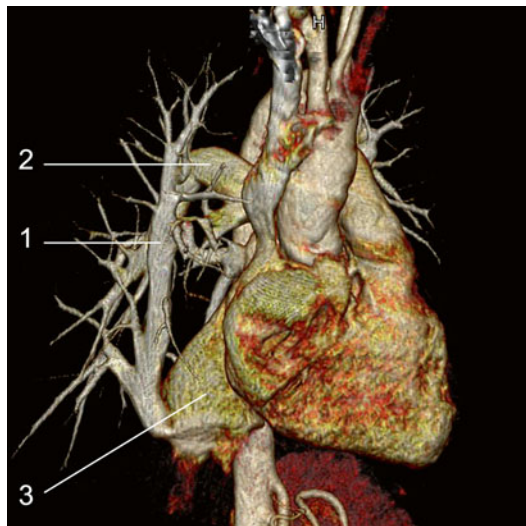


Fig. 3.72 3D VRT colour reconstruction, right anterior oblique plane
1. Pulmonary aberrant venous collector
2. A. pulmonalis dextra
3. V. cava inferior

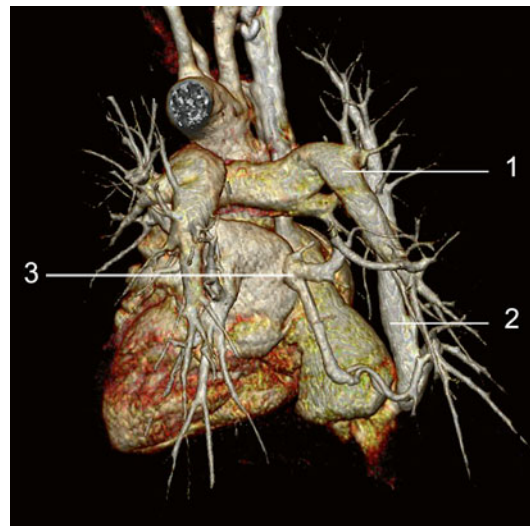


Fig. 3.74 3D VRT colour reconstruction, posterior plane
1. A. pulmonalis dextra
2. Pulmonary aberrant venous collector
3. V. pulmonalis dextra

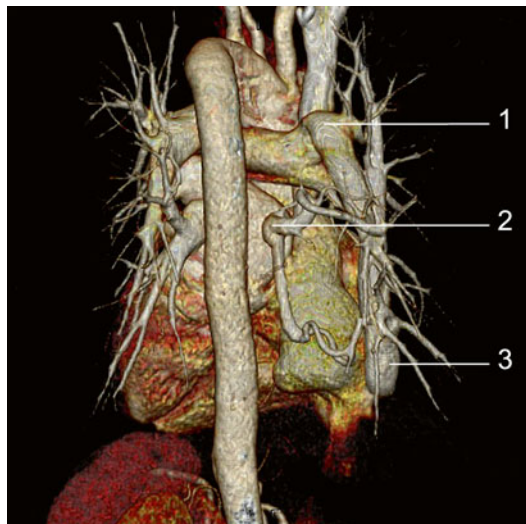


Fig. 3.73 3D VRT colour reconstruction, posterior plane
1. A. pulmonalis dextra
2. V. pulmonalis dextra
3. Pulmonary aberrant venous collector

3.13 Partially Aberrant Venous Drainage

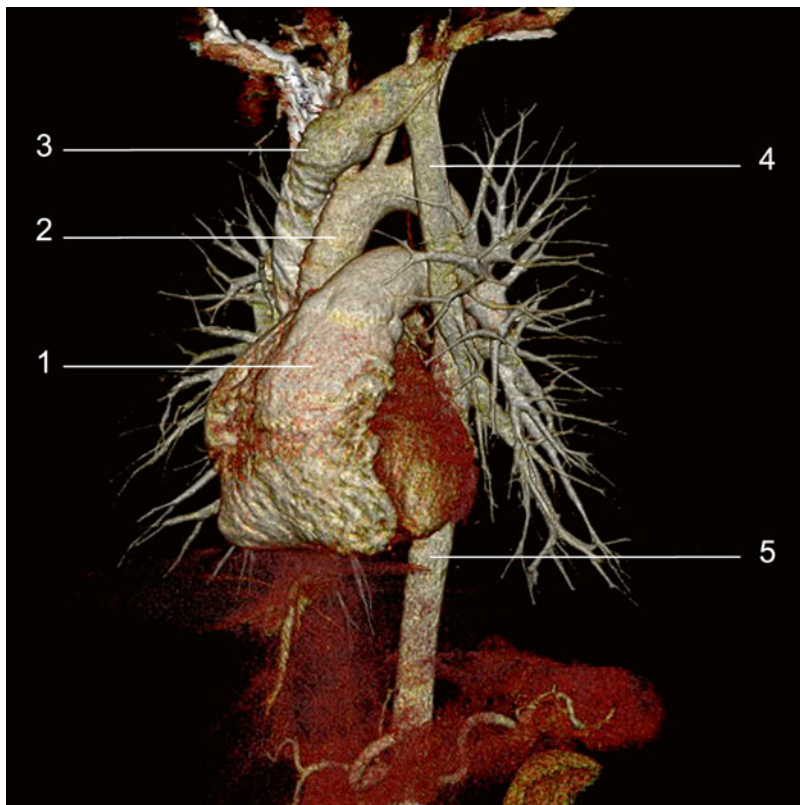


Fig. 3.75 3D VRT colour reconstruction, after removal of the thoracic cage, posterior plane

1. Truncus a. pulmonalis
2. Aorta ascendens
3. Vena cava superior
4. Aberrant venous collector
5. Aorta descendens

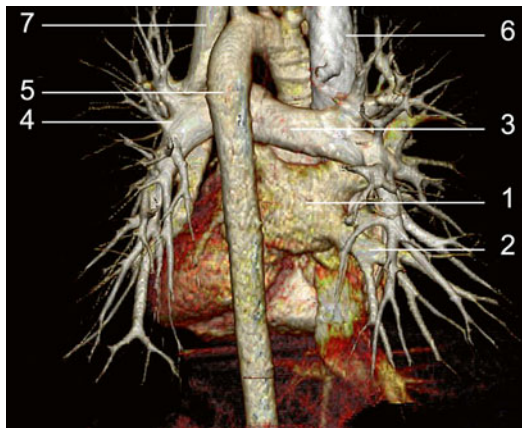


Fig. 3.76 3D VRT colour reconstruction, after removal of the thoracic cage, posterior plane

1. Atrium sinistrum
2. V. pulmonalis dextra inferior
3. A. pulmonalis dextra
4. A. pulmonalis sinistra
5. Aorta descendens
6. V. cava superior
7. Aberrant venous collector

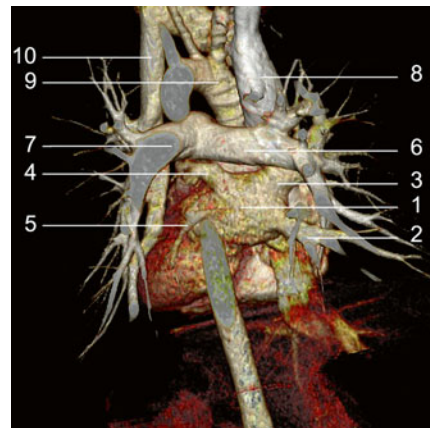


Fig. 3.78 3D VRT colour reconstruction, after removal of the thoracic cage, posterior plane

1. Atrium sinistrum
2. V. pulmonalis dextra inferior
3. V. pulmonalis dextra superior
4. V. pulmonalis sinistra superior
5. V. pulmonalis sinistra inferior
6. A. pulmonalis dextra
7. A. pulmonalis sinistra
8. V. cava superior
9. Arcus aortae
10. Aberrant venous collector



Fig. 3.77 3D VRT colour reconstruction, after removal of the thoracic cage, posterior oblique plane

1. Atrium sinistrum
2. V. pulmonalis sinistra superior
3. A. pulmonalis dextra
4. Arcus aortae
5. Aorta thoracica

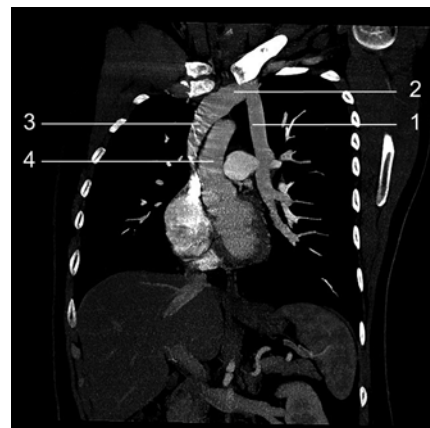


Fig. 3.79 3D MIP reconstruction

1. Aberrant venous collector
2. Truncus brachiocephalicus dexter
3. V. cava superior
4. Aorta ascendens

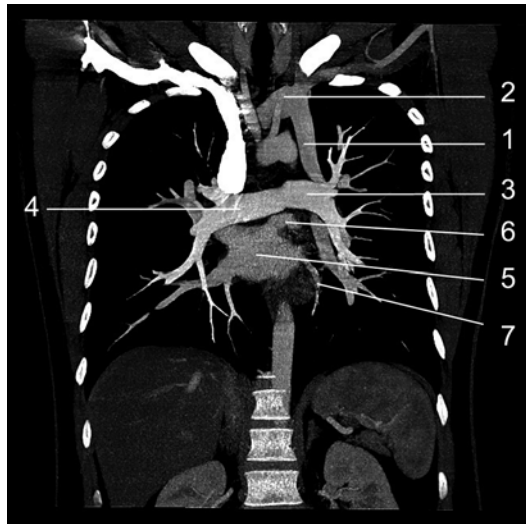


Fig. 3.80 3D MIP reconstruction

1. Aberrant venous collector
2. V. brachiocephalica sinistra
3. A. pulmonalis sinistra
4. A. pulmonalis dextra
5. Atrium sinistrum
6. V. pulmonalis sinistra superior
7. V. pulmonalis sinistra inferior

3.14 Interrupted Arcus Aortae

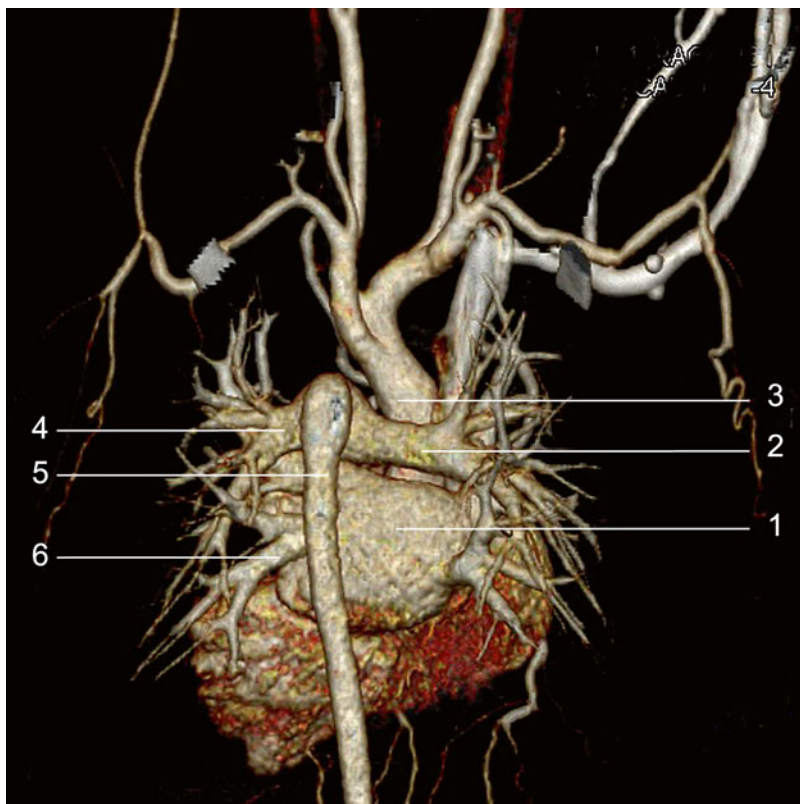


Fig. 3.81 3D VRT colour reconstruction, after removal of the thoracic cage

1. Atrium sinistrum
2. A. pulmonalis dextra
3. Aorta ascendens
4. A. pulmonalis sinistra
5. Aorta descendens
6. V. pulmonalis sinistra

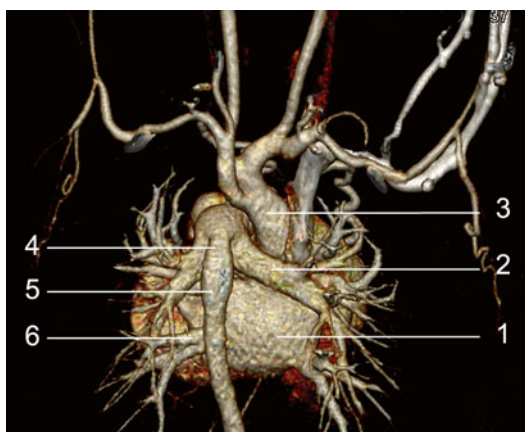


Fig. 3.82 3D VRT colour reconstruction, after removal of the thoracic cage

1. Atrium sinistrum
2. A. pulmonalis dextra
3. Aorta ascendens
4. Persistent arterial channel
5. Aorta descendens
6. V. pulmonalis sinistra

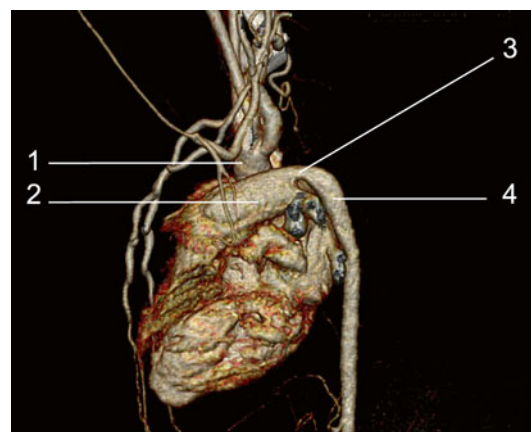


Fig. 3.83 3D VRT colour reconstruction, after removal of the thoracic cage

1. Aorta ascendens
2. Truncus a. pulmonalis
3. Persistent arterial channel
4. Aorta descendens

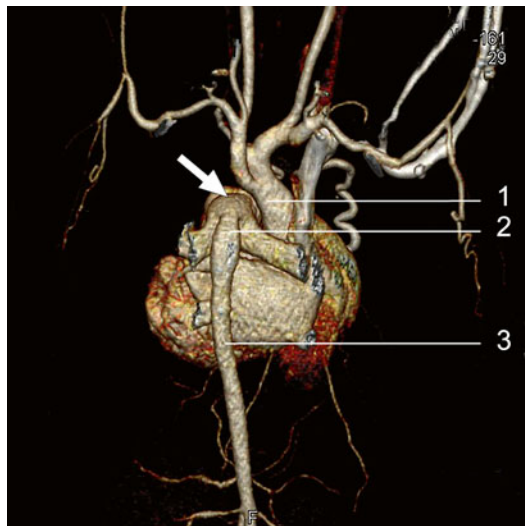


Fig. 3.84 3D VRT colour reconstruction, after removal of the thoracic cage
1. Aorta ascendens
2. Persistent arterial channel
3. Aorta descendens
The full arrow indicates the area in which the arcus aortae is not visualised

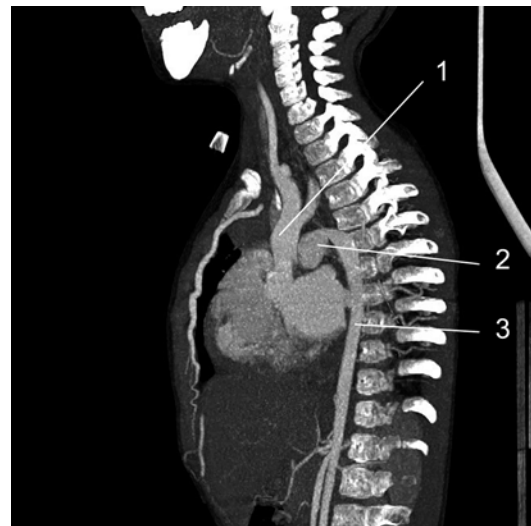


Fig. 3.86 3D MIP reconstruction, sagittal plane
1. Aorta ascendens
2. Persistent arterial channel
3. Aorta descendens

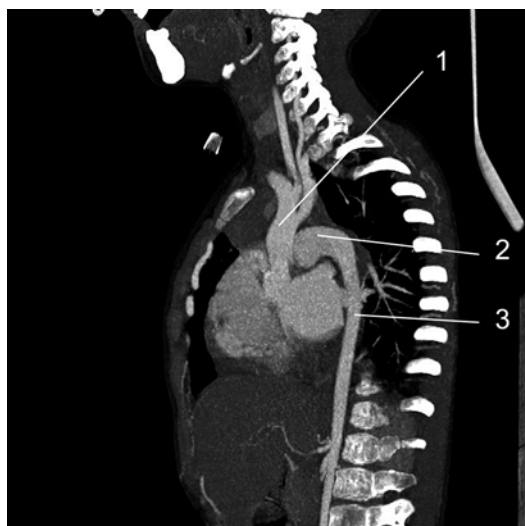


Fig. 3.85 3D MIP reconstruction, sagittal plane
1. Aorta ascendens
2. Persistent arterial channel
3. Aorta descendens

Contents

4.1	Normal Arteriae Coronariae	86
4.2	Abnormal Emergence of the R. Circumflexus	89
4.3	Abnormal Emergence of the A. Coronaria Dextra Placed on the Posterior Aortic Wall	91
4.4	Emergence Through Separate Ostium of the Three A. Coronariae	93
4.5	Abnormal A. Coronaria dextra emergence from the Truncus A. Pulmonalis	95
4.6	Coronary and Aortopulmonary Fistulas	98
4.7	Coronary Calcification	101
4.8	Monovascular Coronary Disease: A. Coronaria Dextra Occlusion	103
4.9	Occlusive Lesion at the Middle Segment of the R. Interventricularis Anterior – Collateral Circulation A. Coronaria Dextra – R. Interventricularis Anterior	105
4.10	Bivascular Coronary Disease	107
4.11	Trivascular Coronary Disease	110
4.12	Aneurysm of the Left Ventricle and R. Interventricularis Anterior Occlusion	113
4.13	Monovascular Coronary Disease Patent Stent in the Middle Segment of R. Interventricularis Anterior	116
4.14	Restenosis at Stent Level	119
4.15	Occlusion of R. Interventricularis Anterior	122
4.16	Coronary Bypass Evaluation	124
4.17	Fallot Tetralogy	126
4.18	Fallot Tetralogy in an Adult Patient	128

4.1 Normal Arteriae Coronariae

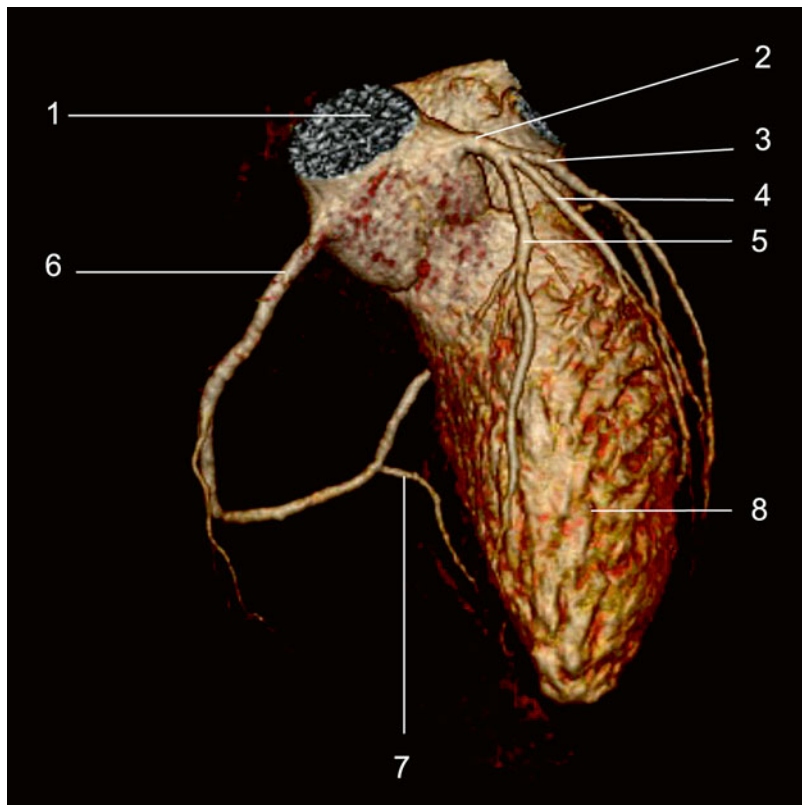
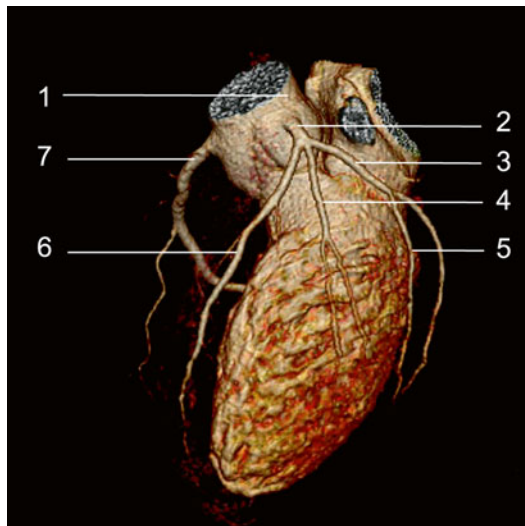
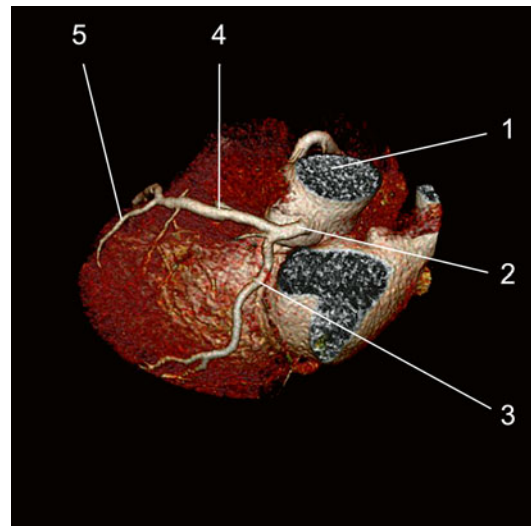


Fig. 4.1 Coronary CT angiography – 3D VRT colour reconstruction

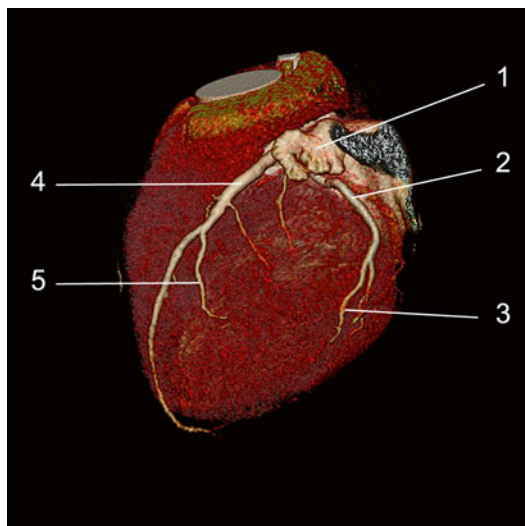
1. Aorta
2. A. coronaria sinistra
3. R. circumflexus
4. R. atrialis intermedius
5. A. interventricularis anterior
6. A. coronaria dextra
7. A. interventricularis posterior
8. Ventriculus sinister

**Fig. 4.2** Coronary CT angiography 3D VRT reconstruction

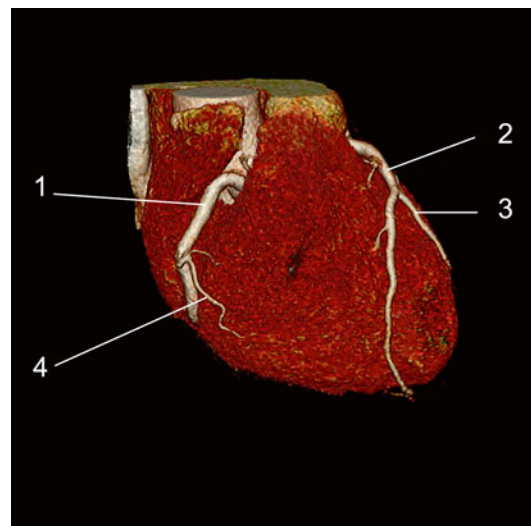
1. Aorta
2. A. coronaria sinistra
3. R. circumflexus
4. R. atrialis intermedius
5. R. marginalis sinister
6. R. interventricularis anterior
7. A. coronaria dextra

**Fig. 4.4** Coronary CT angiography 3D VRT reconstruction

1. Aorta
2. A. coronaria sinistra
3. R. circumflexus
4. R. interventricularis anterior
5. R. marginalis anterior

**Fig. 4.3** Coronary CT angiography 3D VRT reconstruction

1. Auricula sinister
2. R. circumflexus
3. R. marginalis sinister
4. R. interventricularis anterior
5. R. lateralis

**Fig. 4.5** Coronary CT angiography 3D VRT reconstruction

1. A. coronaria dextra
2. R. interventricularis anterior
3. R. diagonalis
4. Arteria marginalis dexter

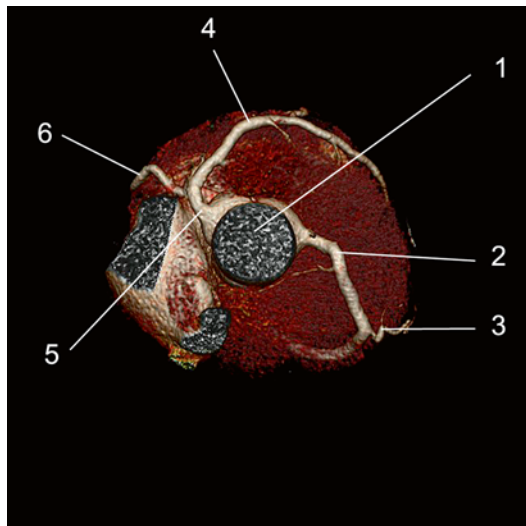


Fig. 4.6 Coronary CT angiography 3D VRT reconstruction

1. Aorta
2. A. coronaria dextra
3. R. marginalis dexter
4. R. interventricularis anterior
5. A. coronaria sinistra
6. R. circumflexus

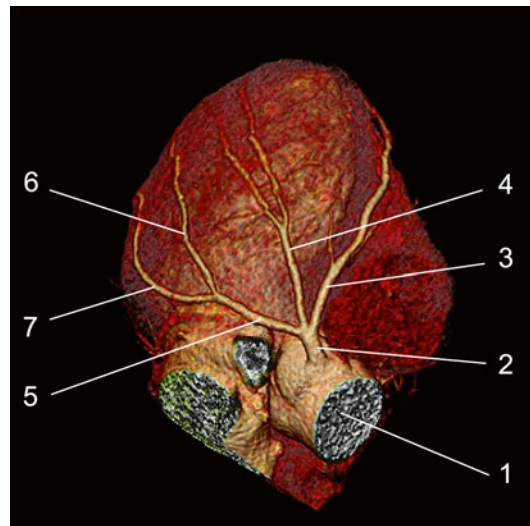


Fig. 4.7 Coronary CT angiography 3D VRT reconstruction

1. Aorta
2. A. coronaria sinistra
3. R. marginalis sinister
4. R. atrialis intermedius
5. R. circumflexus
6. R. marginalis sinister
7. R. marginalis sinister

4.2 Abnormal Emergence of the R. Circumflexus

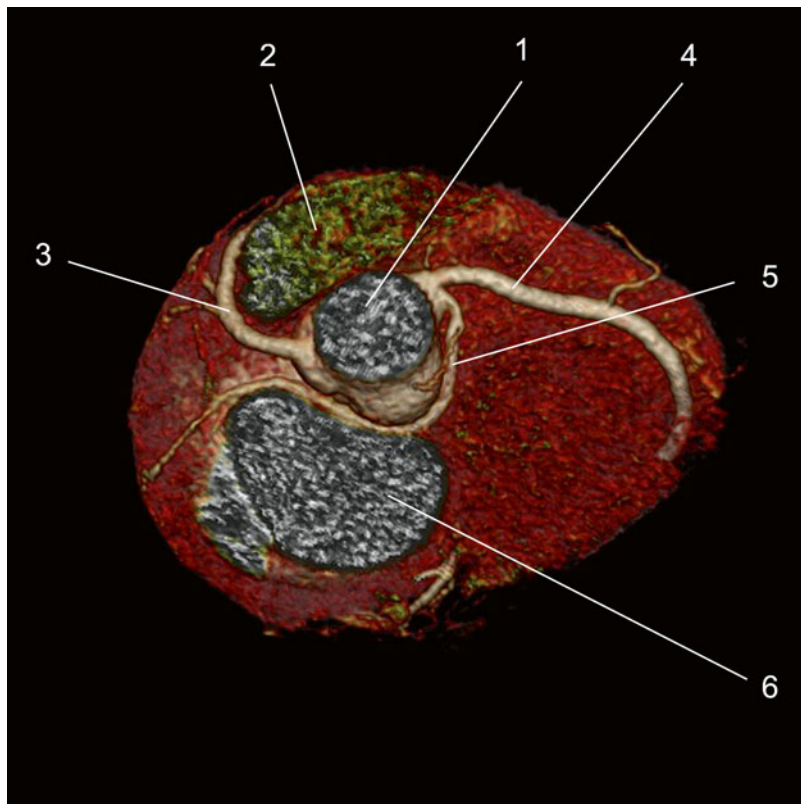


Fig. 4.8 Coronary CT angiography 3D VRT colour reconstruction

1. Aorta
2. Truncus a. pulmonalis cut out during post-processing operation
3. R. interventricularis anterior
4. A. coronaria dextra
5. R. circumflexus with retroaortic course
6. Atrium sinistrum

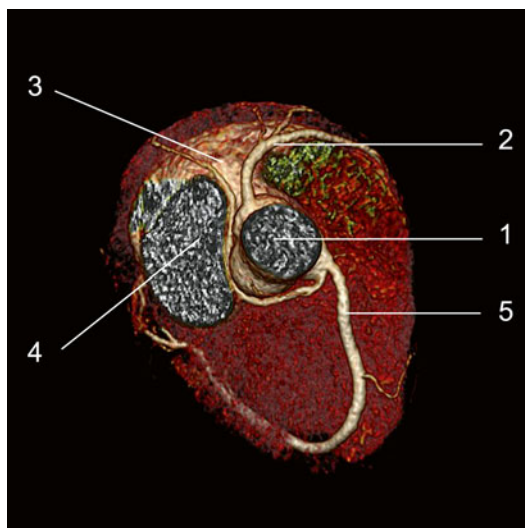


Fig. 4.9 Coronary CT angiography 3D VRT colour reconstruction

1. Aorta
2. R. interventricularis anterior
3. R. circumflexus
4. Atrium sinistrum
5. R. interventricularis posterior

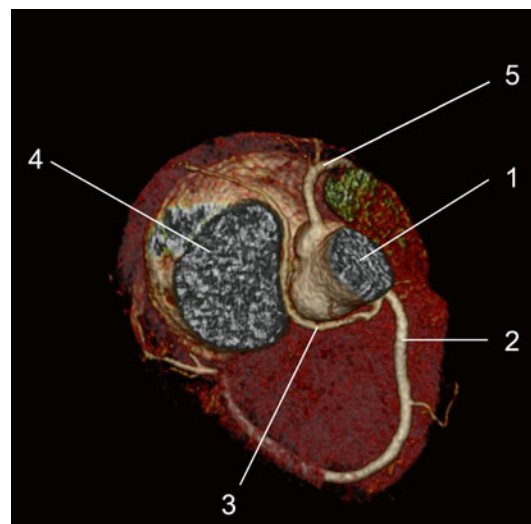


Fig. 4.10 Coronary CT angiography 3D VRT colour reconstruction

1. Aorta
2. Arteria coronaria dextra
3. R. circumflexus
4. Atrium sinistrum
5. R. interventricularis anterior

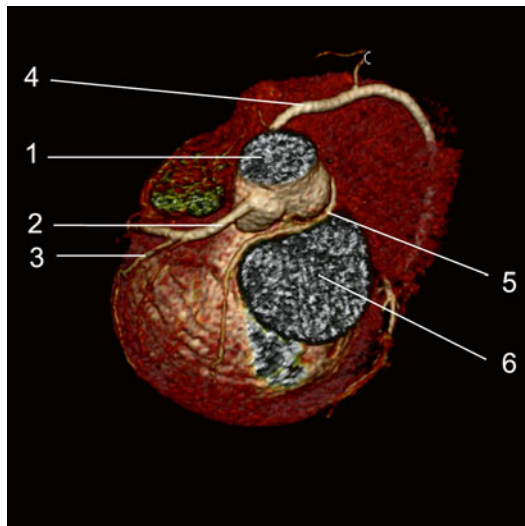


Fig. 4.11 Coronary CT angiography 3D VRT colour reconstruction

1. Aorta
2. R. interventricularis anterior
3. R. lateralis
4. A. coronaria dextra
5. R. circumflexus
6. Atrium sinistrum

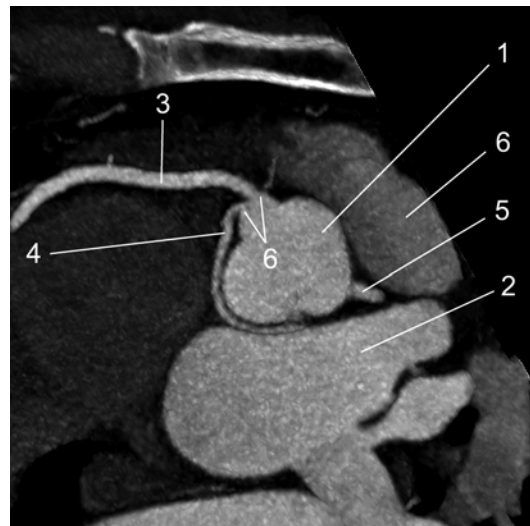


Fig. 4.13 Angiography 3D MIP reconstruction

1. Aorta
2. Atrium sinistrum
3. A. coronaria dextra
4. R. circumflexus
5. R. interventricularis anterior
6. Separate ostium of the two arteriae coronariae (a. coronaria dextra and r. circumflexus)

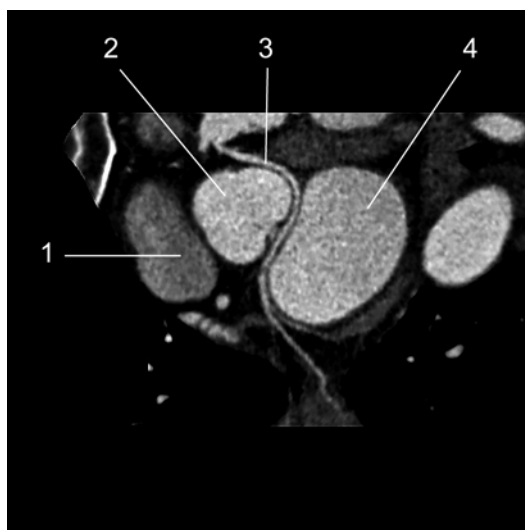


Fig. 4.12 Angiography 3D MIP reconstruction

1. Aorta
2. R. circumflexus with retroaortic course anterior from the atrium sinistrum
3. Atrium sinistrum
4. A. pulmonalis

4.3 Abnormal Emergence of the A. Coronaria Dextra Placed on the Posterior Aortic Wall

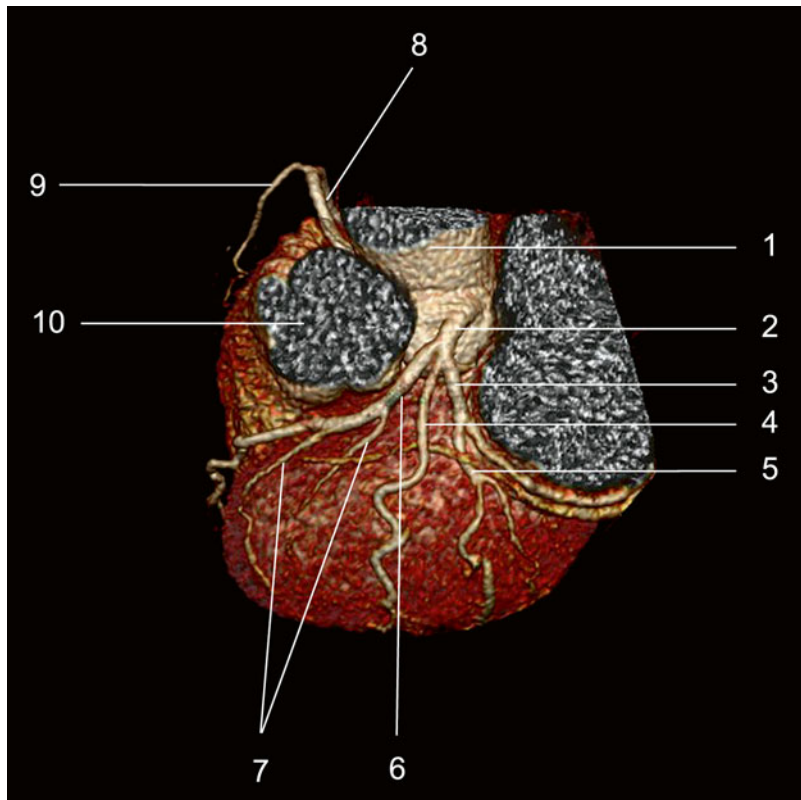


Fig. 4.14 Coronary CT angiography 3D VRT colour reconstruction

1. Aorta
2. Truncus a. coronaria sinistra
3. R. circumflexus
4. R. atrialis intermedius
5. R. marginalis sinister
6. R. interventricularis anterior
7. R. lateralis
8. A. coronaria dextra
9. R. marginalis dexter
10. Truncus a. pulmonalis

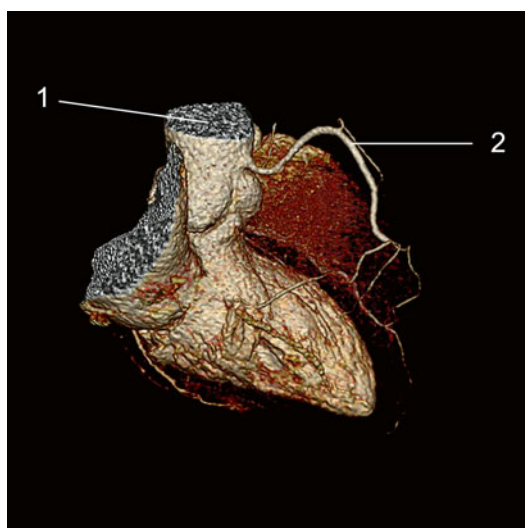


Fig. 4.15 Coronary CT angiography 3D VRT colour reconstruction

1. Aorta
2. Emergent a. coronaria dextra sited on the posterior aortic wall above the sinus aortae

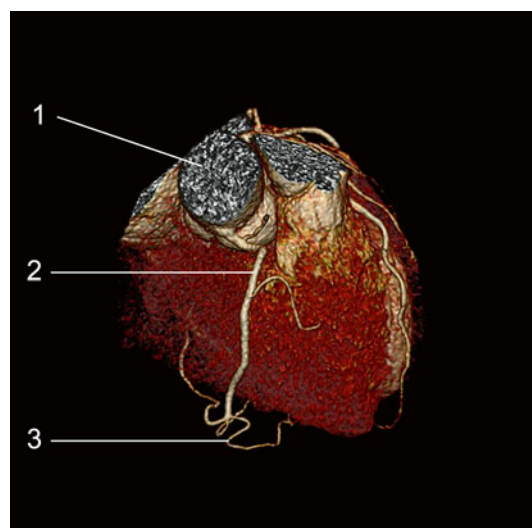


Fig. 4.16 Coronary CT angiography 3D VRT colour reconstruction

1. Aorta
2. Emergent a. coronaria dextra sited on the posterior aortic wall above the sinus aortae
3. R. marginalis dexter

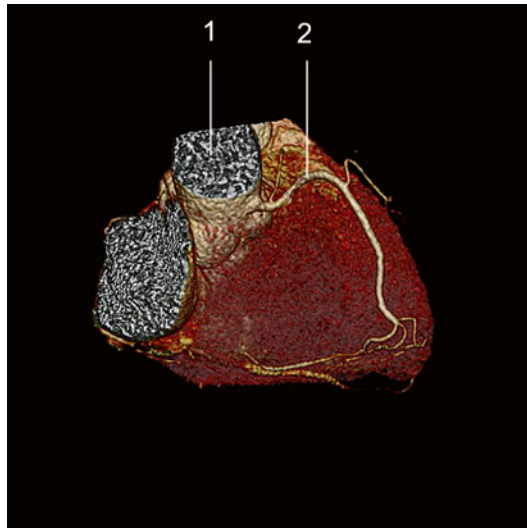


Fig. 4.17 Coronary CT angiography 3D VRT colour reconstruction
1. Aorta
2. A. coronaria dextra

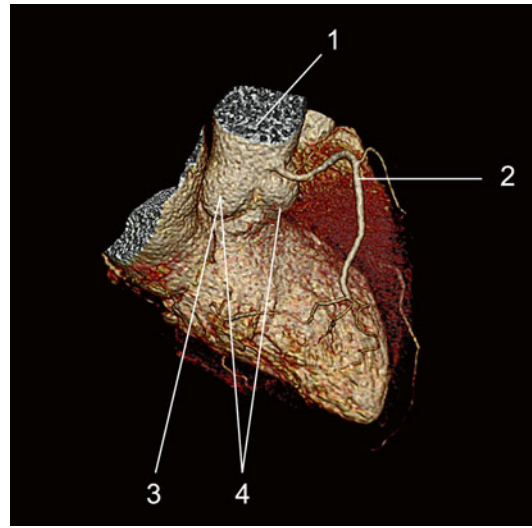


Fig. 4.18 Coronary CT angiography 3D VRT colour reconstruction
1. Aorta
2. A. coronaria dextra
3. Non-coronary cuspis of the sinus aortae
4. Right coronary cuspis, in this case a non-coronary cuspis due to the abnormal emergence of the a. coronaria dextra

4.4 Emergence Through Separate Ostium of the Three A. Coronariae

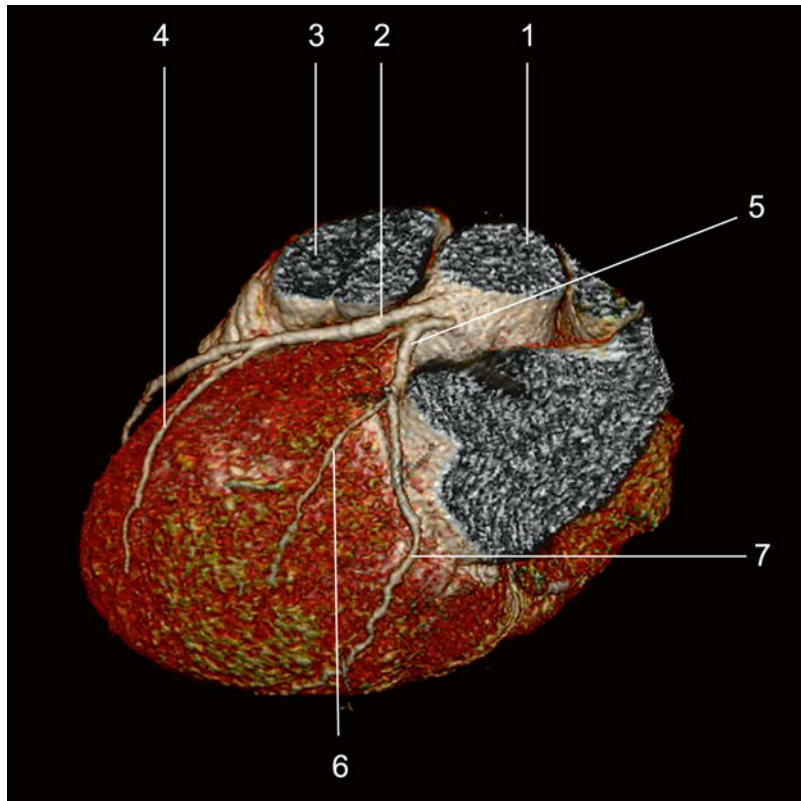


Fig. 4.19 Coronary CT angiography 3D VRT colour reconstruction

1. Aorta
2. A. coronaria sinistra
3. A. pulmonalis
4. R. lateralis
5. R. circumflexus
6. R. marginalis sinister
7. R. marginalis sinister

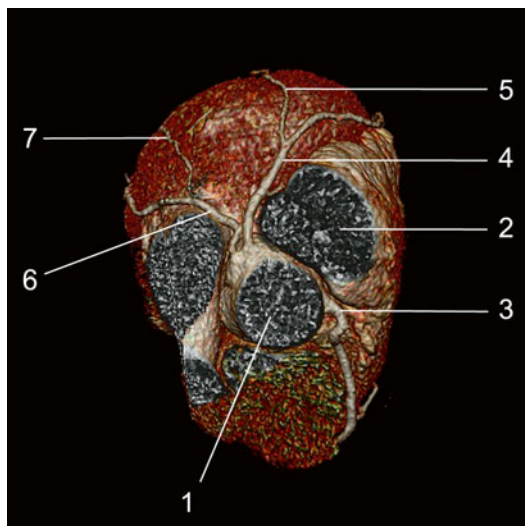


Fig. 4.20 Coronary CT angiography 3D VRT colour reconstruction

1. Aorta
2. A. pulmonalis
3. A. coronaria dextra
4. R. interventricularis anterior
5. R. lateralis
6. R. circumflexus
7. R. marginalis sinister

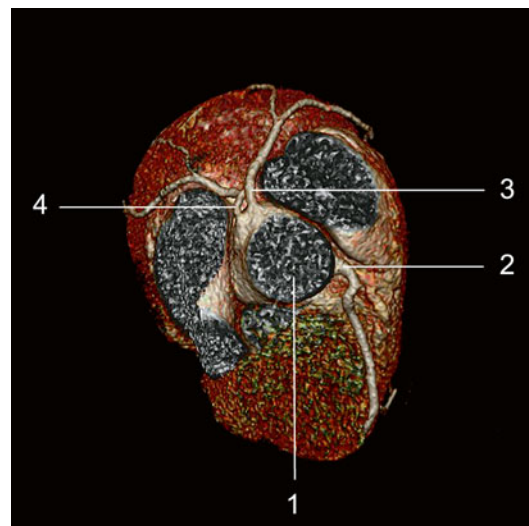


Fig. 4.22 Coronary CT angiography 3D VRT colour reconstruction

1. The aorta with three separated ostium emergencies of the a. coronaria
2. A. coronaria dextra
3. R. interventricularis anterior
4. R. circumflexus

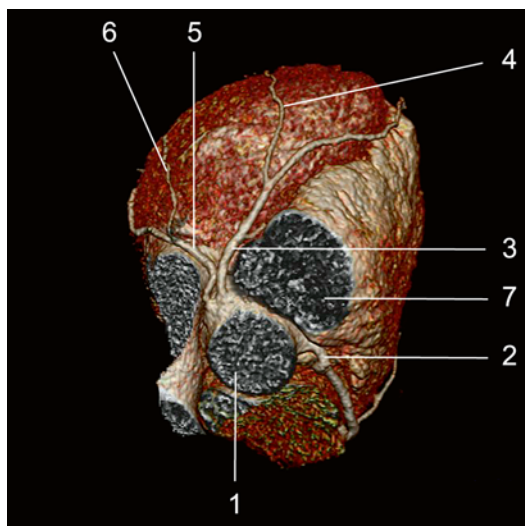


Fig. 4.21 Coronary CT angiography 3D VRT colour reconstruction

1. Aorta
2. A. coronaria dextra
3. R. interventricularis anterior
4. R. lateralis
5. R. circumflexus
6. R. marginalis sinister
7. A pulmonalis

4.5 Abnormal A. Coronaria dextra emergence from the Truncus A. Pulmonalis

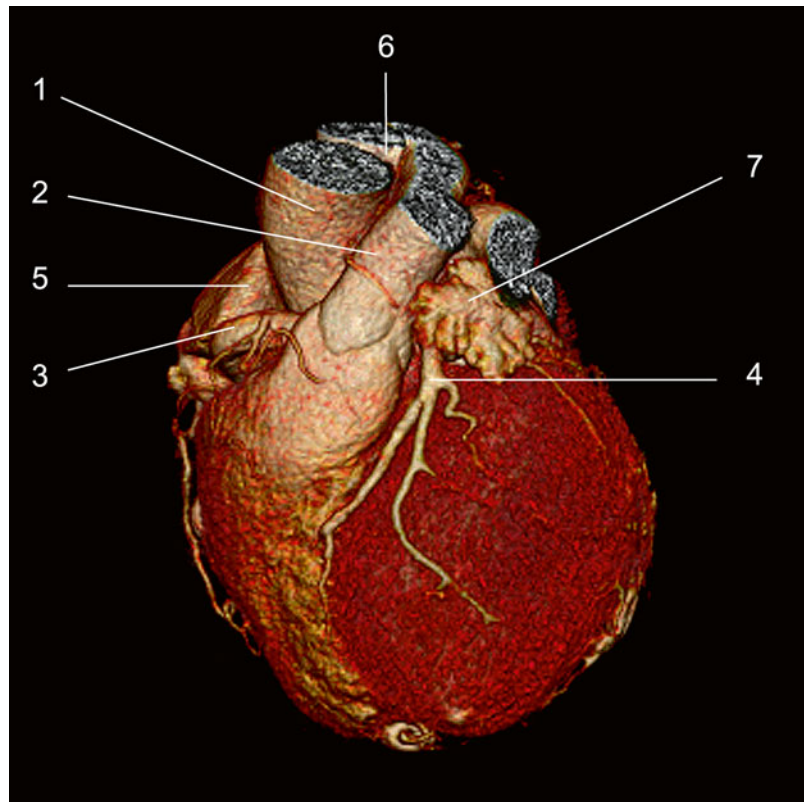


Fig. 4.23 Coronary CT angiography 3D VRT colour reconstruction

1. Aorta
2. Truncus a. pulmonalis
3. A. coronaria dextra
4. A. coronaria sinistra
5. Auricula dextra
6. Vena cava superior
7. Auricula sinistra

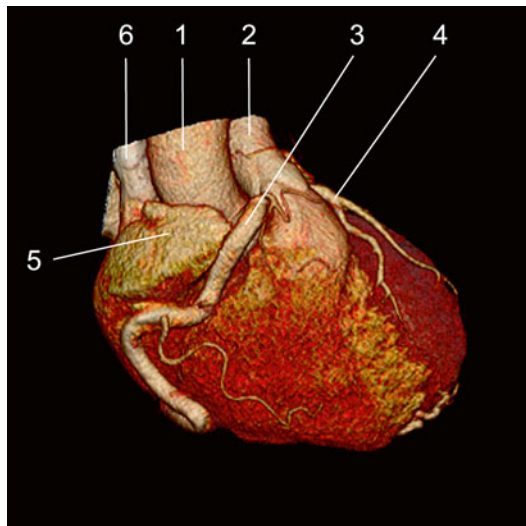


Fig. 4.24 3D VRT colour reconstruction

- 1. Aorta
- 2. Truncus a. pulmonalis
- 3. A. coronaria dextra
- 4. A. coronaria sinistra
- 5. Auricula dextra
- 6. Vena cava superior

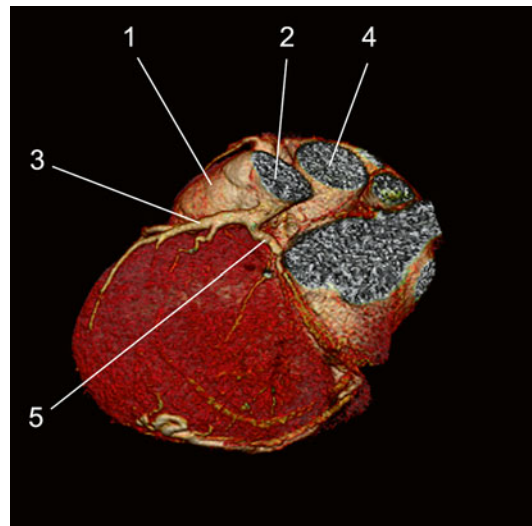


Fig. 4.26 3D VRT colour reconstruction

- 1. Truncus a. pulmonalis
- 2. A. coronaria sinistra
- 3. A. interventricularis anterior
- 4. Aorta
- 5. R. circumflexus

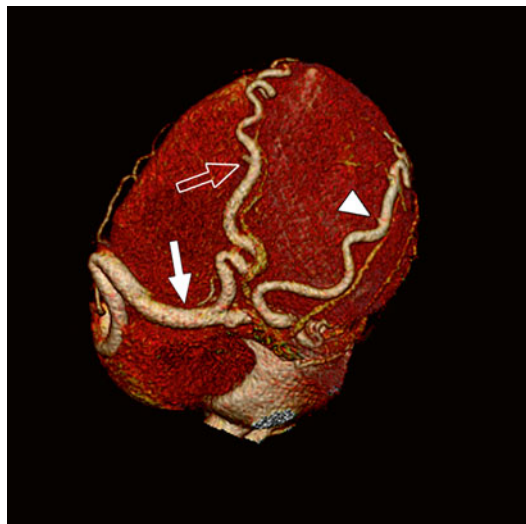


Fig. 4.25 3D VRT colour reconstruction

Full arrow=a. coronaria dextra
Arrow with contour=r.interventricularis posterior
The tip of the arrow=r. posterolateralis dexter

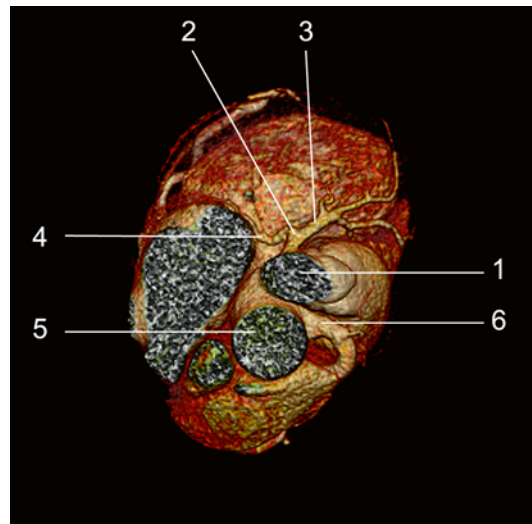
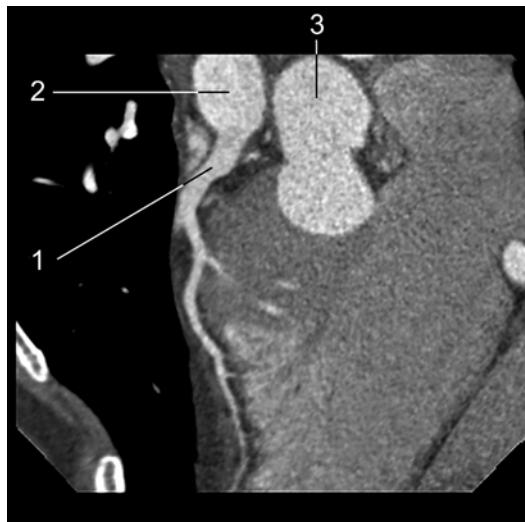
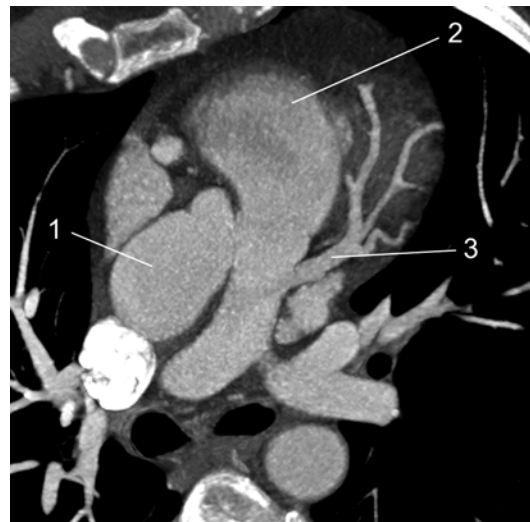


Fig. 4.27 3D VRT colour reconstruction

- 1. Truncus a. pulmonalis
- 2. A. coronaria sinistra
- 3. A. interventricularis anterior
- 4. R. circumflexus
- 5. Aorta
- 6. A. coronaria dextra

**Fig. 4.28** 3D MPR reconstruction

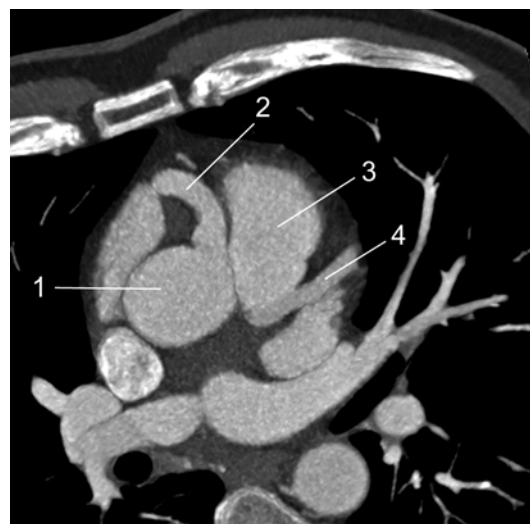
1. Truncus a. coronaria sinistra+r. interventricularis anterior
2. A. pulmonalis
3. Aorta

**Fig. 4.30** 3D MIP reconstruction

1. Aorta
2. Truncus a. pulmonalis
3. Truncus a. coronaria sinistra

**Fig. 4.29** 3D MIP reconstruction

1. Aorta
2. Truncus a. pulmonalis
3. Truncus a. coronaria sinistra

**Fig. 4.31** 3D MIP reconstruction

1. Aorta
2. A. coronaria dextra
3. A. pulmonalis
4. Truncus a. coronaria sinistra

4.6 Coronary and Aortopulmonary Fistulas

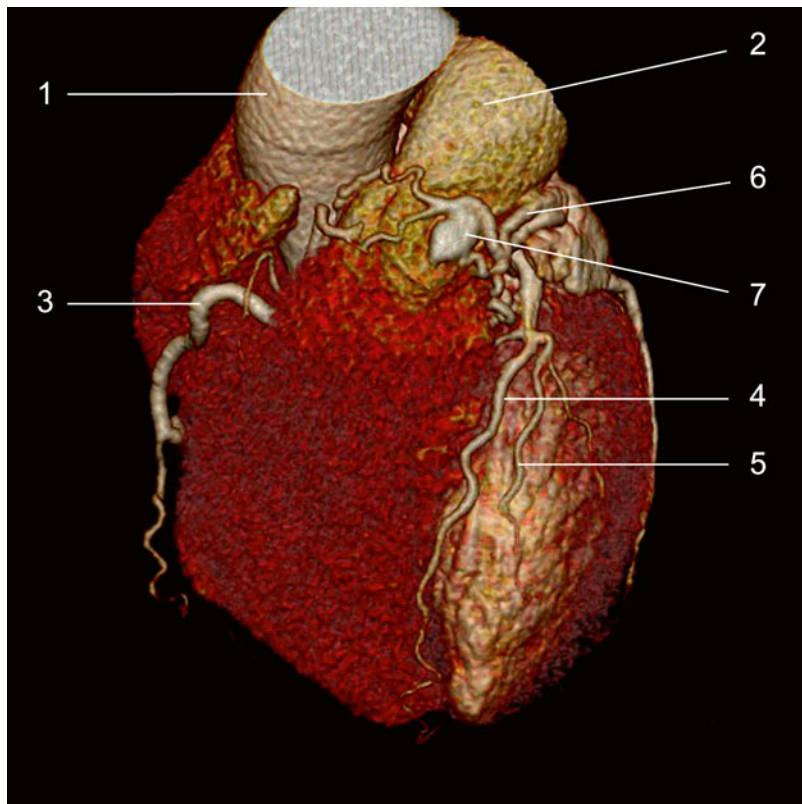
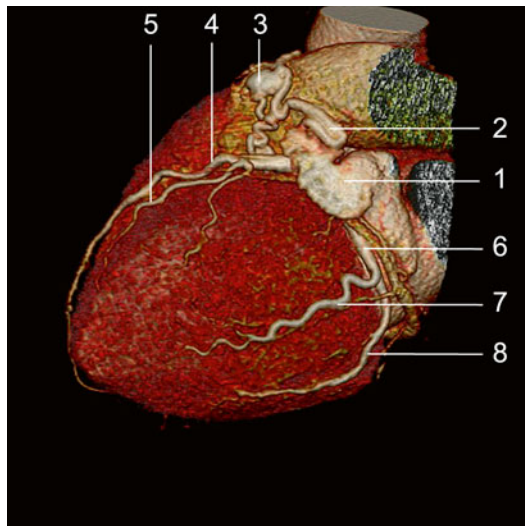
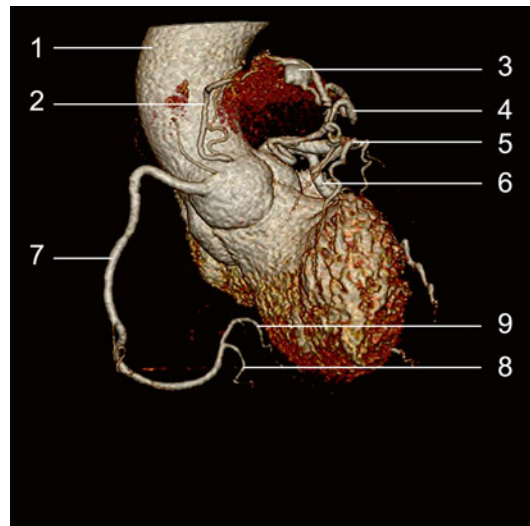


Fig. 4.32 Coronary CT angiography 3D VRT

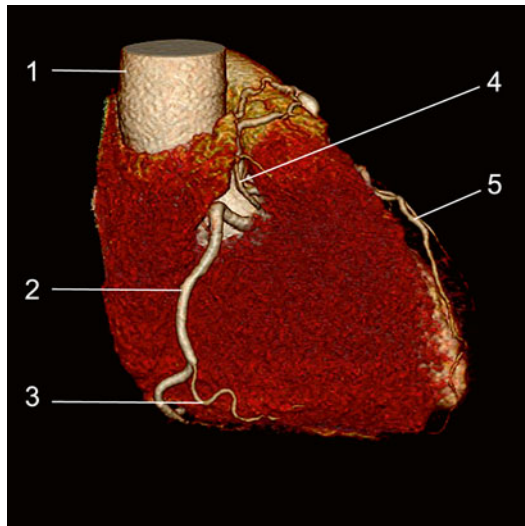
1. Aorta
2. Truncus a. pulmonalis
3. A. coronaria dextra
4. R. interventricularis
5. R. lateralis
6. Fistulous course between r. interventricularis anterior and a. pulmonalis
7. Aneurysmal dilatation at the confluence level of the fistulas' course

**Fig. 4.33** Coronary CTA 3D VRT

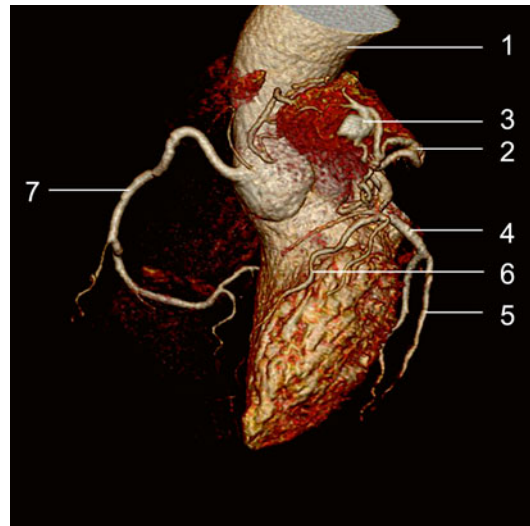
1. Auricula sinistra
2. Fistula
3. Aneurysm
4. R. interventricularis anterior
5. R. lateralis
6. R. circumflexus
7. R. marginalis sinister
8. R. marginalis sinister

**Fig. 4.35** Coronary CTA 3D VRT

1. Aorta
2. From the aorta emergent fistulous course
3. Aneurysmal dilatation
4. From the a. coronaria sinistra emergent fistulous course communicating with a. pulmonalis
5. R. interventricularis anterior
6. R. circumflexus
7. A. coronaria dextra
8. R. interventricularis posterior
9. R. posterolateralis dexter

**Fig. 4.34** Coronary CTA 3D VRT

1. Aorta
2. A. coronaria dextra
3. R. marginalis dexter
4. Frontal aorta emergent fistulous course
5. R. interventricularis anterior

**Fig. 4.36** Coronary CTA 3D VRT

1. Aorta
2. From the r. interventricularis anterior emergent fistulous course communicating with a. pulmonalis
3. Aneurysmal dilatation
4. R. circumflexus
5. R. marginalis sinister
6. R. interventricularis anterior
7. A. coronaria dextra

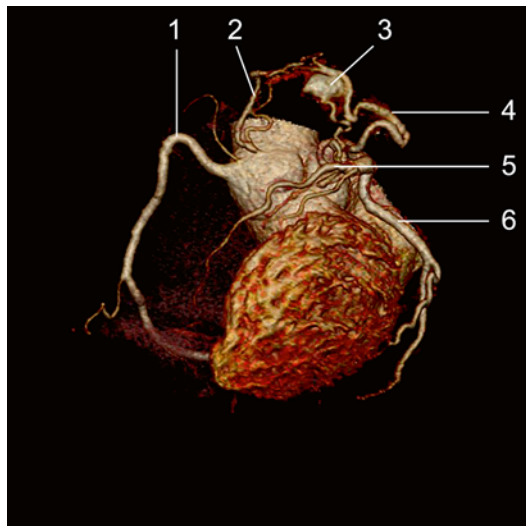


Fig. 4.37 Coronary CTA 3D VRT

1. A. coronaria dextra
2. Fistulous course
3. Aneurysmal dilatation
4. Fistulous course
5. R. interventricularis anterior
6. R. circumflexus

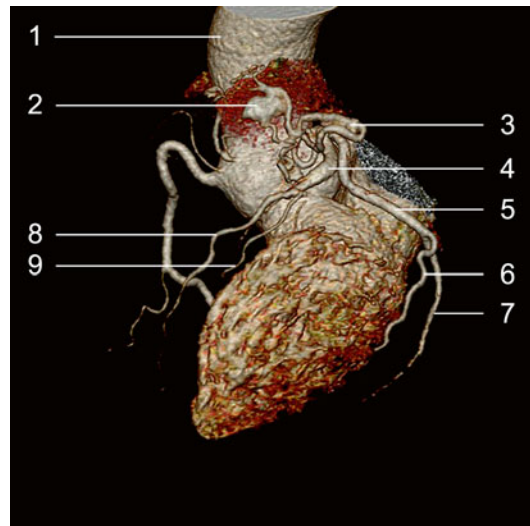


Fig. 4.38 Coronary CTA 3D VRT

1. Aorta
2. Aneurysmal dilatation
3. Fistulous course
4. R. interventricularis anterior, pars proximalis
5. R. circumflexus
6. R. marginalis sinister
7. R. marginalis sinister
8. R. interventricularis anterior
9. R. lateralis

4.7 Coronary Calcification

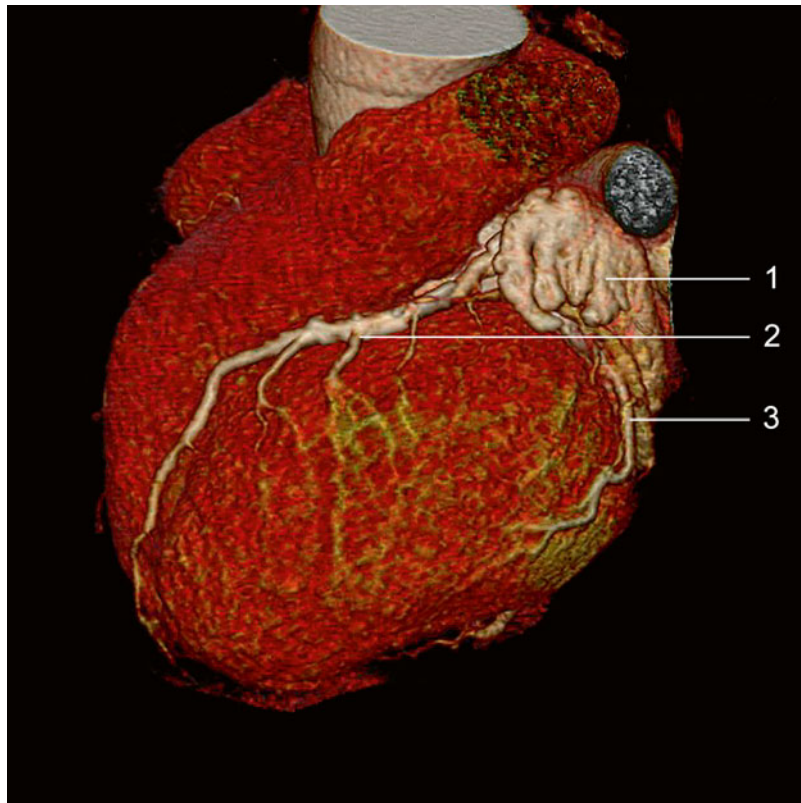


Fig. 4.39 Coronary CTA
3D VRT
1. Auricula sinistra
2. R. interventricularis
anterior
3. R. circumflexus

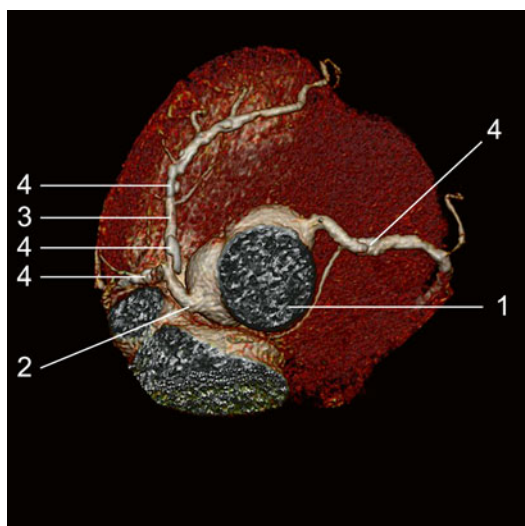


Fig. 4.40 Coronary CTA 3D VRT
1. Aorta
2. Truncus a. coronaria sinistra
3. R. interventricularis anterior
4. Calcified plaques located on the three a. coronariae

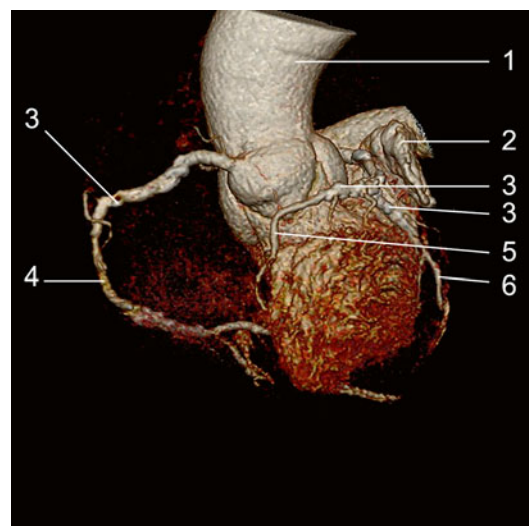


Fig. 4.41 Coronary CTA 3D VRT
1. Aorta
2. Auricula sinistra
3. Calcified plaques located on the three a. coronariae
4. A. coronaria dextra
5. A. interventricularis anterior
6. R. circumflexus

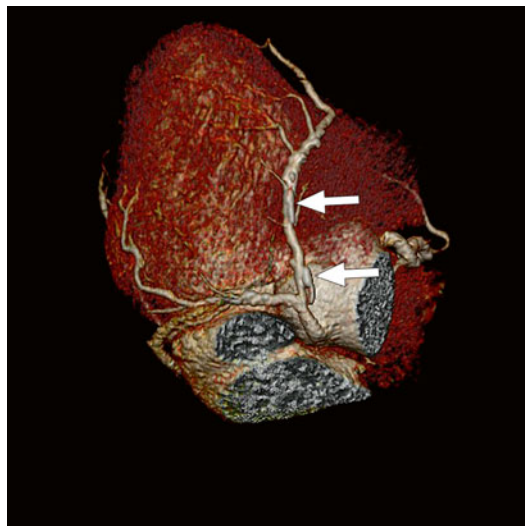


Fig. 4.42 Coronary CT angiography 3D VRT
The *full arrow* indicates calcified atheromatous plaques



Fig. 4.44 Coronary CT angiography 3D VRT
The *full arrow* indicates calcified atheromatous plaques

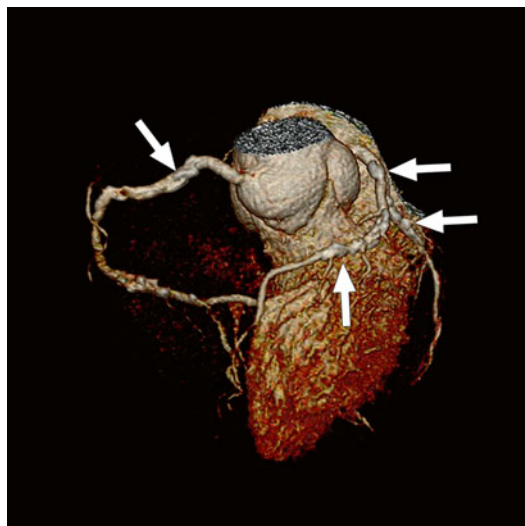


Fig. 4.43 Coronary CT angiography 3D VRT
The *full arrow* indicates calcified atherosomatous plaques

4.8 Monovascular Coronary Disease: A. Coronaria Dextra Occlusion

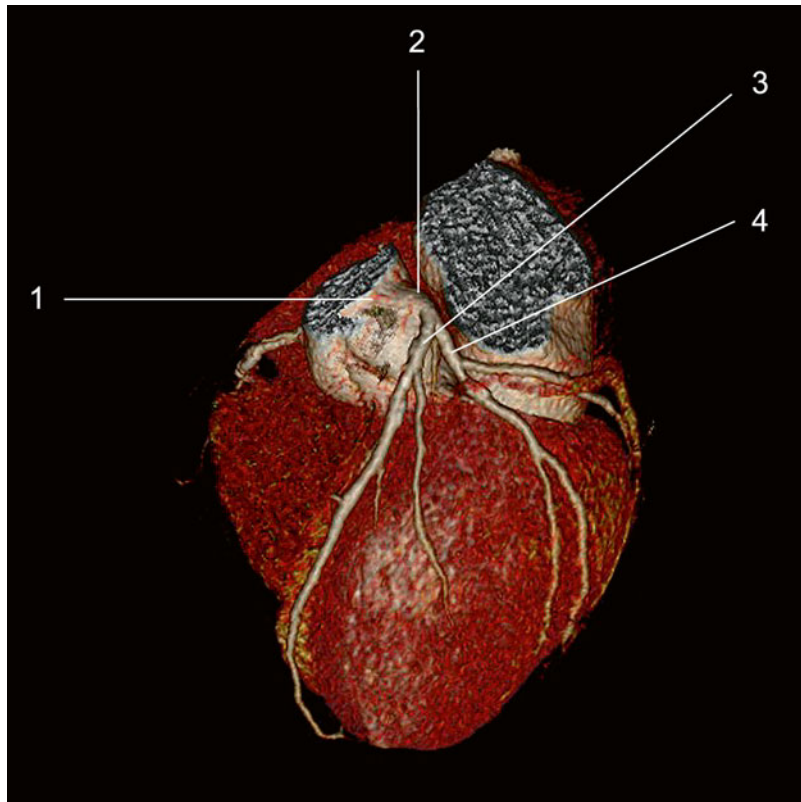
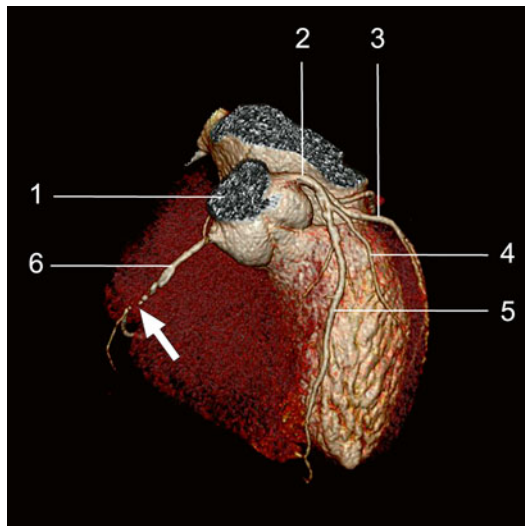
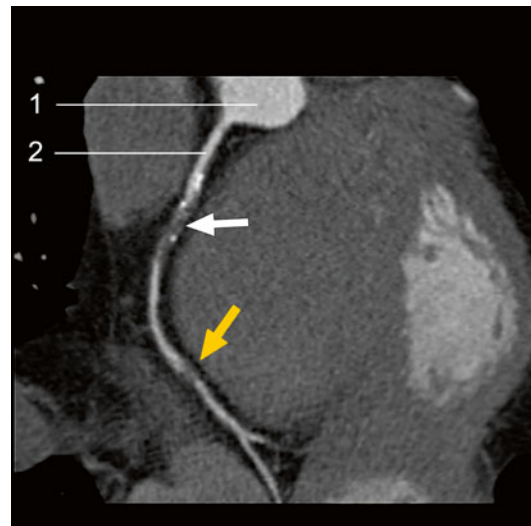


Fig. 4.45 Coronary CT angiography 3D VRT

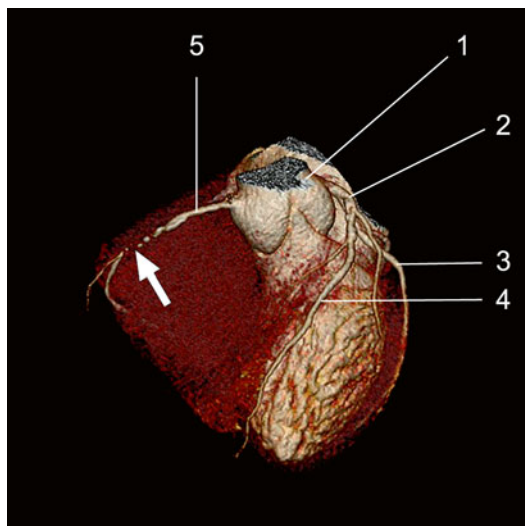
1. Aorta
2. Truncus a. coronaria sinister
3. R. interventricularis sinister
4. R. circumflexus

**Fig. 4.46** Coronary CTA 3D VRT

1. Aorta
 2. Truncus a. coronaria sinister
 3. R. circumflexus
 4. R. lateralis
 5. R. interventricularis anterior
 6. A. coronaria dextra
- The *full arrow* indicates occlusive lesion at the middle segment of a. coronaria dextra

**Fig. 4.48** Coronary CTA 3D MIP

1. Aorta
 2. A. coronaria dextra
- White arrow*=occlusion area at the middle segment of the a. coronaria dextra
Yellow arrow=occlusion area at the distal segment of the a. coronaria dextra

**Fig. 4.47** Coronary CTA 3D VRT

1. Aorta
 2. Truncus a. coronaria sinister
 3. R. circumflexus
 4. R. interventricularis anterior
 5. A. coronaria dextra
- White arrow*=occlusion area at the middle segment of the a. coronaria dextra

**Fig. 4.49** Coronary CTA 3D MIP

1. Aorta
2. A. coronaria dextra
- 3 and 4 occlusional areas at the middle segment and distal segment of a. coronaria dextra

4.9 Occlusive Lesion at the Middle Segment of the R. Interventricularis Anterior – Collateral Circulation A. Coronaria Dextra – R. Interventricularis Anterior

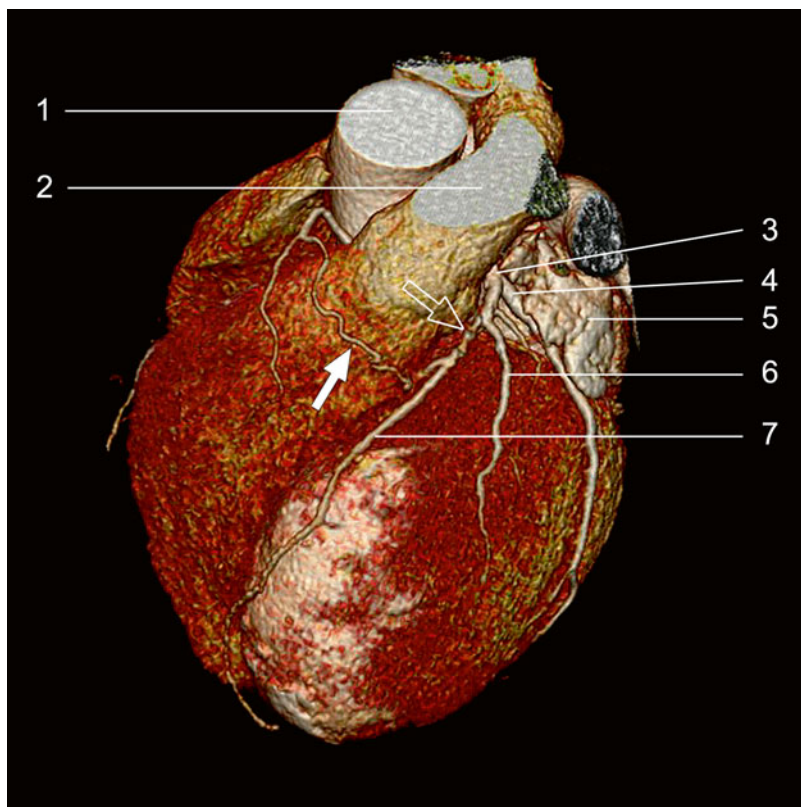


Fig. 4.50 Coronary CTA
3D VRT

1. Aorta
 2. Truncus a. pulmonalis
 3. Truncus a. coronaria sinistra
 4. R. circumflexus
 5. Auricula sinistra
 6. R. lateralis
 7. R. interventricularis anterior – pars media
- White arrow = collateral arteries
Empty arrow = occlusive/subocclusive lesion*

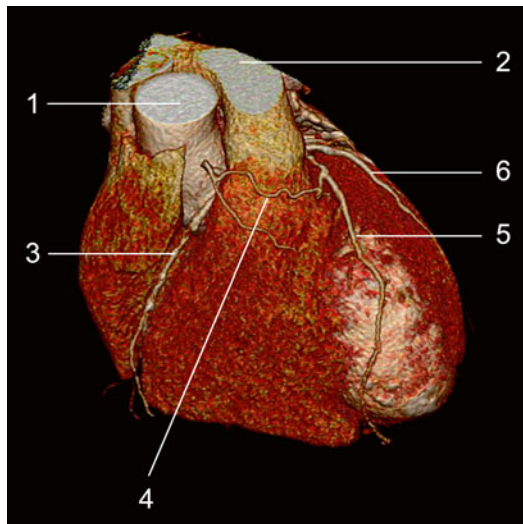


Fig. 4.51 Coronary CTA 3D VRT

1. Aorta
2. Truncus a. pulmonalis
3. A. coronaria dextra
4. Colateralis a. coronaria dextra – r. interventricularis anterior
5. R. interventricularis anterior – pars distalis
6. R. lateralis

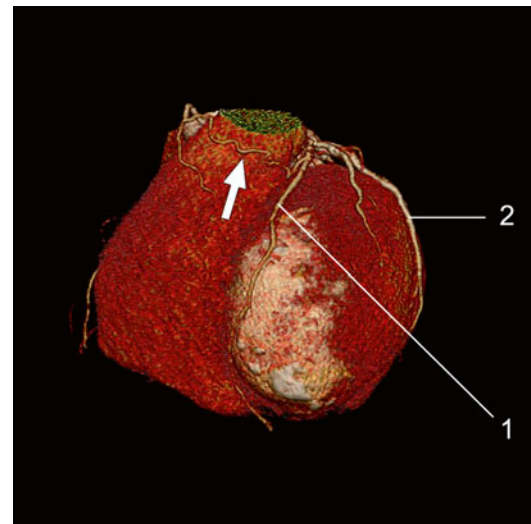


Fig. 4.53 Coronary CTA 3D VRT

1. R. interventricularis anterior
 2. R. circumflexus
- The *full arrow* indicates colateralis a. coronaria dextra r. interventricularis anterior

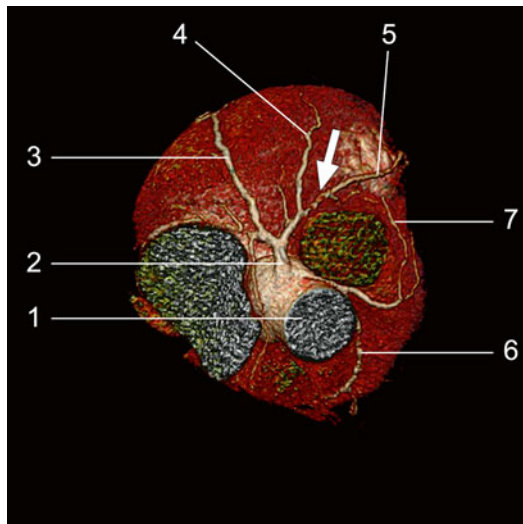


Fig. 4.52 Coronary CTA 3D VRT

1. Aorta
2. Truncus a. coronaria sinistra
3. R. circumflexus
4. R. lateralis
5. R. interventricularis anterior
6. A. coronaria dextra
7. Colateralis a. coronaria dextra – r. interventricularis anterior

The *full arrow* indicates occlusional area of the r. interventricularis anterior pars media

4.10 Bivascular Coronary Disease

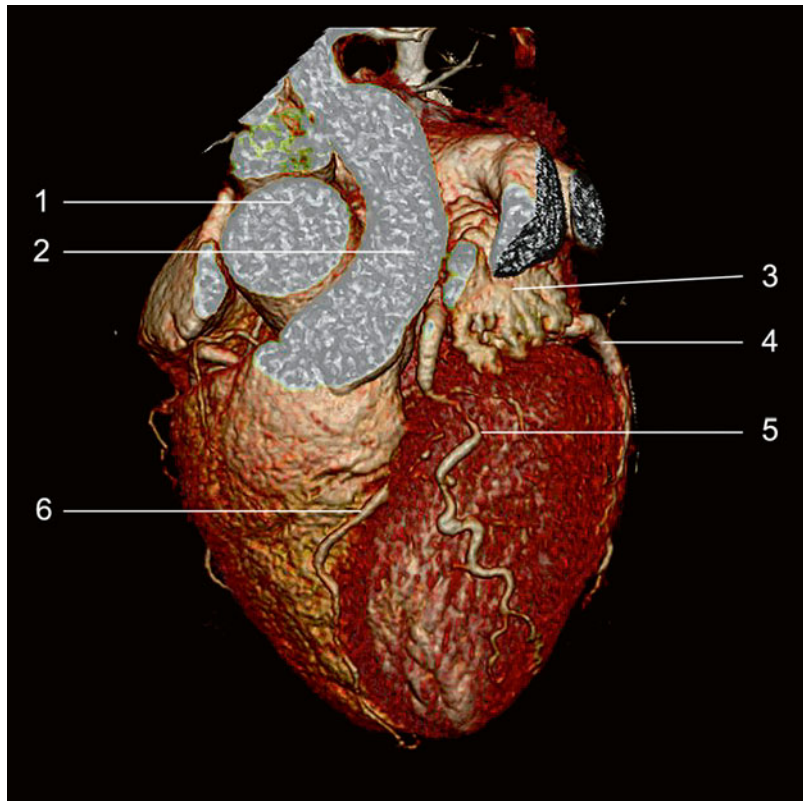


Fig. 4.54 Coronary CTA

- 3D VRT
1. Aorta
 2. A. pulmonalis
 3. Auricula sinistra
 4. R. circumflexus
 5. R. lateralis
 6. R. interventricularis anterior

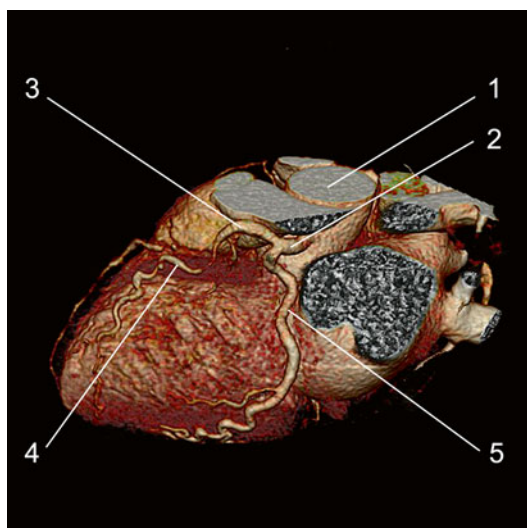


Fig. 4.55 Coronary CTA 3D VRT

1. Aorta
2. Truncus a. coronaria sinistra
3. R. interventricularis anterior
4. R. lateralis
5. R. circumflexus

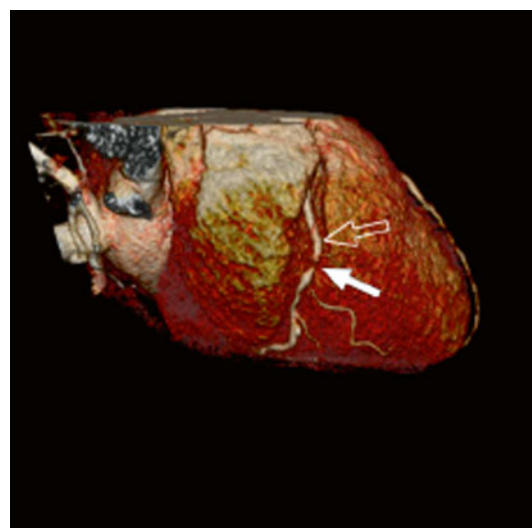


Fig. 4.56 Coronary CTA 3D VRT

Full arrow=stenotic area at the middle segment level
Arrow with contour=a. coronaria dextra

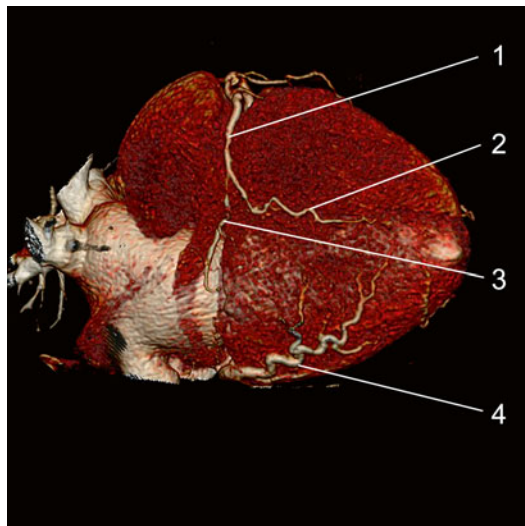


Fig. 4.57 Coronary CTA 3D VRT
 1. A. coronaria dextra – pars distalis
 2. R. interventricularis posterior
 3. R. postero lateralis dexter
 4. R. marginalis sinister

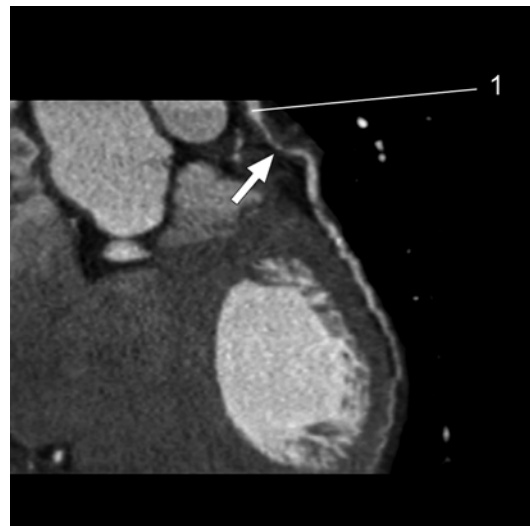


Fig. 4.59 Coronary CTA 3D MPR
 1. R. lateralis
 The full arrow indicates severe stenotic lesions



Fig. 4.58 Coronary CTA 3D MPR
 1. Truncus a. coronaria sinistra
 2. At the pars proximalis patent r. interventricularis anterior
 3. Patent r. interventricularis anterior – pars distalis
 The full arrow indicates occlusional lesion at the level of middle segment

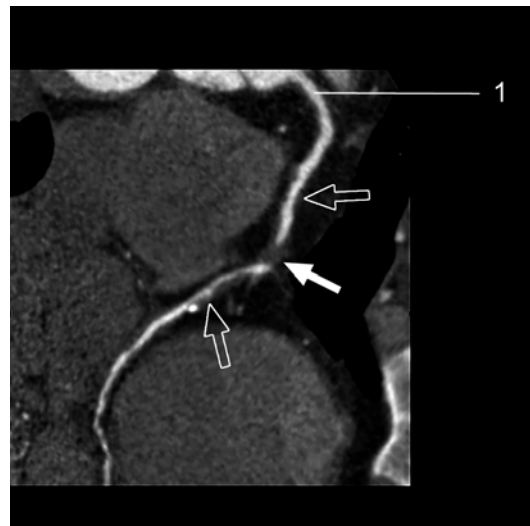


Fig. 4.60 Coronary CTA 3D MPR
 1. A. coronaria dextra
 Full arrow: occlusional lesion at the level of a. coronaria dextra
 Arrow with contour = moderate stenotic atheromatous plaques

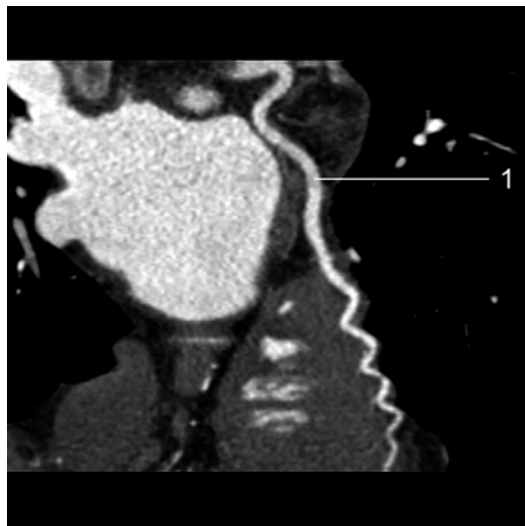


Fig. 4.61 Coronary CTA 3D MPR

1. R. circumflexus+r. marginalis sinister without evident stenotic lesions

4.11 Trivascular Coronary Disease

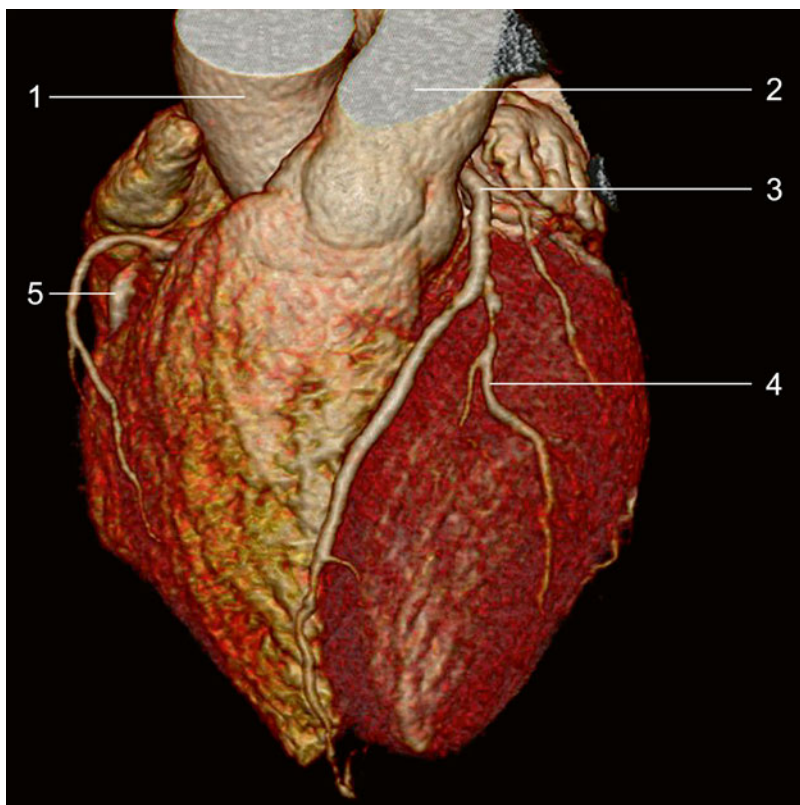


Fig. 4.62 Coronary CTA
3D VRT
1. Aorta
2. Truncus a. pulmonalis
3. R. interventricularis anterior
4. R. lateralis
5. A. coronaria dextra

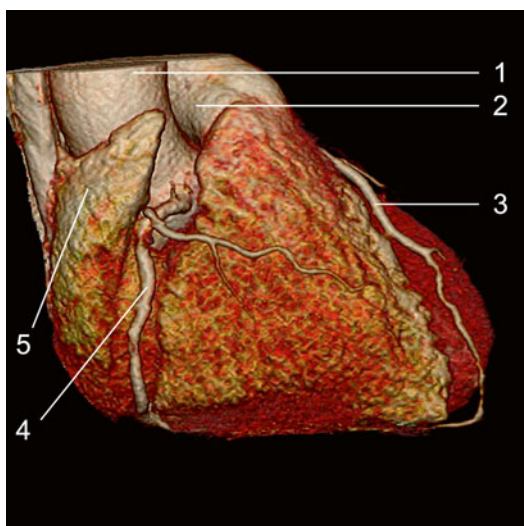


Fig. 4.63 Coronary CTA 3D VRT

1. Aorta
2. Truncus a. pulmonalis
3. R. interventricularis anterior
4. A. coronaria dextra
5. Auricula dextra

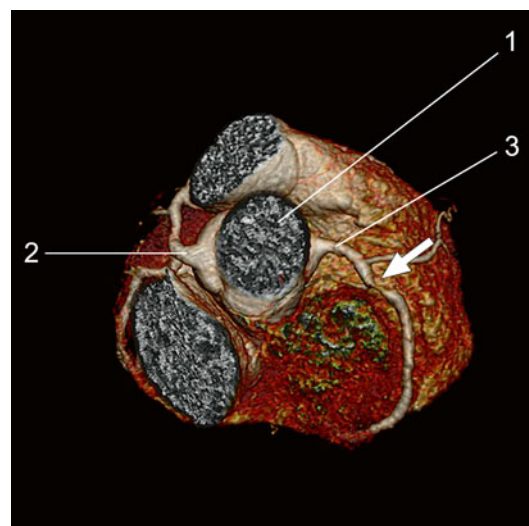
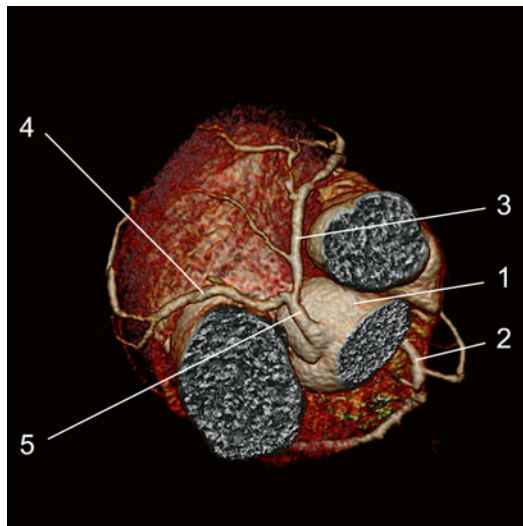
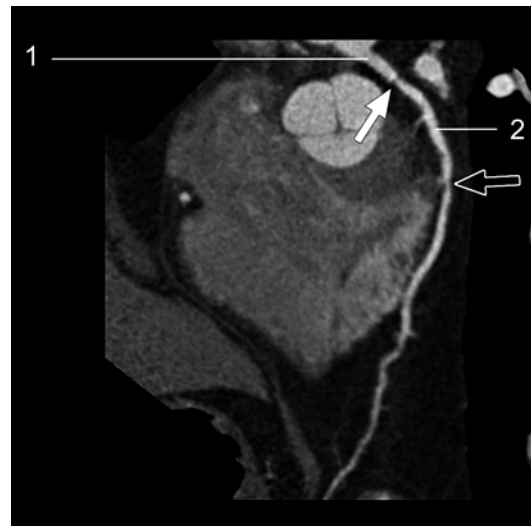


Fig. 4.64 Coronary CTA 3D VRT

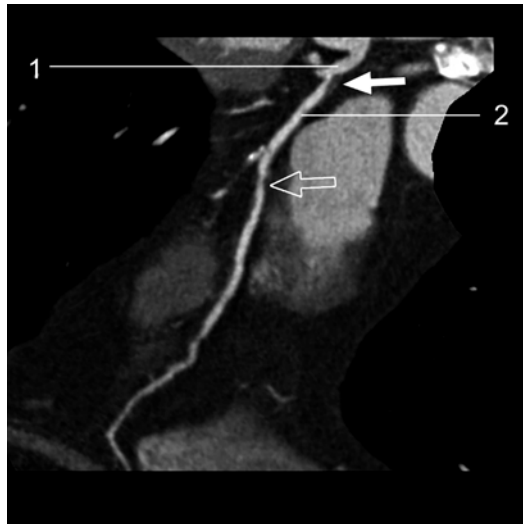
1. Aorta
 2. Truncus a. coronaria sinistra
 3. A. coronaria dextra
- The full arrow indicates stenotic area at the level of a. coronaria dextra pars proximalis

**Fig. 4.65** Coronary CTA 3D VRT

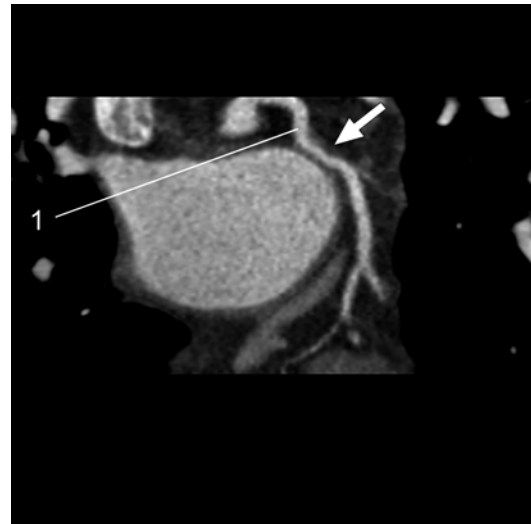
1. Aorta
2. A. coronaria dextra
3. R. interventricularis anterior
4. R. circumflexus
5. Truncus a. coronaria sinistra

**Fig. 4.67** Coronary CTA 3D MPR

1. A. coronaria sinistra
 2. R. interventricularis anterior
- Full arrow* = significant stenotic lesion ostial located at the r. interventricularis anterior
Arrow with contour = ranged non-calcified atherosclerotic plaques located in the middle and distal segments

**Fig. 4.66** Coronary CTA 3D MPR

1. A. coronaria sinistra
 2. R. interventricularis anterior
- The *full arrow* indicates severe stenotic lesion
 The *Empty arrow* indicates severe stenotic lesion

**Fig. 4.68** Coronary angiography 3D MPR

1. R. circumflexus
- The *full arrow* indicates non-calcified mild stenotic plaques located at pars proximalis of r. circumflexus

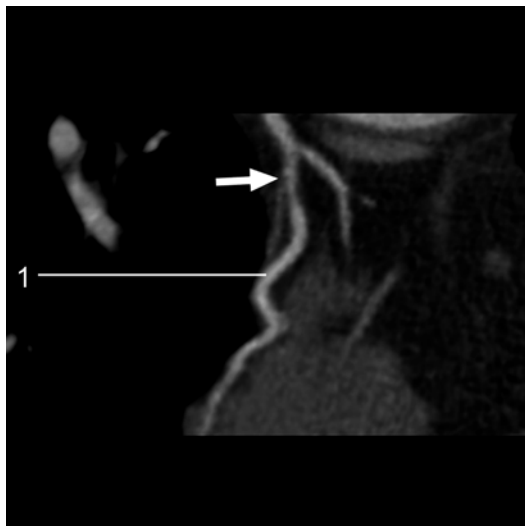


Fig. 4.69 Coronary angiography 3D MPR

1. R. marginalis sinister

The *full arrow* indicates non-calcified significantly stenotic plaques located at pars proximalis of r. marginalis sinister



Fig. 4.70 Coronary angiography 3D MPR

1. A. coronaria dextra

2. R. interventricularis posterior

The *full arrow* indicates non-calcified eccentric plaques, subocclusive located at the pars proximalis of a. coronaria dextra

4.12 Aneurysm of the Left Ventricle and R. Interventricularis Anterior Occlusion

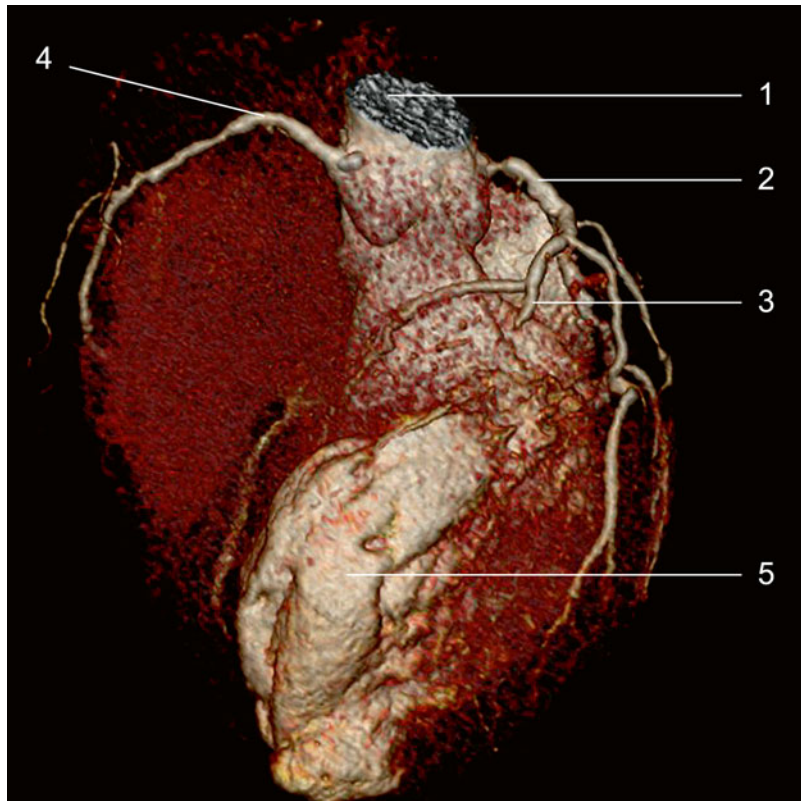
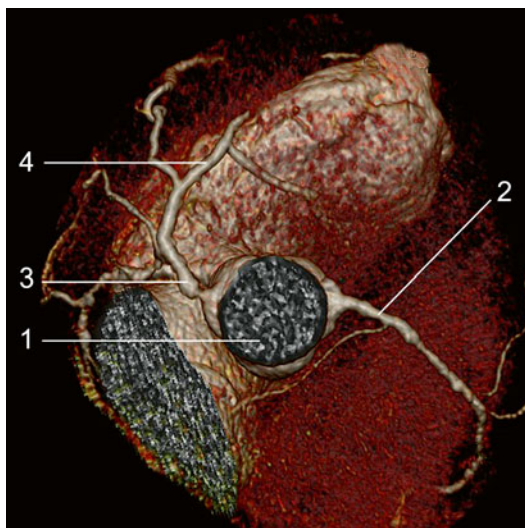


Fig. 4.71 Coronary CTA

3D VRT

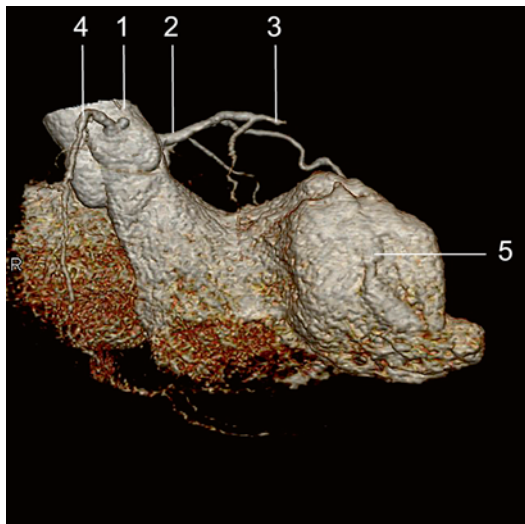
1. Aorta
2. Truncus a. coronaria sinistra
3. Occluded a interventricularis anterior in midle and distal segment
4. A. coronaria dextra
5. Ventriculus sinister aneurysm

**Fig. 4.72** Coronary CTA 3D VRT

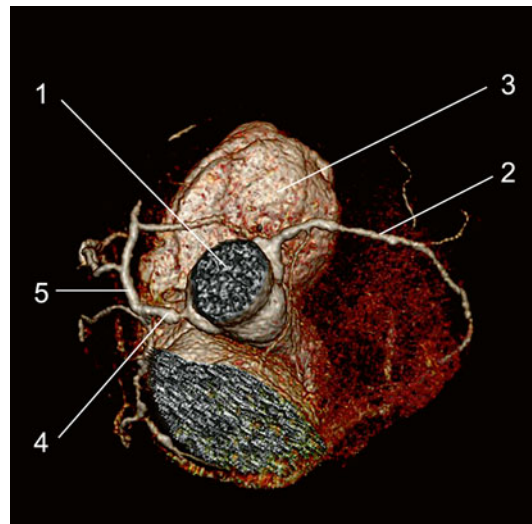
1. Aorta
2. A. coronaria dextra
3. Significantly stenotic lesion of a. coronaria sinistra
4. R. interventricularis anterior with occlusion in the middle part

**Fig. 4.74** Coronary CTA VRT

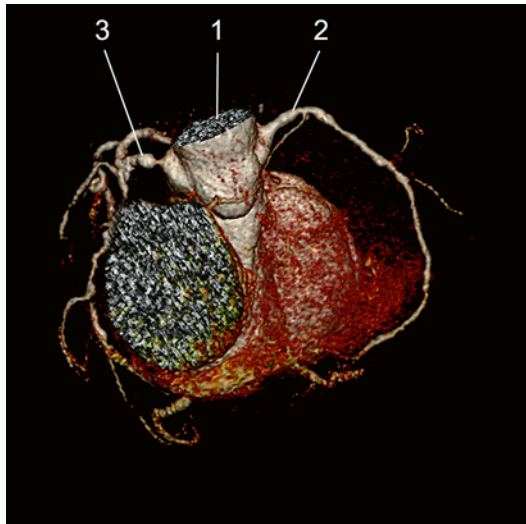
The *full arrow* indicates aneurysm

**Fig. 4.73** Coronary CTA 3D VRT

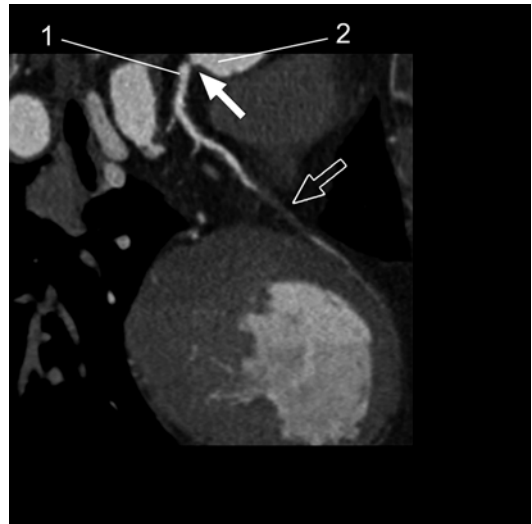
1. Aorta
2. Truncus coronaria sinistra
3. R. interventricularis anterior
4. A. coronaria dextra
5. Ventriculus sinister aneurysm

**Fig. 4.75** Coronary CTA VRT

1. Aorta
2. A. coronaria dextra
3. Ventriculus sinister aneurysm
4. Sever stenotic ostial lesion of truncus a. coronaria sinistra
5. R. interventricularis anterior

**Fig. 4.76** Coronary CTA 3D VRT

1. Aorta
2. A. coronaria dextra
3. Truncus a. coronaria sinistra

**Fig. 4.78** Coronary CTA 3D MPR

1. Truncus a. coronaria sinistra
 2. Aorta
- Full arrow*=severe stenotic lesion of ostium a. coronaria sinistra
Arrow with contour=r. interventricularis anterior with occlusion in the middle part

**Fig. 4.77** Coronary CTA 3D MPR

1. Aorta
 2. R. interventricularis anterior
- Full arrow*=significantly stenotic lesion of ostium a. coronaria sinistra
Arrow with contour=r. interventricularis anterior with occlusion in the middle part

4.13 Monovascular Coronary Disease Patent Stent in the Middle Segment of R. Interventricularis Anterior

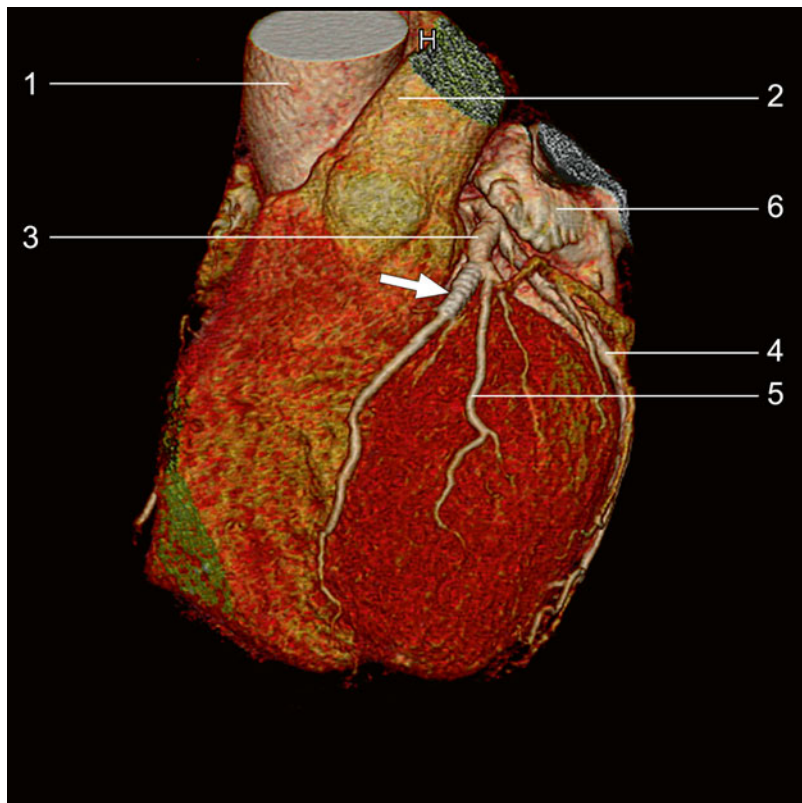
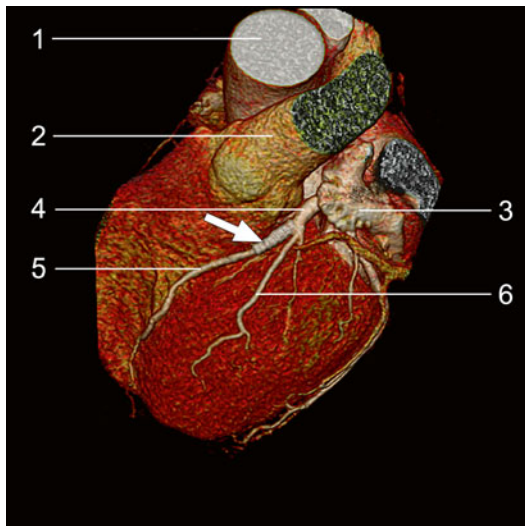


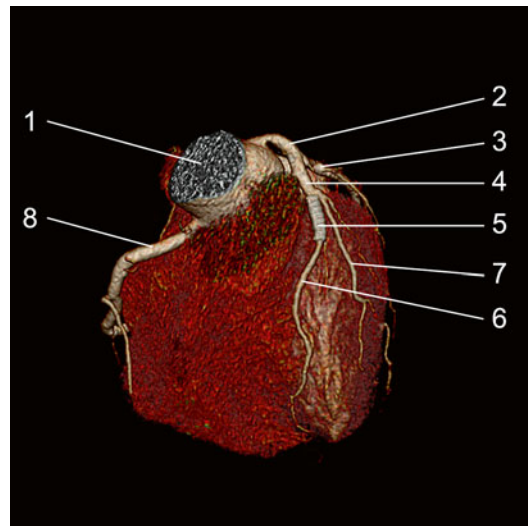
Fig. 4.79 3D VRT colour reconstruction

1. Aorta
 2. Truncus a. pulmonalis
 3. R. interventricularis anterior – pars proximalis
 4. R. circumflexus
 5. R. lateralis
 6. Auricula sinistra
- The full arrow indicates stent

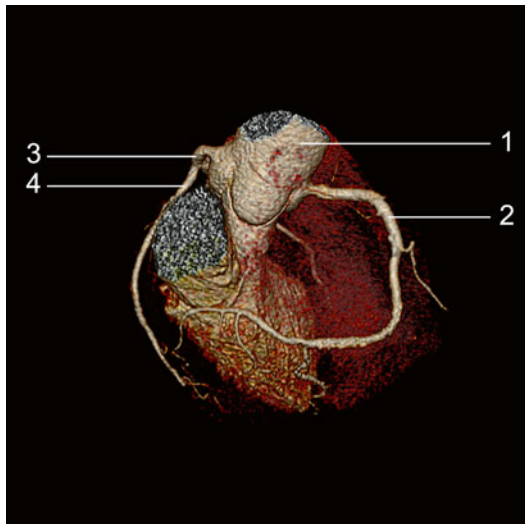
**Fig. 4.80** 3D VRT colour reconstruction

1. Aorta
2. Truncus a. pulmonalis
3. Auricula sinistra
4. R. interventricularis anterior – pars proximalis
5. R. interventricularis anterior – pars distalis
6. R. lateralis

The *full arrow* indicates stent

**Fig. 4.82** 3D VRT colour reconstruction

1. Aorta
2. Truncus a. coronaria sinistra
3. R. circumflexus
4. R. interventricularis anterior – pars proximalis
5. Patent stent on r. interventricularis anterior, middle part
6. R. interventricularis anterior – pars distalis
7. R. lateralis
8. ACD

**Fig. 4.81** 3D VRT colour reconstruction

1. Aorta
2. A. coronaria dextra
3. Truncus a. coronaria sinistra
4. R. circumflexus

**Fig. 4.83** 3D MPR reconstruction

1. Truncus a. coronaria sinistra
2. R. interventricularis anterior – pars proximalis
3. Patent stent
4. Stent
5. R. interventricularis anterior – pars distalis



Fig. 4.84 3D MPR reconstruction

1. Truncus a. coronaria sinistra
2. R. interventricularis anterior – pars proximalis
3. Patent stent
4. Stent
5. R. interventricularis anterior – pars distalis

The *full arrow* indicates calcified atherosomatous plaque

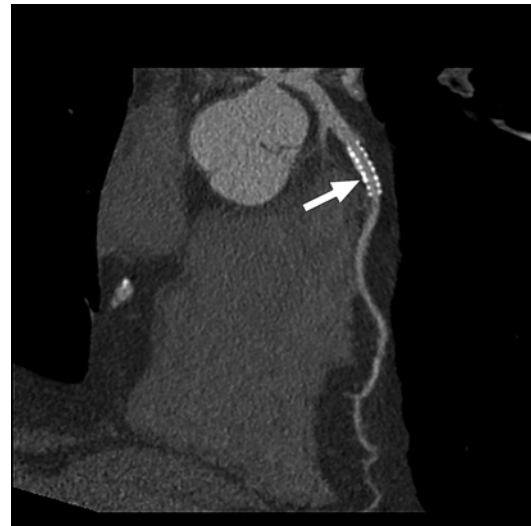


Fig. 4.86 3D MPR reconstruction

The *full arrow* indicates permeable stent at the middle segment of r. interventricularis anterior

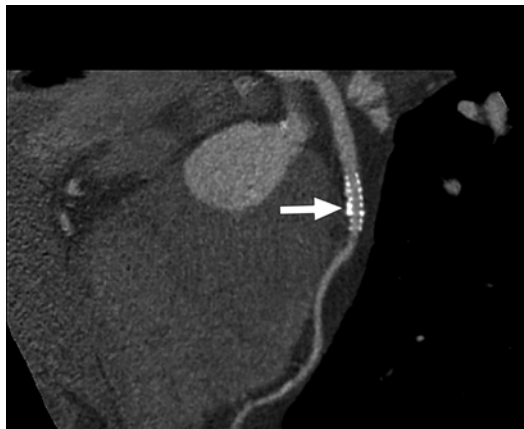


Fig. 4.85 3D MPR reconstruction

The *full arrow* indicates permeable stent at the middle segment of r. interventricularis anterior

4.14 Restenosis at Stent Level

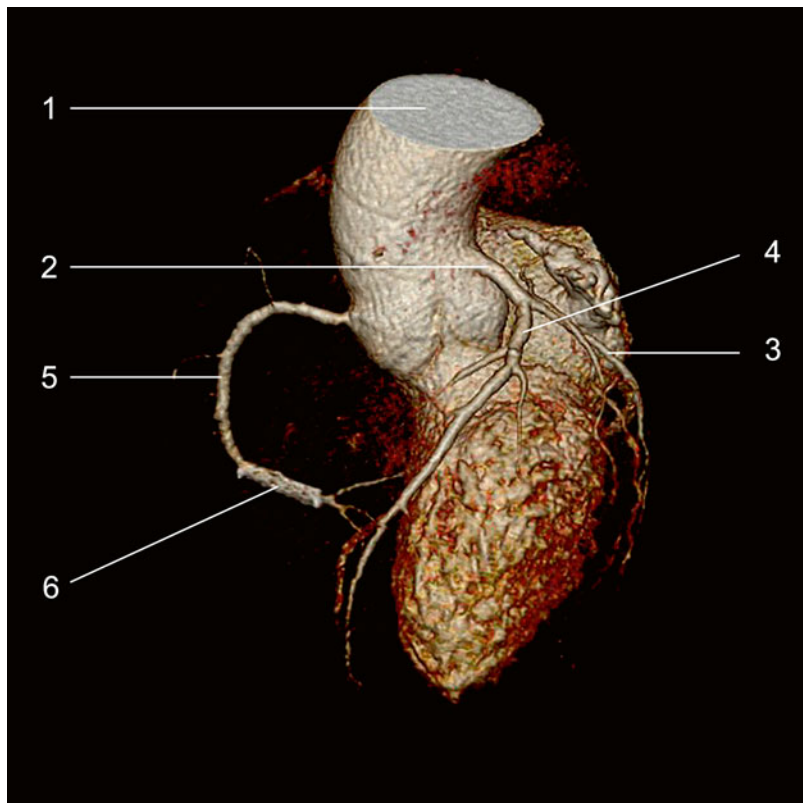


Fig. 4.87 3D VRT colour reconstruction

1. Aorta
2. Truncus coronaria sinistra
3. R. circumflexus
4. R. interventricularis anterior
5. A. coronaria dextra
6. Stent at the level of a. coronaria dextra proximal from crux cordis

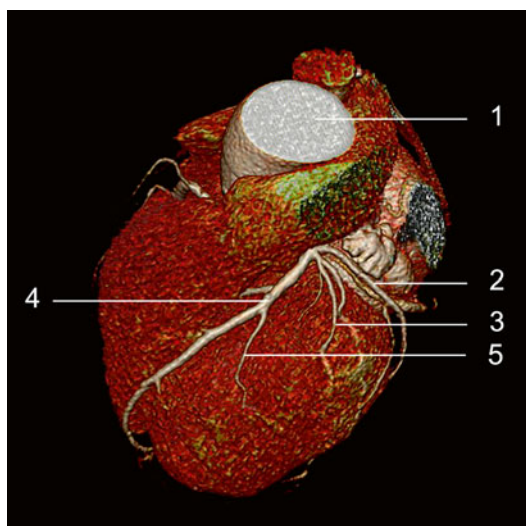


Fig. 4.88 3D VRT colour reconstruction

1. Aorta
2. R. circumflexus
3. R. atrialis intermedius
4. R. interventricularis anterior
5. R. lateralis

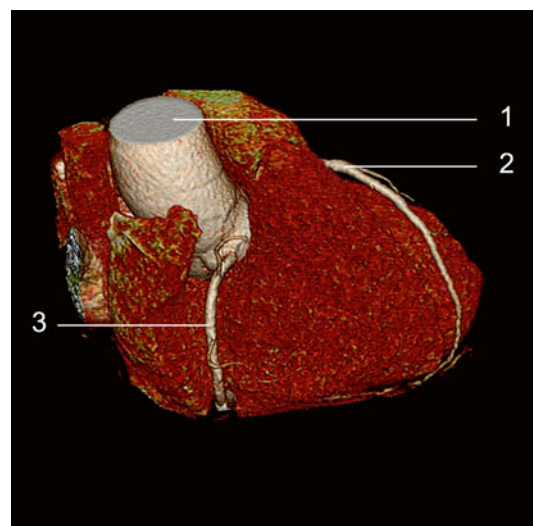


Fig. 4.89 3D VRT colour reconstruction

1. Aorta
2. R. interventricularis anterior
3. A. coronaria dextra

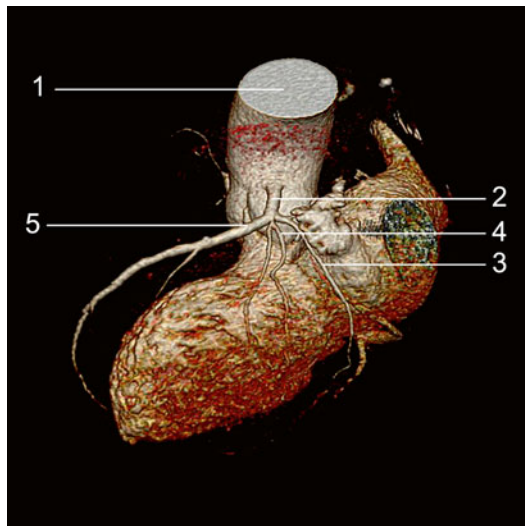


Fig. 4.90 3D VRT colour reconstruction

1. Aorta
2. Truncus a. coronaria sinistra
3. R. circumflexus
4. R. intermedius
5. R. interventricularis anterior



Fig. 4.92 3D MPR reconstruction

1. Aorta
 2. A. coronaria dextra
 3. Stent
 4. Bifurcation
- The *full arrow* indicates restenosis area in stent

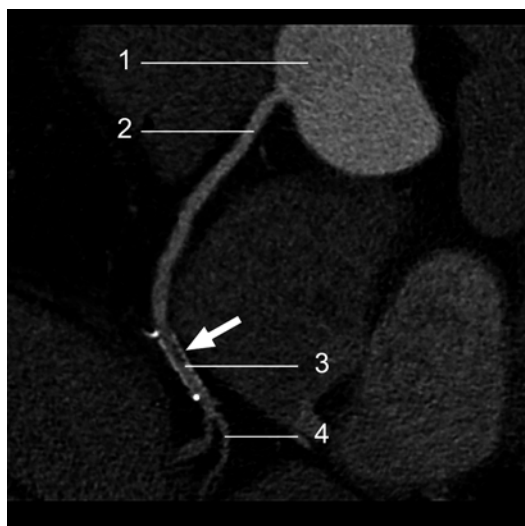


Fig. 4.91 3D MPR reconstruction

1. Aorta
 2. A. coronaria dextra
 3. Stent
 4. Bifurcation
- The *full arrow* indicates restenosis area in stent

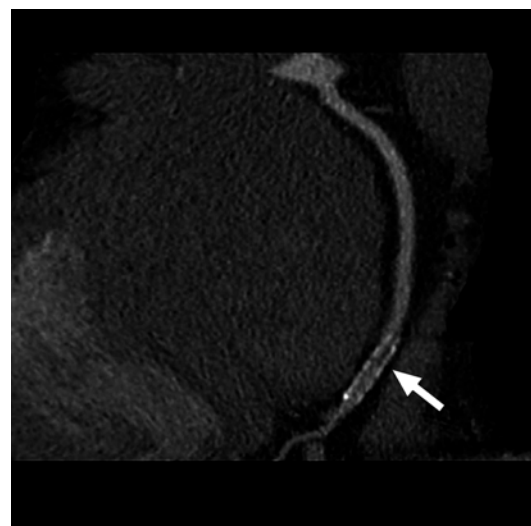


Fig. 4.93 3D MPR reconstruction

The *full arrow* indicates restenosis area in stent



Fig. 4.94 3D MPR reconstruction

The *full arrow* indicates restenosis area in stent

4.15 Occlusion of R. Interventricularis Anterior

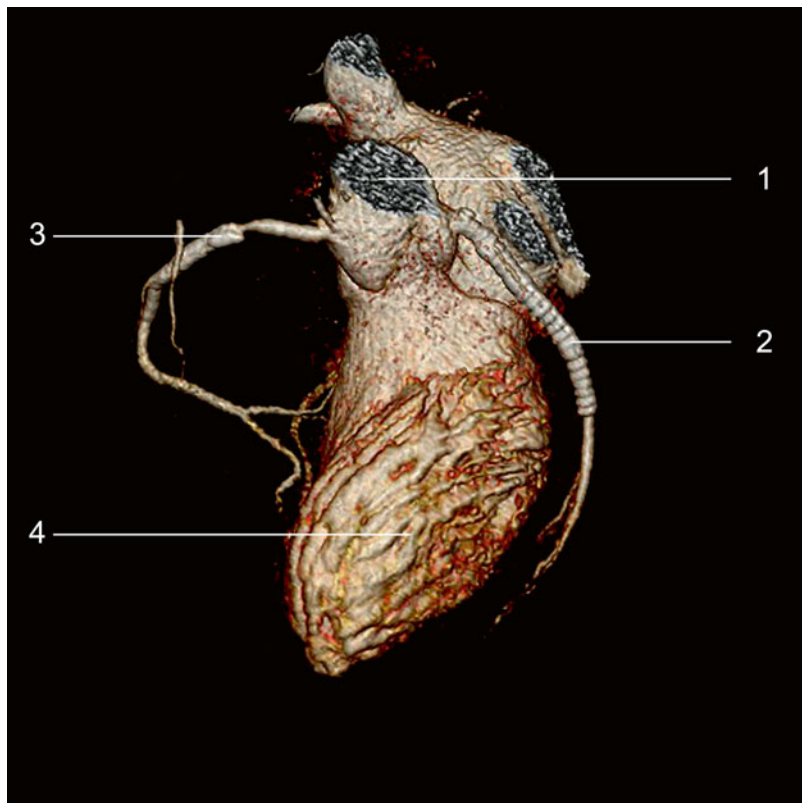


Fig. 4.95 3D VRT colour reconstruction
 1. Aorta
 2. R. circumflexus
 3. A. coronaria dextra
 4. Ventriculus sinister

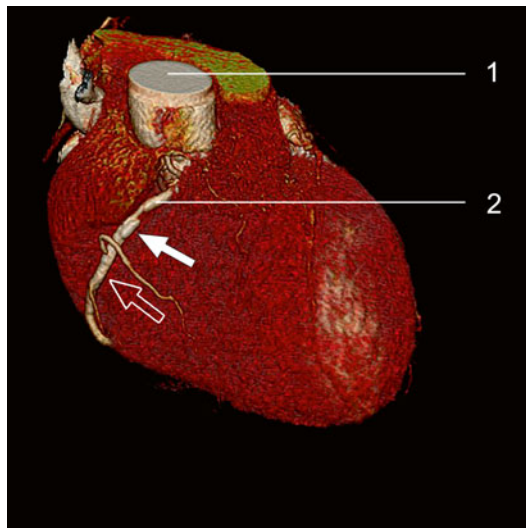


Fig. 4.96 3D VRT colour reconstruction
 1. Aorta
 2. A. coronaria dextra
 Full arrow = calcified atherosclerotic plaque
 Arrow with contour = stent

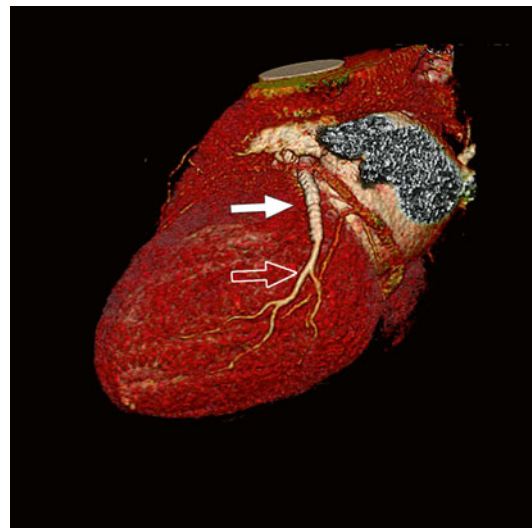
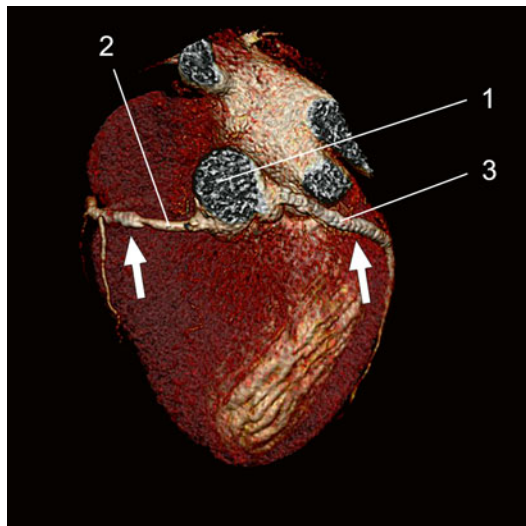
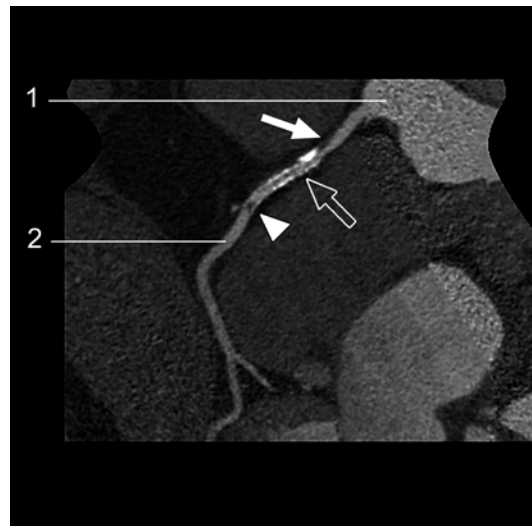


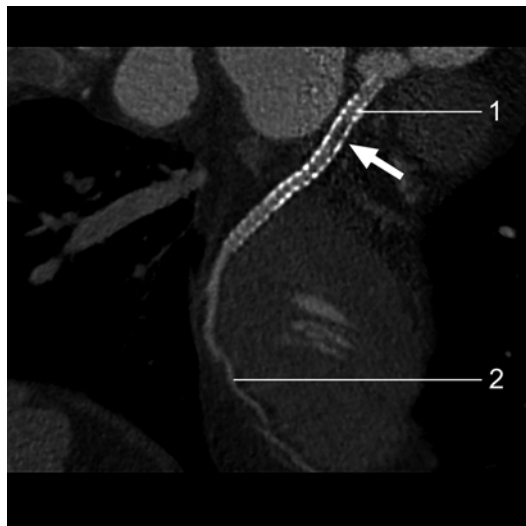
Fig. 4.97 3D VRT colour reconstruction
 Full arrow = stent at the level of r. circumflexus
 Arrow with contour = r. marginalis sinister

**Fig. 4.98** 3D VRT colour reconstruction

1. Aorta
 2. A. coronaria dextra
 3. R. circumflexus
- The *full arrow* indicates stents at the level of a. coronaria dextra and r. circumflexus

**Fig. 4.100** 3D MPR reconstruction

1. Aorta
 2. A. coronaria dextra
- Full arrow* = stenotic lesion proximal stent
Arrow with contour = stenotic area in stent
At the tip of the *arrow* = dissection area distally located from the stent confirmed by invasive angiography

**Fig. 4.99** 3D MPR reconstruction

1. Stents at the level of r. circumflexus
 2. R. marginalis sinister
- The *full arrow* indicates stent restenotic area

4.16 Coronary Bypass Evaluation

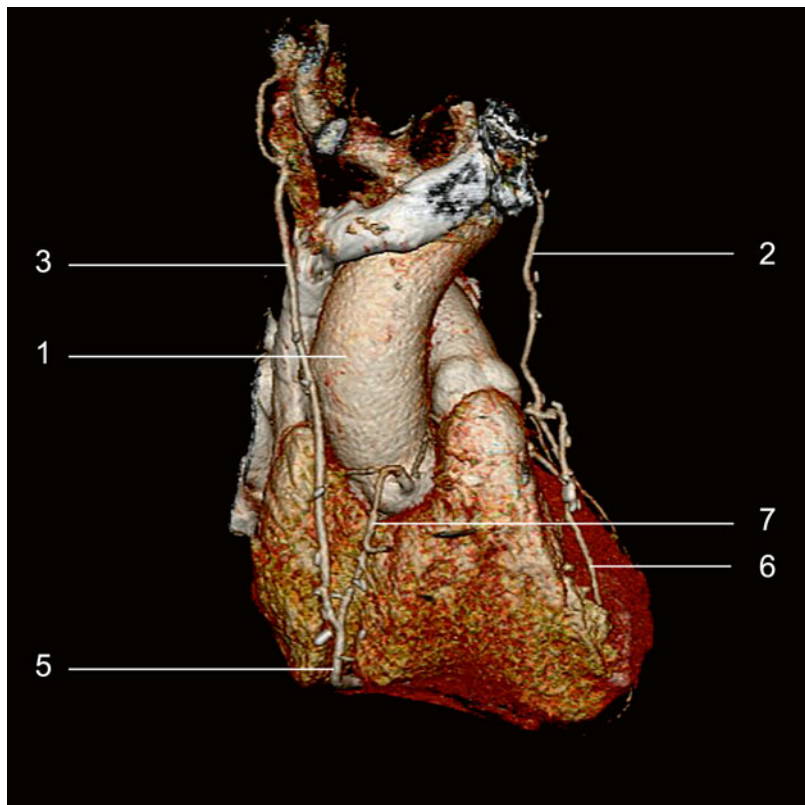


Fig. 4.101 3D VRT colour reconstruction after removal of the thoracic cage

1. Aorta
2. A. thoracica interna grafted at the level of r. interventricularis anterior
3. A. thoracica interna dextra grafted in the middle parts of a. coronaria dextra
4. Truncus a. pulmonalis
5. Post-anastomotic segment of a. coronaria dextra
6. Post-anastomotic segment of r. interventricularis posterior
7. Pars proximalis et media of a. coronaria dextra with occlusive lesions

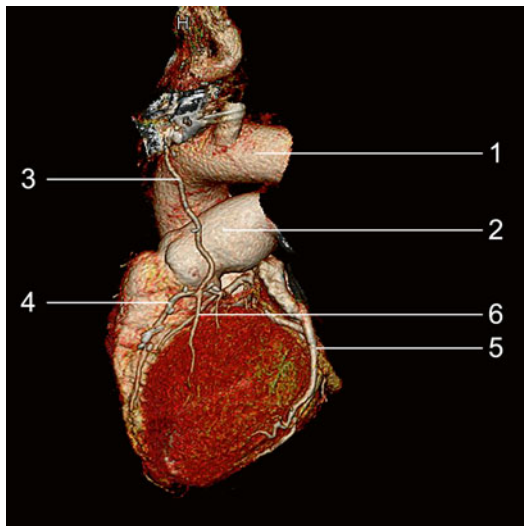


Fig. 4.102 3D VRT colour reconstruction after removal of the costal grill

1. Aorta
2. Truncus a. pulmonalis
3. A. thoracica interna sinistra
4. Post-anastomotic segment of r. interventricularis anterior
5. R. marginalis sinister
6. R. lateralis

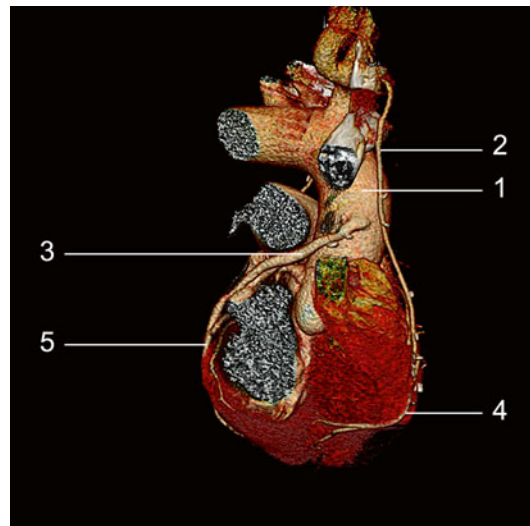


Fig. 4.104 3D VRT colour reconstruction after removal of the thoracic cage

1. Aorta
2. A. thoracica interna dextra grafted to a. coronaria dextra
3. Saphenous venous graft to r. circumflexus
4. Pars distalis of a. coronaria dextra
5. R. marginalis sinister

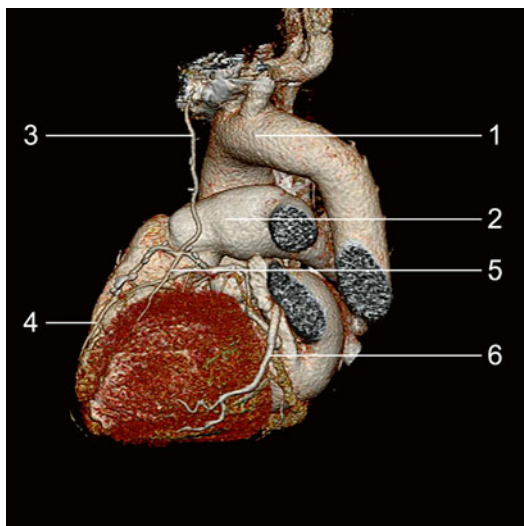


Fig. 4.103 3D VRT colour reconstruction after removal of the thoracic cage

1. Aorta
2. Truncus a. pulmonalis
3. A. thoracica interna sinistra grafted to r. interventricularis anterior
4. Pars distalis of r. interventricularis anterior
5. R. lateralis
6. R. marginalis sinister

4.17 Fallot Tetralogy

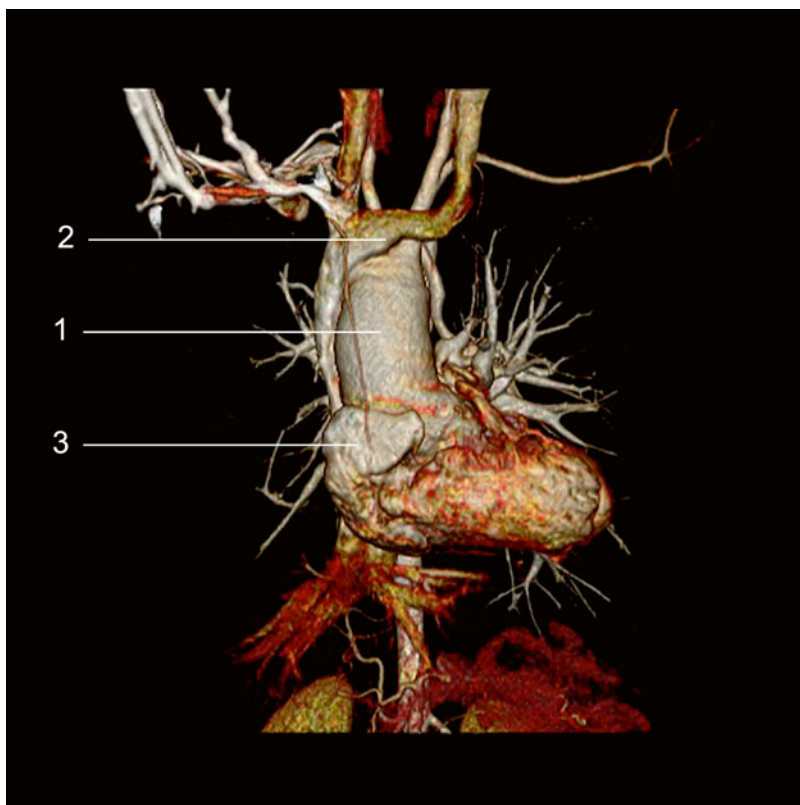


Fig. 4.105 3D VRT colour reconstruction

1. Aorta
2. Vena cava superior
3. Auricula dextra

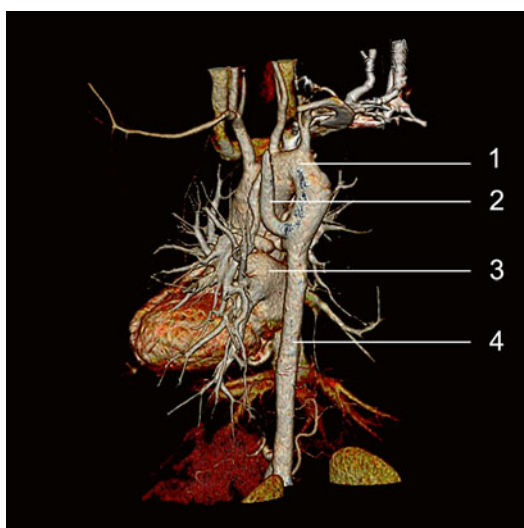


Fig. 4.106 3D VRT colour reconstruction

1. Arcus aortae
2. Colateralis aorto-pulmonalis
3. Atrium sinistrum
4. Aorta descendens

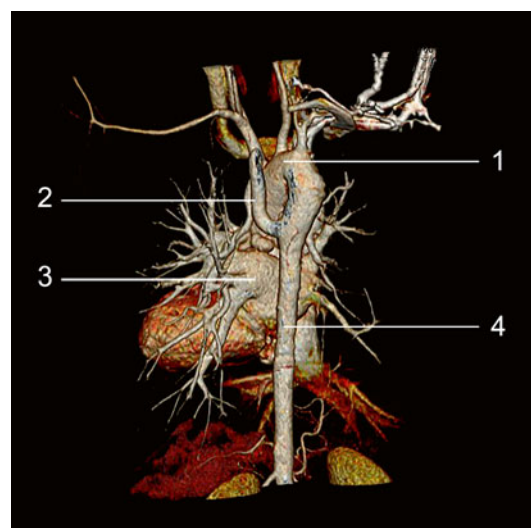
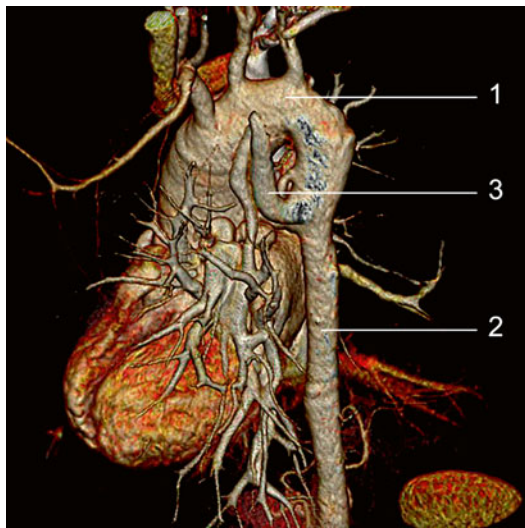


Fig. 4.107 3D VRT colour reconstruction

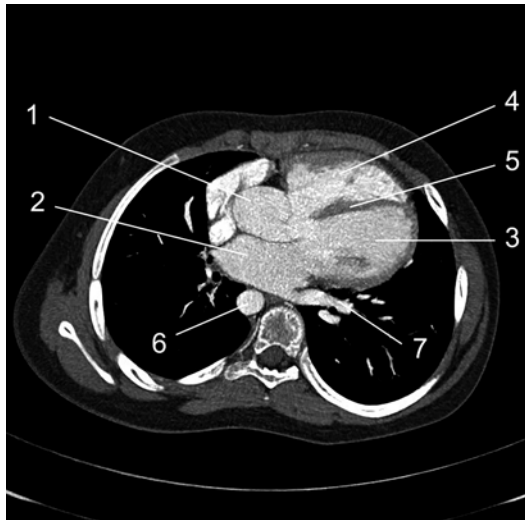
1. Arcus aortae
2. Colateralis aorto-pulmonalis
3. Atrium sinistrum
4. Aorta descendens

**Fig. 4.108** 3D VRT colour reconstruction

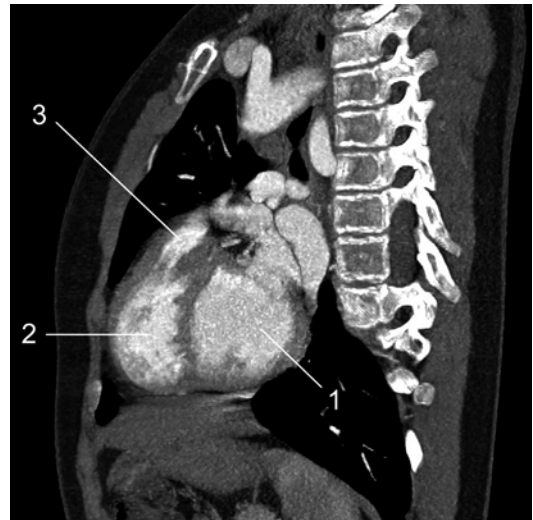
1. Arcus aortae with emergent vessels
2. Aorta descendens
3. Colateralis aorto-pulmonalis

**Fig. 4.110** 3D MIP reconstruction, axial plane

1. Aorta ascendens
2. Aorta descendens
3. Colateralis aorto-pulmonalis

**Fig. 4.109** 3D MIP reconstruction 4CV

1. Aorta "riding" on the septum with predominant ventriculus dexter loading
2. Atrium sinistrum
3. Ventriculus sinister
4. Ventriculus dexter
5. Septum interventricularis
6. Aorta descendens
7. Vena pulmonalis

**Fig. 4.111** 3D MIP reconstruction

1. Ventriculus sinister
2. Ventriculus dexter
3. A. pulmonalis with severe stenosis over and under the valvae (indicated through arrows)

4.18 Fallot Tetralogy in an Adult Patient

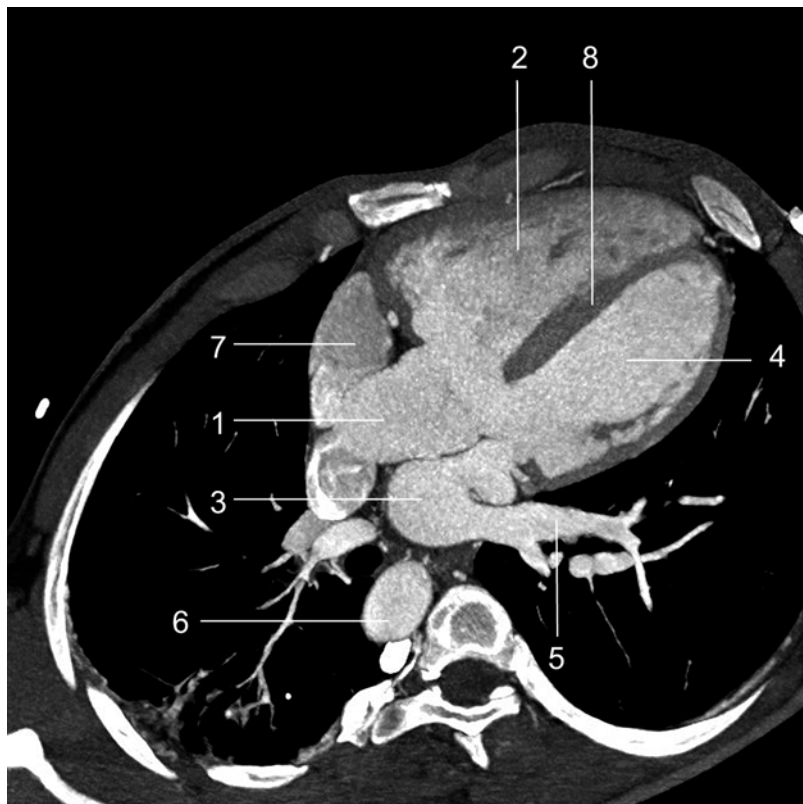
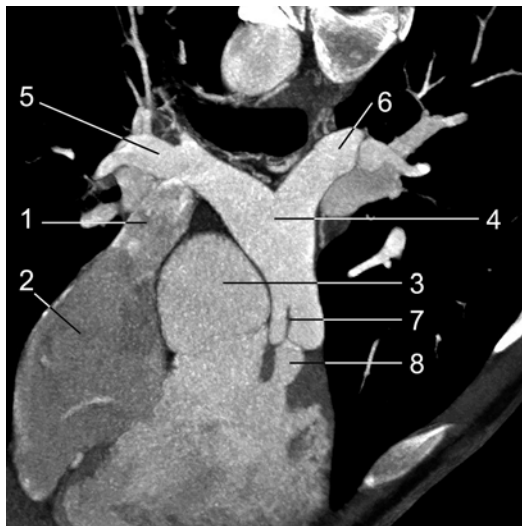
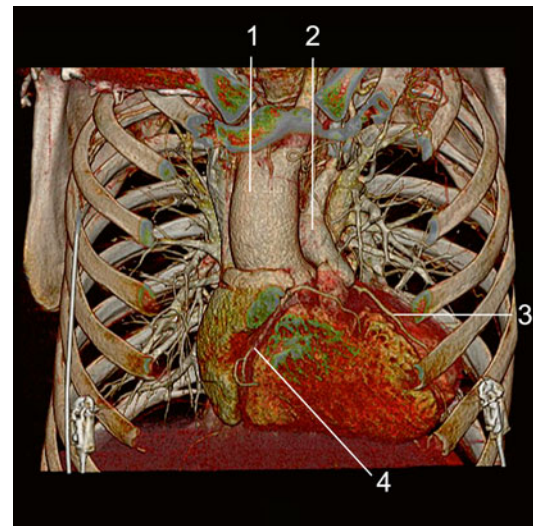


Fig.4.112 3D MIP reconstruction

1. Aorta "riding" on the septum
2. Ventriculus dexter
3. Atrium sinistrum
4. Ventriculus sinister
5. Vena pulmonalis
6. Aorta descendens
7. Atrium dextrum
8. Septum interventricularis

**Fig. 4.113** 3D MIP colour reconstruction

1. Vena cava superior
2. Atrium dextrum
3. Aorta
4. Truncus a. pulmonalis
5. A. pulmonalis dextra
6. A. pulmonalis sinistra
7. Valva trunci pulmonalis
8. Stenosis area under the valvae

**Fig. 4.115** 3D VRT colour reconstruction

1. Aorta
2. A. pulmonalis
3. R. interventricularis anterior
4. A. coronaria dextra

**Fig. 4.114** 3D MIP colour reconstruction

1. Vena cava superior
2. Atrium dextrum
3. Aorta
4. Truncus a. pulmonalis
5. Valva trunci pulmonalis
6. Stenotic area under the valve

Contents

5.1	Normal Abdominal Angiography	132
5.2	Aneurysm of Truncus Coeliacus and Stenotic Lesion of A. Hepatica Communis.....	135
5.3	Left Renal Arteriovenous Fistula	137
5.4	Aorta Abdominalis Aneurysm with Aortoduodenal Fistula	140
5.5	Operated Aorta Abdominalis Aneurysm: Post-operative Complications.....	143
5.6	Stenosis of A. Renalis Sinistra.....	145
5.7	Right A. Renalis Dextra Occlusion Collateral Circulation for Renal Parenchyma	148
5.8	Dissection of Aorta Abdominalis	151
5.9	Separate Emergence of A. Hepatica Communis and A. Splenica Additional Polar Left Superior A. Renalis Sinistra.....	153
5.10	Multiple Aneurysms of A. Splenica Associated with Aneurysm of A. Renalis Dexter	156

5.1 Normal Abdominal Angiography

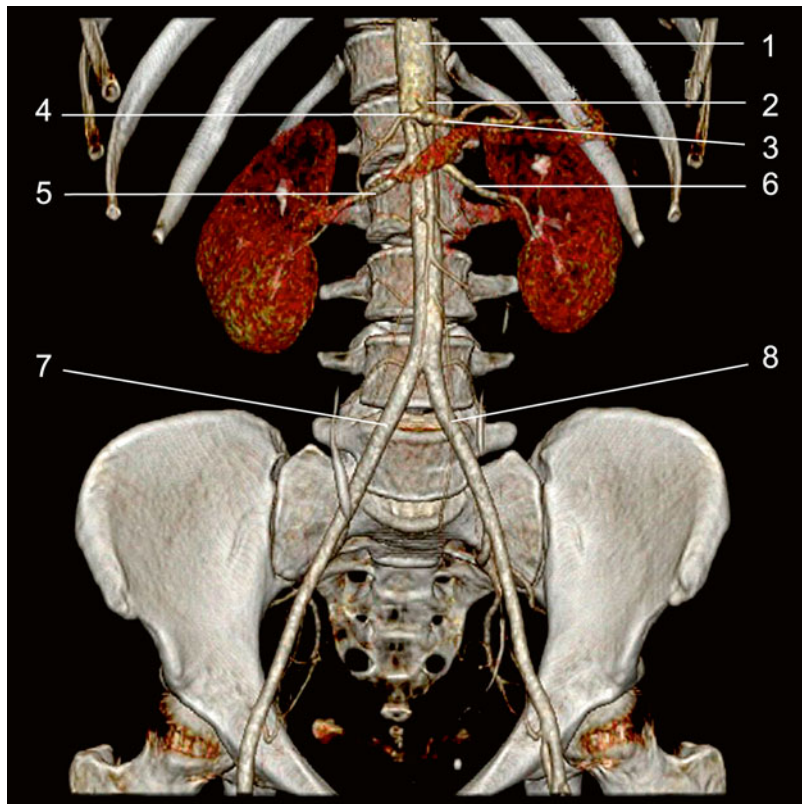


Fig. 5.1 3D VRT colour reconstruction frontal plane

1. Aorta abdominalis
2. Truncus coeliacus
3. A. splenica
4. A. hepatica communis
5. A. renalis dextra
6. A. renalis sinistra
7. A. iliaca communis dextra
8. A. iliaca communis sinistra

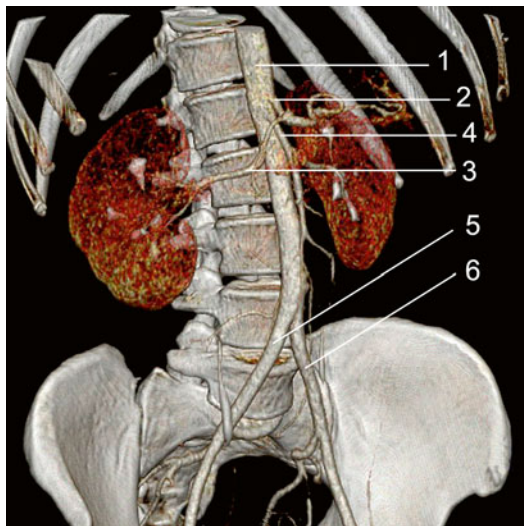


Fig. 5.2 3D VRT colour reconstruction right, anterior oblique plane

1. Aorta abdominalis
2. Truncus coeliacus
3. A. renalis dextra
4. A. mesenterica superior
5. A. iliaca communis dextra
6. A. iliaca communis sinistra

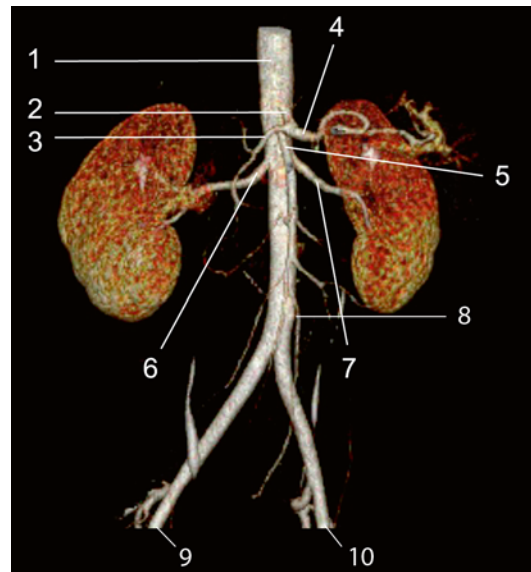


Fig. 5.4 3D VRT colour reconstruction left, after removal of the bone structure

1. A. abdominalis
2. Truncus coeliacus
3. A. hepatica communis
4. A. splenica
5. A. mesenterica superior
6. A. renalis dextra
7. A. renalis sinistra
8. A. mesenterica inferior
9. A. iliaca communis
10. A. iliaca communis

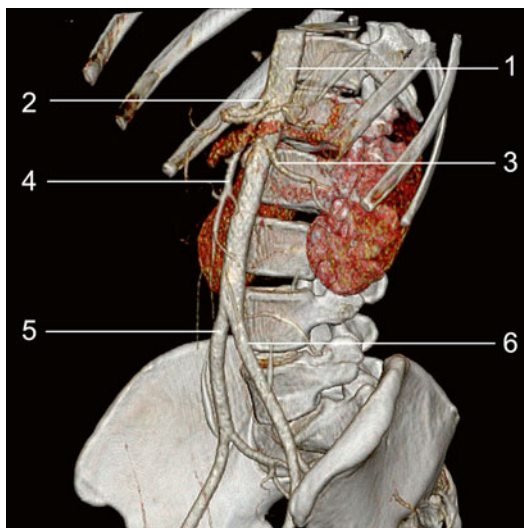


Fig. 5.3 3D VRT colour reconstruction left, anterior oblique plane

1. Aorta abdominalis
2. Truncus coeliacus
3. A. renalis sinistra
4. A. mesenterica superior
5. A. iliaca communis dextra
6. A. iliaca communis sinistra

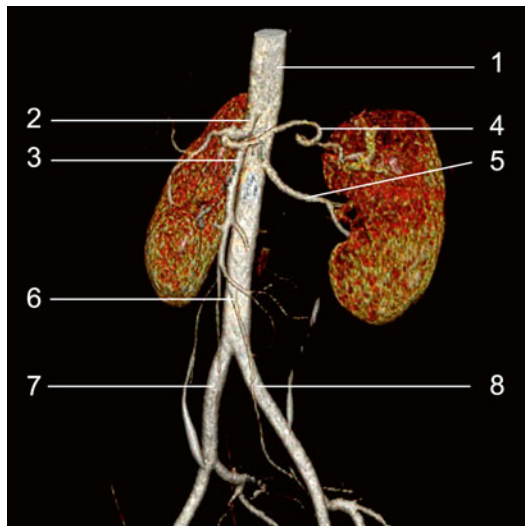


Fig. 5.5 3D VRT colour reconstruction left, after removal of the bone structure

1. A. abdominalis
2. Truncus coeliacus
3. A. mesenterica superior
4. A. splenica
5. A. renalis sinistra
6. A. mesenterica inferior
7. A. iliaca communis
8. A. iliaca communis

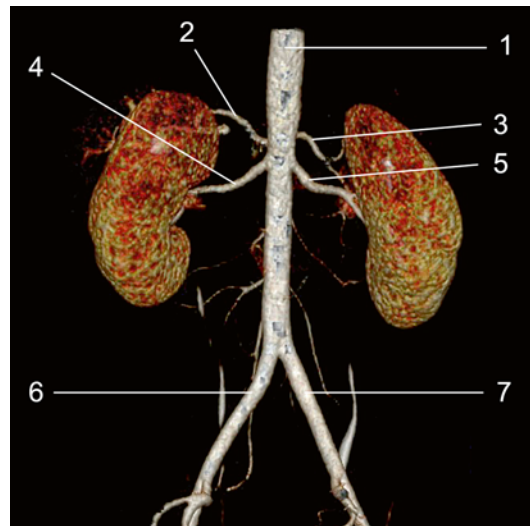


Fig. 5.6 3D VRT colour reconstruction left, after removal of the bone structure, posterior plane

1. A. abdominalis
2. A. splenica
3. A. hepatica communis
4. A. renalis sinistra
5. A. renalis dextra
6. A. iliaca communis
7. A. iliaca communis

5.2 Aneurysm of Truncus Coeliacus and Stenotic Lesion of A. Hepatica Communis

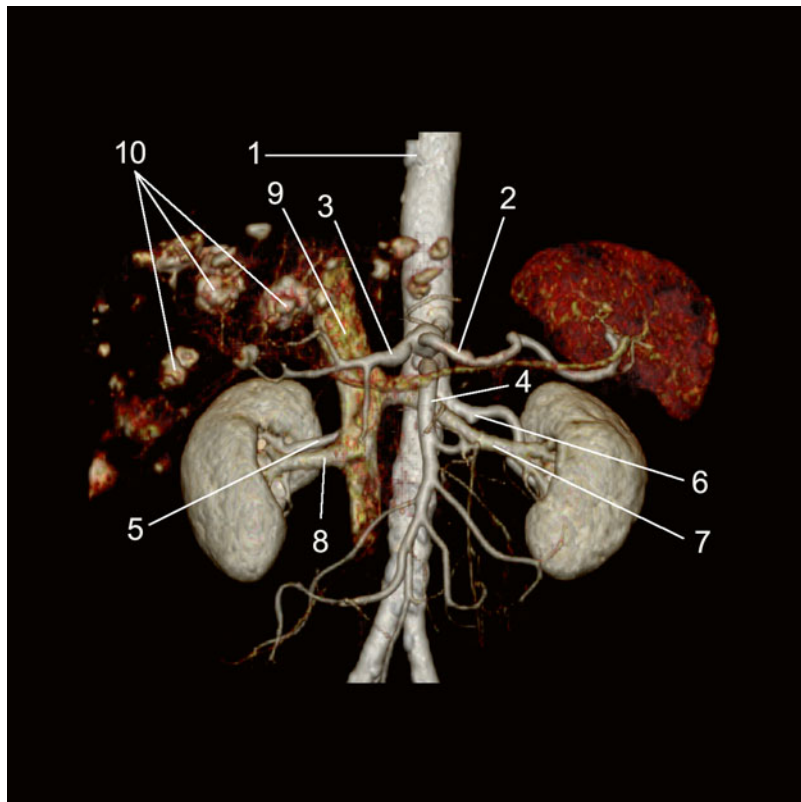


Fig. 5.7 3D VRT reconstruction frontal view

1. Aorta
2. A. splenica
3. A. hepatica communis
4. A. mesenterica superior
5. A. renalis dexter
6. A. renalis sinister
7. V. renalis sinister
8. V. renalis dexter
9. V. cava inferior
10. Hepatic haemangiomas

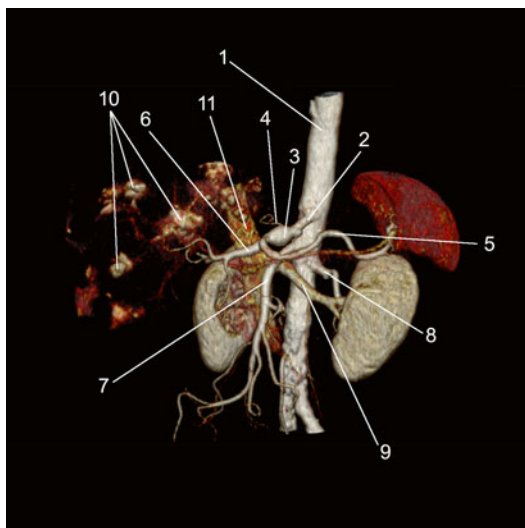


Fig. 5.8 3D VRT reconstruction anterolateral view

1. Aorta
2. Truncus coeliacus
3. Aneurysm of truncus coeliacus
4. A. gastrica sinistra
5. A. splenica
6. A. hepatica communis
7. A. mesenterica superior
8. A. renalis sinistra
9. V. renalis sinistra
10. Haemangiomas of the liver
11. V. cava inferior

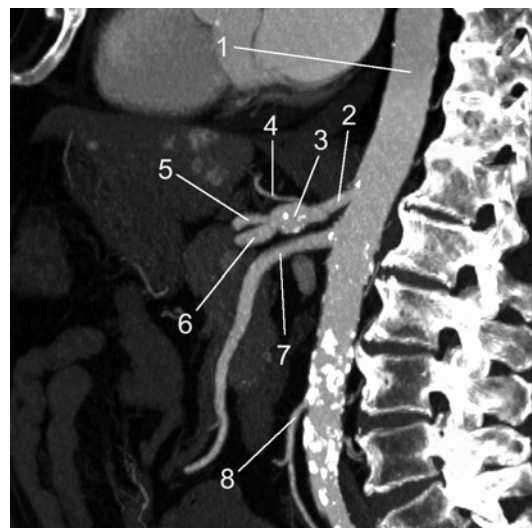


Fig. 5.9 3D MIP reconstruction, sagittal plane

1. Aorta
2. Truncus coeliacus
3. Aneurysm of truncus coeliacus, with calcified plaques
4. A. gastrica sinistra
5. A. splenica
6. A. hepatica communis
7. A. mesenterica superior
8. A. mesenterica inferior



Fig. 5.10 3D MIP reconstruction, transversal plane

1. Aorta
 2. Truncus coeliacus
 3. Aneurysm of truncus coeliacus
 4. A. hepatica communis
 5. A. splenica
 6. Haemangiomas of the liver
- The *full arrow* indicates stenotic lesion of a. hepatica communis

5.3 Left Renal Arteriovenous Fistula

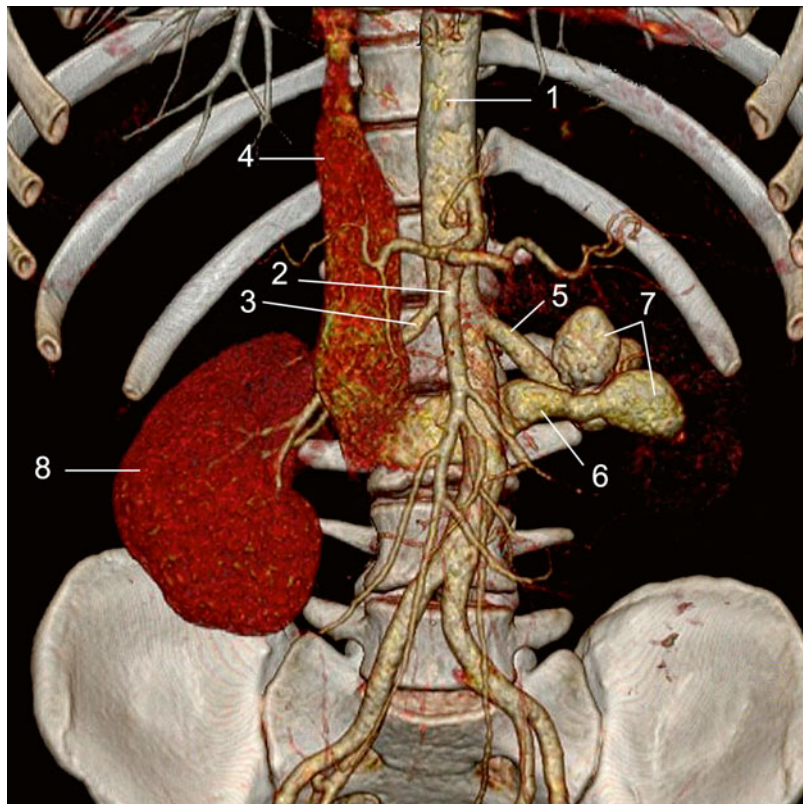


Fig. 5.11 3D VRT colour reconstruction

1. Aorta abdominalis
2. A. mesenterica superior
3. A. renalis dextra
4. Vena cava inferior
5. A. renalis sinistra
6. Vena renalis sinistra
7. Aneurysmal dilatations on the renal arteriovenous fistula's course
8. Normal vascularisation of the right kidney – absence of vascularisation of the left renal parenchyma can be observed

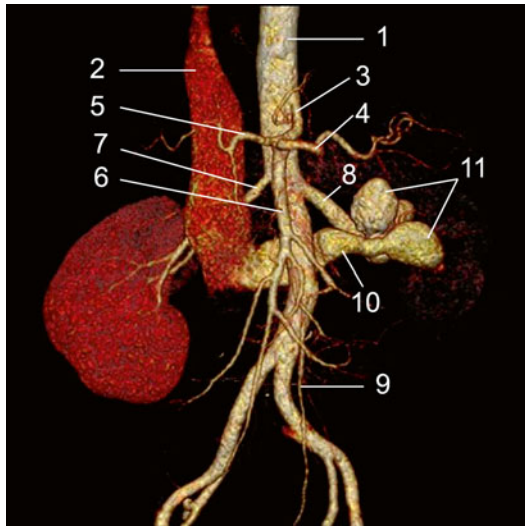


Fig. 5.12 3D VRT colour reconstruction after removal of the bone structure

1. Aorta
2. Vena cava inferior
3. Truncus coeliacus
4. A. splenica
5. A. hepatica
6. A. mesenterica superior
7. A. renalis dextra
8. A. renalis sinistra
9. A. mesenterica inferior
10. Vena renalis sinistra with retroaortic course
11. Aneurysmal dilatations on the left renal arteriovenous fistula's course

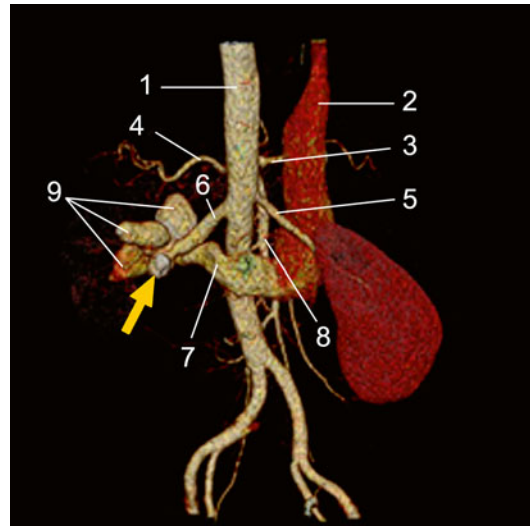


Fig. 5.13 3D VRT colour reconstruction after removal of the bone structure, posterior plane

1. Aorta
 2. Vena cava inferior
 3. A. hepatica
 4. A. splenica
 5. A. renalis dextra
 6. A. renalis sinistra
 7. Vena renalis sinistra with retroaortic course
 8. A. mesenterica superior
 9. Aneurysmal dilatations on the fistula's course
- Full arrow indicates calcification of fistula wall*

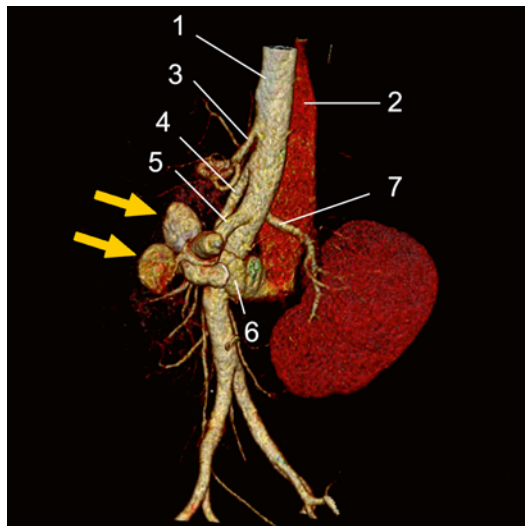


Fig. 5.14 3D VRT colour reconstruction after removal of the bone structure

1. Aorta
2. Vena cava inferior
3. Truncus coeliacus
4. A. mesenterica superior
5. A. renalis sinistra
6. Vena renalis sinistra
7. A. renalis dextra

The full arrow indicates aneurysmal dilated fistula course

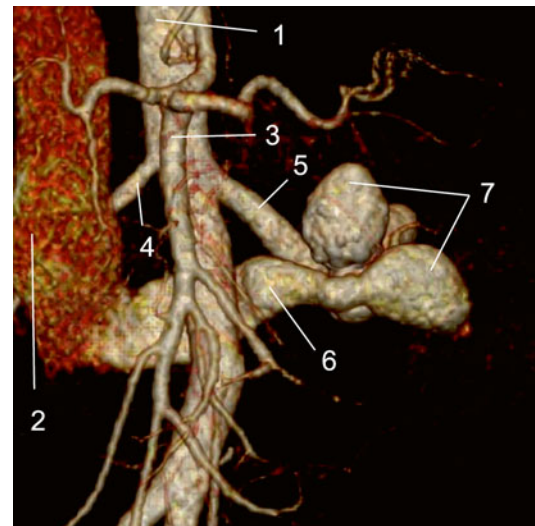


Fig. 5.15 3D VRT colour reconstruction anterior frontal plane (enlarged image)

1. Aorta
2. Vena cava inferior
3. A. mesenterica superior
4. A. renalis dextra
5. A. renalis sinistra
6. Vena renalis sinistra
7. Aneurysmal dilatations on the fistula's course

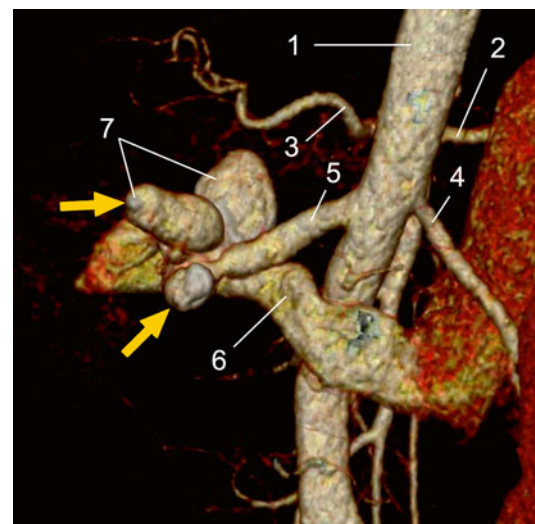


Fig. 5.16 3D VRT colour reconstruction posterior frontal plane (enlarged image)

1. Aorta
2. A. hepatica
3. A. splenica
4. A. renalis dextra
5. A. renalis sinistra
6. V. renalis sinistra
7. Aneurysmal dilatations of fistula with calcified plaques marked through full arrows

5.4 Aorta Abdominalis Aneurysm with Aortoduodenal Fistula



Fig. 5.17 3D MIP reconstruction frontal plane

1. Aneurysmal dilated aortic lumen
 2. Thrombosis area of the aneurysm
- The full arrow indicates aneurysm with parietal calcifications

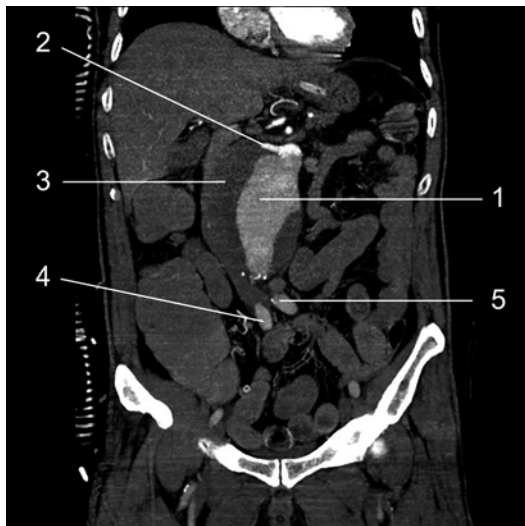


Fig. 5.18 3D MIP reconstruction frontal plane
1. Aneurysmal dilated aortic lumen
2. Emergence and pars proximalis a. renalis dextra
3. Thrombotic area
4. A. iliaca communis
5. A. iliaca communis



Fig. 5.20 3D MIP reconstruction sagittal plane
1. Aneurysmal dilated aorta
2. Mural thrombosis of aneurysm
3. A. iliaca communis

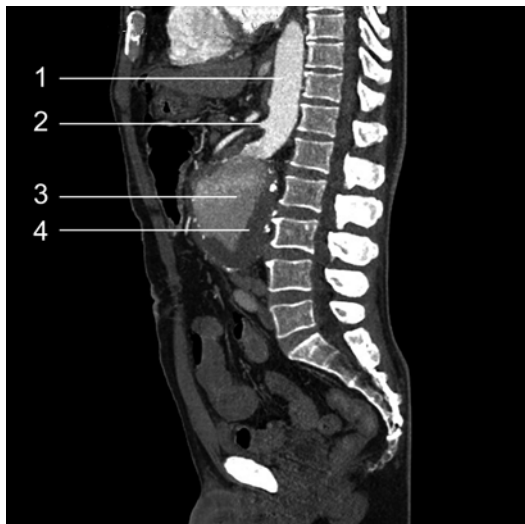


Fig. 5.19 3D MIP reconstruction sagittal plane
1. Aorta abdominalis
2. A. mesenterica superior
3. Aneurysm dilated at the level of aorta abdominalis
4. Mural thrombosis area



Fig. 5.21 3D MIP reconstruction sagittal plane
1. Aneurysmal dilated aorta
2. Parietal thrombosis
3. Fistulas course at the aneurysm level which communicated with duodenum



Fig. 5.22 3D MIP reconstruction sagittal plane
1. Aneurysmal dilated aorta
2. Parietal thrombosis
3. Fistulas course

5.5 Operated Aorta Abdominalis Aneurysm: Post-operative Complications

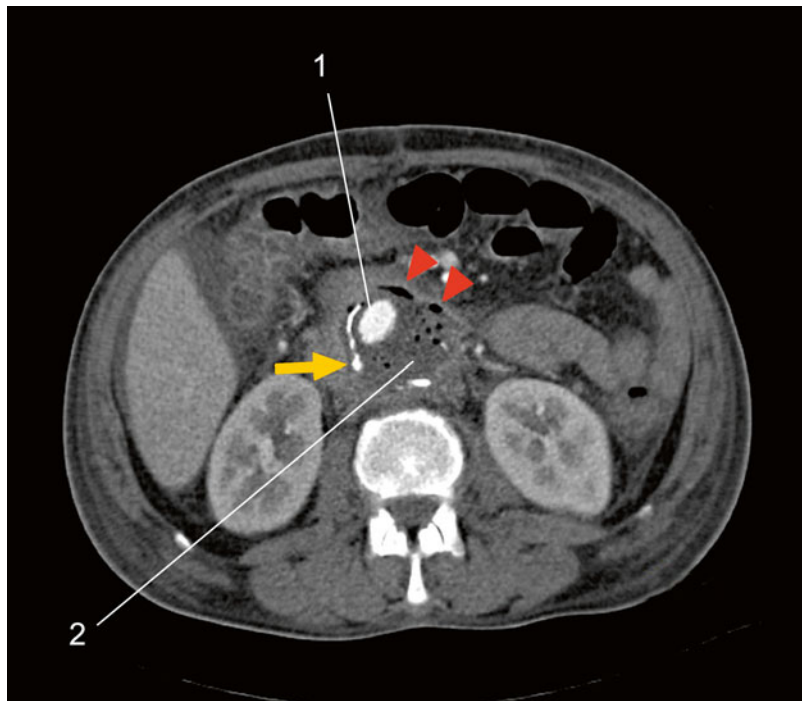


Fig. 5.23 3D MIP reconstruction axial plane

1. Lumen of aortic graft
2. Periprosthetic haematoma

*Full arrow = calcified plaques of the aortic wall
The tip of the arrows = indicate presence of gas bubbles at the level of periprosthetic haematoma suggesting over-infection*

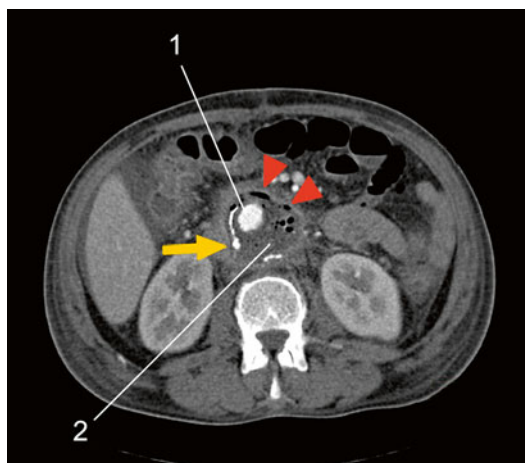


Fig. 5.24 3D MIP reconstruction axial plane

1. Lumen of aortic graft
2. Periprosthetic haematoma

Full arrow = calcified plaques of the aortic wall

The tip of the arrows = indicate presence of gas bubbles at the level of periprosthetic haematoma suggesting over-infection



Fig. 5.25 3D MIP reconstruction frontal plane

1. Lumen of aortic graft
2. Periprosthetic haematoma

Full arrow = calcified plaques of the aortic wall

The tip of the arrows = indicate presence of gas bubbles at the level of periprosthetic haematoma suggesting over-infection



Fig. 5.26 3D MIP reconstruction frontal plane
 1. Lumen of aortic graft
 2. Periprosthetic haematoma
Full arrow=calcified plaques of the aortic wall
 The *tip of the arrows*=indicate presence of gas bubbles at the level of periprosthetic haematoma suggesting over-infection

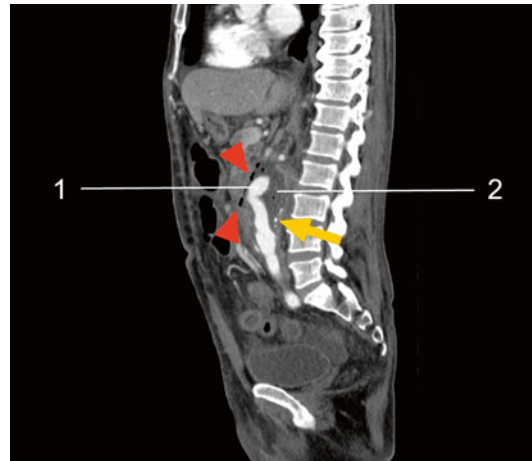


Fig. 5.28 3D MIP reconstruction sagittal plane
 1. Lumen of aortic graft
 2. Periprosthetic haematoma
Full arrow=calcified plaques of the aortic wall
 The *tip of the arrows*=indicate presence of gas bubbles at the level of periprosthetic haematoma suggesting over-infection

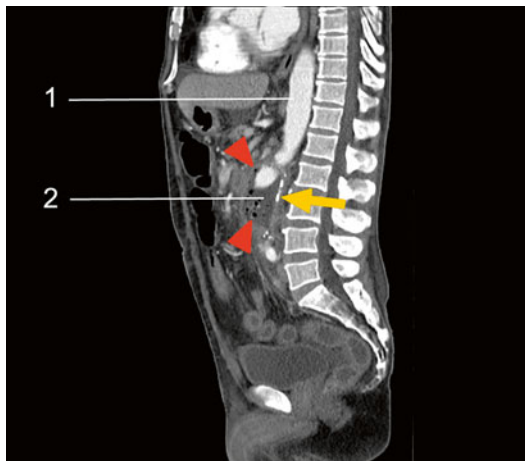


Fig. 5.27 3D MIP reconstruction sagittal plane
 1. Lumen of aortic graft
 2. Periprosthetic haematoma
Full arrow=calcified plaques of the aortic wall
 The *tip of the arrows*=indicate presence of gas bubbles at the level of periprosthetic haematoma suggesting over-infection

5.6 Stenosis of A. Renalis Sinistra

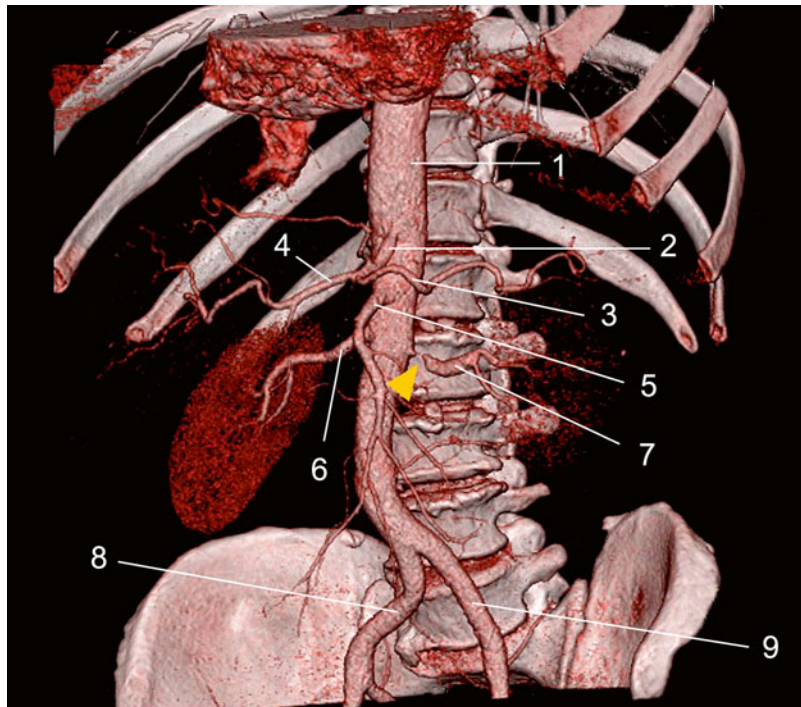


Fig. 5.29 3D VRT colour reconstruction after removal of the bone structure

1. Aorta abdominalis
2. Truncus coeliacus
3. A. splenica
4. A. hepatica
6. A. renalis dextra
7. A. renalis sinistra
8. A. iliaca communae
9. A. iliaca communae

The tip of the arrows indicate severe ostial stenotic area

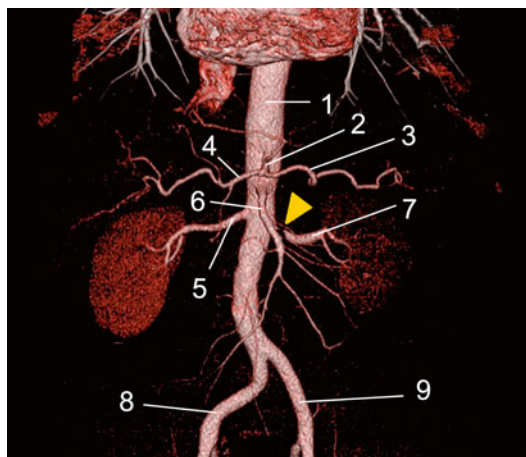


Fig. 5.30 3D VRT colour reconstruction after removal of the bone structure

1. Aorta abdominalis
 2. Truncus coeliacus
 3. A. splenica
 4. A. hepatica
 6. A. renalis dextra
 7. A. renalis sinistra
 8. A. iliaca communae
 9. A. iliaca communae
- The tip of the arrows indicate severe ostial stenotic area

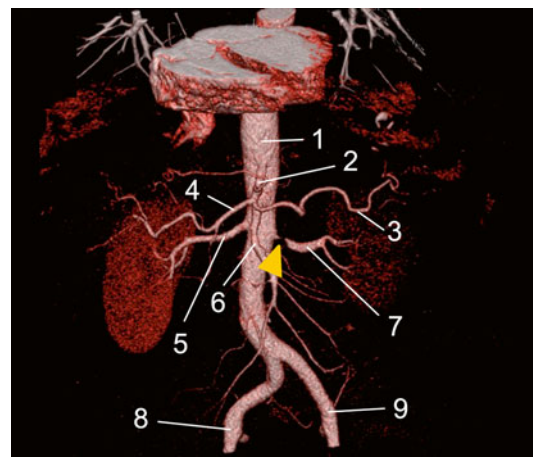


Fig. 5.31 3D VRT colour reconstruction after removal of the bone structure

1. Aorta abdominalis
 2. Truncus coeliacus
 3. A. splenica
 4. A. hepatica
 6. A. renalis dextra
 7. A. renalis sinistra
 8. A. iliaca communae
 9. A. iliaca communae
- The tip of the arrows indicate severe ostial stenotic area

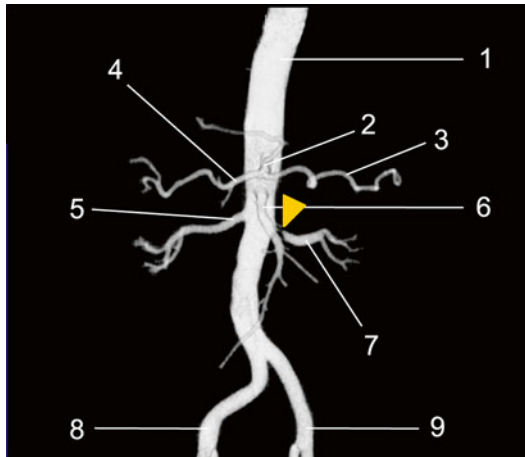


Fig. 5.32 3D MIP reconstruction after removal of the bone structure

1. Aorta abdominalis
2. Truncus coeliacus
3. A. splenica
4. A. hepatica
5. A. renalis dextra
6. A. renalis sinistra
7. A. iliaca communae
8. A. iliaca communae
9. A. iliaca communae

The tip of the arrows indicate severe ostial stenotic area

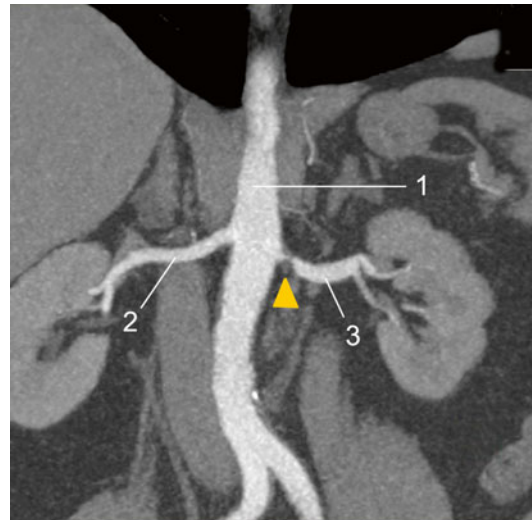


Fig. 5.34 3D MIP reconstruction, frontal plane

1. Aorta
2. A. renalis dextra
3. A. renalis sinistra

The tip of the arrows indicate severe stenotic area

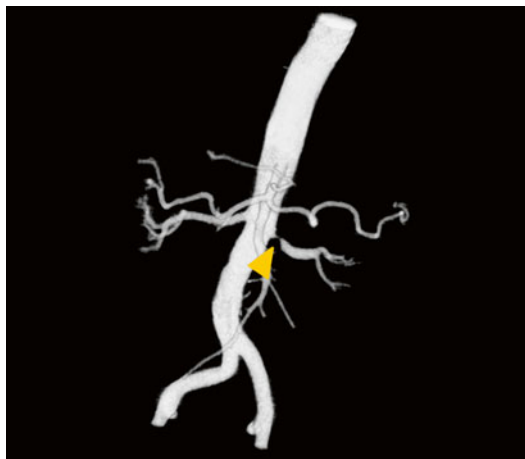


Fig. 5.33 3D VRT reconstruction

The full arrow indicates severe stenosis of a. renalis sinistra



Fig. 5.35 3D MIP reconstruction, frontal plane

1. Aorta
2. A. renalis dextra
3. A. renalis sinistra

The tip of the arrows indicate severe stenotic area

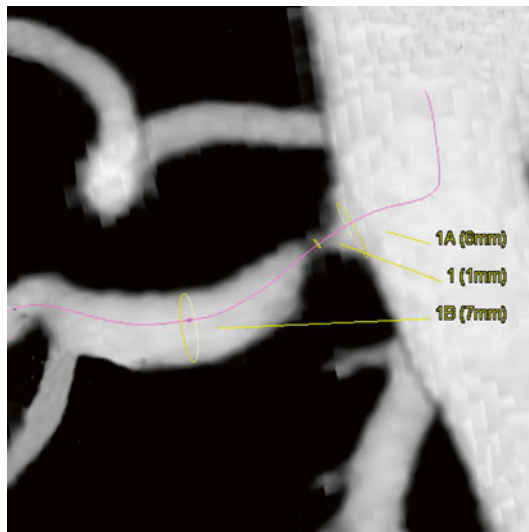


Fig. 5.36 Determination of stenosis grade

5.7 Right A. Renalis Dextra Occlusion Collateral Circulation for Renal Parenchyma

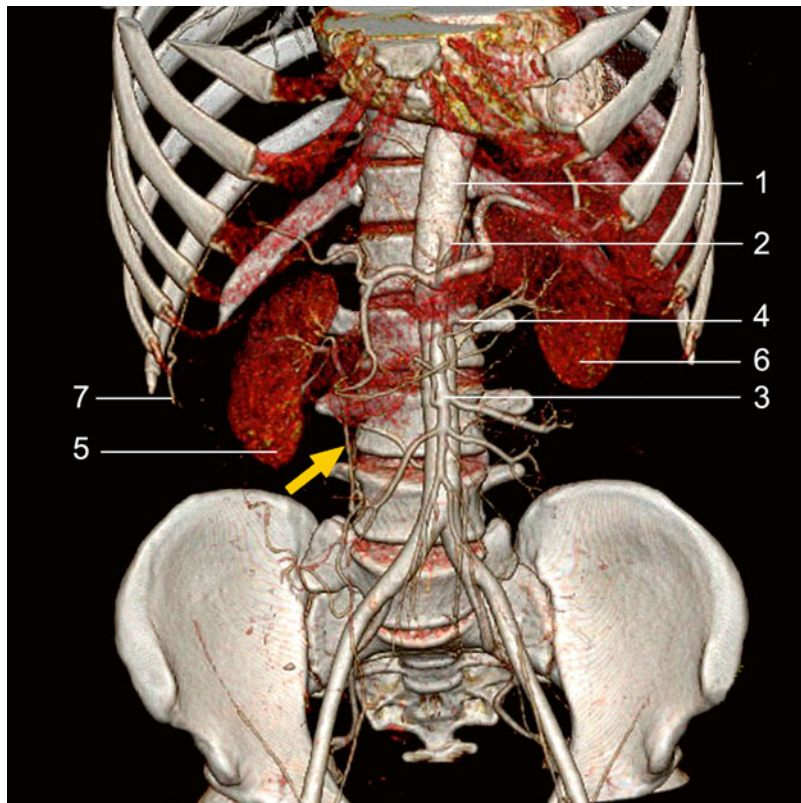


Fig. 5.37 3D VRT colour reconstruction

1. Aorta
 2. Truncus coeliacus
 3. A. mesenterica superior
 4. A. renalis sinistra
 5. Ren dextra
 6. Ren sinistra
 7. A. intercostalis from which hilum renale irrigating collateral develops

The *full arrow* indicates
ren dextra vascularised
through collateral arteries

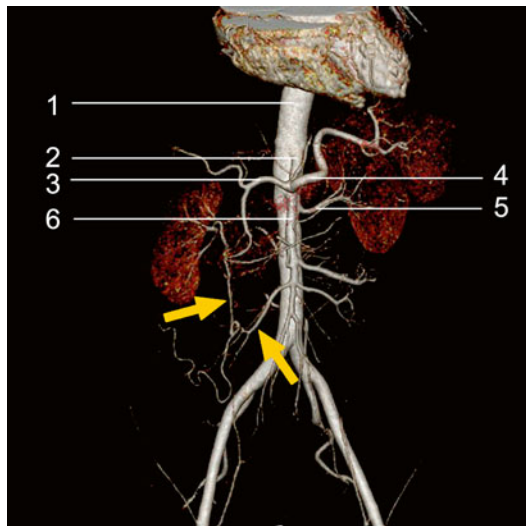


Fig. 5.38 3D VRT colour reconstruction, after removal of the bone structure
1. Aorta
2. Truncus coeliacus
3. A. hepatica communis
4. A. splenica
5. A. renalis sinistra
6. A. mesenterica superior
The arrow indicates ren dextra vascularised through collateral arteries

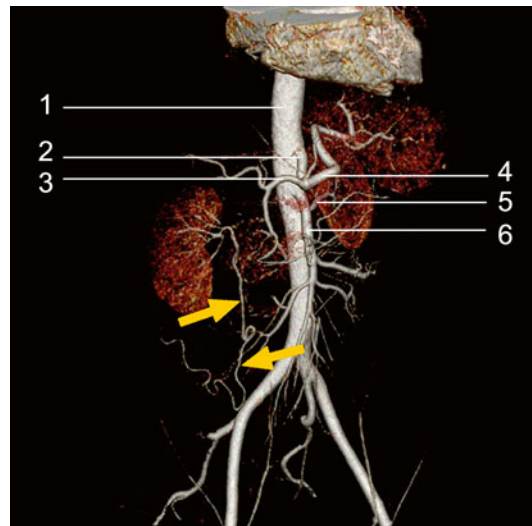


Fig. 5.39 3D VRT colour reconstruction, transversal plane
1. Aorta
2. Truncus coeliacus
3. A. hepatica communis
4. A. splenica
5. A. renalis sinistra
6. A. mesenterica superior
The arrow indicates ren dextra vascularised through collateral arteries

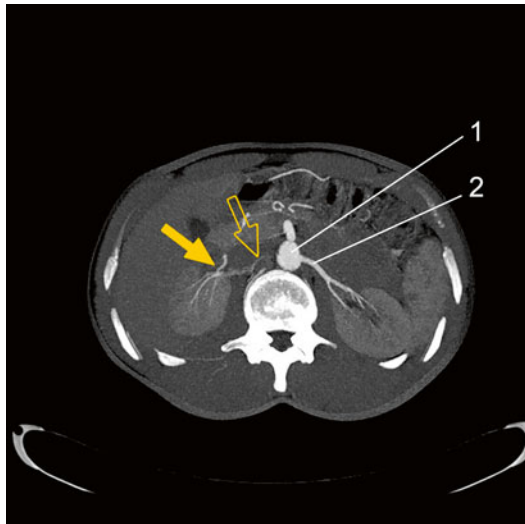


Fig. 5.40 3D MIP reconstruction, coronal plane
 1. Aorta
 2. A. renalis sinistra
Full arrow=vascularised hilum renale dextra
Arrow with contour=a. renalis dextra with chronic occlusion from the emergence



Fig. 5.42 3D MIP reconstruction, coronal plane
 1. Aorta
 The *arrows* indicate collateral course to hilum renale dextra

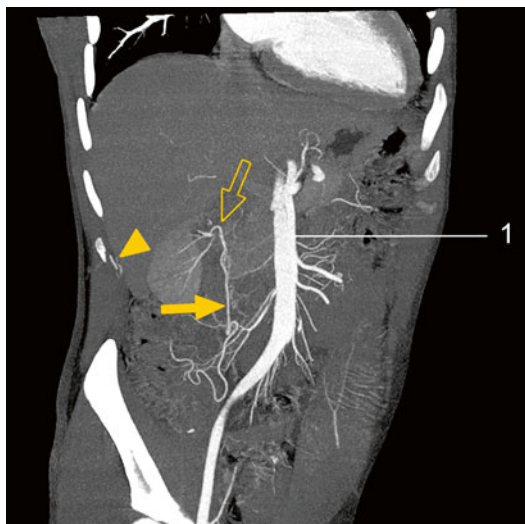


Fig. 5.41 3D MIP reconstruction, coronal plane
 1. Aorta
Full arrow=collateral with ascending course to hilum renale dextra
Arrow with contour=vascularised hilum renale dextra
 The *tip of the arrow*=a. intercostalis from which collateral develops

5.8 Dissection of Aorta Abdominalis

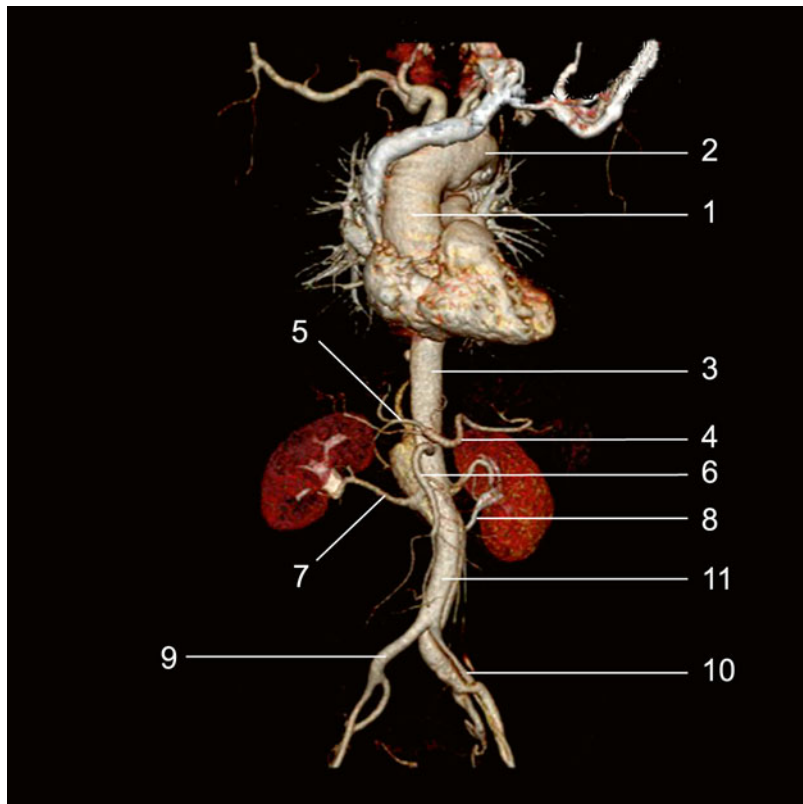
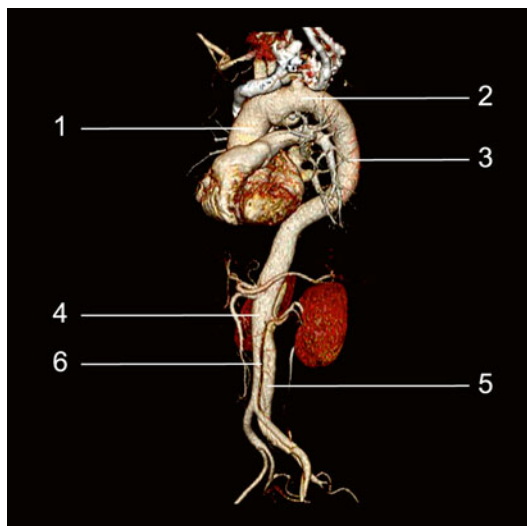
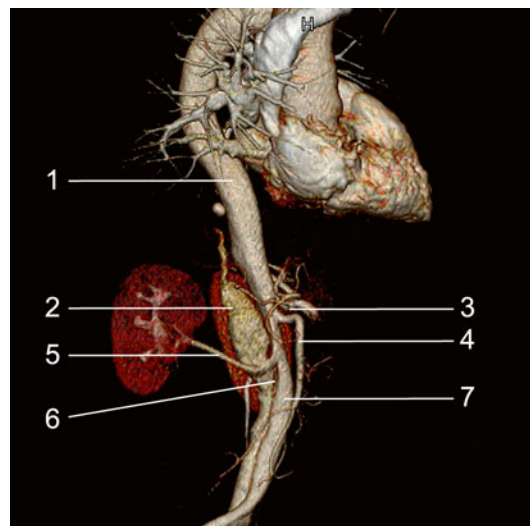


Fig. 5.43 3D VRT colour reconstruction after removal of the bone structure

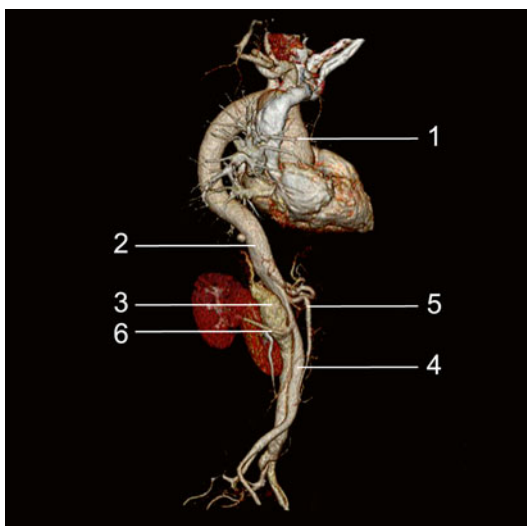
1. Aorta ascendens
2. Arcus aortae
3. Aorta descendens
4. A. splenica
5. A. hepatica
6. A. mesenterica superior
7. A. renalis dextra
8. A. renalis sinistra
9. A. iliaca communis dextra
10. A. iliaca communis sinistra with dissection fold
11. True lumen

**Fig. 5.44** 3D VRT colour reconstruction

1. Aorta ascendens
2. Arcus aortae
3. Aorta thoracica
4. True lumen of aorta abdominalis
5. False lumen
6. Dissection fold

**Fig. 5.46** 3D VRT colour reconstruction

1. Aorta ascendens
2. Aorta descendens
3. False lumen
4. True lumen of aorta abdominalis
5. A. mesenterica superior
6. A. renalis dextra
7. True lumen

**Fig. 5.45** 3D VRT colour reconstruction

1. Aorta abdominalis
2. False lumen
3. From the lumen emerges the iliac trunk
4. A. mesenterica superior
5. From the true lumen emerges a. renalis dextra
6. Dissection fold

5.9 Separate Emergence of A. Hepatica Communis and A. Splenica Additional Polar Left Superior A. Renalis Sinistra

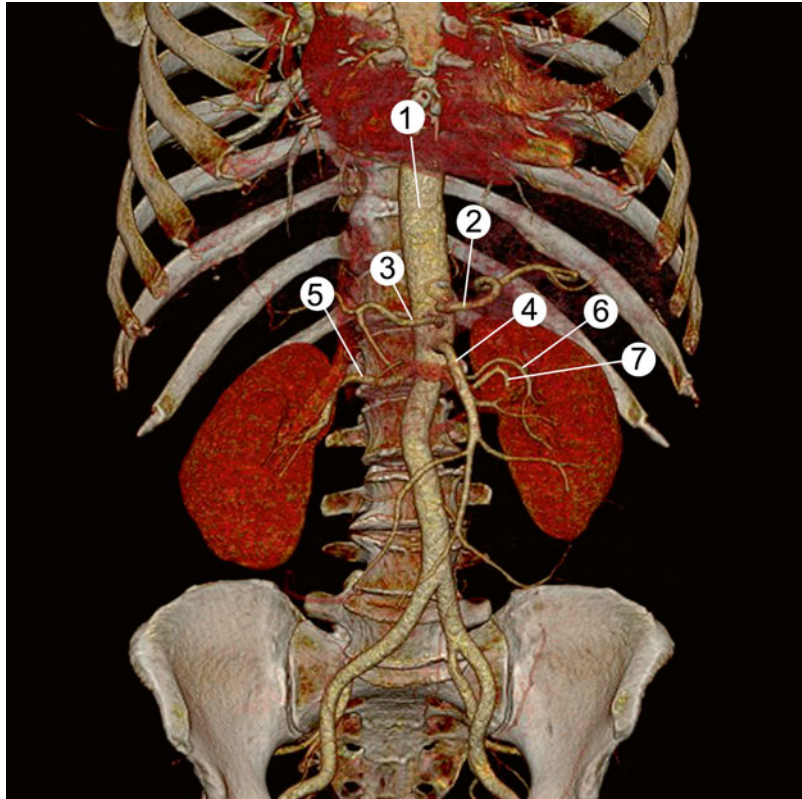
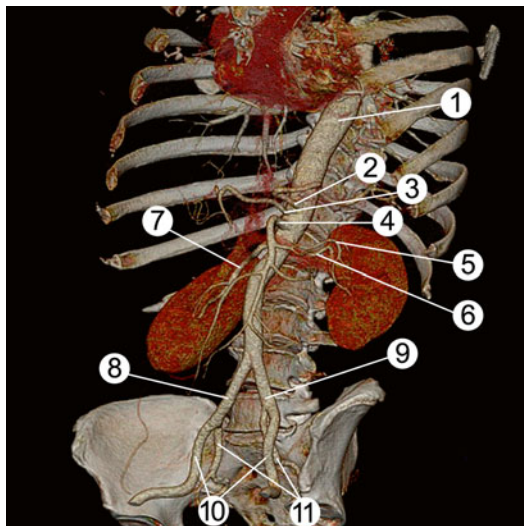
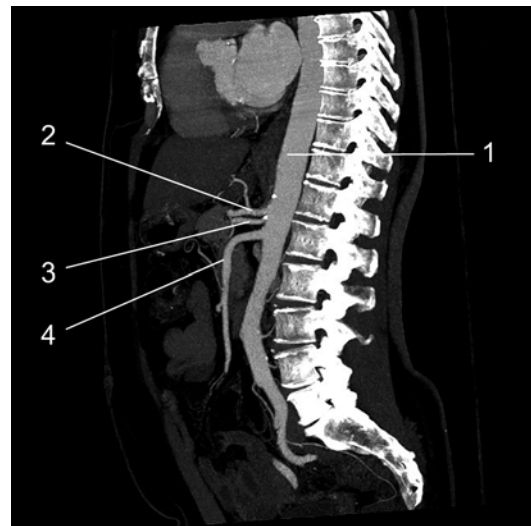


Fig. 5.47 3D VRT colour reconstruction

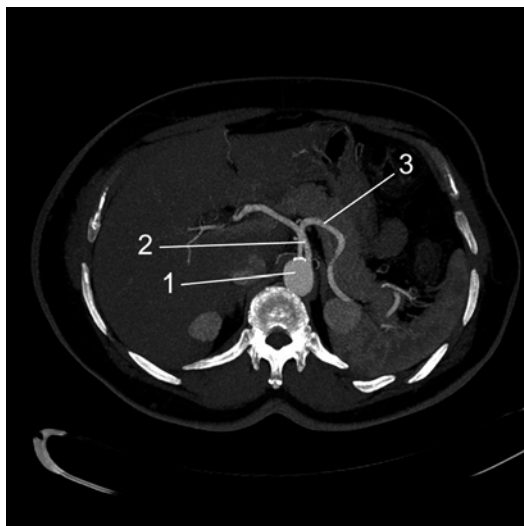
1. Aorta
2. A. splenica
3. A. hepatica communis
4. A. mesenterica superior
5. A. renalis dextra
6. Additional a. renalis sinistra
7. A. renalis sinistra

**Fig. 5.48** 3D VRT colour reconstruction

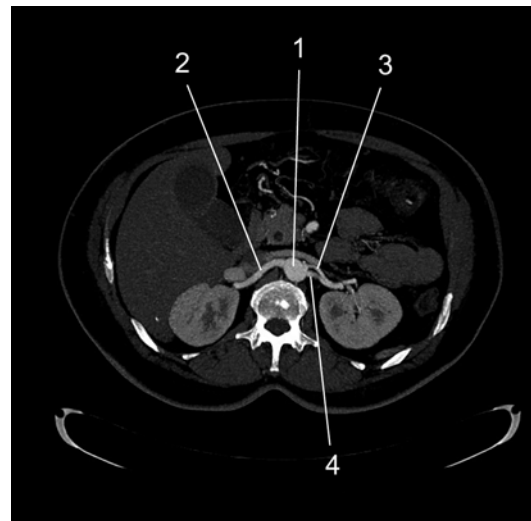
1. Aorta
2. Separate emergence of a. splenica from the aorta abdominalis
3. A. hepatica communis with independent aortic emergence
4. A. mesenterica superior
5. Additional polar left inferior a. renalis
6. A. renalis sinistra
7. A. renalis dextra
8. A. iliaca communia
9. A. iliaca communia
10. A. iliaca externa
11. A. iliaca interna

**Fig. 5.50** 3D MIP reconstruction, sagittal plane

1. Aorta
2. A. splenica
3. A. hepatica communis
4. A. mesenterica superior

**Fig. 5.49** 3D MIP reconstruction, transversal plane

1. Aorta
2. A. hepatica communis
3. A. splenica

**Fig. 5.51** 3D MIP reconstruction, axial plane

1. Aorta
2. A. renalis dextra
3. Additional polar left inferior a. renalis
4. A. renalis sinistra



Fig. 5.52 3D MIP reconstruction, axial plane

1. Aorta
2. A. renalis dextra
3. Additional polar left inferior a. renalis
4. A. renalis sinistra

5.10 Multiple Aneurysms of A. Splenica Associated with Aneurysm of A. Renalis Dexter

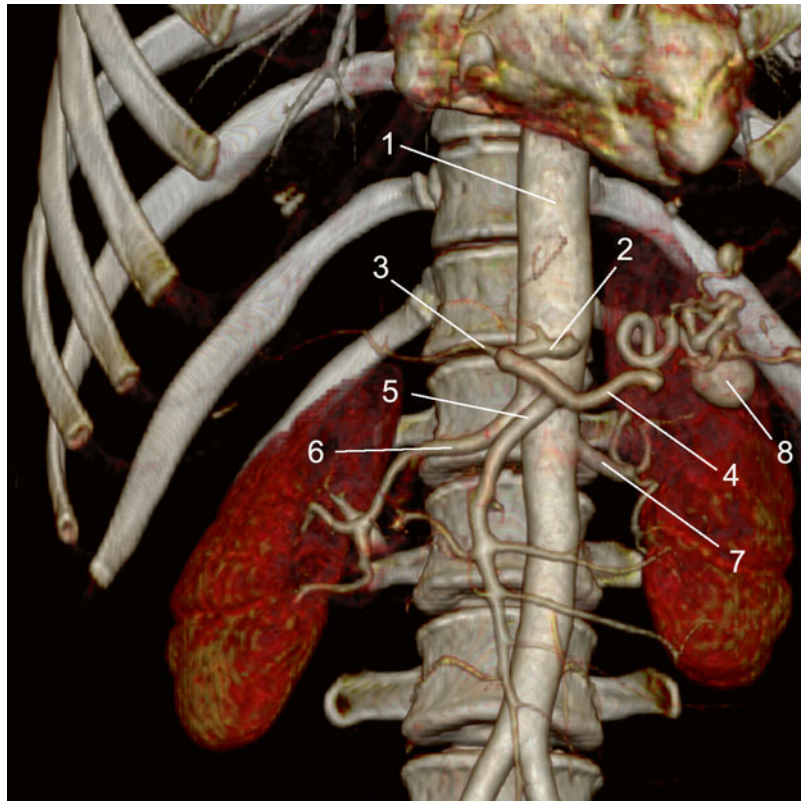


Fig. 5.53 3D VRT reconstruction, frontal plane

1. Aorta
2. Truncus coeliacus
3. A. hepatica communis
4. A. splenica
5. A. mesenterica superior
6. A. renalis dextra
7. A. renalis sinistra
8. Aneurysm of a. splenica

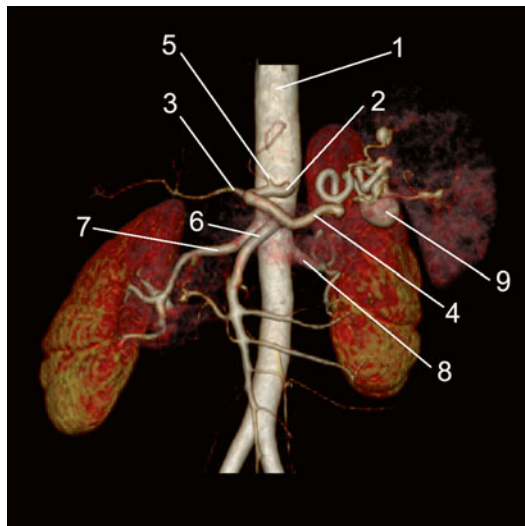


Fig. 5.54 3D VRT reconstruction, frontal plane, after removal of bony structures

1. Aorta
2. Truncus coeliacus
3. A. hepatica communis
4. A. splenica
5. A. gastrica sinistra
6. A. mesenterica superior
7. A. renalis dextra
8. A. renalis sinistra
9. Aneurysms of a. splenica

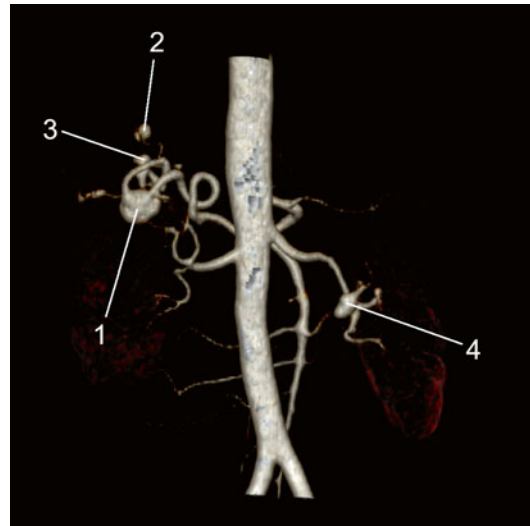


Fig. 5.56 3D VRT reconstruction, posterior view

1. Aneurysms of a. splenica
2. Aneurysms of a. splenica
3. Aneurysms of a. splenica
4. Aneurysm of a. renalis dextra

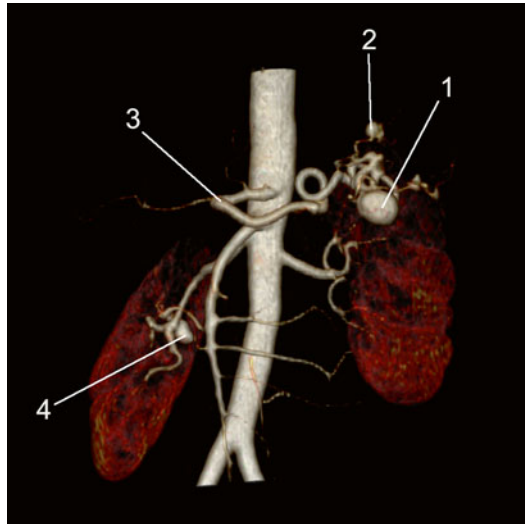


Fig. 5.55 3D VRT reconstruction, anterolateral view

1. Aneurysms of a. splenica
2. Aneurysms of a. splenica
3. Aneurysms of a. splenica
4. Aneurysm of a. renalis dextra

Contents

6.1	Normal Peripheral Angiography	160
6.2	Leriche Syndrome	165
6.3	Leriche Syndrome Axillobifemoral Bypass	167
6.4	Leriche Syndrome Aortobifemoral and Femoropopliteal Graft	170
6.5	Aortobifemoral Graft and Aneurysms at the Level of Anastomosis	174
6.6	Right Arm Occlusion of the Aortobifemoral Graft	177
6.7	Right Femoro-fibular Graft: Occlusion of the Left Lower Limb Arteries	179
6.8	Iliac and Femoral Stents: In-Stent Restenosis	182
6.9	Iliac and Femoral Stents: Occluded Iliac Stents	185
6.10	Autoimmune Vasculitis	187
6.11	Tumour of the Leg	190
6.12	Giant Tumour of the Thigh	192
6.13	CT Angiography of the Right Upper Limb: Occlusion of the Arteria Radialis Dextra	194
6.14	Arteriovenous Malformation in Deltoid Region	196
6.15	CTA Run-Off: Incidental Finding	198

6.1 Normal Peripheral Angiography

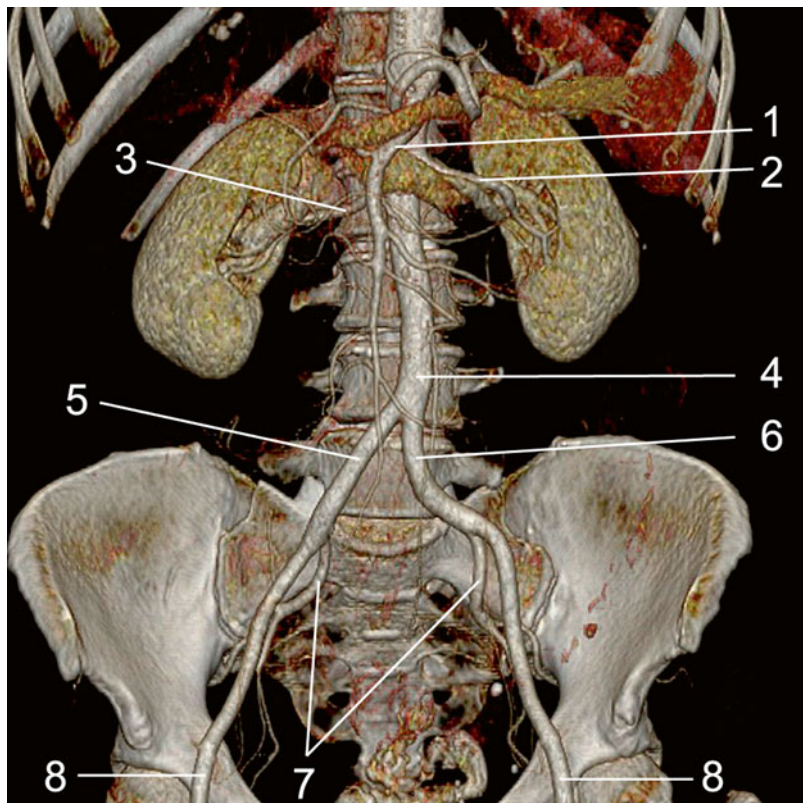


Fig. 6.1 3D VRT colour reconstruction, enlarged image

1. A. mesenterica superior
2. A. renalis sinistra
3. A. renalis dextra
4. Aorta abdominalis
5. A. iliaca communae
6. A. iliaca communae
7. A. iliaca internae
8. A. iliaca externae

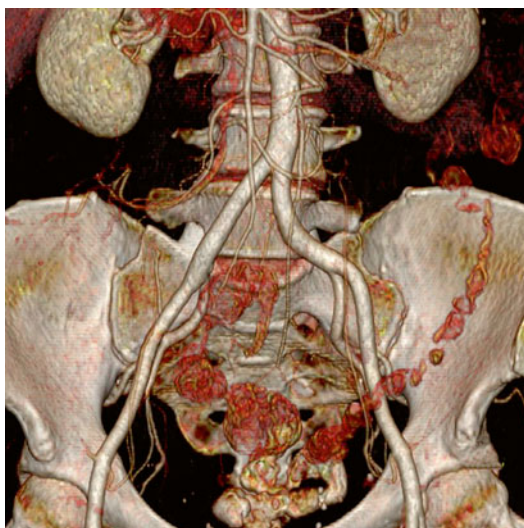


Fig. 6.2 3D VRT colour reconstruction, bifurcation aortae

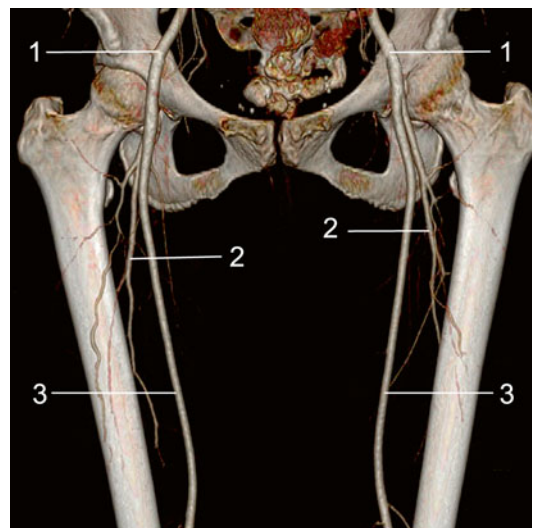


Fig. 6.3 3D VRT colour reconstruction

1. A. iliaca externae
2. A. profunda femoris
3. A. femoralis



Fig. 6.4 3D VRT reconstruction, a. femoralis pars distalis

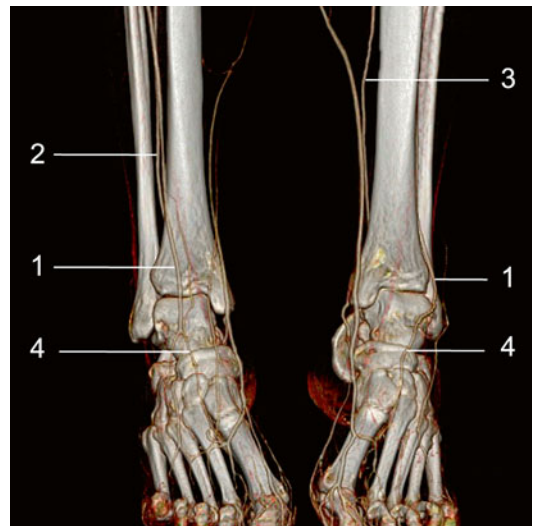


Fig. 6.6 3D VRT reconstruction
1. A. tibialis anterior
2. A. peronea
3. A. tibialis posterior
4. A. dorsalis pedis



Fig. 6.5 3D VRT reconstruction
1. A. tibialis anterior
2. A. peronea



Fig. 6.7 3D VRT reconstruction at the level of dorsum pedis
1. A. tibialis anterior pars distalis
2. A. dorsalis pedis



Fig. 6.8 3D VRT reconstruction with visualisation of regio dorsalis pedis

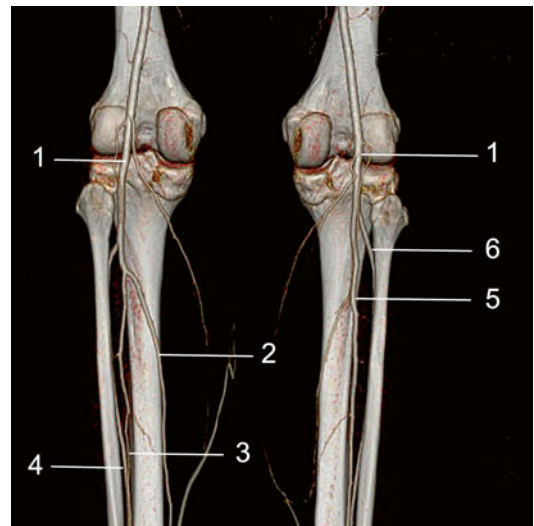


Fig. 6.10 3D VRT reconstruction regio cruris and fossa poplitea

1. A. poplitea
2. A. tibialis posterior sinistra
3. A. peronea sinistra
4. A. tibialis anterior sinistra
5. A. peronea dextra
6. A. tibialis anterior dextra



Fig. 6.9 3D VRT colour reconstruction posterior image at the level of regio cruris

1. A. tibialis posterior sinistra
2. A. peronea sinistra
3. A. tibialis anterior sinistra
4. A. tibialis anterior dextra
5. A. peronea magna
6. Hypoplastic a. tibialis posterior dextra

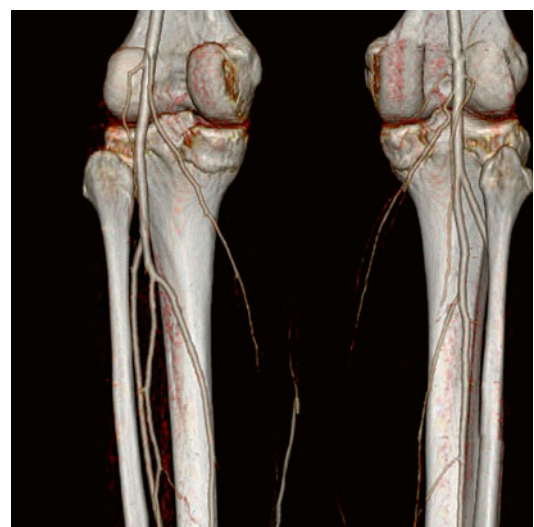


Fig. 6.11 3D VRT reconstruction at the level of fossa poplitea, enlarged image



Fig. 6.12 3D VRT reconstruction at the level of fossa poplitea and 1/3 distal part of crus with visualisation of a. femoralis



Fig. 6.14 3D VRT reconstruction after removal of the bone structure, visualisation of a. femoralis and a. profunda femoris



Fig. 6.13 3D VRT reconstruction at the level of 1/3 medialis part of crus with visualisation of a. profunda femoris



Fig. 6.15 3D VRT reconstruction after removal of the bone structure, at the level of abdomen with visualisation of bifurcation aortae and a. iliaceae and a. femoralis

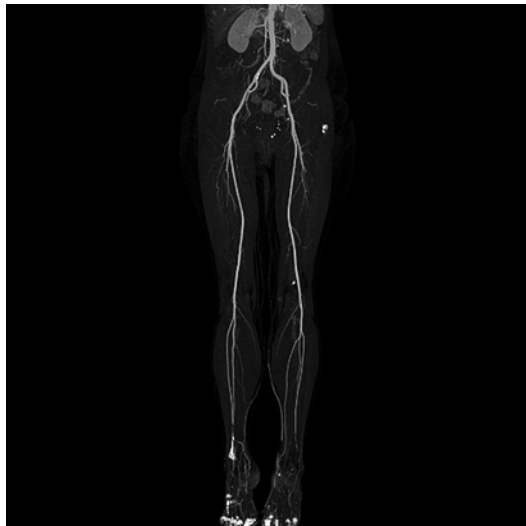


Fig. 6.16 3D VRT reconstruction after removal of the bone structure

6.2 Leriche Syndrome

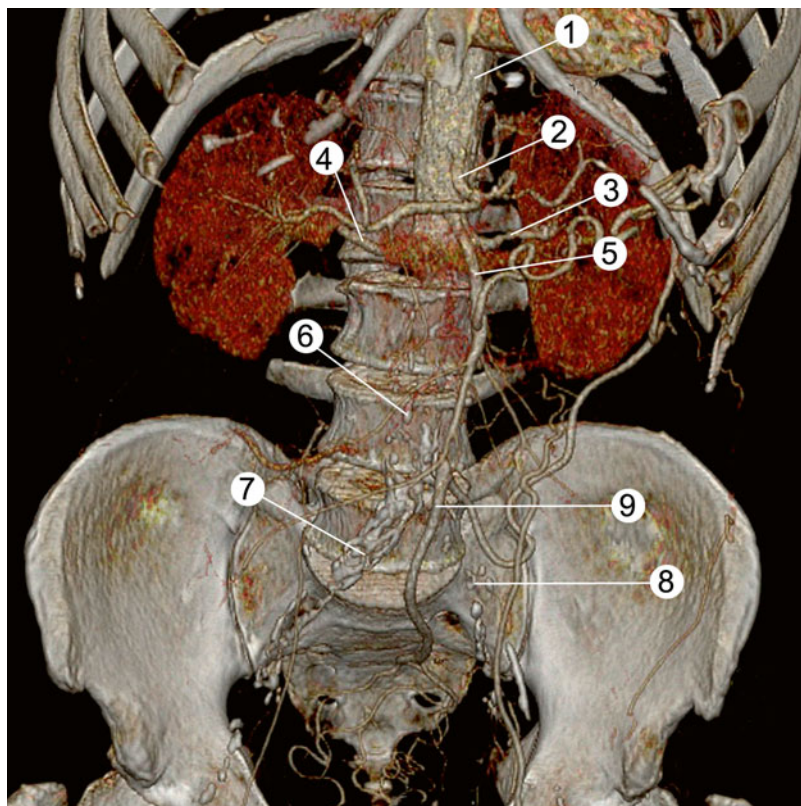
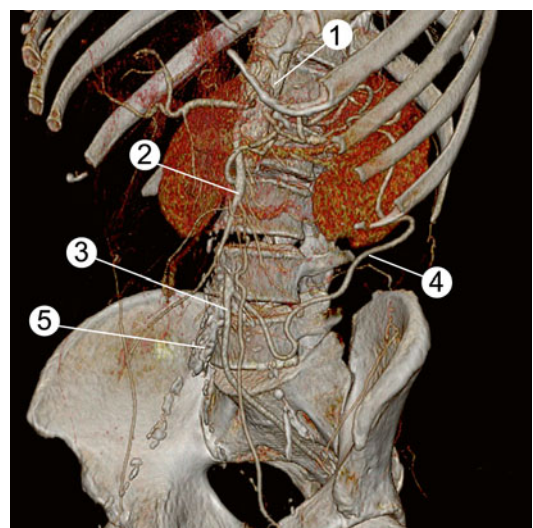


Fig. 6.17 3D VRT colour reconstruction

1. Aorta abdominalis + pars proximalis
2. Truncus coeliacus
3. A. renalis sinistra
4. A. renalis dextra
5. A. mesenterica superior
6. Aorta abdominalis pars distalis + thrombosis and calcification
7. A. iliaca communae et externae thrombosed and calcified
8. A. iliaca communae et externae thrombosed and calcified
9. A. mesenterica superior

Fig. 6.18 3D VRT colour reconstruction

1. Aorta abdominalis
2. A. mesenterica superior
3. A. mesenterica inferior
4. Collateral through a. mesenterica inferior is vascularised
5. A. iliaca communis calcified and thrombosed



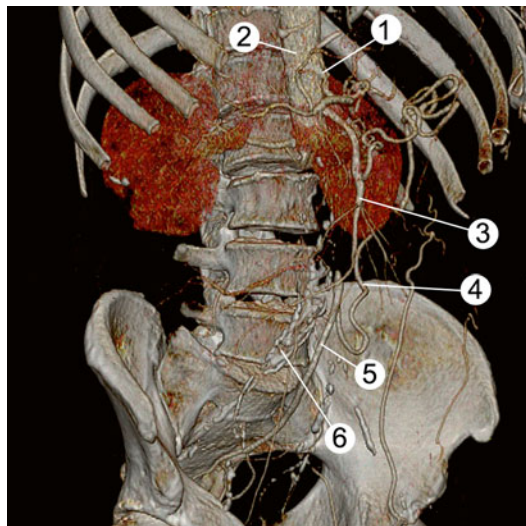


Fig. 6.19 3D VRT colour reconstruction

1. Truncus coeliacus
2. Aorta abdominalis
3. Ar. mesenterica superior
4. Collateral
5. A. mesenterica inferior
6. A. iliaca communae thrombosed and calcified

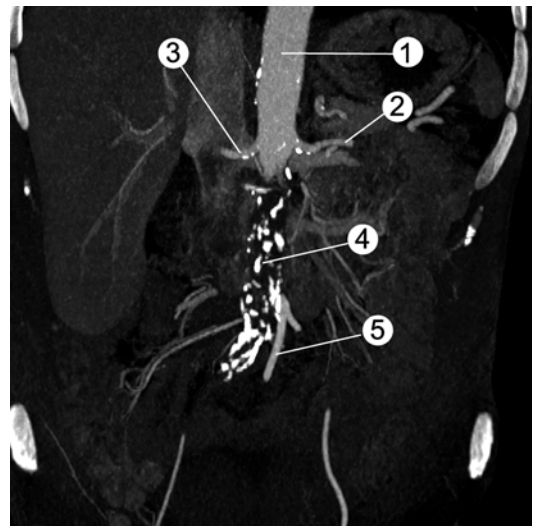


Fig. 6.21 3D MIP reconstruction

1. Aorta abdominalis
2. A. renalis sinistra
3. A. renalis dextra
4. A. abdominalis, pars distalis thrombosed and calcified
5. A. mesenterica inferior

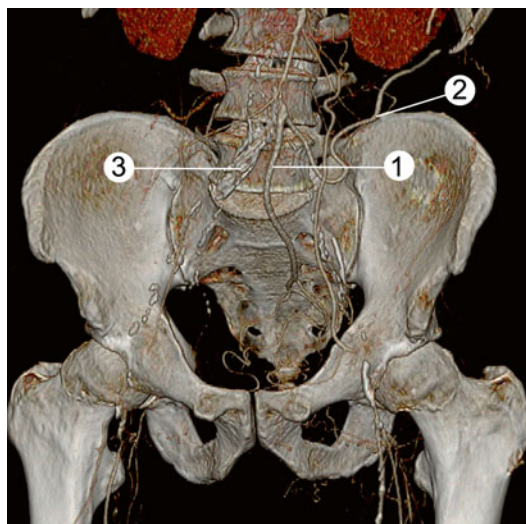


Fig. 6.20 3D VRT colour reconstruction

1. A. mesenterica inferior
2. Collateral
3. A. iliaca communae thrombosed and calcified

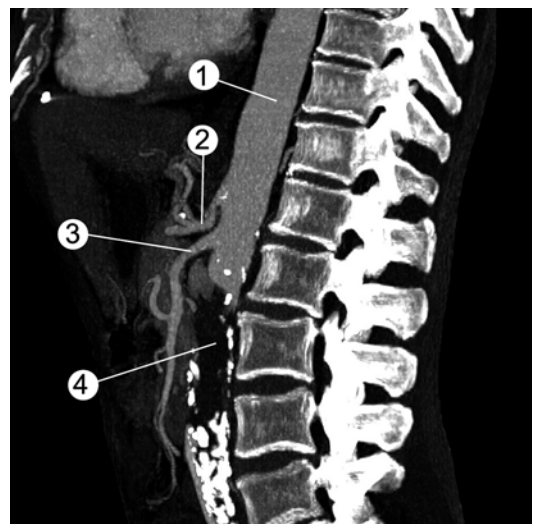


Fig. 6.22 3D MIP reconstruction, sagittal plane

1. A. abdominalis
2. Truncus coeliacus
3. A. mesenterica superior
4. A. abdominalis pars distalis thrombosed and calcified

6.3 Leriche Syndrome Axillobifemoral Bypass

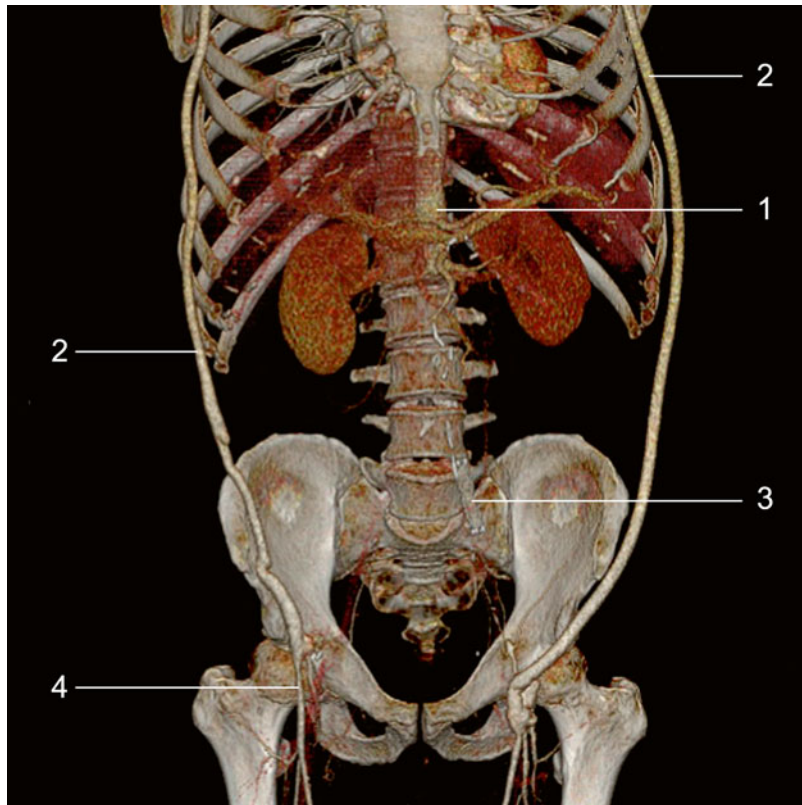


Fig. 6.23 3D VRT colour reconstruction

1. Aorta abdominalis
2. Extraanatomic axillofemoral graft
3. Occluded stent at the level of a. iliaca communis
4. A. femoralis

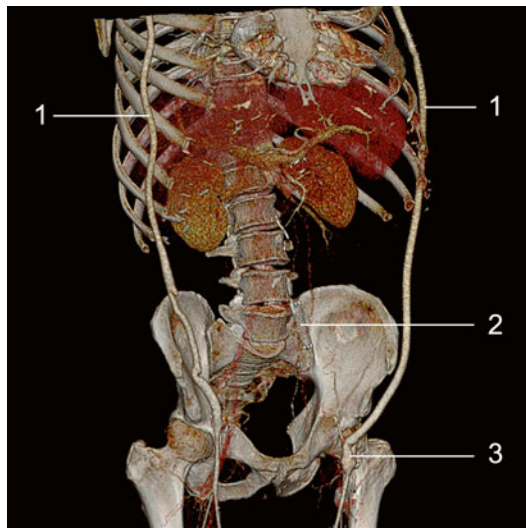


Fig. 6.24 3D VRT colour reconstruction right oblique incidence

1. Axillofemoral grafts
2. Occluded iliac stent
3. Anastomosis of a. femoralis graft

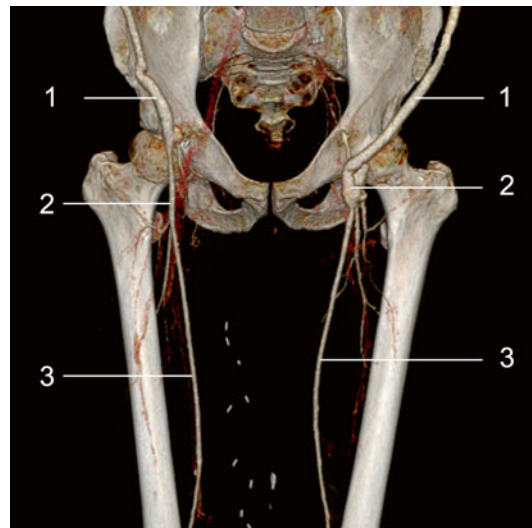


Fig. 6.26 3D VRT colour reconstruction

1. Extraanatomic grafts
2. Graft anastomosis + a. femoralis
3. A. femoralis

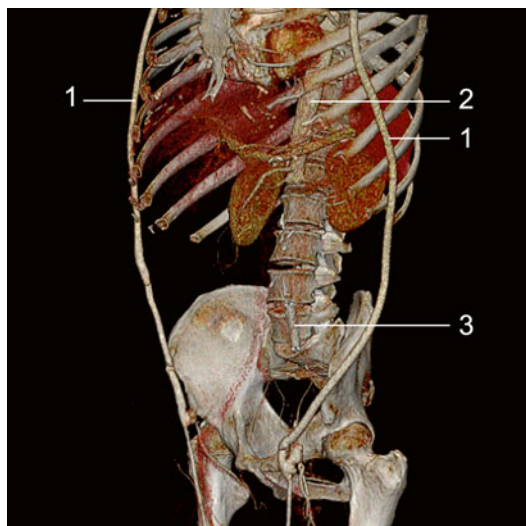


Fig. 6.25 3D VRT colour reconstruction right oblique incidence

1. Axillofemoral grafts
3. Anastomosis of a. femoralis

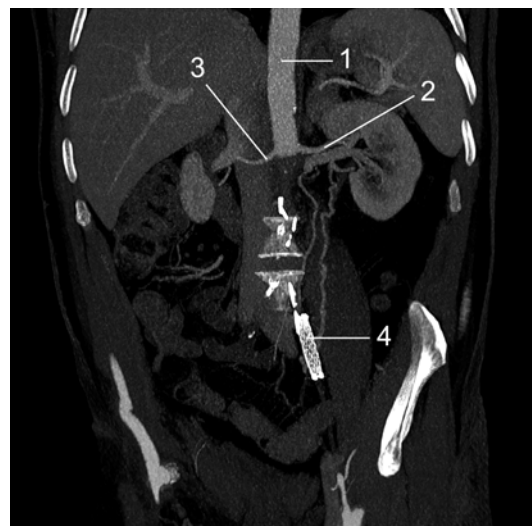


Fig. 6.27 3D MIP reconstruction

1. Aorta abdominalis
2. A. renalis sinistra
3. A. renalis dextra
4. Occluded iliac stent

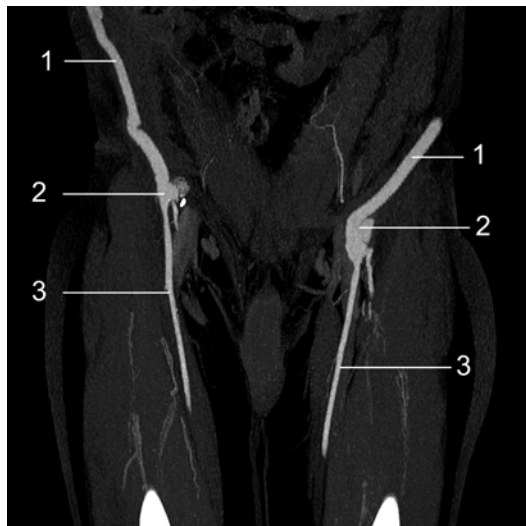


Fig. 6.28 3D MIP reconstruction

1. Axillofemoral grafts
2. Graft anastomosis
3. A. femoralis

6.4 Leriche Syndrome Aortobifemoral and Femoropopliteal Graft

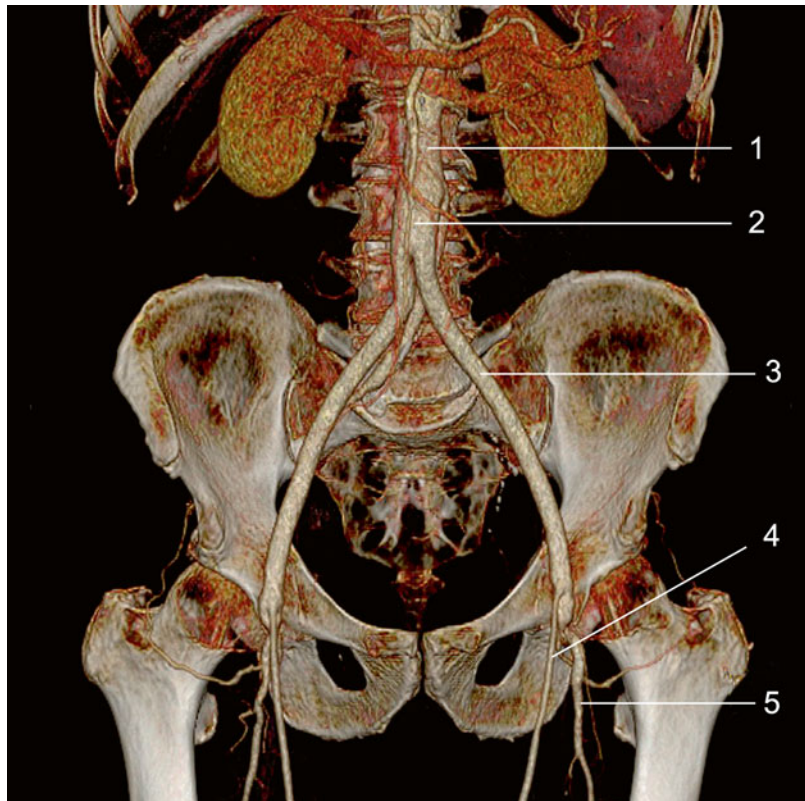


Fig. 6.29 3D VRT reconstruction
1. Aorta abdominalis pars distalis
2. Aortobifemoral graft
3. Arm of aortobifemoral graft
4. Femoropopliteal graft
5. A. profunda femoris

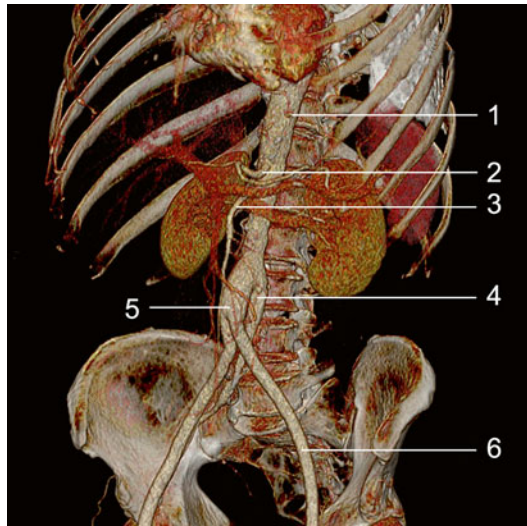


Fig. 6.30 3D VRT reconstruction, left oblique incidence

1. Aorta abdominalis
2. Truncus coeliacus
3. A. mesenterica superior
4. Aorta abdominalis pars distalis
5. Aortobifemoral graft
6. Arms of aortobifemoral graft

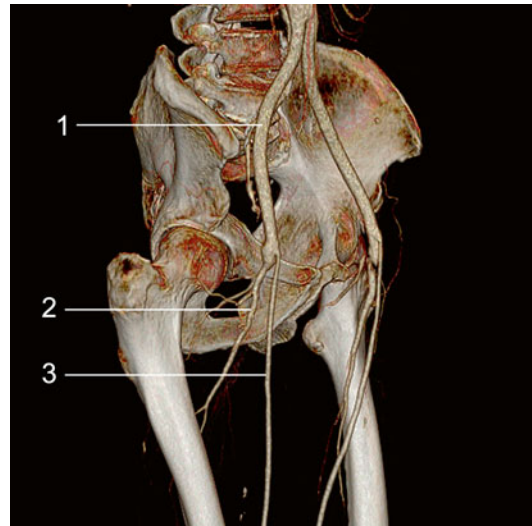


Fig. 6.32 3D VRT reconstruction, right oblique incidence

1. Arm of aortobifemoral graft
2. A. profunda femoris
3. Femoropopliteal graft



Fig. 6.31 3D VRT reconstruction, right oblique incidence



Fig. 6.33 3D VRT reconstruction, left oblique incidence

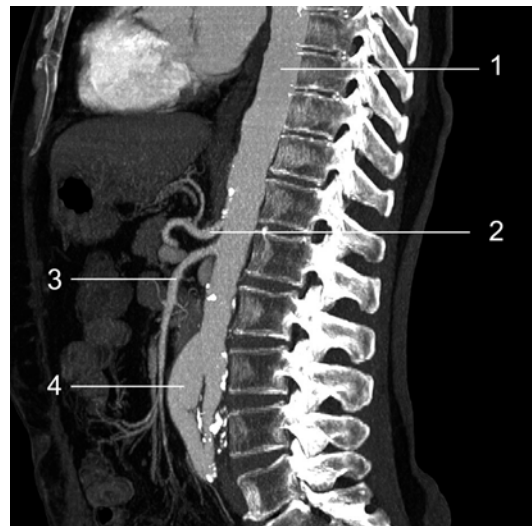


Fig. 6.35 3D MIP reconstruction sagittal plane

1. Aorta abdominalis
2. Truncus coeliacus
3. A. mesenterica superior
4. Pars proximalis of aortobifemoral graft



Fig. 6.34 3D VRT reconstruction, sagittal plane

1. A. profunda femoris
2. Femoropopliteal graft



Fig. 6.36 3D MIP reconstruction frontal plane

1. Arm of aortobifemoral graft
2. A. profunda femoris
3. Femoropopliteal graft

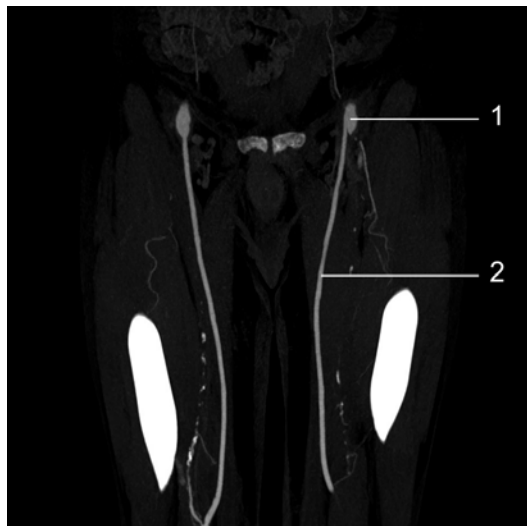


Fig. 6.37 3D MIP reconstruction frontal plane

1. Arm of aortobifemoral graft
2. Femoropopliteal graft

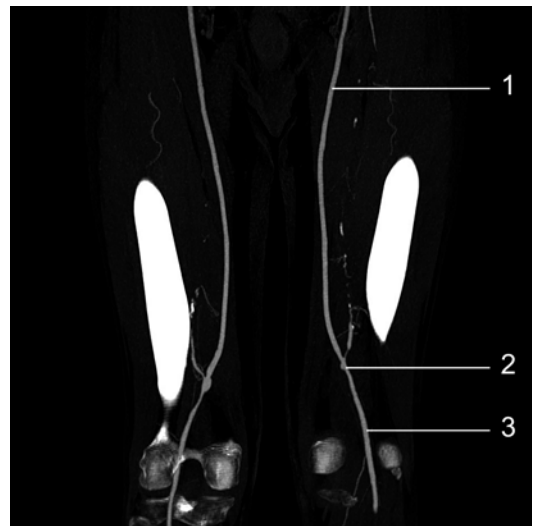


Fig. 6.38 3D MIP reconstruction frontal plane

1. Femoropopliteal graft
2. Femoropopliteal anastomosis
3. A. popliteal

6.5 Aortobifemoral Graft and Aneurysms at the Level of Anastomosis

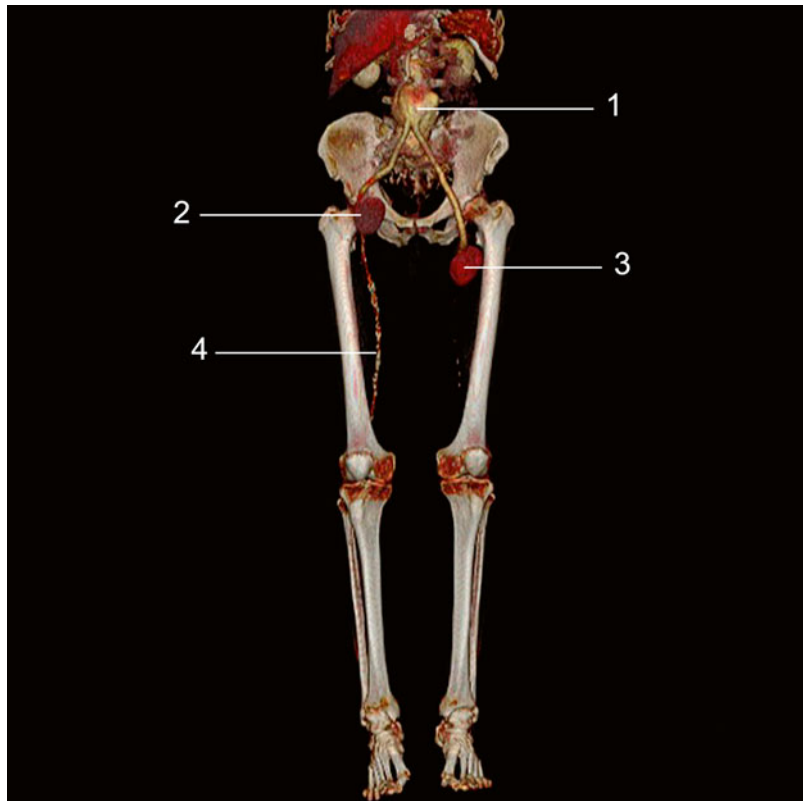


Fig. 6.39 3D VRT colour reconstruction

1. Aorta abdominalis pars distalis with aneurysm at the level of the graft's anastomosis
2. Aneurysm at the level of a. femoralis dextra
3. Aneurysm at the level of a. femoralis sinistra
4. A. femoralis dextra

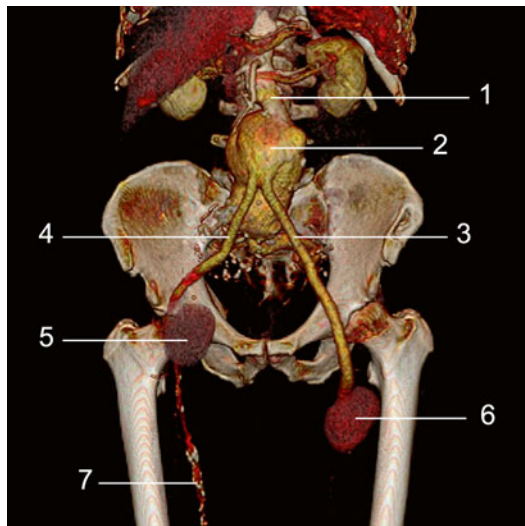


Fig. 6.40 3D VRT colour reconstruction coronary plane, enlarged image

1. Aorta abdominalis
2. Aneurysm at the level of aortobifemoral graft anastomosis
3. Left arm of graft
4. Right arm of graft
5. Aneurysm at the level of anastomosis with a. femoralis dextra
6. Aneurysm at the level of anastomosis with a. femoralis sinistra
7. A. femoralis dextra

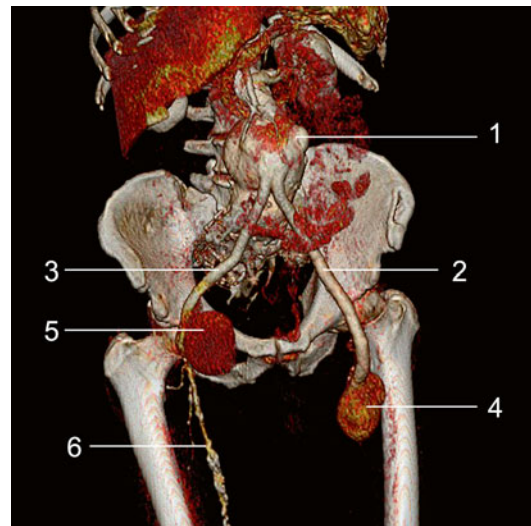


Fig. 6.42 3D VRT colour reconstruction

1. Aneurysm
2. Left arm of graft
3. Right arm of graft
4. Aneurysmal dilatations at the level of anastomosis
5. Aneurysmal dilatations at the level of anastomosis
6. A. femoralis dextra

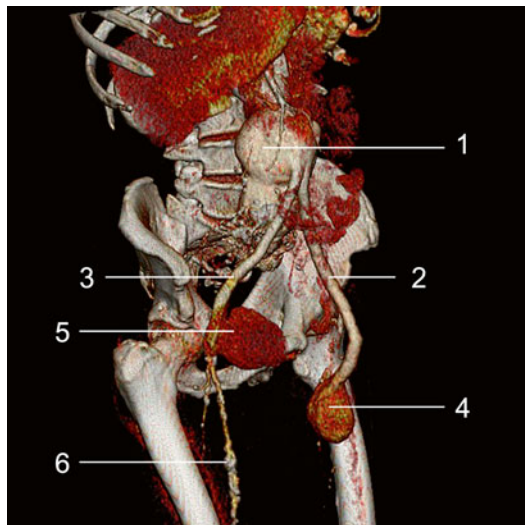
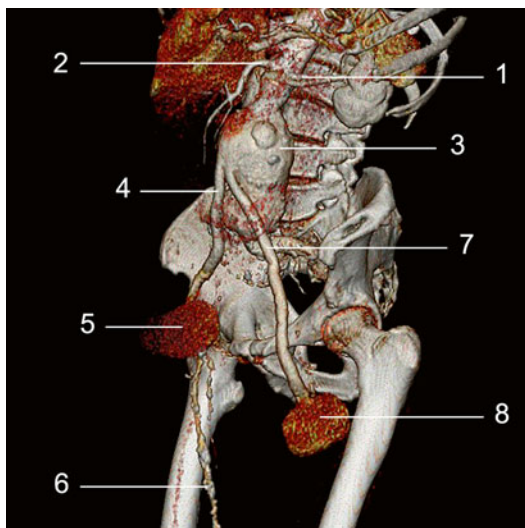
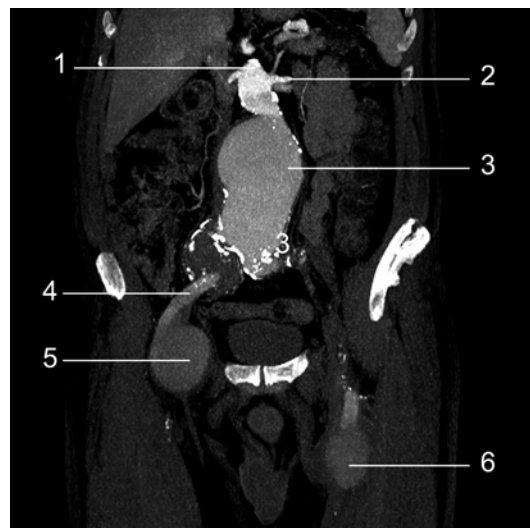


Fig. 6.41 3D VRT colour reconstruction

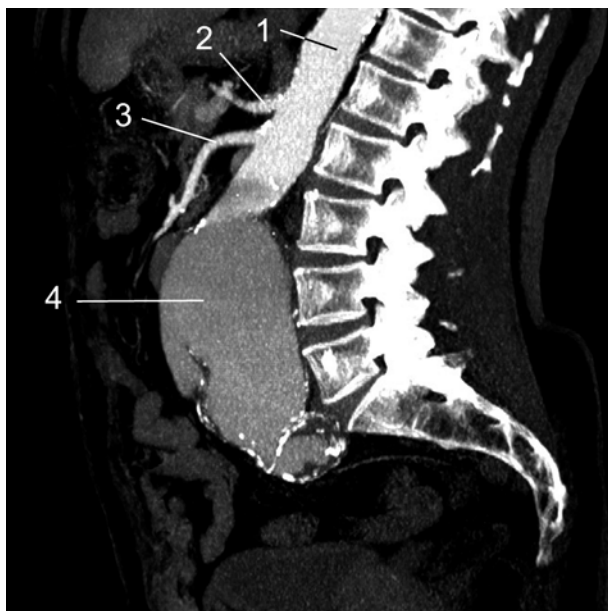
1. Aneurysm
2. Left arm of graft
3. Right arm of graft
4. Aneurysmal dilatations at the level of anastomosis
5. Aneurysmal dilatations at the level of anastomosis
6. A. femoralis dextra

**Fig. 6.43** 3D VRT colour reconstruction

1. Aorta abdominalis
2. A. mesenterica superior
3. Aneurysm
4. Right arm of graft
5. Aneurysm at the level of anastomosis
6. A. femoralis dextra
7. Left arm of graft
8. Aneurysm

**Fig. 6.44** 3D MIP reconstruction

1. Aorta abdominalis
2. A. renalis sinistra
3. Aneurysm
4. Right arm of graft with aneurysmal dilatation on the level of anastomosis (5)
6. Aneurysmal dilatation at the level of left arm anastomosis

**Fig. 6.45** 3D MIP reconstruction, sagittal plane

1. Aorta abdominalis
2. Truncus coeliacus
3. A. mesenterica superior
4. Aneurysmal dilatation

6.6 Right Arm Occlusion of the Aortobifemoral Graft

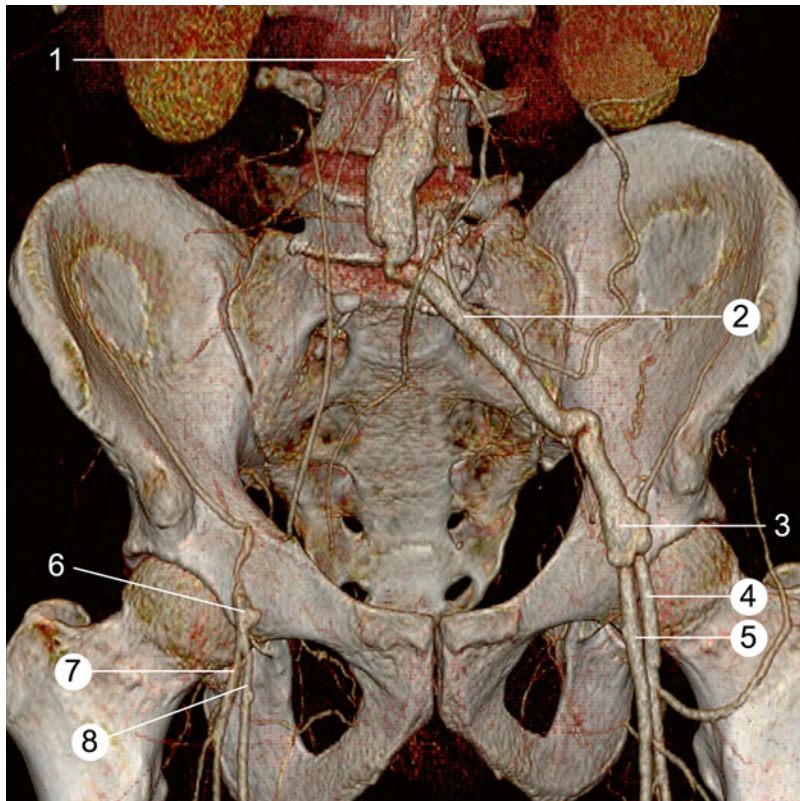


Fig. 6.46 3D VRT reconstruction

1. Proximal part of the graft
2. Left arm of the graft
3. Left arm anastomosis with arteria femoralis
4. Arteria profunda femoris sinistra
5. Arteria femoralis sinistra
6. Arteria femoralis dextra
7. Arteria profunda femoris dextra
8. Arteria femoralis dextra

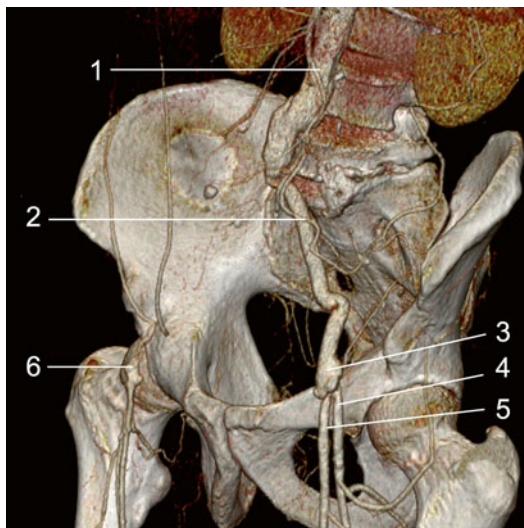


Fig. 6.47 3D VRT reconstruction, oblique view

1. Proximal part of the graft
2. Left arm of the graft
3. Left arm anastomosis with arteria femoralis
4. Arteria profunda femoris sinistra
5. Arteria femoralis sinistra
6. Arteria femoralis dextra

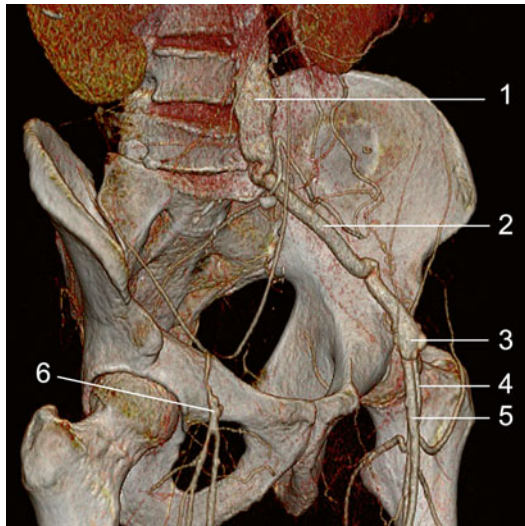


Fig. 6.48 3D VRT reconstruction, oblique view

1. Proximal part of the graft
2. Left arm of the graft
3. Left arm anastomosis with arteria femoralis
4. Arteria profunda femoris sinistra
5. Arteria femoralis sinistra
6. Arteria femoralis dextra

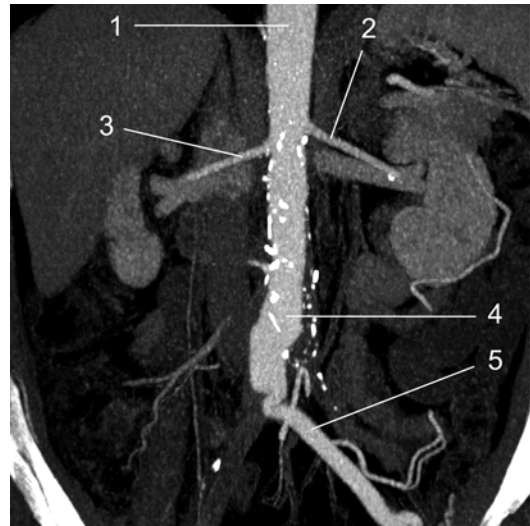


Fig. 6.50 3D MIP reconstruction

1. Aorta abdominalis
2. Arteria renalis sinistra
3. Arteria renalis dextra
4. Aortic graft
5. Left arm of the aortobifemoral graft

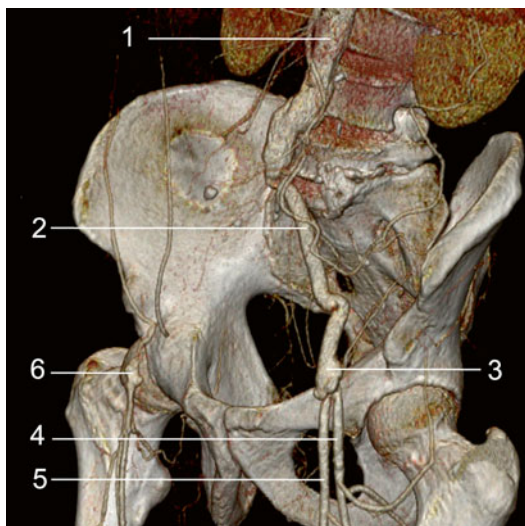


Fig. 6.49 3D VRT reconstruction, oblique view

1. Proximal part of the graft
2. Left arm of the graft
3. Left arm anastomosis with arteria femoralis
4. Arteria profunda femoris sinistra
5. Arteria femoralis sinistra
6. Arteria femoralis dextra



Fig. 6.51 3D MIP reconstruction

1. Aorta
2. Left arm of the graft
3. Arteria femoralis sinistra
4. Arteria profunda femoralis sinistra
5. Arteria femoralis sinistra
6. Arteria femoralis dextra

6.7 Right Femoro-fibular Graft: Occlusion of the Left Lower Limb Arteries

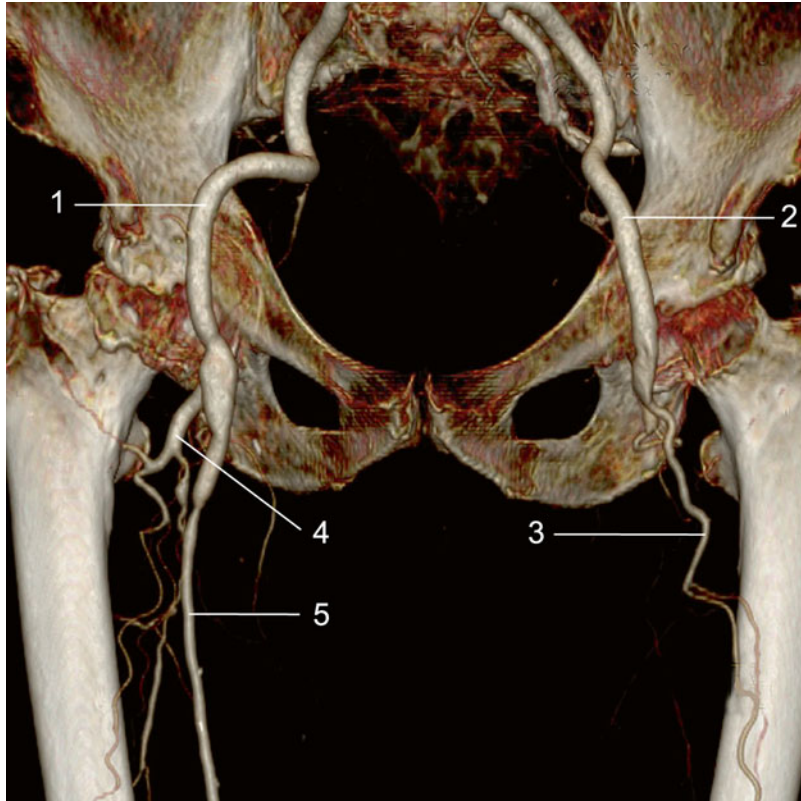


Fig. 6.52 3D VRT reconstruction, coronal view

1. Arteria femoralis dextra
2. Arteria femoralis sinistra
3. Arteria profunda femoris sinistra
4. Arteria profunda femoris dextra
5. Right femoro-fibular venous graft

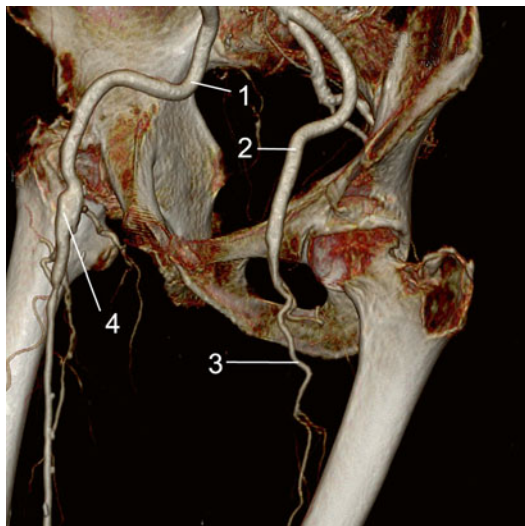


Fig. 6.53 3D VRT reconstruction, oblique view
 1. Arteria iliaca externa dextra
 2. Arteria iliaca externa sinistra
 3. Arteria profunda femoris sinistra
 4. Anastomosis of the venous graft at the distal level of the arteria iliaca externa dextra



Fig. 6.55 3D VRT reconstruction, posterior view, at the level of the popliteal fossa
 1. Venous graft
 2. Collateral arteries



Fig. 6.54 3D VRT reconstruction, posterior view
 1. Right femoro-fibular venous graft
 2. Arteria profunda femoris dextra
 3. Arteria profunda femoris sinistra



Fig. 6.56 3D VRT reconstruction, posterior view at the level of the calf
 1. Arteria fibularis dextra with multiple occlusive lesions
 2. Right femoro-fibular venous graft
 3. Venous graft anastomosis with arteria fibularis dextra
 4. Arteria fibularis dextra



Fig. 6.57 3D VRT reconstruction, posterior view at the level of the calf

1. Arteria fibularis sinistra
2. Anastomosis
3. Arteria fibularis dextra

6.8 Iliac and Femoral Stents: In-Stent Restenosis

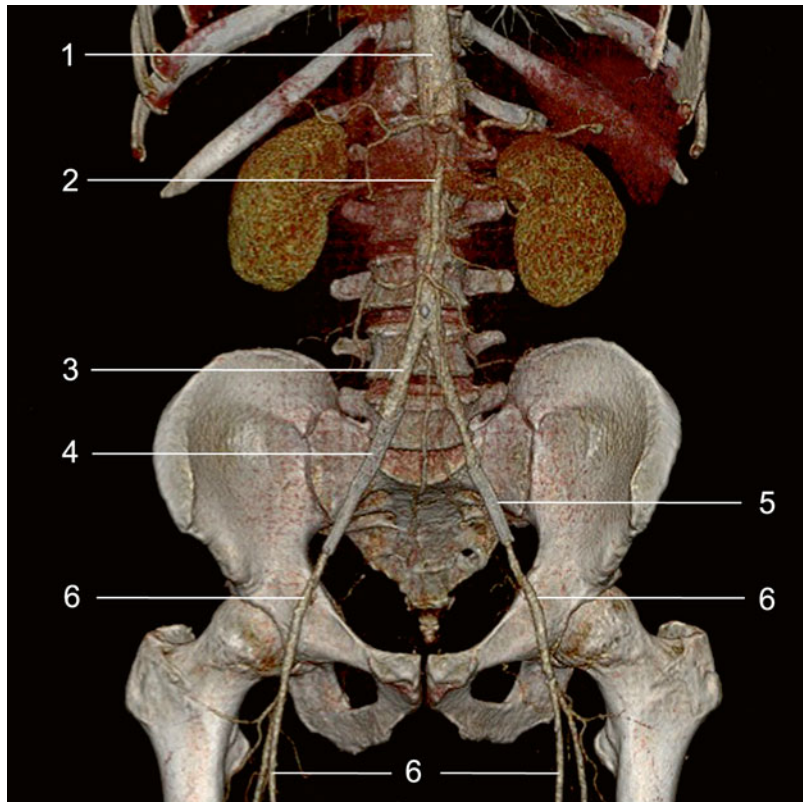


Fig. 6.58 3D VRT reconstruction in coronal plane

1. Aorta abdominalis
2. Arteria mesenterica superior
3. Arteria iliaca communis
4. Arteria iliaca externa
5. Stent at the level of the arteria iliaca externa
6. Arteria femoralis

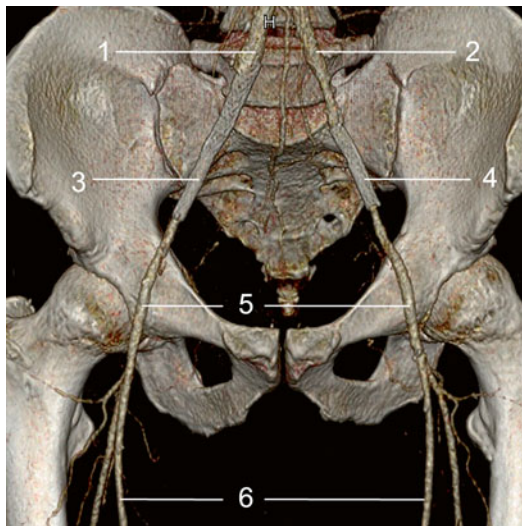


Fig. 6.59 3D VRT reconstruction in coronal plane
1. Arteria iliaca communis dextra
2. Arteria iliaca communis sinistra
3. Stent in the arteria iliaca externa dextra
4. Stent in the arteria iliaca externa sinistra
5. Arteria femoralis
6. Arteria femoralis

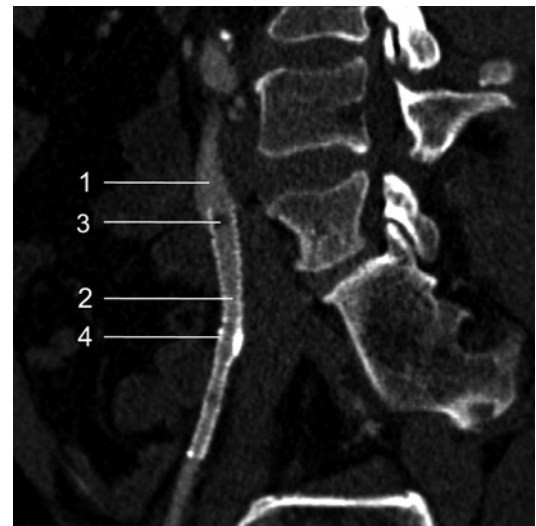


Fig. 6.61 Curved 3D MPR
1. Arteria iliaca externa dextra
2. Patent in-stent lumen
3. Proximal in-stent restenosis
4. Stent



Fig. 6.60 3D VRT reconstruction
1. Arteria femoralis dextra
2. Stent in arteria femoralis dextra
3. Arteria femoralis sinistra

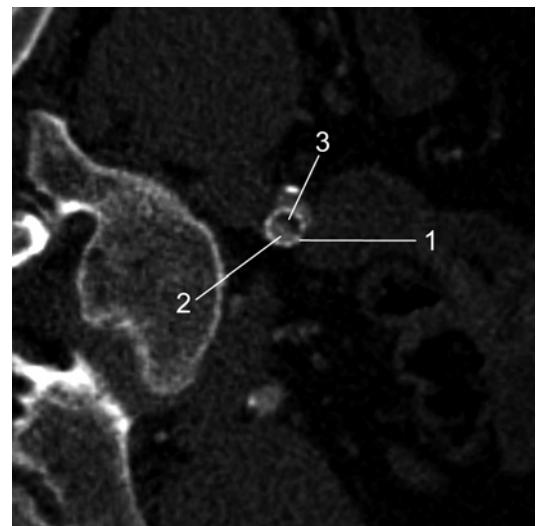


Fig. 6.62 Axial 3D MPR
1. Stent
2. Patent lumen
3. Neointimal proliferation (restenosis)

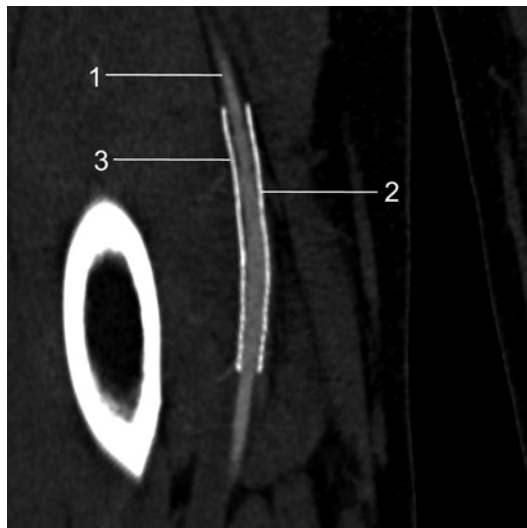


Fig. 6.63 3D MPR at the femoral level

1. Patent lumen at the level of arteria femoralis dextra
2. Stent
3. Area with neointimal hyperplasia

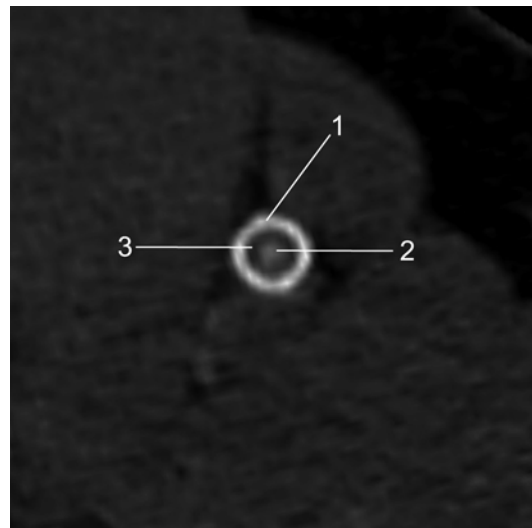


Fig. 6.64 3D MPR, axial plane

1. Stent
2. Patent lumen
3. Neointimal hyperplasia

6.9 Iliac and Femoral Stents: Occluded Iliac Stents

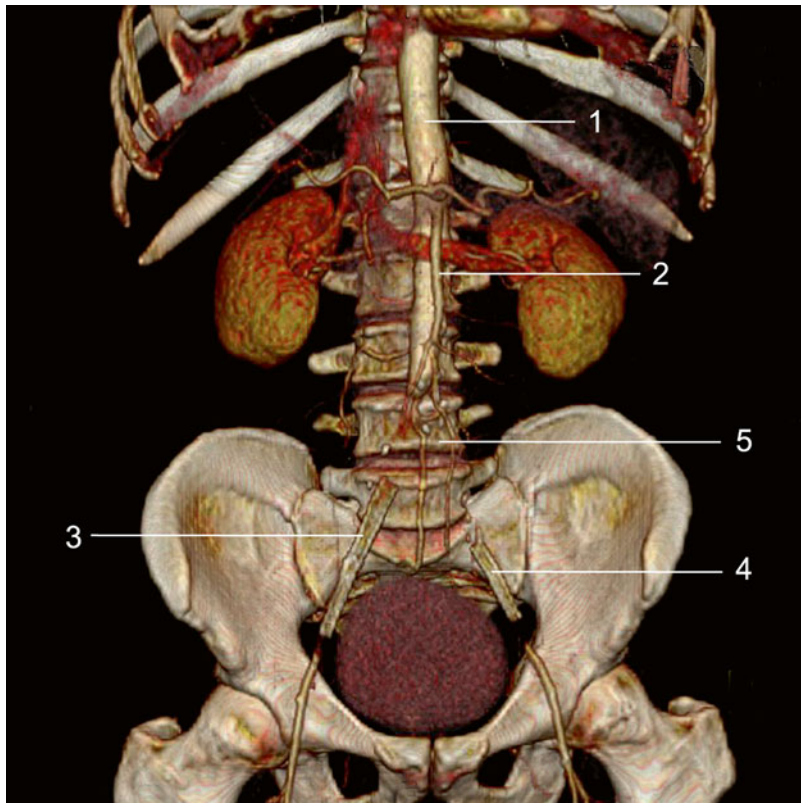
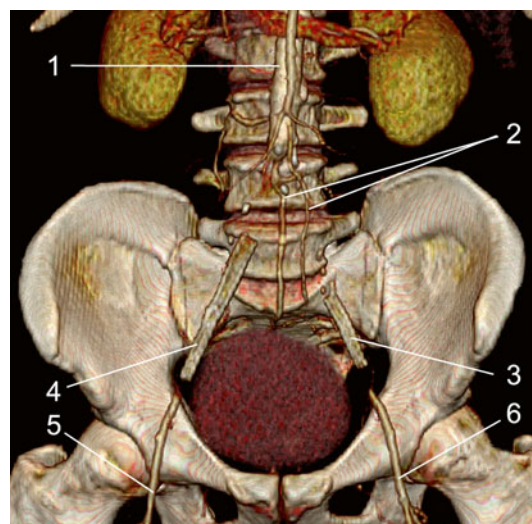
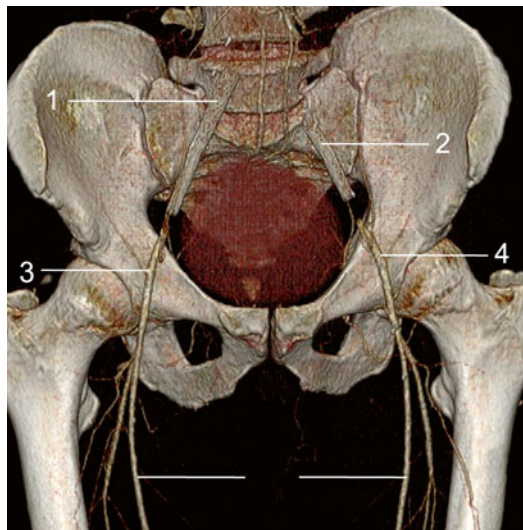


Fig. 6.65 3D VRT reconstruction
 1. Aorta abdominalis
 2. Arteria mesenterica superior
 3. Thrombosis at the level of arteria iliaca communis and arteria iliaca externa dextra
 4. Thrombosis at the level of arteria iliaca communis and arteria iliaca externa sinistra
 5. Thrombosis of a. iliaca communis

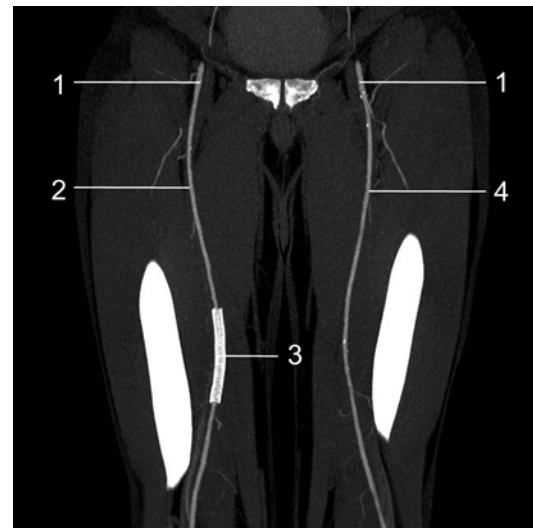
Fig. 6.66 3D VRT reconstruction

1. Aorta abdominalis
2. Occlusion at the level of arteria iliaca communis sinistra
3. Occluded stent at the level of arteria iliaca externa sinistra
4. Occluded stent at the level of arteria iliaca externa dextra
5. Arteria femoralis dextra
6. Arteria femoralis sinistra

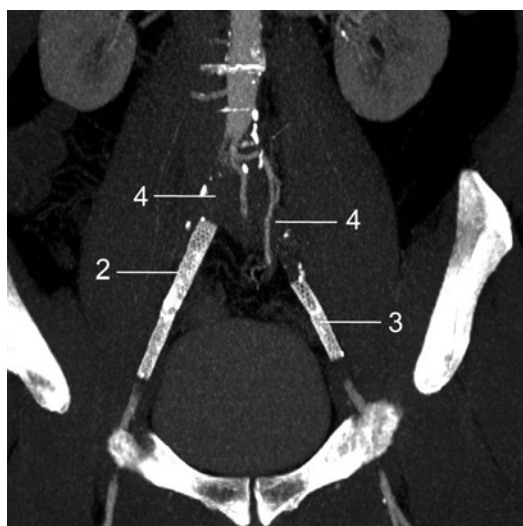


**Fig. 6.67** Reconstruction 3D VRT

1. Occluded stents at the level of arteria iliaca communis and arteria iliaca externa dextra
2. Occluded stent at the level of arteria iliaca externa sinistra
3. Arteria femoralis
4. Arteria femoralis

**Fig. 6.69** 3D MIP reconstruction at the thigh level

1. Arteria iliaca externa
2. and 4. Arteria femoralis
3. Patent stent at the level of arteria femoralis dextra

**Fig. 6.68** 3D MIP reconstruction

1. Aorta abdominalis
2. and 3. Occluded stents

**Fig. 6.70** 3D MPR reconstruction

1. Occluded stents
2. Occluded stents

6.10 Autoimmune Vasculitis

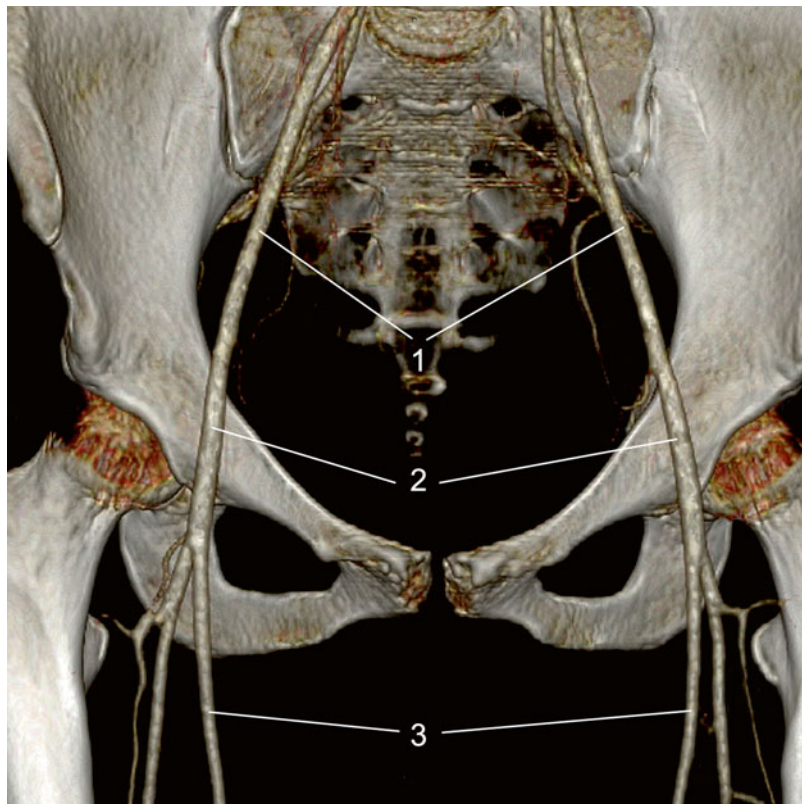


Fig. 6.71 3D VRT reconstruction
1. Arteria iliaca externa
2. Arteria femoralis
3. Arteria femoralis



Fig. 6.72 3D VRT reconstruction
1. Arteria femoralis
2. Arteria profunda femoris

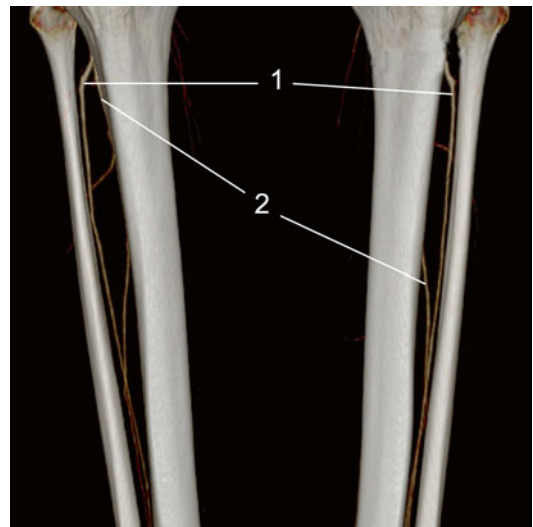


Fig. 6.73 3D VRT reconstruction
1. Arteria tibialis posterior
2. Arteria fibularis



Fig. 6.74 3D VRT reconstruction of the distal segment of the calf with absence of arteria tibialis anterior and arteria dorsalis pedis



Fig. 6.76 3D VRT reconstruction, posterior view
1. Arteria tibialis posterior
2. Arteria fibularis



Fig. 6.75 3D VRT reconstruction of the distal segment of the calf with absence of arteria tibialis anterior and arteria dorsalis pedis

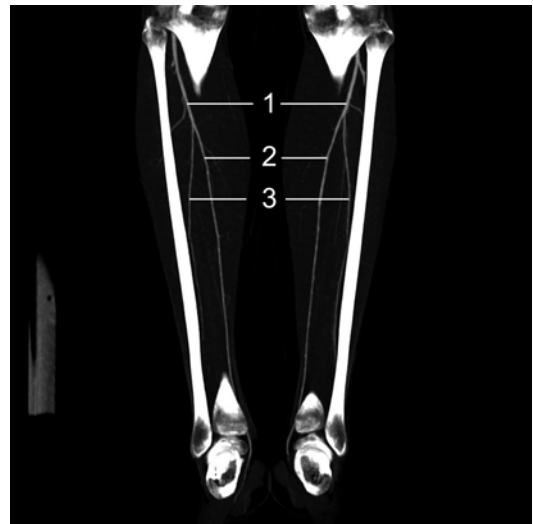


Fig. 6.77 3D MIP reconstruction
1. Arteria tibialis posterior
2. Arteria tibialis posterior
3. Arteria fibularis

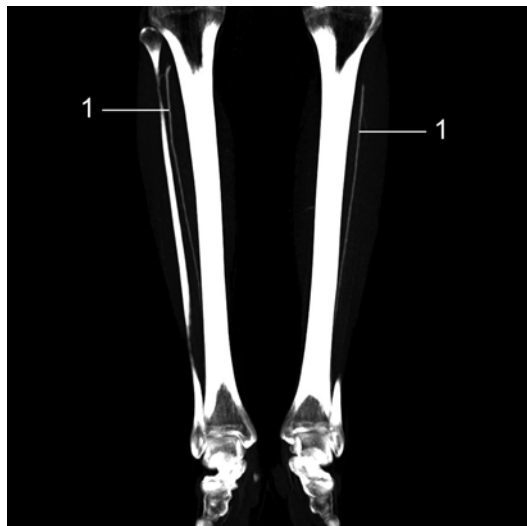


Fig. 6.78 3D MIP reconstruction

1. Arteria tibialis anterior (artery can be visible only to the middle third of the leg)

6.11 Tumour of the Leg

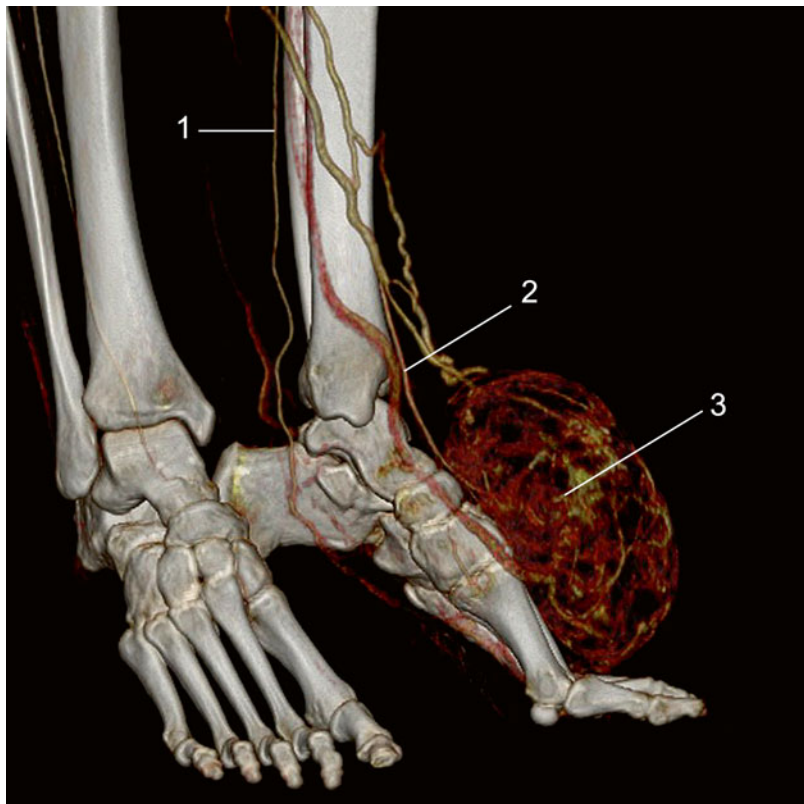


Fig. 6.79 3D VRT reconstruction, arterial phase

1. Arteria tibialis posterior sinistra
2. Arteria tibialis anterior sinistra
3. Hypervascular tumour

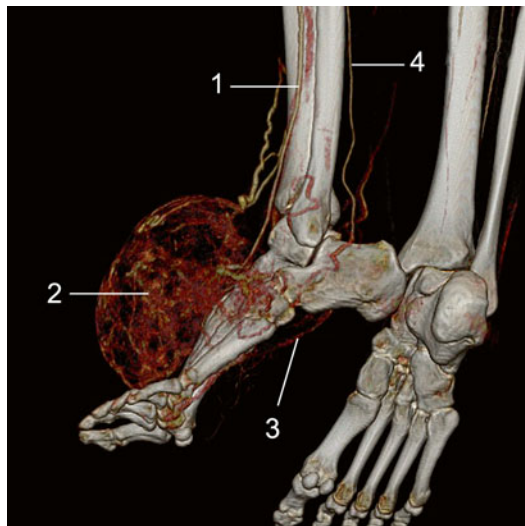


Fig. 6.80 3D VRT reconstruction, arterial phase

1. Arteria tibialis anterior sinistra
2. Hypervascular tumour
3. Arteria plantaris
4. Arteria tibialis posterior sinistra

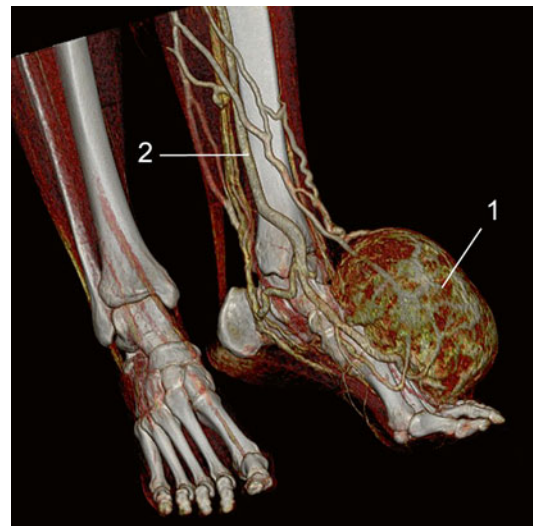


Fig. 6.82 3D VRT reconstruction, venous phase

1. Tumoural mass
2. Superficial and profound venous system



Fig. 6.81 3D VRT reconstruction, venous phase

1. Tumoural mass
2. Superficial and profound venous system

6.12 Giant Tumour of the Thigh

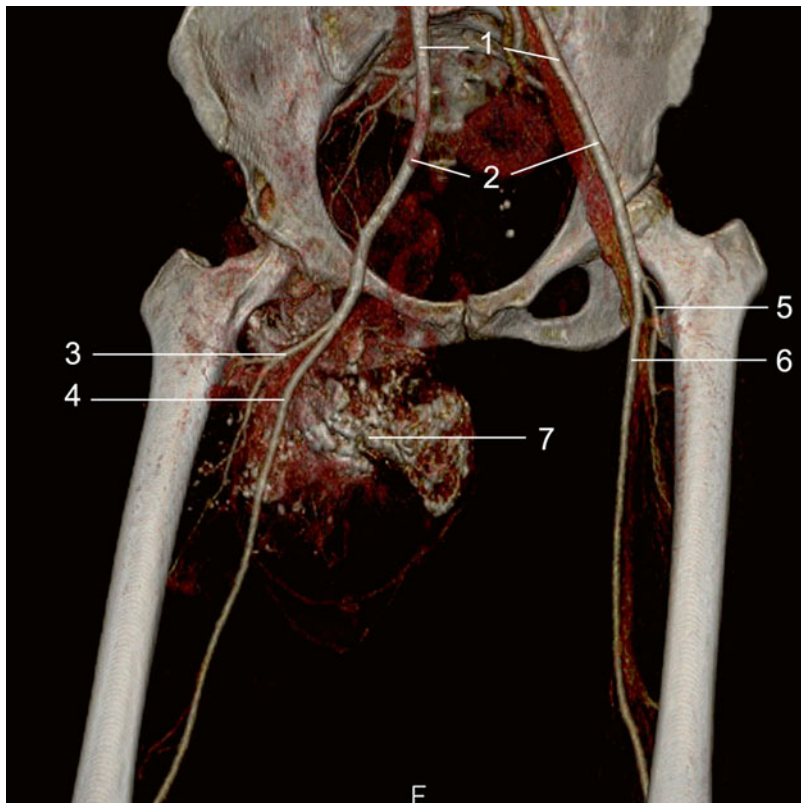
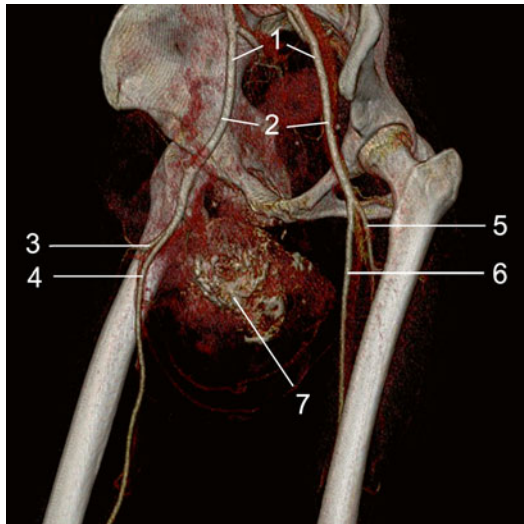
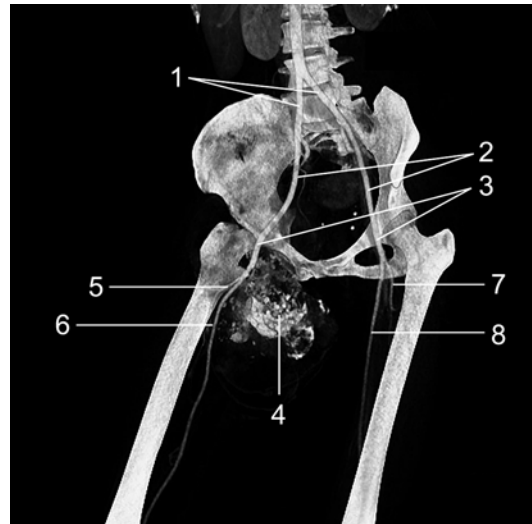


Fig. 6.83 3D VRT reconstruction, pelvis and thigh

1. Arteria iliaca externa
2. Arteria iliaca externa
3. Arteria profunda femoris dextra
4. Arteria femoralis dextra
5. Arteria profunda femoris sinistra
6. Arteria femoralis sinistra
7. Tumoural mass with calcification and vascularisation, without embedding of the vascular package

**Fig. 6.84** 3D VRT reconstruction, pelvis and thigh

1. Arteria iliaca externa
2. Arteria iliaca externa
3. Arteria profunda femoris dextra
4. Arteria femoralis dextra
5. Arteria profunda femoris sinistra
6. Arteria femoralis sinistra
7. Tumoural mass with calcification and vascularisation, without embedding of the vascular package

**Fig. 6.85** 3D VRT reconstruction

1. Arteria iliaca communis
2. Arteria iliaca externa
3. Arteria iliaca externa
4. Tumoural mass with calcification
5. Arteria profunda femoris dextra
6. Arteria femoralis dextra
7. Arteria profunda femoris sinistra
8. Arteria femoralis sinistra

**Fig. 6.86** 3D VRT reconstruction

1. Arteria iliaca communis
2. Arteria iliaca externa
3. Arteria iliaca externa
4. Tumoural mass with calcification and invasion in the pelvis
5. Arteria profunda femoris dextra
6. Arteria femoralis dextra

6.13 CT Angiography of the Right Upper Limb: Occlusion of the Arteria Radialis Dextra

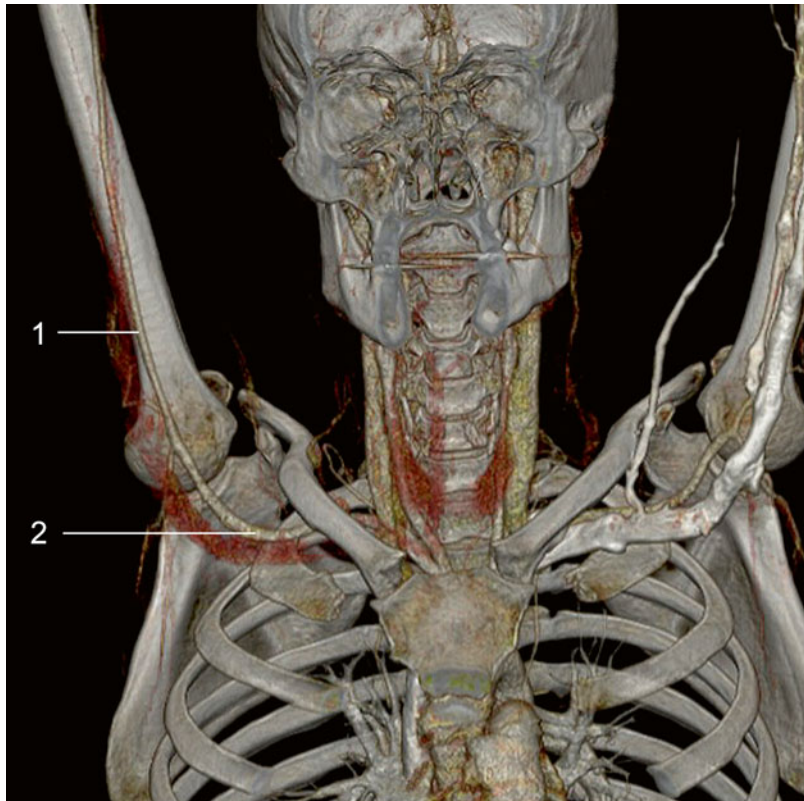


Fig. 6.87 3D VRT reconstruction
1. Arteria brachialis dextra
2. Arteria axillaris dextra



Fig. 6.88 3D VRT reconstruction

1. Arteria ulnaris dextra
2. Arteria radialis dextra (occluded)

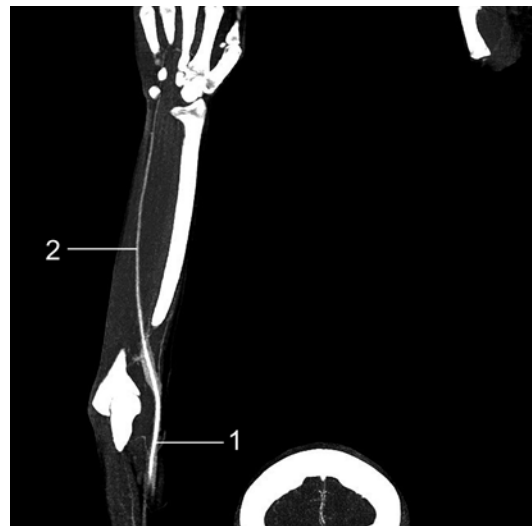


Fig. 6.90 3D MIP reconstruction

1. Arteria brachialis dextra
2. Arteria ulnaris dextra

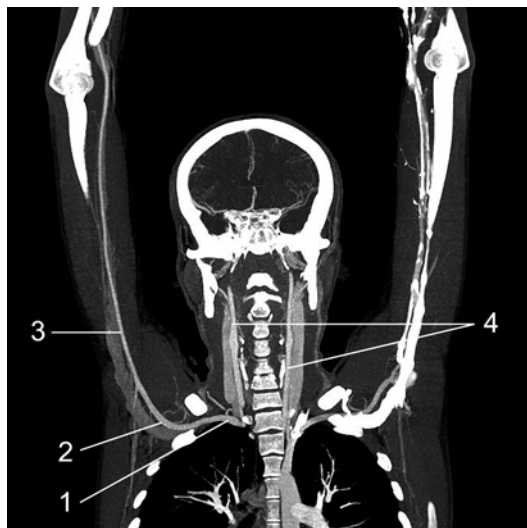


Fig. 6.89 3D MIP reconstruction

1. Arteria subclavia dextra
2. Arteria axillaris dextra
3. Arteria brachialis dextra
4. Arteria carotis communis

6.14 Arteriovenous Malformation in Deltoid Region

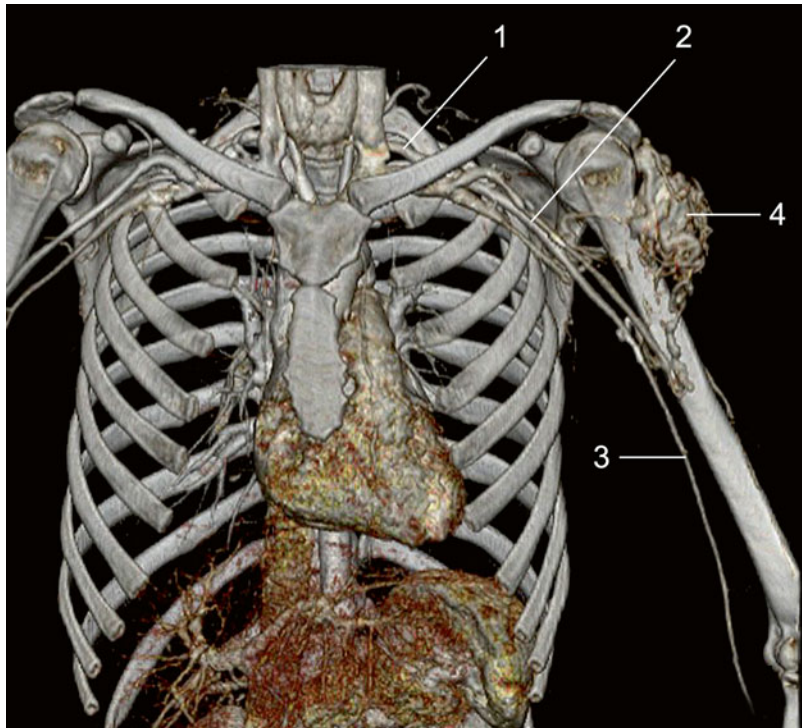


Fig. 6.91 3D VRT reconstruction, coronal view

1. Arteria subclavia sinistra
2. Arteria axillaris sinistra
3. Arteria brachialis sinistra
4. Arteriovenous malformation

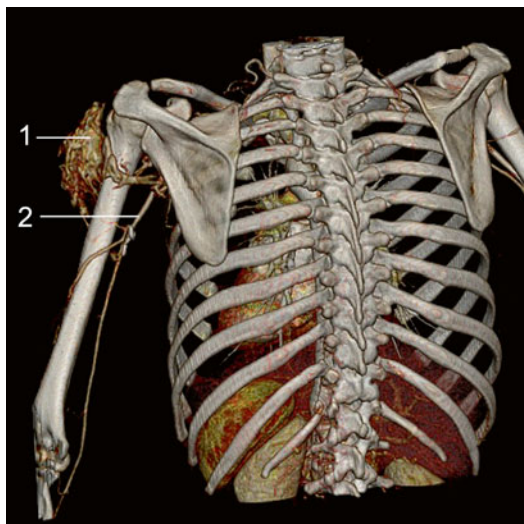


Fig. 6.92 3D VRT reconstruction, posterior view

1. Arteriovenous malformation
2. Arteria brachialis sinistra

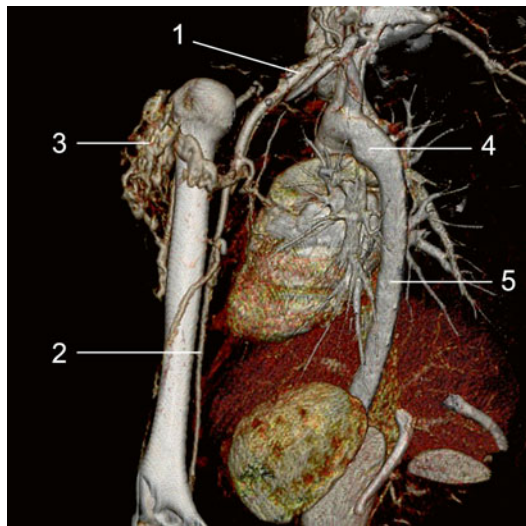


Fig. 6.93 3D VRT reconstruction, after removing the thoracic cage

1. Arteria subclavia and arteria axillaris sinistra
2. Arteria brachialis sinistra
3. Arteriovenous malformation
4. Arcus aortae
5. Aorta descendens

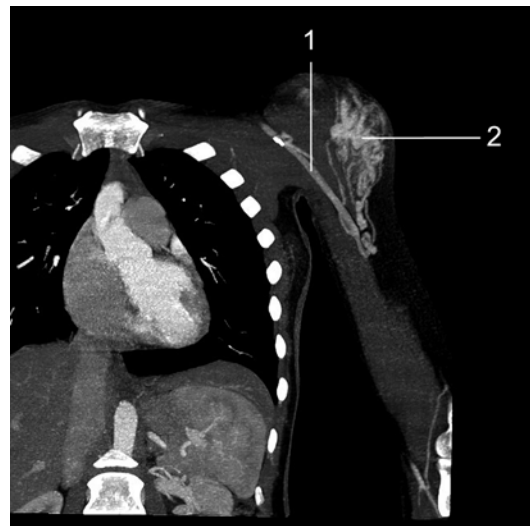


Fig. 6.95 3D MIP reconstruction

1. Arteria axillaris sinistra
2. Arteriovenous malformation

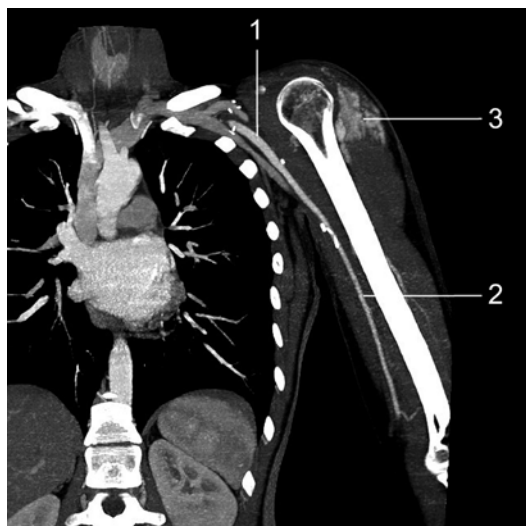


Fig. 6.94 3D MIP reconstruction

1. Arteria subclavia sinistra
2. Arteria brachialis sinistra
3. Arteriovenous malformation



Fig. 6.96 3D MIP reconstruction
Arteriovenous malformation

6.15 CTA Run-Off: Incidental Finding

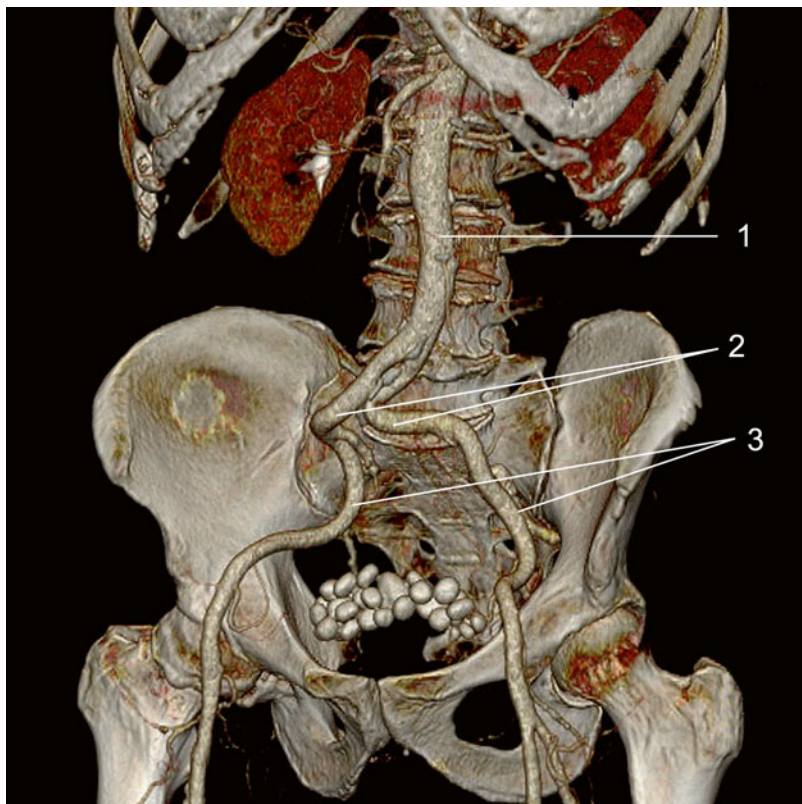


Fig. 6.97 3D VRT reconstruction
1. Aorta abdominalis
2. Arteria iliaca communis
3. Arteria iliaca externa
4. Stones in the urinary bladder